University of Alberta

Neuronal Mechanisms Underlying Spasticity Following Chronic Spinal Cord Injury

by

Yunru Li 

A thesis submitted to the Faculty of Graduate Studies and Research in partial fulfillment of the requirements for the degree of Doctor of Philosophy

Centre for Neuroscience
Edmonton, Alberta
Fall 2004

Your file Votre référence
ISBN: 0-612-95969-4
Our file Notre référence
ISBN: 0-612-95969-4

Dedicated to my family ----

To my father for his eternal encouragement,

to my mother for her endless support,

to my husband for being proud of me

and to my brother for his belief in me

ACKNOWLEDGMENTS

I would like to express my deepest thanks to my supervisor, Dr. David Bennett for providing me with the opportunity to come to Canada and work with him. His enthusiasm and insights in research have always inspired me. I appreciate not only his supervision in academic work, but also his attitude of helping young people in all aspects. He is not only a great mentor, but also a wonderful guide in one's life. I have been immensely fortunate to have such a considerate and supportive supervisor.

I am sincerely grateful to the members of my supervisory committee, Dr. Richard Stein and Dr. Peter Smith. Their brilliant and creative minds amazed me and their valuable advice benefited me throughout my graduate studies. In addition, I would like to thank Dr. Monica Gorassini for her continuous help, support, interest and constructive suggestion with my research. Many thanks to the members of my examination committee, Dr. Kelvin Jones and Dr. Robert Lee (external examiner), for their time and effort in providing me with feedback on my thesis.

I would also like to thank Mr. Leo Sanelli for the excellent technical support I have received from him and to Mrs. Carol Ann Johnson and Mrs. Brenda Topliss for their excellent administrative support over the past five years.

Finally, I would like to extend my thanks to my fellow graduate students and the faculty and staff in the Centre for Neuroscience. Each one helped me with techniques and new ideas and their sense of humor provided a very friendly and encouraging atmosphere in which to work.

LIST OF CONTENTS

LIST OF TABLE

LIST OF FIGURES

LIST OF ABBREVIATIONS

Caudal	Ca
Calcium persistent inward current	Ca PIC
Discontinuous current clamp	DCC
Excitatory post synaptic potentials	EPSPs
γ-aminobutyric acid	GABA
Late-Accelerating Self-sustained	LAS
Low-threshold Linear Self-sustained	LLS
Modified artificial cerebral spinal fluid	mACSF
Norepinephrine	NE
Normal artificial cerebral spinal fluid	nACSF
Persistent inward current	PIC
Sodium persistent inward current	Na PIC
Sacral	S
Tetrodotoxin	TTX
Threshold	T

Chapter 1: Introduction

SPINAL CORD INJURY AND SPASTICITY

There are about 250,000 to 400,000 existing spinal cord injury patients in the USA and approximately 8,000 new victims each year. More than 80% of them experience spasticity (Levi et al. 1995), which can severely impede residual motor function and can be very painful. Spasticity in these patients is poorly treated by conventional therapies (Little et al. 1989), in large part because we do not fully understand the underlying mechanisms.

Although spasticity is classically defined as a velocity-dependent increase in tonic stretch reflexes (muscle tone) with exaggerated tendon jerks, clonus and clasp-knife response (Lance and Burke 1974; Noth 1991), spasticity developed in patients after chronic spinal cord injury is mainly characterized by, and leads to frequent complaints about the long-lasting flexor/extensor spasms and exaggerated cutaneous reflexes evoked by numerous non-noxious stimuli (Kuhn and Macht 1948; Young 1994). It usually takes more than several weeks for the full spasticity syndrome to develop after a complete spinal cord injury. That is, immediately after the spinal cord injury, the spinal cord is at first completely areflexic, known as spinal shock, which usually lasts from days to weeks (Nacimiento and Noth 1999). About 1 to 3 weeks after the injury, various muscle reflexes to nociceptive plantar stimulus (flexor withdraw reflex), including the Babinski sign, gradually recover. The flexor activity first starts from distal muscles, such as ankle muscles, and later moves proximally, such as to the knee and hip. Tendon jerk reflexes reappear about 1 month post injury and become exaggerated with time. The threshold of

the flexor reflex decreases gradually and finally a very slight stimulation to the plantar surface of the foot can produce strong contraction of the flexors lasting for a long period of time (Ashby and McCrea 1987; Kuhn and Macht 1948). The extensor activity recovers later than the flexor activity, and, in contrast to the flexor reflexes, which are most readily evoked by cutaneous stimulation, the most effective stimulation to extensor reflex is proprioceptive, like changing body or limb positions. As the threshold decreases, squeezing of thigh musculature, rubbing and light tactile stimulation can become sufficient to elicit powerful extension (Ashby and McCrea 1987; Kuhn and Macht 1948). Very often, the flexor and the extensor muscles contract simultaneously and produce a rigidity of the limb that can last for several seconds. Flexion of the knee may then suddenly release the extensor spasm, i.e., the clasp-knife response (Ashby and McCrea 1987). Once these symptoms of spasticity occur, they usually persist throughout the patient's life.

IONIC MECHANISMS UNDERLYING SPASTICITY

Initial studies of spasticity have been focused on the reflex changes after chronic spinal cord injury. In animals with chronic spinal cord injury, the monosynaptic reflex (including tendon jerk) is exaggerated (Hultborn and Malmsten 1983b; Robert and Young 1994), and associated with decreased presynaptic inhibition (Ashby et al. 1974; Nielsen et al. 1995). Changes in other segmental circuits could also contribute to spasticity, including changes in Renshaw inhibition (Delwaide 1985; cf. Katz et al. 1982), reciprocal Ia inhibition (Delwaide 1985, cf. Ashby and Wiens 1989) and autogenic Ib inhibition (Delwaide and Oliver 1988).

Changes in these monosynaptic and other short acting reflex pathways, although interesting, likely only play a minor role in producing the clinical manifestation of spasticity after spinal cord injury, since most of the clinical symptoms are produced by the long-lasting reflexes, i.e. the polysynaptic part of the recorded reflexes, such as exaggerated cutaneous/flexor reflexes (Bennett et al. 1999; Remy-Neris et al. 1999) and increased tonic stretch reflexes (Burke et al. 1970; Powers et al. 1989; Thilmann et al. 1991). Thus, the present study focuses on the ionic mechanisms underlying these exaggerated long-lasting spastic reflexes through intracellular recording from the motoneurons.

One obvious and important outcome of a complete spinal cord injury is the elimination of descending inputs from the brainstem that control the baseline levels of excitability for

both interneurons and motoneurons (Baldissera et al. 1981). The reticulospinal system is particularly important for this tonic control, with its most powerful effects mediated by the monoaminergic axons (Jankowska 1992a), including axons that contain 5-HT (Maxwell et al. 1996) originating from the raphe nucleus and axons that contain NE originating from the locus ceruleus nucleus (Patel et al. 1997). Both kinds of axons project densely throughout the cord (Alvarez et al. 1998; Björklund and Skagerberg 1982; Giroux et al. 1999a). Therefore, it seems worthwhile to review how the monoamines, especially 5-HT, affect the motoneuron and interneuron excitability in the spinal cord.

Excitatory effect of monoamines on the spinal motoneurons

BISTABLE BEHAVIOR: One major effect of monoamines on spinal motoneurons is the production of bistable behavior (Hounsgaard et al. 1988; Hounsgaard and Kiehn 1989). In a bistable motoneuron, a brief synaptic input or intracellular current injection activates prolonged depolarizations, which can remain active for many seconds after the stimulation has ceased. The sustained depolarizations (plateau potentials) either stop spontaneously or can be turned off by a hyperpolarization. Bistable behavior is a latent property of motoneurons. It only appears in motoneurons in anesthetized preparations if pharmacological agents (TEA or cesium) are applied to suppress K^+ currents (Powers and Binder 2000; Schwindt and Crill 1980). However, bistable behavior can occur spontaneously in motoneurons without such agents in the unanesthetized decerebrate cat preparation (Hounsgaard et al. 1988) because this preparation has tonic activity in fibers

that originate in the brainstem and release the monoamines serotonin (5-HT) and norepinephrine (NE). Therefore, the activation of plateau potentials in motoneurons depends critically on the facilitation of monoamines. When the descending monoaminergic input is eliminated by acute spinal transection, no plateau potential is activated in motoneurons below the level of injury, which can be restored by exogenous administration of monoaminergic receptor agonists (Conway et al. 1988; Hounsgaard et al. 1988).

PERSISTENT INWARD CURRENTS: A persistent inward current (PIC) is needed to generate the plateau potentials and bistable behavior (Carlin et al. 2000; Lee and Heckman 1998; Svirskis and Hounsgaard 1998). A large part of the PIC is mediated by the L-type calcium (Ca) currents (Carlin et al. 2000; Hounsgaard and Kiehn 1989). L-type channels have been considered to be high-voltage activated (HVA), but recent studies show that there are two main neuronal variants, CaV 1.2 and 1.3 (Xu and Lipscombe 2001). CaV 1.2 is an HVA channel, but CaV 1.3 has a threshold for activation of –50 mV or less. CaV 1.3 is also 10-fold less sensitive to the L-type Ca channel antagonists nimodipine and nifedipine. Spinal motoneurons have both CaV 1.2 and 1.3 (Carlin et al. 2000; Westenbroek et al. 1998), but motoneuron PICs display the hallmarks of 1.3, including both the low-voltage range for activation (e.g., Lee and Heckman 1998) and the insensitivity to nifedipine (Hounsgaard and Kiehn 1989; Mills and Pitman 1997; Voisin and Nagy 2001). A persistent sodium (Na) current is now known to also generate a substantial portion of the PIC in rat motoneuron (Hsiao et al. 1998) and many other neurons (Angstadt and Choo 1996; Elson and Selverston 1997; Rekling and Laursen

1989; Sandler et al. 1998; Schwindt and Crill 1995; Stafstrom et al. 1982). A Ca-mediated cation channel may also play a significant role in some cells (Perrier and Hounsgaard 1999; Rekling and Feldman 1997; Zhang and Harris-Warrick 1995).

RECOVERY OF BISTABILITY AFTER CHRONIC INJURY: After spinal cord injury, monoamines from the descending inputs are almost completely eliminated; however, some 5-HT does persist in the injured cord (Newton and Hamill 1988a; Shapiro 1997a). For example, the spinal cord contains serotonergic neurons as part of its autonomic system along the edge of the spinal gray matter (Newton and Hamill 1988). In addition, axons containing NE in the vasculature may sprout into the injured cord (cf. McNicholas et al. 1980). Although the amount of 5-HT or NE from these sources are much lower than the original (2-12%), there is evidence that, with chronic spinal transection, spinal receptors caudal to the injury become supersensitive to residual monoamines such as 5-HT (Hains et al. 2002). If this supersensitivity is strong enough, then even very low levels of monoamines persisting after injury could maintain their original effects. Indeed, preliminary data in cats with chronic spinal cord injury have shown that, after the exaggerated reflexes have developed, intracellular recording from motoneurons indicated that bistable behavior recovered in these motoneurons (Eken et al. 1989), even after the abolishment of any sign of bistability in motoneurons after acute spinal cord injury (Hounsgaard et al. 1988). Recordings from motor unit in humans and animals after injury also suggested that some changes in intrinsic membrane properties of motoneurons have occurred after chronic injury, including sustained poorly regulated discharges, unusually low minimum firing

rates and generally inefficient control of firing rate in force production (Matthews 1996; Zijdewind and Thomas 2003, 2001).

Inhibitory effect of monoamines on the dorsal root reflexes

One remaining problem is that the activation of persistent inward currents is usually slow, whereas muscle spasms are activated even with a very brief stimulation. Interestingly, it has been found that, although excitatory to motoneurons, the monoamines are inhibitory to the dorsal horn. In large part, this inhibition is presynaptic and focused on sensory afferents that mediate both high and low threshold cutaneous input (Clarke et al. 2002) and high threshold muscle afferents (groups III, and IV) (Cleland and Rymer 1990; Jankowska 1992b; Miller et al. 1995). Therefore, after spinal cord injury, with decreased inhibition from 5-HT, the excitatory postsynaptic potentials (EPSPs) produced by dorsal root stimulation actually increased (Baker and Chandler 1987). In contrast to the gradual recovery of motoneuron excitability, this happens right after injury. This prolonged EPSP may play an important role in the activation of persistent inward current. In acute spinal cord injury, due to the loss of persistent inward currents in the motoneurons, no long-lasting reflexes could be activated. However, when a hemisection occurred in the dorsal half of the spinal cord, the increased EPSP and the preserved motoneuron excitability contribute to spasticity right after injury.

In summary, it is very likely that plateau potentials and associated PICs are re-activated in motoneurons after chronic spinal cord injury in motoneurons, which, in combination

with the dis-inhibited and thus prolonged EPSPs, contribute to the production of spasticity. To test this hypothesis, a new model of spasticity was employed in the present study.

NEW MODEL OF SPASTICITY

Part of the reason that it is so hard to study spasticity is that it is very difficult to replicate experimentally. Complete spinal cord transection in animals, such as cats, leads to good spasticity but makes it hard to maintain the animals in a healthy state. They require daily bladder expression, and bladder infection and pressure sores can be a chronic problem (Ashby and McCrea 1987; Naftchi et al. 1979). Although animals with incomplete spinal cord injury can be easily maintained, they only demonstrate mild hyperreflexia without prominent spasticity; thus they are even less favorable experimental models (Ashby and McCrea 1987; Hultborn and Malmsten 1983a).

Bennett et. al. (1999) have developed a new model for the study of spasticity, in which complete spinal cord injury is made in adult rats at the S_2 level of the spinal cord. The level S_2 was chosen because first of all, the locomotion and bowel/bladder functions are preserved at this injury level, making the animal easy to care for. Second, the cord below the level of the injury innervates mainly the tail, which is readily accessible to manipulate and record EMG from, and it closely resembles the muscular structure of the axonal muscles of the back in human beings. Third, histological study and electrical study have shown that, although the motoneurons may be slightly fewer in regions below S_2, the motoneuron size and electrical properties remain almost the same. Finally, and most importantly, the sacrocaudal part of the spinal cord is very small, so it can survive as a whole when maintained *in vitro*; thus, it has all the benefit of *in vitro* studies, such as controllable external environment and much more stable recording (Bennett et al. 1999).

For the first two weeks after injury, the affected tail is flaccid; no responses can be elicited anywhere on the tail except at the base, which is partly innervated by the S_1 root above the lesion site. At about two weeks, tonic muscle activity that flexes the tail ventrally emerges, usually triggered by cutaneous stimulation or muscle stretch. As time passes, the muscle tone in the affected tail markedly increases, and the threshold of the stretch and cutaneous evoked reflexes decreases. As a result, brief stimulation that normally does not induce activities in normal animals evokes long-lasting reflexes in these chronic spinal rats. These reflexes produce powerful whole tail contractions (spasms), so that the tail does not move in a smooth arch as in the normals, and it coils with jerky movements, with the tip often rotating more than 360 degrees. The tail spasticity grows progressively more severe over the months after injury, with increased involvement of extensor muscles. Thus, the development of spasticity in the rat tail muscles follows a similar time course to that in human limbs, suggesting similar underlying mechanisms (Bennett et al. 1999).

BRIEF SUMMARY OF OUR WORK

The main purpose of the present thesis is to study the ionic mechanisms underlying spasticity, using the animal model described above, recorded *in vitro*. We first verified that the long-lasting reflexes recorded *in vivo* that contributed to spasticity are reproducible when the whole sacrocaudal cord is removed and maintained *in vitro*, with similar threshold, duration and intensity (Li et al. 2004b). Then we recorded from the motoneurons intracellularly and proved that motoneurons recover their ability to activate PICs and associated plateau potentials after chronic spinal cord injury. These PICs cause the spastic long-lasting reflexes that play a major role in the production of spasticity (whereas no plateaus or long-lasting reflexes could be recorded in motoneurons of acute spinal rats) (Bennett et al. 2001b). To study the ionic mechanisms of the PICs underlying plateau potentials, we voltage-clamped the motoneurons and found that PICs are mediated by a low-threshold Cav1.3 L-type calcium current and a persistent sodium current (Li and Bennett 2003). Both currents contribute to the production of the spastic long-lasting reflexes in the chronic spinal rats, and each current, with its own specific dynamic characteristics, contributes to the unique firing behaviors of motoneurons after chronic spinal cord injury (Li et al. 2004a). Finally, to study how baclofen, a widely used anti-spasticity medicine, relieves spasticity, we examined its effect on the long-lasting reflexes and PIC activation in these chronic spinal rats, and demonstrated that baclofen relieves spasticity mainly by decreasing presynaptic neurotransmitter release (Li et al. 2004c).

REFERENCES

Alvarez F, Pearson J, Harrington D, Dewey D, Torbeck L, and Fyffe R. Distribution of 5-hydroxytryptamine-immunoreactive boutons on alpha- motoneurons in the lumbar spinal cord of adult cats. *J Comp Neurol* 393: 69-83, 1998.

Angstadt JD and Choo JJ. Sodium-dependent plateau potentials in cultured Retzius cells of the medicinal leech. *J Neurophysiol* 76: 1491-1502, 1996.

Ashby P and McCrea DA. Neurophysiology of spinal spasticity. In: *Handbook of the Spinal Cord*, edited by Davidoff RA. New York: Marcel Dekker Inc., 1987, p. 120-143.

Ashby P, Verrier M, and Lightfoot E. Segmental reflex pathways in spinal shock and spinal spasticity in man. *J Neurology, Neurosurgery, and Psychiatry* 37: 1352-1360, 1974.

Ashby P and Wiens M. Reciprocal inhibition following lesions of the spinal cord in man. *J Physiol* 414: 145-157, 1989.

Baker LL and Chandler SH. Characterization of postsynaptic potentials evoked by sural nerve stimulation in hindlimb motoneurons from acute and chronic spinal cats. *Brain Res* 420: 340-350, 1987.

Baldissera F, Hultborn H, and Illert M. Integration in spinal neuronal systems. In: *Handbook of Physiology. The Nervous system. Motor Control*, edited by VB B. Bethesda: American Physiological Society, 1981, p. 509-595.

Bennett DJ, Gorassini M, Fouad K, Sanelli L, Han Y, and Cheng J. Spasticity in rats with sacral spinal cord injury. *J Neurotrauma* 16: 69-84, 1999.

Bennett DJ, Li Y, and Siu M. Plateau potentials in sacrocaudal motoneurons of chronic spinal rats, recorded in vitro. *J Neurophysiol* 86: 1955-1971, 2001.

Björklund A and Skagerberg G. Descending monoaminergic projections to the spinal cord. In: *Brain Stem Control of Spinal Mechanisms*, edited by Sjolund B and Bjorklund A. Amsterdam: Elsevier Biomedical Press, 1982, p. 55-88.

Burke D, Gillies JD, and Lance JW. The quadriceps stretch reflex in human spasticity. *J Neurol Neurosurg Psychiatry* 33: 216-223, 1970.

Carlin KP, Jones KE, Jiang Z, Jordan LM, and Brownstone RM. Dendritic L-type calcium currents in mouse spinal motoneurons: implications for bistability. *Eur J Neurosci* 12: 1635-1646, 2000.

Clarke RW, Eves S, Harris J, Peachey JE, and Stuart E. Interactions between cutaneous afferent inputs to a withdrawal reflex in the decerebrated rabbit and their control by descending and segmental systems. In: *Neuroscience*, 2002, p. 555-571.

Cleland CL and Rymer WZ. Neural mechanisms underlying the clasp-knife reflex in tha cat. I. Characteristics of the reflex. In: *Journal of Neurophysiology*, 1990, p. 1303-1318.

Conway BA, Hultborn H, Kiehn O, and Mintz I. Plateau potentials in alpha-motoneurones induced by intravenous injection of L-dopa and clonidine in the spinal cat. *J Physiol* 405: 369-384, 1988.

Delwaide PJ. Electrophysiological testing of spastic patients: its potential usefulness and limitations. In: *Clinical neurophysiology in spasticity. Restorative neurology*, edited by Delwaide PJ and Young RR. Amsterdam: Elsevier, 1985, p. 186-203.

Delwaide PJ and Oliver E. Short-latency autogenic inhibition (IB inhibition) in human spasticity. *J Neurology, Neurosurgery, and Psychiatry* 51: 1546-1550, 1988.

Eken T, Hultborn H, and Kiehn O. Possible functions of transmitter-controlled plateau potentials in alpha motoneurones. *Prog Brain Res* 80: 257-267; discussion 239-242, 1989.

Elson RC and Selverston AI. Evidence for a persistent Na+ conductance in neurons of the gastric mill rhythm generator of spiny lobsters. *J Exp Biol* 200 (Pt 12): 1795-1807, 1997.

Giroux N, Rossignol S, and Reader TA. Autoradiographic study of alpha1- and alpha2-noradrenergic and serotonin1A receptors in the spinal cord of normal and chronically transected cats. *J Comp Neurol* 406: 402-414, 1999.

Hains BC, Everhart AW, Fullwood SD, and Hulsebosch CE. Changes in serotonin, serotonin transporter expression and serotonin denervation supersensitivity: involvement in chronic central pain after spinal hemisection in the rat. *Exp Neurol* 175: 347-362, 2002.

Hounsgaard J, Hultborn H, Jespersen B, and Kiehn O. Bistability of alpha-motoneurones in the decerebrate cat and in the acute spinal cat after intravenous 5-hydroxytryptophan. *J Physiol* 405: 345-367, 1988.

Hounsgaard J and Kiehn O. Serotonin-induced bistability of turtle motoneurones caused by a nifedipine-sensitive calcium plateau potential. *J Physiol* 414: 265-282, 1989.

Hsiao CF, Del Negro CA, Trueblood PR, and Chandler SH. Ionic basis for serotonin-induced bistable membrane properties in guinea pig trigeminal motoneurons. *J Neurophysiol* 79: 2847-2856, 1998.

Hultborn H and Malmsten J. Changes in segmental reflexes following chronic spinal cord hemisection in the cat. I. Increased monosynaptic and polysynaptic ventral root discharges. *Acta Physiol Scand* 119: 405-422, 1983a.

Hultborn H and Malmsten J. Changes in segmental reflexes following chronic spinal cord hemisection in the cat. II. Conditioned monosynaptic test reflexes. *Acta Physiol Scand* 119: 423-433, 1983b.

Jankowska E. Interneuronal relay in spinal pathways from proprioceptors. *Prog Neurobiol* 38: 335-378, 1992a.

Jankowska E. Interneuronal relay in spinal pathways from proprioceptors. In: *Progress in Neurobiology*, 1992b, p. 335-378.

Katz R, Pierrot-Deseilligny E, and Hultborn H. Recurrent inhibition of motoneurones prior to and during ramp and ballistic movements. *Neurosci Lett* 31: 141-145, 1982.

Kuhn RA and Macht MB. Some manifestations of reflex activity in spinal man with particular reference to the occurrence of extensor spasm. *Bull Johns Hopkins Hosp* 84: 43-75, 1948.

Lance JW and Burke D. Mechanisms of spasticity. *Arch Phys Med Rehabil* 55: 332-337, 1974.

Lee RH and Heckman CJ. Bistability in spinal motoneurons in vivo: systematic variations in persistent inward currents. *J Neurophysiol* 80: 583-593, 1998.

Levi R, Hultling C, and Seiger A. The Stockholm Spinal Cord Injury Study: 2. Associations between clinical patient characteristics and post-acute medical problems. *Paraplegia* 33: 585-594, 1995.

Li Y and Bennett DJ. Persistent sodium and calcium currents cause plateau potentials in motoneurons of chronic spinal rats. *J Neurophysiol* 90: 857-869, 2003.

Li Y, Gorassini MA, and Bennett DJ. Role of persistent sodium and calcium currents in motoneuron firing and spasticity in chronic spinal rats. *J Neurophysiology* 91: 767-783, 2004a.

Li Y, Harvey PJ, Li X, and Bennett DJ. Spastic long-lasting reflexes in the chronic spinal rat, studied *in vitro*. *J Neurophysiology* (in press), 2004b.

Li Y, Li X, Harvey PJ, and Bennett DJ. Effect of baclofen on spinal reflexes and persistent inward currents in motoneurons of acute and chronic spinal rats. *J Neurophysiology* (submitted), 2004c.

Little JW, Micklesen P, Umlauf R, and Britell C. Lower extremity manifestations of spasticity in chronic spinal cord injury. *Am J Phys Med Rehabil* 68: 32-36, 1989.

Matthews PB. Relationship of firing intervals of human motor units to the trajectory of post-spike after-hyperpolarization and synaptic noise. *J Physiol* 492 (Pt 2): 597-628, 1996.

Maxwell L, Maxwell D, Neilson M, and Kerr R. Confocal microscopic survey of serotoninergic axons in the lumbar spinal cord of the rat: co-localization with glutamate decarboxylase and neuropeptides. *Neuroscience* 75: 471-480, 1996.

McNicholas L, Martin W, Sloan J, and Nozaki M. Innervation of the spinal cord by sympathetic fibers. *Exp Neurol* 69, 1980.

Miller JF, Paul KD, Rymer WZ, and Heckman CJ. 5-HT1B/1D agonist CGS-12066B attenuates clasp knife reflex in the cat. In: *J. Neurophysiol.*, 1995, p. 453-456.

Mills JD and Pitman RM. Electrical properties of a cockroach motor neuron soma depend on different characteristics of individual Ca components. *J Neurophysiol* 78: 2455-2466, 1997.

Nacimiento W and Noth J. What, if anything, is spinal shock? *Arch Neurol* 56: 1033-1035, 1999.

Naftchi N, Schlosser W, and Horst W. Correlation of changes in the GABA-ergic system with the development of spasticity in paraplegic cats. *Adv Exp Med Biol*: 431-450, 1979.

Newton BW and Hamill RW. The morphology and distribution of rat serotoninergic intraspinal neurons: an immunohistochemical study. *Brain Res Bull* 20: 349-360, 1988.

Nielsen J, Petersen N, and Crone C. Changes in transmission across synapses of Ia afferents in spastic patients. *Brain* 118: 995-1004, 1995.

Noth J. Trends in the pathophysiology and pharmacotherapy of spasticity. *J Neurol* 238: 131-139, 1991.

Patel R, Kerr R, and Maxwell D. Absence of co-localized glutamic acid decarboxylase and neuropeptides in noradrenergic axons of the rat spinal cord. *Brain Res* 749: 164-169, 1997.

Perrier JF and Hounsgaard J. Ca(2+)-activated nonselective cationic current (I(CAN)) in turtle motoneurons. *J Neurophysiol* 82: 730-735, 1999.

Powers RK and Binder MD. Summation of effective synaptic currents and firing rate modulation in cat spinal motoneurons. *J Neurophysiol* 83: 483-500, 2000.

Powers RK, Campbell DL, and Rymer WZ. Stretch reflex dynamics in spastic elbow flexor muscles. *Ann Neurol* 25: 32-42, 1989.

Rekling JC and Feldman JL. Calcium-dependent plateau potentials in rostral ambiguus neurons in the newborn mouse brain stem in vitro. *J Neurophysiol* 78: 2483-2492, 1997.

Rekling JC and Laursen AM. Evidence for a persistent sodium conductance in neurons from the nucleus prepositus hypoglossi. *Brain Res* 500: 276-286, 1989.

Remy-Neris O, Barbeau H, Daniel O, Boiteau F, and Bussel B. Effects of intrathecal clonidine injection on spinal reflexes and human locomotion in incomplete paraplegic subjects. *Exp Brain Res* 129: 433-440, 1999.

Robert R and Young MD. Spasticity: a review. *Neurology* 44(Suppl 9): 12-20, 1994.

Sandler VM, Puil E, and Schwarz DW. Intrinsic response properties of bursting neurons in the nucleus principalis trigemini of the gerbil. *Neuroscience* 83: 891-904, 1998.

Schwindt PC and Crill WE. Amplification of synaptic current by persistent sodium conductance in apical dendrite of neocortical neurons. *J Neurophysiol* 74: 2220-2224, 1995.

Schwindt PC and Crill WE. Properties of a persistent inward current in normal and TEA-injected motoneurons. *J Neurophysiol* 43: 1700-1724, 1980.

Shapiro S. Neurotransmission by neurons that use serotonin, noradrenaline, glutamate, glycine, and gamma-aminobutyric acid in the normal and injured spinal cord. *Neurosurgery* 40: 168-176; discussion 177, 1997.

Stafstrom CE, Schwindt PC, and Crill WE. Negative slope conductance due to a persistent subthreshold sodium current in cat neocortical neurons in vitro. *Brain Res* 236: 221-226, 1982.

Svirskis G and Hounsgaard J. Transmitter regulation of plateau properties in turtle motoneurons. *J Neurophysiol* 79: 45-50, 1998.

Thilmann AF, Fellows SJ, and Garms E. The mechanism of spastic muscle hypertonus. Variation in reflex gain over the time course of spasticity. *Brain* 114 (Pt 1A): 233-244, 1991.

Voisin DL and Nagy F. Sustained L-type calcium currents in dissociated deep dorsal horn neurons of the rat: characteristics and modulation. *Neuroscience* 102: 461-472, 2001.

Westenbroek RE, Hoskins L, and Catterall WA. Localization of Ca2+ channel subtypes on rat spinal motor neurons, interneurons, and nerve terminals. *J Neurosci* 18: 6319-6330, 1998.

Xu W and Lipscombe D. Neuronal Ca(V)1.3alpha(1) L-type channels activate at relatively hyperpolarized membrane potentials and are incompletely inhibited by dihydropyridines. *J Neurosci* 21: 5944-5951, 2001.

Young RR. Spasticity: a review. *Neurol* 44: S12-S20, 1994.

Zhang B and Harris-Warrick RM. Calcium-dependent plateau potentials in a crab stomatogastric ganglion motor neuron. I. Calcium current and its modulation by serotonin. *J Neurophysiol* 74: 1929-1937, 1995.

Zijdewind I and Thomas CK. Motor unit firing during and after voluntary contractions of human thenar muscles weakened by spinal cord injury. *J Neurophysiol* 89: 2065-2071, 2003.

Zijdewind I and Thomas CK. Spontaneous motor unit behavior in human thenar muscles after spinal cord injury. *Muscle Nerve* 24: 952-962, 2001.

Chapter 2: Spastic long-lasting reflexes of the chronic spinal rats, studied *in vitro*

(Revised from Li et al. J. Neurophysiol. 91: 2236-2246, 2004)

INTRODUCTION

Spasticity that appears in the months following spinal cord injury involves a generalized syndrome of muscle hyperreflexia, clonus and hypertonus (Kuhn and Macht 1948; Young 1994). Though spasticity can severely impair residual motor function, it remains poorly understood and standard antispastic drugs are often not well tolerated by patients (Penn 1990). To date, the study of spasticity has been restricted to human or whole adult animal *in vivo* preparations (Ashby and McCrea 1987; Heckman 1994; Taylor et al. 1997), because spinal cord injury usually occurs in adults and spasticity can take months to be fully manifested. Thus, one purpose of this paper was to develop and validate a new *in vitro* preparation for the study of spasticity in adult rats, where the whole chronically injured adult spinal cord is explanted and maintained in artificial cerebral spinal fluid (ACSF). This enables full control of the extracellular environment, and thus detailed testing of the pharmacological basis of hyperreflexia associated with spasticity. To validate this *in vitro* preparation we have begun by quantifying the ventral root hyperreflexia seen *in vitro* to demonstrate that it is similar to the hyperreflexia seen in the corresponding awake rats (Bennett et al. 1999a; Bennett et al. 2003). Related intracellular motoneuron recordings are reported in Bennett et al. (2001c).

Recently, it is has been shown that a full spasticity syndrome develops in the tail musculature of rats about one month after a low spinal transection (at the S_2 sacral cord; chronic spinal state (Bennett et al. 1999a)). This tail spasticity is functionally relevant to spasticity after higher level injury in humans, because the anatomy, mechanics and

segmental control of tail muscles is similar to other proximal muscles, especially those of the axial muscles of the back and neck (Richmond and Loeb 1992; Richmond et al. 1992; Wada et al. 1994a; Wada et al. 1994b), which can have major spasms after spinal cord injury in humans (Stauffer 1974). Further, descending supraspinal and propriospinal innervation of the sacrocaudal spinal cord are similar to those at other spinal cord levels (Masson et al. 1991; Wada et al. 1993), and thus spinal cord injury has similar descending tract denervation. The hyperreflexia associated with tail spasticity has been quantified in the awake chronic spinal rat by examining the muscle reflexes (EMG) in response to stimulation of the caudal nerve trunk supplying the tail (Bennett et al. 1999a; Bennett et al. 2003). The hallmark of these spastic reflexes is the emergence of a *long-lasting reflex* that is evoked by low threshold afferent stimulation, facilitated by repeated stimulation, and mediates the flexor/extensor spasms seen in these chronic spinal rats.

An interesting aspect of this low spinal model of spasticity is that the affected sacrocaudal spinal cord is small enough that it should, in principle, survive whole when explanted and maintained *in vitro*. Indeed, Long et al. (1988) have shown that the sacrocaudal spinal cord of normal adult rat can survive *in vitro*, though they used a sagittal hemisection to improve oxygenation. In the current experiments we removed the whole sacrocaudal spinal cord of chronically injured adult rats, and examined the ventral root reflex responses to dorsal root stimulation, and compared these reflexes to those seen in the awake chronic spinal rat (Bennett et al. 1999a; Bennett et al. 2003). The results described in this paper indicate that the long-lasting reflexes were remarkably well preserved *in vitro*, compared to *in vivo*, with a similar threshold, duration and facilitation

with repetition. Interestingly, we found that it was important to study the whole sacrocaudal cord with minimal tissue cutting during the preparation process. For example, an additional sagittal hemisection (method used by Long et al. 1988) eliminated the long-lasting reflexes, suggesting an important involvement of the contralateral and/or midline circuitry in the long-lasting spastic reflexes.

One characteristic of the awake acute spinal rat (as opposed to chronic spinal rat) that we found difficult to replicate in the *in vitro* preparation was the facilitation of low-threshold long-lasting reflexes by vigorous cutaneous stimulation (Bennett et al. 2003), mainly because pure cutaneous stimulation is difficult to evoke from dorsal root stimulation *in vitro*. However, we did find that by raising the excitability of the reflexes by altering extracellular K^+ or Mg^{++} concentrations long-lasting reflexes appeared in the *in vitro* sacrocaudal cord of acute spinal rats (similar to the results of Long et al. 1988). Specific monoaminergic neuromodulators, such as NE or 5-HT, also facilitated the long-lasting reflexes in acute spinal rats. Interestingly, similar applications of monoaminergic neuromodulators in chronic spinal rats prolonged the already large long-lasting reflexes and had effects at much lower doses, suggesting major changes in sensitivity to these substances. Parts of this work have been presented in abstract form (Bennett et al. 1999b).

METHODS

The whole sacrocaudal spinal cord of adult female Sprague-Dawley rats (60 to 250 days old) was removed and studied in an *in vitro* recording apparatus (modified from Long et al. 1988). In the main experimental group, rats had a previous chronic transection at the S_2 sacral spinal level, 1 - 6 month before (transection made in adult rats at > 50 days of age). This produced pronounced spasticity in the tail musculature (chronic spinal group). See methods in Bennett et al. (1999a; 2003). The sacrocaudal spinal cord was removed by transecting above the previous chronic transection, so as not to re-injure the sacrocaudal cord (Fig. 1*A*). In control rats there was no previous injury and the transection during removal and preparation of the spinal cord was considered an acute injury (acute spinal group). All procedures were approved by the University of Alberta animal welfare committee.

Surgery

CORD REMOVAL. Chronic spinal and normal rats were deeply anesthetized with urethane (0.18 g / 100 g; maximum of 0.45 g per rat for rats over 250 g) and a T_{13}-L_6 dorsal laminectomy was performed to expose the lumbar and sacrocaudal spinal cord. The dura was opened and modified artificial cerebral spinal fluid (mACSF; at 21°C) was dripped liberally onto the cord for the remainder of the surgery. A suction line removed excess mACSF and blood. The rat was then given pure oxygen to breathe for about 5 mins with a mask, until the dorsal vein of the cord appeared hyper-oxygenated (bright red).

Following this, the carotids and jugular were cut to lower the blood pressure and minimize blood in the cord. The spinal cord was then quickly removed by cutting the sacrocaudal roots as they traversed the L_6 vertebra and then transecting the lumbar cord and gently lifting the cord caudally while cutting lumbar roots as they appeared. The cord was placed in a dissection dish containing oxygenated mACSF at 21°C. The rat was euthanized with a sodium pentobarbital overdose.

DISSECTION DISH. In the dissection dish, the long dorsal and ventral roots of the sacrocaudal cord were untangled, identified (see below) and cut to a manageable 1 - 2 cm length in preparation for stimulation and recording. The excess spinal cord was cut away by re-transecting the cord just rostral to the S_2 sacral spinal level (i.e. rostral to the chronic transection site). In some cases (not standard) the cord was also mid-sagittally hemisected (Long et al. 1988). The mACSF was changed to wash out the remaining urethane and tissue debris, and the cord was left to recover in the mACSF for 1 hour.

ROOT IDENTIFICATION AND PREPARATION. In pilot experiments (4 rats) we traced the roots deep into the sacrum to find their entry points to identify them and their relation to the anatomy of the cord. The caudal roots were tightly attached to the terminae fibrum of the cord, which was characterized by the pigtail-like anterior artery that adhered to it (attached root shown in top of Fig. 1*A*). Moving more rostrally, the first root that was *unattached* to the terminae fibrum was usually the S_4 sacral dorsal root (dorsal root arrow in Fig. 1*A*). Thus, during the standard preparation for an *in vitro* experiment this S_4 root was used as a landmark, and the two separate roots rostral to this were assumed to be S_3

and S_2 (not shown in Fig. 1*A* for simplicity, though S_2 lesion shown). The relatively large caudal dorsal root adhering to the terminae fibrum was gently teased free, at which point it was usually possible to find an extremely fine caudal ventral root, which was then also teased free. Both these caudal roots are in the text referred to as Ca_1, though they may also contain fibres from more caudal Ca_2, Ca_3, etc. roots. All the sacrocaudal dorsal roots are much larger in diameter than the ventral roots.

Though the sacral roots were unattached to the terminae fibrum, they adhered to the spinal cord for at least a segment before entering the dorsal horn (and for greater distances in older animals; > 4 months; not drawn in Fig. 1*A*). Because of their large size, they interfered with oxygenation of the dorsal sacrocaudal cord. Thus, these roots were gently teased away from the cord, and this procedure markedly increased the length of time for which the long-lasting polysynaptic reflexes were viable (from 1 hour to > 5 hours; see Results).

Recording chamber

After recovery in the dissection dish, the sacrocaudal cord was transferred to a recording chamber, and bathed with normal ACSF flowing at 4 - 6 ml/min and maintained at 24-25°C. The cord was usually placed on its lateral side with dorsal and ventral roots from one side upward, and easily accessible for recording. The chamber had a narrow channel (5.5 mm wide) to hold the spinal cord, and this channel opened at one end to form a wider but shallow area for holding the long roots before mounting them for recording. ACSF flowed by gravity into the narrow channel near the rostral end of the cord and

drained out through a wick placed in the wide shallow area near the end of the cord. The cord was held in place by pins at the rostral and caudal extremes, and supported on 2 layers of porous nappy paper pinned to a Sylgard bottom surface. The bottom of the narrow channel was angled to fit the tapering profile of the cord, and thus allowed the ACSF level to be maintained as shallow as possible. Thus the total chamber volume was 0.25 ml, giving 20 bath changes/min at the 5 ml/min flow rate.

Root stimulation and recording

Ventral and dorsal roots were mounted for monopolar recording and stimulation on up to 8 chlorided silver wires suspended just above the ACSF at the root entry points. The root was wrapped around the wire in the air and then quickly covered with a Vaseline/mineral oil mixture (1:1 by weight). Usually we mounted at least S_4, and Ca_1 dorsal and ventral roots on the left side of the cord, and then a further 4 roots from the remaining ipsilateral and contralateral roots. Three additional sliver wires were placed directly in the ACSF for the stimulation-return, monopolar recording reference and instrumentation ground.

Dorsal roots were stimulated with 0.1 ms current pulses, usually at 0.1 mA (about 10 x threshold; 10xT; T = 0.009 - 0.01 mA, as described below; Isoflex stimulator, AMPI, Isreal). The anode (+) was connected to the root and the cathode (-) to the nearby stimulation-return wire in the bath. Tests with stimulating one end of a root and recording the other end of the same root (see below) indicated that this simulation arrangement recruited the nerve effectively and did not cause any stray stimulation of nearby roots. Originally, we stimulated with the reverse polarity (cathode on the root and anode in

bath), but found that this produced some anodal block (above 2-5xT), which presumably occurred when the action potential propagated past the oil/water interface into the bath (which was positive). From the faster conduction times in our standard stimulation arrangement (anode on nerve), compared to the reverse polarity, we suppose that action potentials were initiated near the oil/water interface in our standard arrangement.

Ventral roots were recorded with a custom-built differential preamplifier (QT5), with one lead connected to the root and a second to the reference wire in the bath near the ventral roots. The root recordings were highpass filtered at 100 Hz, lowpass filtered at 3kHz, amplified by 5000x and sampled at 6 - 10 kHz (the latter with Axoscope, Axon Inst., USA). Dorsal root stimulation was repeated > 5 times with an inter-stimulation interval normally set at 20 sec to give multiple ventral root reflexes for averaging. Before each experiment we transferred a piece of unused dorsal root to the recording chamber and recorded one end while stimulating the other. This gave an estimate of the stimulation threshold (T; consistently 0.008 - 0.01 mA) and the conduction velocity (16-24 m/s at 25°C).

CSF and drug applications

The normal ACSF used in the recording chamber had a composition (in mM) of: 122 NaCl, 24 $NaHCO_3$, 3 KCl, 2.5 $CaCl_2$, 1 $MgSO_4$, 12 glucose mixed in distilled water (osmolatity of 298 mOsm). The ACSF was bubbled with 95% O_2 and 5% CO_2 to give a pH of 7.4. During dissection and recovery a modified ACSF (mACSF) was used to minimize neural and general metabolic activity. Originally, we made mACSF from

normal ACSF mixed with urethane (Long et al. 1988), but found that ACSF with NaCl replaced by sucrose (at equal osmolarity; 0 mM NaCl, 214 mM sucrose) or ACSF made with Kynurenic acid (a broad spectrum glutamate transmission blocker, Kekesi et al. 2002) worked better. The mACSF made with Kynurenic acid became our standard method and yielded the most healthy preparations; its composition was (in mM): 118 NaCl, 24 $NaHCO_3$, 1.5 $CaCl_2$, 3 KCl, 5 $MgCl_2$, 1.4 NaH_2PO_4, 1.3 $MgSO_4$, 25 D-glucose and 1 Kynurenic acid (note the low Ca^{++} and high Mg^{++}, to further reduce excitotoxicity). Ventral root reflex responses were tested in normal ACSF and during manipulations of the ACSF, including: removal of Mg^{++} (0 mM $MgCl_2$, 3.5 mM $CaCl_2$), increase in K^+ (7 mM KCl, 121 mM NaCl), and the addition of 5-HT, NE, L-DOPA, methoxamine or clonidine (Sigma, RBI). We added the later drugs in increasing doses to give cumulative concentration-response relations, with >15 mins between each dose for steady-state responses to be reached at each dose.

Data analysis

Ventral root reflexes were quantified using custom software written in Matlab (Mathworks, USA). The data was highpass filtered at 800 Hz (1^{st} order filter), lowpass filtered at 3 kHz (4^{th} order Butterworth filter) and then rectified. The rectified data was averaged over a 100 – 1100 ms window post-stimulus to estimate the tonic long-lasting reflex, and over a 2 – 4 ms window to estimate the monosynaptic reflex. Background ventral root activity just before the stimulus was also averaged (in a 100 ms window). Such window averages were computed for each trial, and a grand mean and standard deviation was computed across trials for each reflex component (5 trials per average).

When there was no activity, the mean ventral root average was not zero, due to noise in the data that was rectified and thus not removed by averaging. This average noise signal was subtracted from all other measurements to remove its effect. In the text and Figures means ± standard deviations are shown. Statistical differences were computed with a Student t-test at the 95% confidence level.

RESULTS

Acute spinal state

When the whole sacrocaudal spinal cord of normal rats was acutely transected and transferred to the *in vitro* recording chamber (transected at S_2 level), long-lasting ventral root reflexes were never observed, regardless of the dorsal root stimulation intensity or rate (n = 22 rats; Fig. 1*B*). There was at times a brief short-latency reflex in the most caudal roots (n = 7/22), including a small monosynaptic response (0.33 ± 0.42 mV; top arrow in Fig. 1*B*), which was significantly smaller than the monosynaptic reflex in chronic spinal rats, as described below. This is consistent with the relatively areflexic state seen in the tail of awake acute sacral spinal rats or normal intact rats (see Fig. 1 in Bennett et al. 2003).

Chronic spinal state

In contrast, the sacrocaudal spinal cord of chronic spinal rats (> 30 days after S_2 transection, Fig. 1*A*) had large and long-lasting ventral root reflexes in response to dorsal root stimulation when tested in normal ACSF (Figs. 1*C*, *D*; n = 30 rats). Again, this is consistent with the long-lasting reflexes seen in the tail muscles of awake chronic spinal rats (see Figs. 1*D,E* in Bennett et al. 2003). Further, the awake chronic spinal rats that were most spastic prior to *in vitro* testing (top spasticity rating in Bennett et al. 2003) always had larger *in vitro* ventral root reflexes, compared to less spastic rats.

The preservation of the long-lasting reflexes *in vitro* probably occurred because the spinal cord was relatively unaffected when transferred to the *in vitro* recording chamber as it was left whole and removed by cutting above the original transection. The main difference between the *in vivo* and the *in vitro* states was the temperature, which was 25°C in the latter. When the temperature was raised beyond 27°C, the reflexes disappeared irreversibly.

The reflexes generally increased and then stabilized in the first 30 min after transferring the sacrocaudal cord to the recording chamber, after which they remained stable for hours. Over time, the reflexes on the most rostral roots (S_3) disappeared first (after > 5 hours), presumably because of the poorer viability of the larger diameter spinal cord. Reflexes in more caudal roots lasted longer, for up to 18 hours, though they gradually diminished with time.

The long-lasting reflex response to Ca_1 dorsal root stimulation was always largest, compared to other dorsal root stimulation. Thus, we either stimulated the Ca_1 root by itself (Fig. 2; n = 67 roots tested from 19 rats) or the ipsilateral S_3, S_4 and Ca_1 dorsal roots together (Fig. 1, n = 52 roots from 14 rats), which in awake rats would be similar to stimulating the tip of the tail or the whole caudal nerve trunk respectively (Ca_1 innervates tip of the tail, Bennett et al. 2003). Either dorsal root stimulation arrangement evoked long-lasting reflexes in the Ca_1 and S_4 ventral roots (n = 99/117 roots), and occasionally in S_3 roots (n = 13/32). The reflexes lasted for on average 2.1 ± 0.47 seconds (Fig. 1*D*) and had similar components to those in the awake rat (Bennett et al. 2003): *i,* a short

latency initial peak, including a major polysynaptic component (double arrow in Fig. 1*C*); *ii*, a 50 ms pause in activity following the initial peak; and *iii*, a long-lasting tonic component (Fig. 1*C*, *D*). The tonic component of the long-lasting reflex was quantified by averaging the rectified reflexes over a 1 sec window, starting 100 ms after the stimulus (see Methods and Figs. 2-4) and is the main focus of this paper (term spastic long-lasting reflex).

The one clear difference to the awake rat was that there was often a substantial monosynaptic component to the reflex recorded *in vitro* (mean 1.9 ± 0.91 mV; Fig. 1*C*, single arrow; see also Fig. 5*B* described below), whereas in the awake rat the monosynaptic reflex was small or absent (Bennett et al. 2003). The larger monosynaptic reflex might have been a result of the lower temperature, which is known to enhance synaptic transmission (Barron and Matthews 1938; Brooks et al. 1955; Pierau et al. 1976). The monosynaptic reflex recorded *in vitro* was significantly larger in chronic spinal rats than in acute spinal rats (1.9 mV compared to 0.33 mV, as detailed above).

REFLEX THRESHOLD. The long-lasting reflex in the *in vitro* chronic spinal preparation was of very low threshold, and thus in part mediated by group I muscle afferents or Aβ skin afferents, as in the awake rat (Bennett et al. 2003). That is, it could be evoked by stimuli just above afferent threshold (which was 0.008 - 0.01mA; n = 20/20 roots pairs tested at threshold; Fig. 2*B* and top left of Fig. 2*A*). Likewise, the monosynaptic reflex was of low threshold (Fig. 2*C*). In most ventral roots, the long-lasting reflex got significantly larger with increasing stimulus intensity (up to about 20xT; n = 16/20; Fig. 2*A*, and solid

symbols in Fig. 2*B*, group means, normalized to the maximum reflex, %max), and thus was also in part due to higher threshold afferents. In other roots high threshold afferent stimulation had an inhibitory effect (n = 4/20), with the long-lasting reflex decreasing with intensities above 5xT (example shown in Fig. 2*B*, open symbols).

ENHANCEMENT OF REFLEX WITH REPETITION. Like in the awake rat (Bennett et al. 2003), the *in vitro* ventral root reflexes were enhanced by repeated stimulation (n = 36/39 roots tested). A two second interval was used to test this effect, since it produced the maximal enhancement in the awake rat, and the reflexes usually lasted for about 2 seconds, allowing interactions between successive stimuli (Fig. 3*A*). The long-lasting component built up in amplitude and duration with repetition (Fig. 3*A*,*C*), although there was considerable variability in the responses (e.g. second pulse in Fig. 3*A*). In contrast, the monosynaptic component was always depressed by this repeated simulation (Fig. 3*B*,*D*), consistent with the effects of rate-depression and associated presynaptic mechanisms (Thompson et al. 1998). Rate-depression of the monosynaptic reflexes also occurred in the acute spinal rat (not shown). A longer interval of 20 sec produced no significant interactions between reflexes (neither monosynaptic nor long-lasting components; not shown).

Reflexes evoked by stimulation trains

Recently, we have shown that motoneurons of chronic spinals rats have pronounced persistent inward currents (PICs; sodium and calcium currents) that amplify the synaptic currents and prolong the motoneuron discharge and ultimately produce the long-lasting

reflexes in the present sacrocaudal preparation (see Discussion and Bennett et al. 2001c; Li and Bennett 2003; Li et al. 2003). However, because these PICs are only slowly activated, short stimuli, such as from a single dorsal root stimulation pulse, should not be as effective as longer stimuli in evoking PICs that produce long-lasting reflexes (Li and Bennett 2003; Li et al. 2003). Therefore we also examined the responses to 0.5 sec long 100 Hz stimulation trains at primary afferent intensity (1.5xT). In all cases stimulation trains evoked significantly longer duration responses (6.0 ± 2.8 sec; Fig. 4*A*) than the responses to single shocks (2.1 ± 0.47 sec; Fig. 4*C*; n = 37 roots tested; note that Fig. 4*B* is an expanded copy of Fig. 4*A*, on the same time scale as Fig. 4*C*). Further, these long-lasting responses to stimulation trains were more robust than the single pulse responses, in that they occurred more reliably in all ventral roots (including S_3), they were often largest at the lowest stimulation threshold (compare Fig. 4*B* and E) and they continued to occur for longer periods as the preparation deteriorated (at > 5 hours). Also, they were more resistant to pharmacological manipulations, as described below.

Interestingly, a brief low threshold stimulation train (0.5 sec) at times triggered two or more long lasting bursts of activity (1 - 10 sec each; two bursts shown in Fig. 4*A*; n = 10/37 roots), similar to the repeated spasms seen in awake chronic spinal rats (compare to Fig. 5 of Bennett et al. 2003). Likely this occurred because these stimulation trains mimicked the large afferent barrage that occurred during the mechanical stimulation that was used to evoke spasms in the awake rat (Bennett et al. 1999a; Bennett et al. 2003). This spasm-like activity was usually irregular, though there was at times rhythmic activity that occurred reciprocally in left and right roots (not shown). Spasm-like bursting

could also be evoked with higher threshold stimulation (10xT; n = 12/37; Fig. 4*D*). Longer duration trains (2 sec) were also effective, though very long stimuli (7 sec) often produced inhibition of ongoing activity (not shown). Stimulation trains never evoked long-lasting activity in acute spinal rats, regardless of the intensity or duration.

Contralateral long-lasting reflexes

The standard single dorsal root stimulation pulse also evoked long-lasting reflexes in the contralateral ventral roots (Fig. 5*C*; n = 28/30 rats). These contralateral reflexes were in most respects identical to those on the ipsilateral side (Fig. 5*A*): they had a short latency polysynaptic component (Fig. 5*D*) and they were low threshold, enhanced with repetition, and altered by neuromodulators (see below). However, there was never a monosynaptic component in contralateral ventral root responses (Fig. 5*D*). Interestingly, the contralateral long-lasting reflexes (Fig. 5*C*) were significantly larger than the ipsilateral reflexes (Fig. 5*A*), with a given dorsal root stimulation (23 ± 16 % increase). Likewise, a given ventral root responded with a significantly larger long-lasting reflex response to its contralateral dorsal root stimulation (Fig. 5*E*,*H*), compared to its corresponding ipsilateral dorsal root (Figs. 5*F*,*G*; n = 56 root pairs tested). These crossed reflexes were reciprocally organized, since stimulating both ipsi- and contra-lateral dorsal roots together gave a smaller response compared to individually (n = 4/4; not shown). This crossed reciprocal organization functionally corresponds to the withdrawal reflexes seen in the awake chronic spinal rat, where the tail is flexed away from a cutaneous contact (Bennett et al. 2001a).

Lesions and localization of neurons involved in long-lasting reflex

The importance of the contralateral side of the spinal cord in the long-lasting reflexes was also made clear from lesion experiments. After the contralateral side was removed by a midsagittal hemisection (half the cord removed while cord in mACSF), the long-lasting reflexes on the remaining ipsilateral roots were eliminated (n = 10/10 rats). In contrast, this sagittal hemisection caused a significant increase in the monosynaptic reflex (Harvey et al. 1999), so at least we know that the ipsilateral primary afferents and motoneurons were not injured by this procedure.

Other lesions also reduced or eliminated the long-lasting reflexes in chronic spinal rats. For example, minor injury to the dorsal cord during removal of the dorsal vein and attached pia (which we only did in initial trials to improve oxygenation) resulted in a preparation with weak long-lasting reflexes, even though the awake rat was initially very spastic (n = 3 rats). Thus, the dorsal surface of the cord is important for the reflexes, and this is consistent with the additional finding that leaving the large sacral dorsal roots attached over the dorsolateral funiculus greatly reduced the long-lasting reflexes, presumably through interfering with oxygenation (see Methods). Slightly stretching the caudal end of the cord during preparation, likewise could reduce or eliminate the reflexes (n = 5 rats). In contrast, complete transections at the S_3 level, below the chronic S_2 lesion did not disrupt the long-lasting reflexes (n = 3 rats). Thus, it appears that the contralateral, dorsal and caudal portions of the cord are minimally essential for the production of long-lasting reflexes.

Facilitation of reflexes in acute spinal rat

In the awake acute spinal rat some sustained reflex activity could be evoked in the tail muscles by high-threshold cutaneous/nociceptive afferent stimulation of the tip of the tail, and this could be used as a conditioning stimulation to facilitate the low-threshold, long-lasting reflexes (Bennett et al. 2003). In contrast, in the *in vitro* preparation sustained ventral root activity could never be evoked in the acute spinal preparation, perhaps because it was not feasible to likewise selectively stimulate the cutaneous afferents. However, we found that the low-threshold, long-lasting reflexes could be facilitated *in vitro* in acute spinal rats by pharmacological means. For example, simply raising the K^+ to 7 mM (to generally depolarize cells and lower K^+ currents) enabled long-lasting reflexes (n = 5; Fig. 6*B*), though these reflexes were significantly smaller and shorter than in the chronic spinal rat (see Fig. 6*F*; compare time scales in Fig. 6 and 7), and usually only in the caudal roots. Likewise, increasing neuronal excitability, by lowering the Mg^{++} also enabled a similar long-lasting reflex (n = 10; Fig. 6*C*; at times in all ventral roots, S_3-Ca_1), consistent with Long et al. (1988). However, again these reflexes were significantly smaller than in the chronic spinal rat (Fig. 6*F*).

The neuromodulatory transmitters 5-HT (20 – 100 μM; n = 10) and NE (20 – 100 μM; n = 5), and associated agonist methoxamine (10 – 30 μM; n = 6), could at times facilitate the long-lasting reflexes in acute spinal rats, analogously to the facilitation of the long-lasting flexor reflex afferent (FRA) responses in the acute spinal cat by monoamines (L-DOPA, Jankowska et al. 1967). However, these reflexes were variable and required large doses (Fig. 6*D*,*E*), in comparison to in chronic spinal rats. That is, 5-HT had no effect at

doses below 20 to 30 μM, and above this dose there were long-lasting reflexes though much smaller than in the chronic spinal rat (20 – 100 μM; Fig. 6*D*,*F*). These high doses usually evoked brief periods of spontaneous ventral root discharges (lasting about 5 mins, just after the application of 5-HT), and the long-lasting reflexes were still small during this spontaneous activity (Fig. 6*D*). Likewise, NE only facilitated long-lasting reflexes and spontaneous activity at high doses (20 - 100 μM). Furthermore, these reflexes could only be evoked by stimulation trains (Fig. 6*E*) and the single stimulation pulses never gave a long-lasting reflex (Fig. 6*F*).

Facilitation of reflexes activity in chronic spinal rat

In the chronic spinal rat the long-lasting reflexes were significantly increased in duration by raising the K^+ to 7 mM (compare Figs. 7*A* and *B*), though the reflex amplitude measured in the first second of activity was not significantly increased (Fig. 7*F*; n = 7 roots tested). Interestingly, with high K^+ the reflex responses to a single stimuli fluctuated markedly (Fig. 7*B*), with repeated spasm-like activity, as was seen in the awake rat, and as also seen with 100 Hz stimulation trains (see above). When the excitability was raised by lowering the Mg^{++}, the long-lasting reflex duration was likewise increased (Fig. 7*C*), and in this case the reflex amplitude was also significantly increased (Fig. 7*F*; n = 8).

The neuromodulatory transmitters 5-HT and NE also altered the long-lasting reflexes (Figs. 7*D*,*E*), though with a complex concentration dependence (Figs. 8 & 9; n = 13 and 12 roots tested with 5- HT and NE respectively; L-DOPA acted similarly to NE, not shown). The chronic spinal rat was much more sensitive to these substances than the

acute spinal rat, with enhanced reflexes at concentration orders of magnitude lower than the doses to evoke activity in acute spinal rats (0.1 - 1 μM; compare Figs. 6 and 7). With this low concentration of 5-HT or NE the long-lasting reflex to a *single* pulse was significantly increased in amplitude (67%; Fig. 7F; see solid circles in Fig. 9*A*,*B*) and duration (54%, Fig. 8C). Likewise, the long-lasting reflex responses to a stimulation train were significantly increased in amplitude and duration (Fig. 8*D*, see open circles in Fig. 9*A*,*B*). In contrast, the monosynaptic was not increased (see squares in Fig. 9*A*,*B*).

Paradoxically, when higher doses were used in the chronic spinal rat (10 - 30 μM NE), the long-lasting reflex to a *single* dorsal root stimulus was reduced, and often nearly eliminated (Fig. 8*F* and Fig. 9*A*,*B*, *solid* circles). This high dose of NE (or 5-HT) evoked long periods of spontaneous activity (5 – 10 mins), usually shortly after application (Fig. 8*E*). However, the reflexes were still inhibited during this activity (at arrow in Fig. 8*E*), and even when this activity had subsided the reflexes remained lowered (Fig. 8*F*). The monosynaptic reflexes were not blocked by high doses, though they were somewhat reduced in 30 μM NE (Fig. 9*B*, squares). Furthermore, the associated long-lasting responses to a stimulation train were also not blocked by high doses of 5-HT or NE (no inhibition at high doses Fig. 8*G* compared to 8*B*), and instead were significantly larger than control levels at all doses at or above 0.1 μM (Fig. 9*A*,*B*, open circles; see Discussion). Washout of these drugs took long periods to reverse the changes in reflexes (> 1 hr) and was thus unreliable.

The α_1-adreneric receptor agonist methoxamine facilitated the long-lasting reflex to a single dorsal root pulse at all doses (n = 6 root pairs tested), in both duration (to 18.6 ± 11 from 2.1 ± 0.5 sec; significant increase) and amplitude (Fig. 9*C*, solid circles; amplitude change not significant, due to high variability), consistent with its action on facilitating PICs on motoneurons (see Discussion). No high dose inhibition was seen, unlike with NE. Further, methoxamine had no inhibitory effect on the monosynaptic reflex (squares), and markedly facilitated the long-lasting response to a 100 Hz stimulation train (Fig. 9*C*, open circles; significant increase).

In contrast, at very low doses the α_2-adrenergic receptor agonist clonidine significantly reduced the long-lasting response to a single stimulation pulse (0.03 μM; n = 8 roots tested) and at higher doses (≤0.1 μM) eliminated the reflex in most ventral roots tested (n = 6/8 roots; Fig. 9*D*, solid circles), consistent with its action on blocking polysynaptic reflexes (see Discussion). All doses of clonidine only marginally reduced the monosynaptic reflex (only significant reduction at 0.1 dose in Fig. 9*D*, squares), and did not significantly reduce the long-lasting response to a stimulation train (Fig. 9*D*, open circles), with a moderate increase in this train-evoked reflex at the highest dose (Fig. 9*D*).

DISCUSSION

We have shown that the hyperreflexic state of the sacrocaudal spinal cord in awake chronic spinal rats (*in vivo*) persists when the whole cord is explanted and maintained *in vitro* in oxygenated artificial CSF. In particular this is the first demonstration that the low threshold, long-lasting reflexes, which are the hallmark of spasticity in this and other types of spinal cord injury (i.e., spasms and spastic stretch reflexes, Bennett et al. 1999a; Bennett et al. 2003; Burke et al. 1970b; Kuhn and Macht 1948; Noth 1991; Powers et al. 1989) can be seen in vitro with ventral root recordings and dorsal root stimulation. With this new preparation we have provided evidence that the long-lasting reflexes in these spastic rats are enhanced by neuromodulators such as 5-HT, and have a major contralateral component. The mechanisms for these results are discussed further below. First, however, we will summarize the close parallels between the reflexes in the *in vivo* and *in vitro* preparations, and thus help validate the study of spinal cord injury and spasticity using this *in vitro* method, despite the many arbitrary factors of *in vitro* preparations such as ACSF composition, osmolarity, pH, tissue oxygenation, temperature, etc (Jiang et al. 1991; Kerkut and Bagust 1995).

Comparison of in vivo and in vitro reflexes

The ventral root reflexes to dorsal root stimulation in the *in vitro* sacrocaudal spinal cord are very similar to the tail muscle reflexes seen with stimulation of the caudal nerve trunk of the tail in the awake rat, including their: long duration, detailed reflex components (short latency initial peak, pause, and tonic discharge), involvement of the lowest

threshold afferents, particular sensitivity to the most caudal tail afferents and enhancement with repeated stimulation (Bennett et al. 2003). Likewise, in the acute spinal state the reflexes recorded *in vitro* and *in vivo* are similar in that they are small and of short duration, and in these preparations long-lasting reflexes can be facilitated by strong cutaneous stimulation or drug applications to enhance the excitability of the spinal cord. The one clear difference in the reflexes recorded *in vitro* is the presence of a moderately large monosynaptic reflex, not usually seen in the tail muscle responses of awake rats (Bennett et al. 2003). This may be related to the lower temperature required for tissue survival *in vitro* (25°C), which is known to increase synaptic transmission (Barron and Matthews 1938; Brooks et al. 1955; Pierau et al. 1976), though many other factors might increase the monosynaptic reflex in the sacrocaudal spinal cord, including damage to the contralateral or midline parts of the spinal cord (see Results and Harvey et al. 1999).

Because the sacrocaudal cord mediating these reflexes in chronic spinal rats is at the end of the neural axis (Fig. 1*A*), it can be removed and transferred to a recording chamber without any additional injury to the cord, which most likely assures that the long-lasting reflexes to dorsal root stimulation are well preserved. Indeed, when additional injury is deliberately made to the dorsal, contralateral or caudal cord (e.g. hemisection), then the long-lasting reflexes are eliminated.

Role of contralateral spinal cord in spasticity

We had not anticipated the large contralateral reflexes seen in the *in vitro* preparation, though in retrospect, this was a mistake, due to the special anatomy and function of the sacrocaudal spinal cord (Jankowska et al. 1978; Ritz et al. 1991; Ritz et al. 1989; Ritz et al. 2001). There is crossed segmental reflex control in the sacral cord, not seen at higher spinal segments, including: crossed disynaptic inhibition, crossed monosynaptic excitation from Ia afferents and even crossed presynaptic inhibition of afferents (Akatani et al. 2002; Harvey et al. 1999; Jankowska et al. 1978; Wada and Shikaki 1999). Functionally, motoneurons to muscles on both sides of the tail must at times be reciprocally coordinated and at others cocontracted, as we have observed (Fig. 5), because the tail acts as a single axial appendage. For example, the muscles on the left side of the tail are activated to withdraw the tail from a noxious stimulation on the right side, whereas left and right ventral tail muscles are co-contracted to flex the tail down away from a dorsal stimulation, and both these responses occur in the chronic spinal rat (Bennett et al. 2001a). The finding that ablation of the contralateral cord, by sagittal hemisection, eliminates the long-lasting spastic reflexes further stresses the importance of crossed or midline circuitry in spasticity of axial musculature.

Neuromodulatory control over the long-lasting spastic reflex

Following chronic spinal cord injury there are major changes in the neuronal excitability of the spinal cord caudal to the injury, which ultimately lead to long-lasting spastic reflexes (Bennett et al. 2001c; Li and Bennett 2003; Li et al. 2003). In particular, motoneurons exhibit a marked increase in excitability, as a result of the emergence of large voltage-gated persistent inward currents (PICs, Li and Bennett 2003), not seen in

acute spinal rats. These PICs are regeneratively activated once a critical depolarization of the motoneuron occurs, and produce subthreshold plateau potentials and self-sustained firing that ultimately cause the many second long, portion of the long-lasting reflex (Fig. 10 of Li et al. 2003). However, because these PICs have relatively slow kinetics, they are only activated by moderately long depolarizations (0.1 - 1 sec, depending on amplitude, Bennett et al. 2001c, Li and Bennett, 2003). Short depolarizations, such as from a monosynaptic EPSP, are not sufficient to evoke full PICs or associated long-lasting reflexes. However, repeated high frequency stimulation (100 Hz, 0.5 sec trains) summates both short and long EPSPs, and these stimulation trains are particularly effective in evoking PICs and long-lasting reflexes (Bennett et al. 2001b; Li et al. 2003). This is consistent with the very large train-evoked long-lasting reflexes described in the Results, and the facilitation of the train evoked reflexes by methoxamine, clonidine, NE and 5-HT, all of which facilitate PICs/plateaus (Hounsgaard and Kiehn 1989; Lee and Heckman 1999).

Oddly enough, a single stimulation pulse to the caudal dorsal roots can activate PICs and a corresponding long-lasting reflex in chronic spinal rats (Bennett et al. 2001c; Li et al. 2003), despite the slow activation of PICs. This occurs because caudal dorsal root stimulation evokes a relatively prolonged polysynaptic EPSP (pEPSP; 0.5 sec long) that can be seen when the PICs are blocked either pharmacologically or by hyperpolarization (Li et al. 2003). This pEPSP is sufficiently long to trigger the PICs in motoneurons of chronic spinal rats, and thus triggers a many second long-lasting reflex response. Thus, long-lasting reflexes triggered by a single stimulation shock require both pEPSPs and

motoneuron PICs, whereas long-lasting reflexes triggered by a stimulation train do not require a pEPSP and only require PICs and a short EPSP that will summate. Therefore, the present finding that the $\alpha 2$ agonist clonidine (or high dose NE or 5-HT) blocks the long-lasting response to a single stimulation shock, but not a stimulation train, suggests that clonidine likely inhibits the pEPSP that triggers the PICs and long-lasting reflex, consistent with its known inhibitory action on polysynaptic pathways (Chau et al. 1998) (Stone et al. 1998) and lack of inhibitory action on motoneuron plateaus/PICs (Conway et al. 1988). Clonidine does not block the monosynaptic reflex and facilitates PICs/plateaus (Conway et al. 1988), and thus in the presence of clonidine a stimulation train still produces a prolonged synaptic excitation that likely activates a PIC and long-lasting reflex. In contrast, the $\alpha 1$ agonist methoxamine likely does not block the pEPSP, since it does not inhibit the single dorsal root response, and instead enhances it, likely by enhancing the PICs.

Supersensitivity to monoamines in chronic compared to acute spinal rats

The concentration of 5-HT and NE required to facilitate the long-lasting reflexes in acute spinal rats were 100 times more than those in chronic spinal rats, and thus there is a remarkable supersensitivity to monoamines that occurs with long-term injury, as previously reported (Barbeau and Bedard 1981). The long-lasting reflexes induced by these monoamines in acute spinal rats likely resulted from induction of PICs (Bennett et al. 2001c), though apparently a higher dose was required in acute compared to chronic spinal rats to affect the PICs. In acute spinal cats, the noradrenergic precursor L-DOPA

likewise evokes late, long-lasting reflexes (FRA reflexes, Jankowska et al. 1967) and these are in part mediated by PICs/plateau potentials on motoneurons (Hounsgaard et al. 1988).

Summary and functional implications

Our results demonstrate that the long-lasting spastic reflex that emerges following spinal cord injury can be studied *in vitro* in the sacrocaudal cord; and thus, this preparation enables the detailed study of the pharmacological basis for spasticity, and ultimately can be used to develop and test new antispastic drugs. So far we have shown that the long-lasting spastic reflexes depend critically on the spontaneous emergence of plateau potentials (Bennett et al. 2001a,c) and associated PICs in motoneurons (L-type Ca^{++} and persistent Na^{+} currents; Li and Bennett, 2003), and emergence of polysynatpic EPSPs that are sufficiently long to activate PICs (Li et al. 2003). Furthermore, bath application of 5-HT, NE or the α_1-adrenergic receptor agonist methoxamine enhance the long-lasting reflexes at unusually low doses (supersensitivity, Figs. 7 – 9), perhaps due to a facilitation of plateaus/PICs.

Following complete spinal transection, 5-HT and NE levels below the injury are much reduced, but not eliminated (Newton and Hamill 1988), and thus may still play a major role in spasticity, given the pronounced supersensitivity to these neuromodulators (see above). Further, in incomplete spinal cord injured patients, NE and 5-HT derived from spared descending pathways could further modulate spasticity, and may thus in part explain the high variability of spastic reflexes in patients with spinal cord injury and

observation that incomplete injury can produce a more exaggerated spastic syndrome. We have found that the neuromodulators 5-HT and NE can both facilitate and inhibit the long-lasting reflexes depending on the dose, with inhibition likely being mediated by a block of pEPSPs. Importantly, this inhibition can be mimicked by the α_2-adrenergic receptor agonist clonidine, and thus the antispastic action of clonidine (Anderson et al. 1982) or related drugs such as tizanidine (Nance et al. 1997) may be to block these polysynaptic pathways.

TABLE

Ventral root reflexes	Acute spinal rats	Chronic spinal rats
Monosynaptic reflex:		
Amplitude	0.33 ± 0.42 mV	1.9 ± 0.91 mV*
Threshold	Low threshold	Low threshold
Effect of stimulus repetition	Reduction	Reduction
Contralateral stimulation	No reflex	No reflex
Contralateral lesion	Reflex enhanced	Reflex enhanced
Long-lasting reflex:		
Threshold	No long-lasting reflex	Low threshold
Duration	N/A	2.1 ± 0.47 sec*
Effect of stimulus repetition	N/A	Enhancement
Contralateral stimulation	N/A	23 ± 16 % increase*
Contralateral lesion	N/A	Reflex eliminated

TABLE 2-1. SUMMARY OF REFLEXES IN ACUTE AND CHRONIC SPINAL RATS.

Reflex response recorded in ventral roots in response to a single ipsilateral dorsal root stimulation pulse. A * indicates significant difference from acute spinal, or significant increase with contralateral instead of ipsilateral stimulation. All reflexes were evoked near afferent threshold and indicated as 'low threshold'. The contralateral lesion was a complete removal of the contralateral cord.

FIGURES

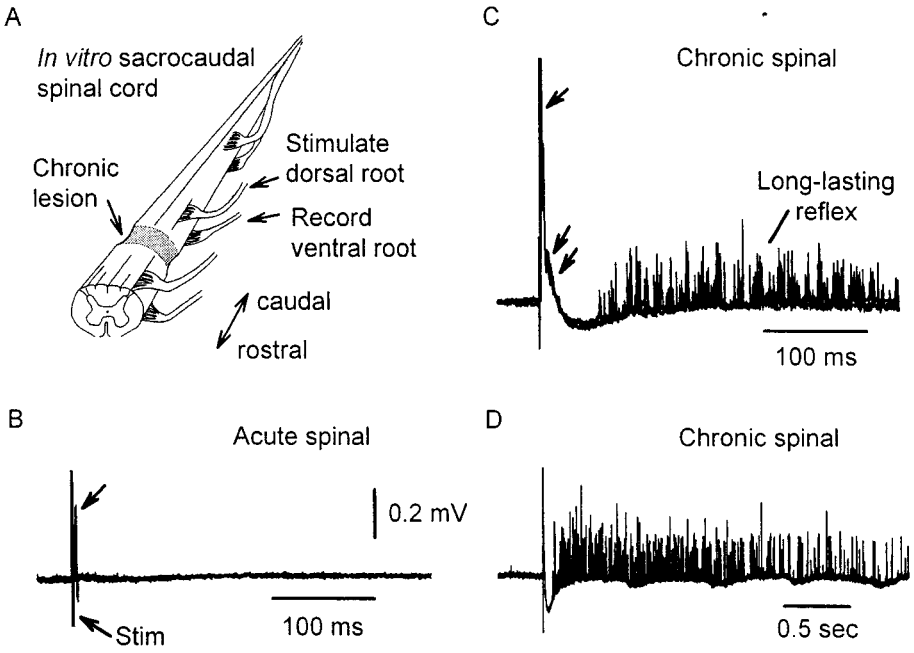

FIGURE 2-1. LONG-LASTING REFLEXES IN THE IN VITRO SACROCAUDAL SPINAL CORD.

A: schematic of chronically transected sacrocaudal spinal cord (S_2 lesion), with example dorsal and ventral roots used for reflex testing (not all roots shown). B: the S_4 ventral root response to ipsilateral dorsal root stimulation in an acute spinal rat (S_3-Ca_1 dorsal roots stimulated together with single pulse; 0.1 ms, 0.1 mA, 0.05 Hz; 3 overlaid sweeps). Note the small monosynaptic reflex (upper arrow) just after stimulus artefact. C: long-lasting S_4 ventral root reflex response to dorsal root stimulation in a chronic spinal rat (62 days post lesion, same stimulus as in B). Single and double arrows indicate monosynaptic and short latency polysynaptic reflexes respectively. Note the long-lasting reflex. D:

same as C, but on longer time scale. Normal ACSF, with no drug applications as also in Figs. 2- 5.

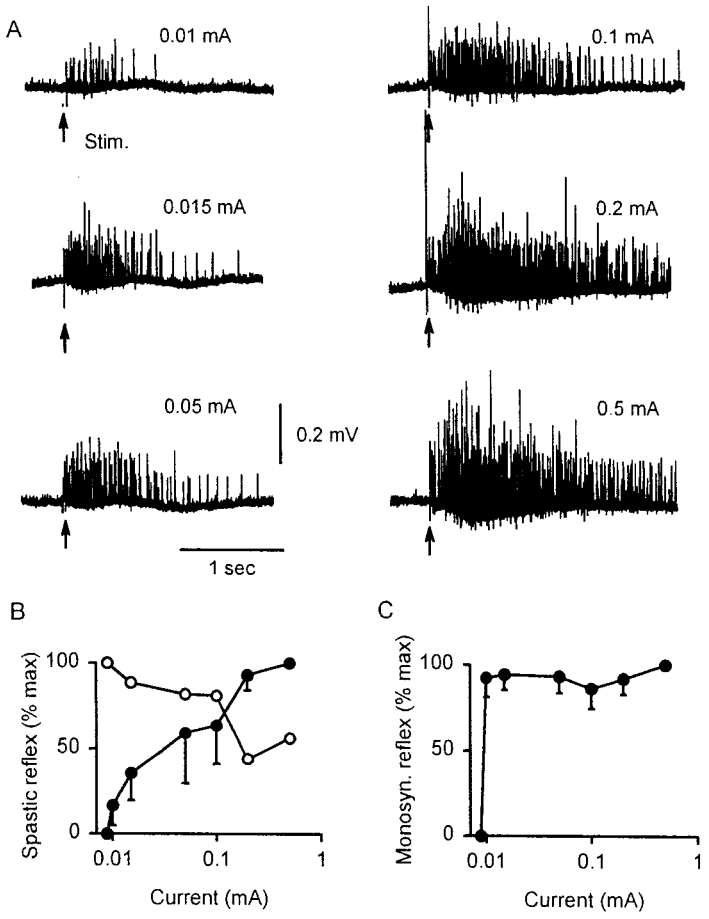
A
0.01 mA
Stim.
0.015 mA
0.05 mA
0.1 mA
0.2 mA
0.5 mA
0.2 mV
1 sec
B
Spastic reflex (% max)
100
50
0
0.01
0.1
1
Current (mA)
C
Monosyn. reflex (% max)
100
50
0
0.01
0.1
1
Current (mA)

FIGURE 2-2. EFFECT OF STIMULUS INTENSITY ON LONG-LASTING REFLEX IN CHRONIC SPINAL RATS.

A: long-lasting Ca_1 ventral root responses to single Ca_1 dorsal root stimuli at varying intensities relative to afferent threshold (T = 0.009 mA). Note that the reflex persisted even near threshold (0.01 mA, 1.1xT), but was larger and longer for higher intensities (up to 50xT). B: solid symbol, group mean long-lasting reflex amplitude as a function of stimulus intensity (n = 20). Open symbol, example of ventral root reflex decreasing with stimulus intensity, unlike the group mean (not included in mean, Ca_1 root). C: mean monosynaptic response amplitudes (n = 20). Reflexes in B and C are normalized to the maximum response in each root. Error bars indicate standard deviations, as in all Figures.

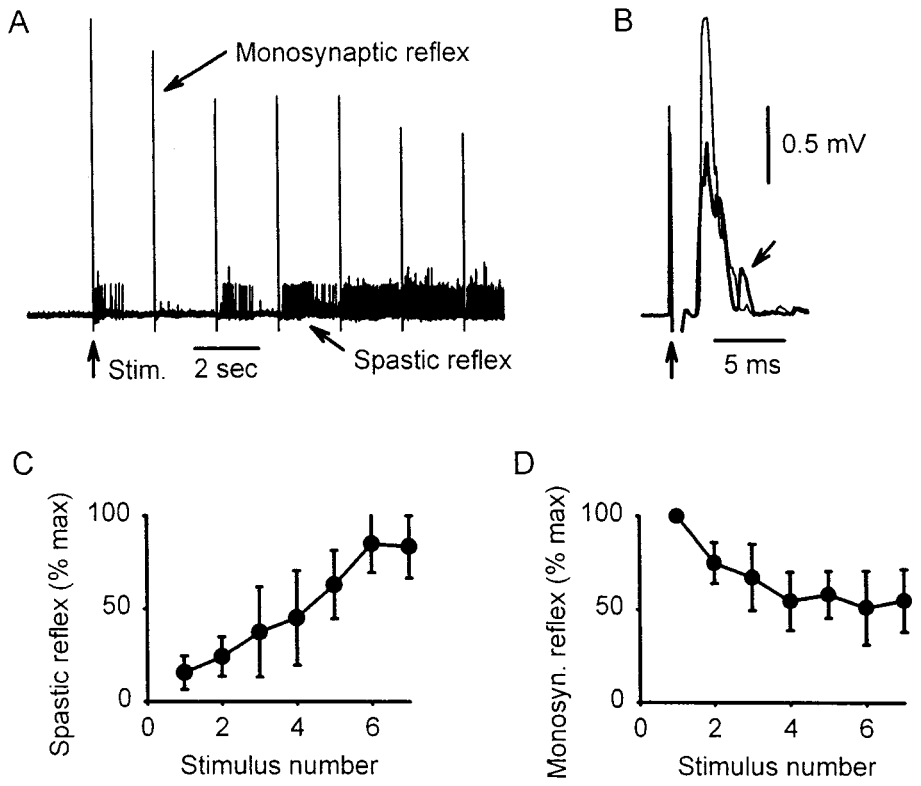

FIGURE 2-3. EFFECT OF REPEATED STIMULATION ON LONG-LASTING REFLEX IN CHRONIC SPINAL RATS.

A: increase in long-lasting reflex in the S_4 ventral root with stimulation pulse repeated at 2 sec intervals (stimulation at 0.1 mA on Ca_1 dorsal root). B: monosynaptic reflexes to first (thin line) and last (thick line) stimuli in A. Note the decrease in monosynaptic reflex with repetition (rate-depression), and increase in short latency polysynaptic reflex (right arrow). C: group mean long-lasting reflex amplitude as a function of number of stimuli delivered at 2 sec intervals (see text). D: same as C, but monosynaptic reflex. Reflexes normalized to maximum of each root.

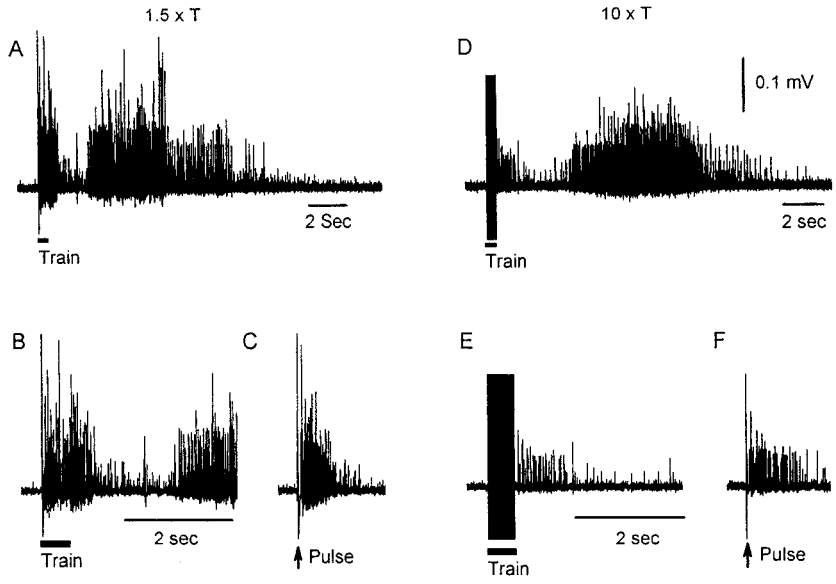

FIGURE 2-4. LONG-LASTING REFLEXES EVOKED BY HIGH FREQUENCY STIMULUS TRAINS.

A: very long-lasting reflex in S_4 ventral root in response to a brief low threshold stimulus train (0.5 sec, 100 Hz, 0.015 mA on Ca_1 dorsal root, 1.5xT). Note the two bursts of spasm-like activity. B: same as A, but on shorter time scale. C: response of same S_4 ventral root to a single low threshold pulse (0.015 mA on Ca_1 dorsal root). D-F: same sequence as in A-C, but in a different rat with a higher stimulus intensity (0.1 mA, 10xT). Parts B,C,E, and F on same time scale.

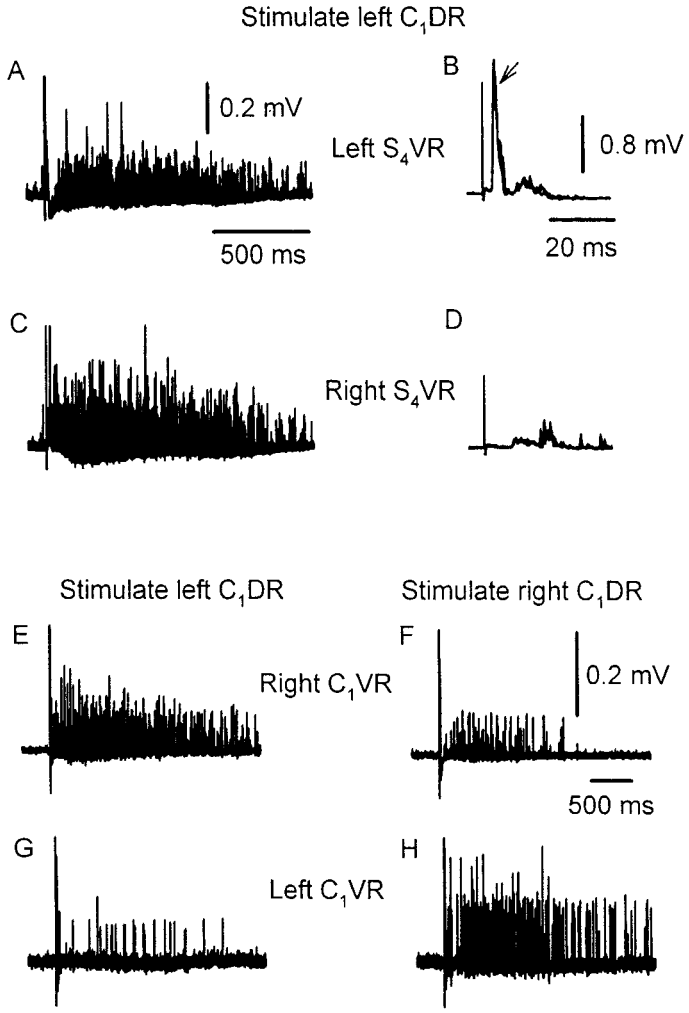

FIGURE 2-5. CONTRALATERAL LONG-LASTING REFLEXES IN CHRONIC SPINAL RATS.

A: long-lasting reflex of S_4 ventral root (VR) in response to ipsilateral Ca_1 dorsal root (DR) stimulation pulse (0.1 mA). B: expanded time scale to show monosynaptic reflex (at arrow). C-D: same as A-B, but recording from contralateral S_4 ventral root with the same DR stimulation. Note larger long-lasting reflex, and lack of monosynaptic reflex in this contralateral response. E-F: comparison of stimulating the left and right Ca_1 dorsal

roots (0.01mA) in a different rat. Note again the larger reflexes in the respective contralateral Ca_1 ventral roots (E,H), compared with the ipsilateral roots (F,G).

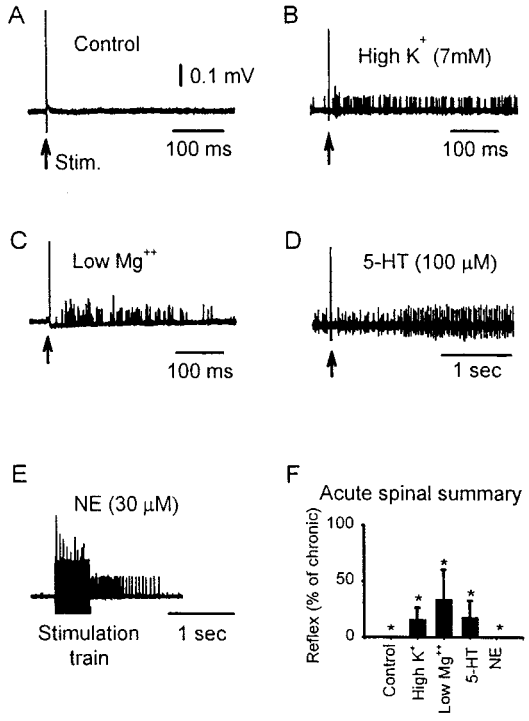

FIGURE 2-6. FACILITATION OF LONG-LASTING REFLEXES IN ACUTE SPINAL RATS.

A: acute spinal rat with no ventral root reflexes to dorsal root stimulation with normal ACSF (0.1 mA pulse on Ca_1 dorsal root, recording from S_4 ventral root). B: long-lasting reflex emerged when the K^+ was raised from 3 mM to 7mM (eliminated with wash; not shown). C: long-lasting reflex re-emerged when the Mg^{++} was eliminated from the ACSF. D: long-lasting reflex to the same stimulation was caused by application of a high dose of 5-HT (100 μM) in another acute spinal rat that was initially without reflexes in normal ACSF. Note the spontaneous activity produced by the 5-HT prior to the stimulus

pulse (prior to arrow). E: high dose of NE (30 μM) likewise facilitated the long-lasting reflex, but only in response to train stimuli (0.5 s, 100 Hz, 0.1 mA pulse). Doses lower than 20 μM had no effect. F: summary of long-lasting reflex amplitudes, normalized by average long-lasting reflex in chronic spinal rats in normal ACSF (doses 30 - 100 μM; n > 5 roots per condition, see text). All reflexes significantly less than in chronic spinal rat.

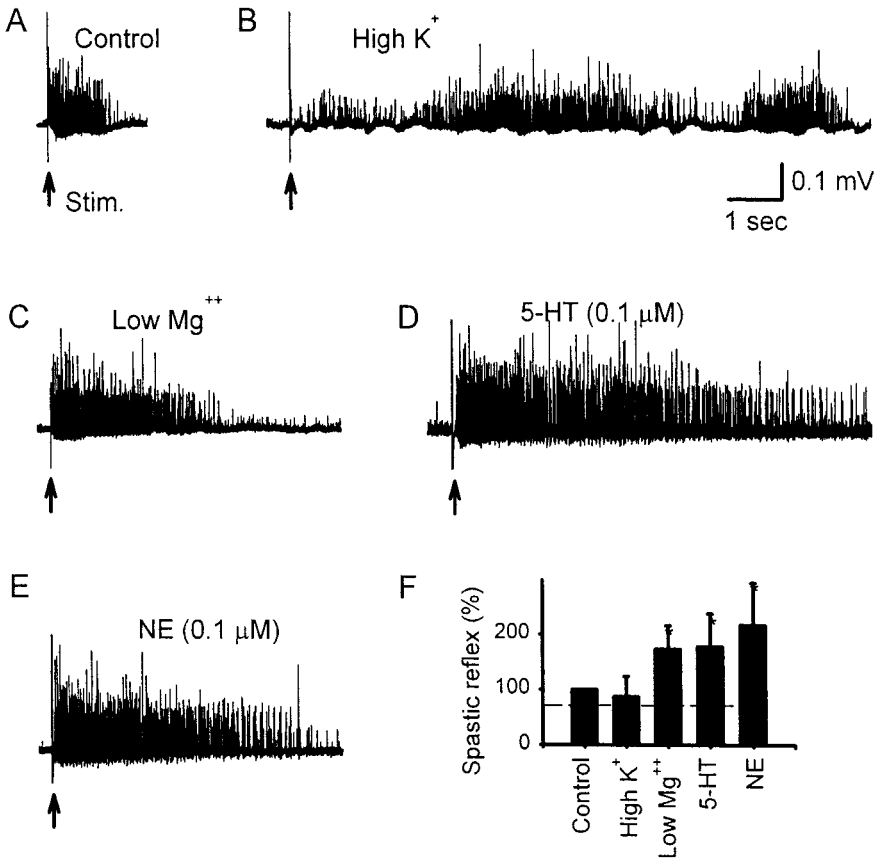

FIGURE 2-7. FACILITATION OF LONG-LASTING REFLEXES IN CHRONIC SPINAL RATS.

A: chronic spinal rat with long-lasting reflex in normal ACSF (0.1 mA pulse on Ca_I dorsal root, recording from S_4 ventral root). B–F: same format as Fig. 6, except the doses of 5-HT and NE required to facilitate reflexes were much lower (0.03-0.1 μM for NE and 0.1 - 1 μM for 5-HT; averages in F were from these dose ranges).

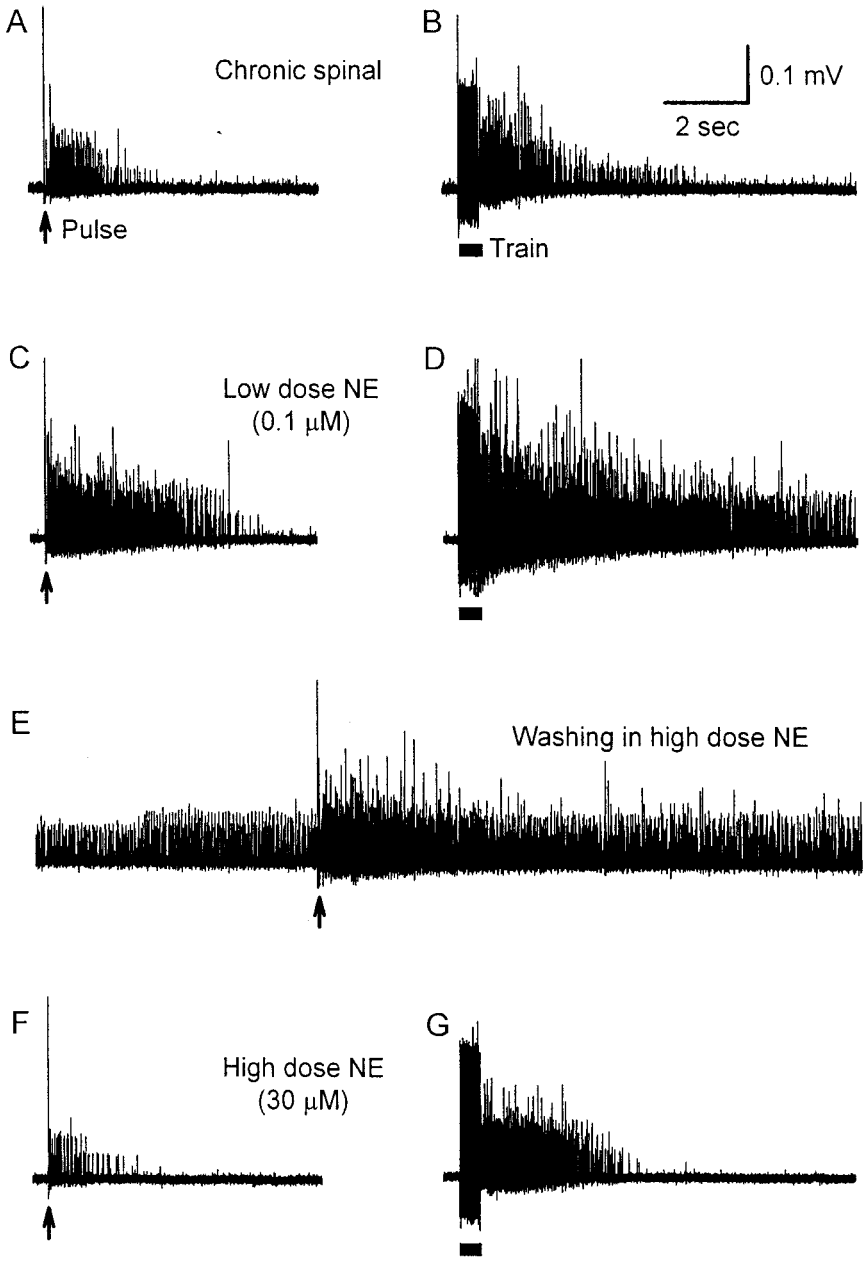
A
Chronic spinal
Pulse
B
0.1 mV
2 sec
Train
C
Low dose NE
(0.1 μM)
D
E
Washing in high dose NE
F
High dose NE
(30 μM)
G

FIGURE 2-8. PARADOXICAL DOSE-RESPONSE RELATION FOR NE IN CHRONIC SPINAL RAT.

A-B: long-lasting reflex in S4 ventral root in responses to a Ca1 dorsal root stimulation pulse at arrow (A, 0.1 mA; 10xT) or train at bar (B, 0.5 sec, 100 Hz, 0.015 mA; 1.5xT) in normal ACSF. C-D: enhanced long-lasting reflexes in low dose NE (0.1 μM). E: spontaneous activity that occurred 5 mins after start of application of high dose NE (30 μ M). At this time the long-lasting reflex response to a pulse (at arrow) was markedly reduced, and obscured by the spontaneous activity. F-G: long-lasting reflexes 15 mins after application of NE. Note that spontaneous activity had subsided, and reflex response to a single pulse was very small (F), though the train stimulation still evoked a large long-lasting reflex (G).

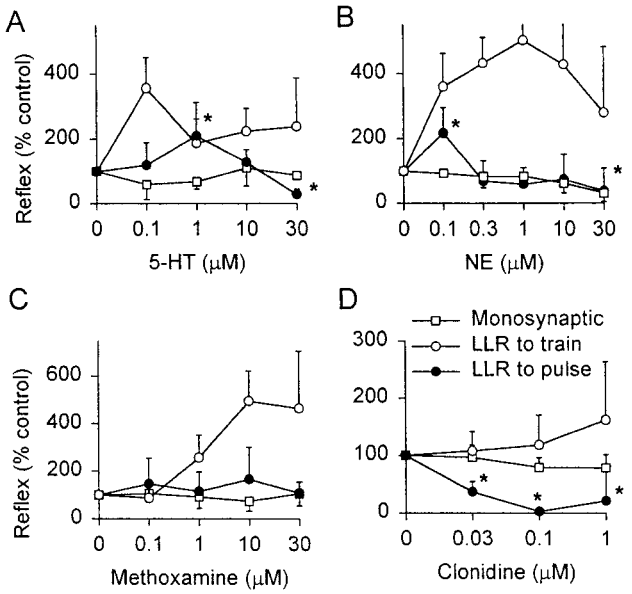

FIGURE 2-9. SUMMARY OF NEUROMODULATORY EFFECTS ON LONG-LASTING REFLEX IN CHRONIC SPINAL RATS.

A: cumulative dose-response relation for 5-HT. Long-lasting reflex responses to a single pulse (0.1 mA) and a train (0.5 sec, 100 Hz, 0.015 mA) are indicated by solid and open circles respectively. Open square symbols indicate monosynaptic reflex amplitudes. Data normalized to reflex amplitude for each root in normal ACSF. The * indicates significantly difference in single pulse long-lasting reflex (solid circles) compared to normal ACSF conditions (100%). Note the biphasic single pulse response, increasing at 1 μM and decreasing at 30 μM. In contrast, all doses significantly elevated the train evoked reflex (squares), compared to control. B-D: dose-response relations for NE,

methoxamine and clonidine. Same format as A. Note that NE behaved as 5-HT. Methoxamine, in contrast, produced an increase in the single pulse reflex at all doses. Clonidine did not cause a low-dose increase in reflex, but mimicked the inhibition of the reflex seen in high dose NE. Also, NE and methoxamine caused a significant increase in the long-lasting response to the train stimulation. For each dose $n > 5$ roots tested.

REFERENCES

Akatani J, Wada N, and Kanda K. Intersegmental neuronal pathways in sacrococcygeal spinal cord (S3-Co3) activated by electrical stimulation of tail muscle nerves with low threshold in low spinal cats. *Brain Res* 924: 30-38, 2002.

Anderson RJ, Brigham P, Cady WJ, and Kellar KJ. Role of alpha-2 adrenergic affinity in the action of a non-sedative antispasticity agent. *Acta Neurol Scand* 66: 248-258, 1982.

Ashby P and McCrea DA. Neurophysiology of spinal spasticity. In: *Handbook of the Spinal Cord.*, edited by Davidoff RA. New York: Marcel Dekker Inc., 1987, p. 120-143.

Barbeau H and Bedard P. Denervation supersensitivity to 5-hydroxytryptophan in rats following spinal transection and 5,7-dihydroxytryptamine injection. *Neuropharmacology* 20: 611-616, 1981.

Barron DH and Matthews BHC. Dorsal root reflexes. *J Physiol* 94: 26-29P, 1938.

Bennett DJ, Gorassini M, Fouad K, Sanelli L, Han Y, and Cheng J. Spasticity in rats with sacral spinal cord injury. *J Neurotrauma* 16: 69-84, 1999a.

Bennett DJ, Gorassini MA, and Siu M. In vitro preparation to study spasticity in chronic spinal rats. *Soc Neuroscience Abst* 25: 1394, 1999b.

Bennett DJ, Li Y, Harvey PJ, and Gorassini M. Evidence for plateau potentials in tail motoneurons of awake chronic spinal rats with spasticity. *J Neurophysiol* 86: 1972-1982, 2001a.

Bennett DJ, Li Y, and Sanelli L. Role of NMDA in spasticity following sacral spinal cord injury in rats. *Soc Neurosci Abstr* 31: 933.11, 2001b.

Bennett DJ, Li Y, and Siu M. Plateau potentials in sacrocaudal motoneurons of chronic spinal rats, recorded in vitro. *J Neurophysiol* 86: 1955-1971, 2001c.

Bennett DJ, Sanelli L, and Cooke C. Spastic long-lasting reflexes in the awake rat after sacral spinal cord injury. *J Neurophysiol*: submitted, 2003.

Brooks CM, Koizumi K, and Malcolm JL. Effects of changes in temperature on reactions of the spinal cord. *J Neurophysiol* 18: 205-216, 1955.

Burke D, Gillies JD, and Lance JW. The quadriceps stretch reflex in human spasticity. *J Neurol Neurosurg Psychiat* 33: 216-223, 1970.

Chau C, Barbeau H, and Rossignol S. Effects of intrathecal alpha1- and alpha2-noradrenergic agonists and norepinephrine on locomotion in chronic spinal cats. *J Neurophysiol* 79: 2941-2963, 1998.

Conway BA, Hultborn H, Kiehn O, and Mintz I. Plateau potentials in alpha-motoneurones induced by intravenous injection of L-dopa and clonidine in the spinal cat. *J Physiol* 405: 369-384, 1988.

Harvey PJ, Gorassini MA, Yakovenko S, Gritsenko V, and Bennett DJ. Contralateral presynaptic inhibition of the monosynaptic reflex in the sacral spinal cord. *Soc Neuroscience Abst* 25: 1394, 1999.

Heckman CJ. Alterations in synaptic input to motoneurons during partial spinal cord injury. *Med Sci Sports Exerc* 26: 1480-1490, 1994.

Hounsgaard J, Hultborn H, Jespersen B, and Kiehn O. Bistability of alpha-motoneurones in the decerebrate cat and in the acute spinal cat after intravenous 5-hydroxytryptophan. *J Physiol* 405: 345-367, 1988.

Hounsgaard J and Kiehn O. Serotonin-induced bistability of turtle motoneurones caused by a nifedipine-sensitive calcium plateau potential. *J Physiol* 414: 265-282, 1989.

Jankowska E, Jukes MG, Lund S, and Lundberg A. The effect of DOPA on the spinal cord. 5. Reciprocal organization of pathways transmitting excitatory action to alpha motoneurones of flexors and extensors. *Acta Physiol Scand* 70: 369-388, 1967.

Jankowska E, Padel Y, and Zarzecki P. Crossed disynaptic inhibition of sacral motoneurones. *J Physiol* 285: 425-444, 1978.

Jiang C, Agulian S, and Haddad GG. O2 tension in adult and neonatal brain slices under several experimental conditions. *Brain Res* 568: 159-164, 1991.

Kekesi G, Joo G, Csullog E, Dobos I, Klimscha W, Toth K, Benedek G, and Horvath G. The antinociceptive effect of intrathecal kynurenic acid and its interaction with endomorphin-1 in rats. *Eur J Pharmacol* 445: 93-96, 2002.

Kerkut GA and Bagust J. The isolated mammalian spinal cord. *Prog Neurobiol* 46: 1-48, 1995.

Kuhn RA and Macht MB. Some manifestations of reflex activity in spinal man with particular reference to the occurrence of extensor spasm. *Bull Johns Hopkins Hosp* 84: 43-75, 1948.

Lee RH and Heckman CJ. Enhancement of bistability in spinal motoneurons in vivo by the noradrenergic alpha1 agonist methoxamine. *J Neurophysiol* 81: 2164-2174, 1999.

Li Y and Bennett DJ. Persistent sodium and calcium currents cause plateau potentials in motoneurons of chronic spinal rats. *J Neurophysiol* 90: 857-869, 2003.

Li Y, Gorassini MA, and Bennett DJ. Role of peristent sodium and calcium currents in motoneuron firing and spasticity in chronic spinal rats. *J Neurophysiol*: in press, 2003.

Long SK, Evans RH, Cull L, Krijzer F, and Bevan P. An in vitro mature spinal cord preparation from the rat. *Neuropharmacology* 27: 541-546, 1988.

Masson RL, Jr., Sparkes ML, and Ritz LA. Descending projections to the rat sacrocaudal spinal cord. *J Comp Neurol* 307: 120-130, 1991.

Nance PW, Sheremata WA, Lynch SG, Vollmer T, Hudson S, Francis GS, O'Connor P, Cohen JA, Schapiro RT, Whitham R, Mass MK, Lindsey JW, and Shellenberger K. Relationship of the antispasticity effect of tizanidine to plasma concentration in patients with multiple sclerosis. *Arch Neurol* 54: 731-736, 1997.

Newton BW and Hamill RW. The morphology and distribution of rat serotoninergic intraspinal neurons: an immunohistochemical study. *Brain Res Bull* 20: 349-360, 1988.

Noth J. Trends in the pathophysiology and pharmacotherapy of spasticity. *J Neurol* 238: 131-139, 1991.

Penn RD. Medical and surgical treatment of spasticity. *Neurosurg Clin N Am* 1: 719-727, 1990.

Pierau FR, Klee MR, and Klussmann FW. Effect of temperature on postsynaptic potentials of cat spinal motoneurones. *Brain Res* 114: 21-34, 1976.

Powers RK, Campbell DL, and Rymer WZ. Stretch reflex dynamics in spastic elbow flexor muscles. *Ann Neurol* 25: 32-42, 1989.

Richmond FJ and Loeb GE. Electromyographic studies of neck muscles in the intact cat. II. Reflexes evoked by muscle nerve stimulation. *Exp Brain Res* 88: 59-66, 1992.

Richmond FJ, Thomson DB, and Loeb GE. Electromyographic studies of neck muscles in the intact cat. I. Patterns of recruitment underlying posture and movement during natural behaviors. *Exp Brain Res* 88: 41-58, 1992.

Ritz LA, Bailey SM, Carter RL, Sparkes ML, Masson RL, and Rhoton EL. Crossed and uncrossed projections to cat sacrocaudal spinal cord: II. Axons from muscle spindle primary endings. *J Comp Neurol* 304: 316-329, 1991.

Ritz LA, Brown PB, and Bailey SM. Crossed and uncrossed projections to cat sacrocaudal spinal cord: I. Axons from cutaneous receptors. *J Comp Neurol* 289: 284-293, 1989.

Ritz LA, Murray CR, and Foli K. Crossed and uncrossed projections to the cat sacrocaudal spinal cord: III. Axons expressing calcitonin gene-related peptide immunoreactivity. *J Comp Neurol* 438: 388-398, 2001.

Stauffer E. Trauma. In: *Spinal Deformity in Neurological and Muscular Disorders*, edited by Hardy J. St, Louis: C.V. Mosby, 1974, p. 219 - 239.

Stone LS, Broberger C, Vulchanova L, Wilcox GL, Hokfelt T, Riedl MS, and Elde R. Differential distribution of alpha2A and alpha2C adrenergic receptor immunoreactivity in the rat spinal cord. *J Neurosci* 18: 5928-5937, 1998.

Taylor JS, Friedman RF, Munson JB, and Vierck CJ, Jr. Stretch hyperreflexia of triceps surae muscles in the conscious cat after dorsolateral spinal lesions. *J Neurosci* 17: 5004-5015, 1997.

Thompson FJ, Parmer R, and Reier PJ. Alteration in rate modulation of reflexes to lumbar motoneurons after midthoracic spinal cord injury in the rat. I. Contusion injury. *J Neurotrauma* 15: 495-508, 1998.

Wada N, Miyata H, and Tokuriki M. Histochemical fiber composition of cat's tail muscles. *Arch Ital Biol* 132: 53-58, 1994a.

Wada N, Nakata A, Koga T, and Tokuriki M. Anatomical structure and action of the tail muscles in the cat. *J Vet Med Sci* 56: 1107-1112, 1994b.

Wada N and Shikaki N. Neuronal pathways for spinal reflexes activated by group I and group II muscle afferents in the spinal segment (Co1) innervating the tail in the low spinalized cat. *Exp Brain Res* 125: 129-138, 1999.

Wada N, Sugita S, Jouzaki A, and Tokuriki M. Descending projections to coccygeal spinal segments in the cat. *J Anat* 182 (Pt 2): 259-265, 1993.

Young RR. Spasticity: a review. *Neurol* 44: S12-S20, 1994.

Chapter 3: Plateau potentials in sacrocaudal motoneurons of chronic spinal rats, recorded *in vitro*

(Revised from Bennett et al. J. Neurophysiol. 86: 1955-1971, 2001[1])

[1] The author contributed to data collection and analysis, writing and revising the manuscript.

INTRODUCTION

Following spinal cord injury, exaggerated reflexes and muscle tone often emerge, which contribute to a general spasticity syndrome in humans (Ashby & McCrea, 1987; Kuhn & Macht, 1948; Noth, 1991; Young, 1994) and animals (Ashby & McCrea, 1987; Bennett et al. 1999a; Heckman, 1994; Taylor et al. 1997). A central complaint of patients with spasticity involves intense muscle contractions, lasting for many seconds, that are triggered by numerous stimuli. These are related to various long-lasting reflexes that have been described experimentally in humans and animals with injury, including: spastic stretch reflexes (Burke et al. 1970; Powers et al. 1989; Thilmann et al. 1991), cutaneous/flexor-afferent reflexes (Bennett et al. 1999a; Kuhn & Macht, 1948; Remy-Neris et al. 1999), general oligosynaptic reflexes (Hultborn & Malmsten, 1983a,b; Mailis & Ashby, 1990), and radiating muscle spasms (Kuhn & Macht, 1948). Such long-lasting reflexes may have numerous causes, including: (1) loss of inhibition from descending and segmental pathways (Cavallari & Pettersson, 1989; Heckman, 1994; Mailis & Ashby, 1990; Thompson et al. 1998), (2) neuronal sprouting (Krenz & Weaver, 1998) and (3) direct changes in intrinsic properties of spinal neurons (Eken et al. 1989).

The possibility that the intrinsic properties of spinal motoneurons change with spinal cord injury is consistent with data from motor unit firing in humans and animals after injury, including: sustained poorly modulated discharges (Gorassini et al. 1999a; Thomas & Ross, 1997), unusually low minimum firing rates (Carp et al. 1991; Powers & Rymer, 1988; Thomas & Ross, 1997) and generally inefficient control of firing rate in force

production (Blaschac et al. 1988; Wiegner et al. 1993). The objective of the present paper was thus to investigate whether long-lasting reflexes that emerge after injury result, in part, from changes in intrinsic excitability of motoneurons, such that relatively uncontrolled firing can be triggered by a brief stimulation (e.g., due to plateau potentials; Russo & Hounsgaard, 1999).

Although motoneurons usually fire in proportion to the net excitatory input, their response can also be altered substantially by numerous voltage-dependent currents intrinsic to the motoneuron membrane (Binder et al. 1996; Rekling et al. 2000; Russo & Hounsgaard, 1999). For example, voltage-dependent persistent inward currents (PIC) can at times be activated by a brief stimulus and regeneratively cause sustained depolarizations (i.e. plateau potentials; abbreviated plateau) and firing (Bennett et al. 1998a,b; Hounsgaard et al. 1988; Hounsgaard & Kiehn, 1989; Lee & Heckman 1998a,b; Schwindt & Crill, 1984;). Persistent inward currents are likely present in most motoneurons, but are only manifested as plateaus when they are either: (1) directly facilitated or (2) uncovered by reducing opposing outward currents (e.g. Ca^{++}-dependent K^+ current), both of which may occur with extrinsically administered serotonin (5-HT; Hultborn & Kiehn, 1992; Russo & Hounsgaard, 1999). The PIC responsible for plateaus is often mediated by L-type calcium channels (Hounsgaard & Kiehn, 1989), although any relatively long-lasting voltage-gated inward current could also be involved, including persistent sodium currents (Schwindt & Crill, 1995), and ligand-gated currents from NMDA receptors (Guertin & Hounsgaard, 1998; Hochman et al. 1994; Kiehn et al. 1996).

The existence of plateaus in motoneurons appears to normally require monoaminergic facilitation from the brainstem (5-HT, NE). That is, plateaus occur in brainstem-intact decerebrate cats, are largely eliminated by acute spinalization, and return with application of monoaminergic drugs (Conway et al. 1988; Hounsgaard et al. 1988). As there are few sources of 5-HT or NE within the spinal cord below a chronic spinal transection (except perhaps related to the autonomic system, McNicholas et al. 1980; see also Newton & Hamill, 1988) it is unlikely that plateaus mediated by monoamines could re-emerge with long-term complete spinal cord transection. However, because the inward currents (PIC) are ubiquitous, as discussed above, and PIC and plateaus are facilitated by various other neuromodulators (acetylcholine, substance-P and glutamate; via metabotropic receptors; Russo et al. 1997; Russo & Hounsgaard, 1999), plateaus may still play a role in chronic injury. Indeed, the similarity of the long-lasting reflexes in the chronic spinal cat to the tonic stretch reflex in the decerebrate cat led Hultborn's group to propose that both are mediated by plateaus on motoneurons (Eken et al. 1989; Nielsen & Hultborn, 1993). Their preliminary evidence, from motoneurons recorded in two chronic spinal cats, supports this hypothesis.

In the present study, we have made intracellular recordings from motoneurons of chronic spinal rats to test for the presence of plateaus. The spinal cord transection was made at the sacral level, which, within a month, leads to pronounced spasticity in the tail muscles while sparing bladder and locomotor function (Bennett et al. 1999a). In these chronic spinal rats there was often sustained tail motor unit firing, suggestive of the involvement

of plateaus (Bennett et al. 2001). This preparation has the unique advantage that the affected adult sacrocaudal spinal cord is small enough to survive when acutely explanted and studied in vitro (whole adult cord; Bennett et al. 1999b; Li et al. 2004; Long et al. 1988). Ventral root recordings were used to verify that the spastic reflex behaviour persisted in vitro (Bennett 1999b), and intracellular recordings were made from identified motoneurons. As anticipated, we found that, with chronic spinal cord injury, the motoneurons recovered their ability to exhibit plateau behaviour. These plateaus could be triggered by dorsal root stimulation, and they markedly prolonged reflex responses, thus playing a major role in the long-lasting spastic reflexes seen after chronic spinal cord injury.

METHODS

Intracellular recordings were made from sacrocaudal motoneurons of adult female Sprague-Dawley rats (age: 1.5 - 7 months; 200-800 g) following sacral spinal cord injury. The spinal cord was transected at the S_2 sacral spinal level either acutely (acute spinal condition; n = 29 cells, n = 14 rats) or at least one month prior to the experiment (chronic spinal, 1 - 5 months post lesion, n = 35 cells, n = 14 rats), as described in Bennett et al. (1999a). In the latter group, only rats with clear spasticity symptoms were used (rating 3-5 in Table 1 of Bennett et al. 1999a). Recordings were made while the whole sacrocaudal spinal cord was maintained in vitro (Bennett et al. 1999b; Li et al. 2004). All procedures were approved by a local animal welfare committee.

Surgery

The in vitro whole sacrocaudal adult rat preparation has been described previously (Bennett et al. 1999b; Li et al. 2004; Long et al. 1988) and is only briefly summarized here. Normal and chronic spinal rats were deeply anesthetized with urethane (0.18 g/100 g; maximum of 0.45 g per rat, for rats over 250 g), and the spinal cord caudal to the T_{12} vertebrae was transferred to a dissection dish containing oxygenated modified cerebral spinal fluid (mCSF) at room temperature (20 - 21°C). In the dissection dish, a transection was made at the upper S_2 level with fine iridectomy scissors, just rostral to the original transection site in the chronic spinal rats. In normal rats, this S_2 transection was also made and served to provide an acute spinal lesion. Following a 1 hour resting period in

mCSF, the cord was transferred to a recording chamber, where it was submerged in normal CSF flowing at 6 ml/min and maintained at 25°C. The cord was supported on a nappy paper mesh, and secured by passing insect pins through lateral vasculature and connective tissue and into a Sylgard base below the nappy paper.

Solutions

The normal CSF had the following composition (in mM): 122 NaCl, 24 $NaHCO_3$, 3 KCl, 2.5 $CaCl_2$, 1 $MgSO_4$, 12 Glucose in distilled water, bubbled with 95% O_2 and 5% CO_2 and pH 7.4. Modified CSF (mCSF) was used during dissection and recovery to prevent excitotoxic injury. Initially mCSF consisted of CSF with NaCl replaced by sucrose at equal osmolarity (0 NaCl, 213.6 mM Sucrose (295 mOsm; Aghajanian & Rasmussen, 1989). Later we noticed that sucrose tended to toughen the pia, making subsequent intracellular penetrations more difficult (e.g., dimpling occurred). We thus changed to a mCSF based on Kynurenic acid, a broad spectrum antagonist of glutamate transmission. This mCSF composition was (in mM): 118 NaCl, 24 $NaHCO_3$, 3 KCl, 1.5 $CaCl_2$, 1.3 $MgSO_4$, 25 Glucose, 1.4 NaH_2PO_4, 5 $MgCl_2$; 1 Kynurenic acid (McQuiston & Madison, 1999). Regardless of the mCSF used, recordings were made in the same normal CSF, and qualitatively similar results were obtained, though in general we noticed that the cords prepared with kynurenic-based mCSF were healthier, with larger reflexes and more pronounced plateaus. Serotonin (5-HT; 10-100 μM) was at times added to the CSF in some acute spinal preparations, after the main recordings in normal CSF.

Intracellular and root recording

The long ventral and dorsal roots (at least sacral S_3, S_4 and caudal Ca_1) were mounted on silver-chloride wires supported above the recording chamber, and covered in grease. Brief dorsal root stimulations were used to evoke long-lasting reflexes in spastic rats, and also to confirm the viability of the preparation (Bennett et al. 1999b). Reflex responses were recorded in the ventral roots and intracellularly on the motoneurons. Ventral roots were also stimulated to antidromically activate motoneurons for identification.

All segments of the in vitro sacrocaudal spinal cord could produce ventral root reflexes and thus had viable motoneurons (see also: Li et al. 2004). However, we focused on motoneurons in the caudal Ca_1 and sacral S4 regions because: (1) this is the smallest, and presumably best oxygenated, portion of the cord in vitro, (2) ventral root reflexes were largest and remained viable for the longest periods (>5 hours and up to 18 hours) and (3) motoneurons in this region innervate only the tail muscles, as opposed to bladder and pelvic regions served by higher sacral segments (Bennett et al. 1999a; Steers, 1994).

Sharp intracellular electrodes were made from thick-walled glass capillary tubing (Warner, GC150F-10, 1.5mm o.d.) with a Narishige puller (PE-2), filled with 2 M potassium acetate and beveled with a rotary grinder (Sutter, BV-10) to give a final resistance of 50 - 100 MΩ. An Axoclamp2b intracellular amplifier (Axon Instr.) was used, either in bridge or discontinuous current clamp modes (DCC; 4 - 5 kHz switching;

all Figures are from DCC recordings), with capacitance maximally compensated. The electrode was advanced with a stepper-motor micromanipulator (660, Kopf), while observing the electrode resistance changes and antidromic ventral root field potentials. Final cell penetration was achieved either by passing high frequency current (buzz), or making a fast step with a piezoelectric element (WPI) mounted on the tip of the Kopf manipulator. Upon penetration, antidromic spike properties were measured. Only cells with >55 mV resting potential and >60 mV spike amplitude were accepted for analysis. For approximate classification, the injected current required to initiate firing during a slow current ramp (0.5 nA/s; see below; recruitment current) was computed. All cells with a recruitment current less than the mean (1.75nA, mean of all acute and chronic cells) were considered low recruitment threshold cells, and the remainder high threshold. The intracellular current and membrane potential was low-pass filtered at 6 kHz and sampled at 16 kHz with an Axoscope system (Axon Inst).

Usually the cord was placed horizontally in the recording chamber with the ventral side upwards, and the intracellular electrode was advanced vertically, perpendicular to the cord, directly into the motor nucleus. The disadvantage of this approach was that dimpling of the pia during penetration could damage underlying neurons.

An alternate longitudinal approach through a transverse cut was used in some of the animals, as follows. After removal of the cord from the animal, it was transferred to a vibratome in mCSF and a transverse cut was made at the S4 level. Then, following the usual incubation in mCSF, the remaining S_4 and caudal cord was transferred to the

recording chamber and supported on a 30o ramp with the cut face pointing up the ramp. The cord was not submerged as usual, but covered with nappy paper superfused with CSF through a wick near the cut face of the cord (Long et al. 1988). The intracellular electrode was advanced into the cut face, longitudinally to the cord, directly into the motor nucleus near the visible interface of the white and gray matter (thus avoiding the pia). The main disadvantage of this approach is that the transverse cut is an additional injury and the reflexes recorded in the remaining S_4 and caudal Ca_1 roots were diminished. However, we did not notice differences in the intracellular plateau properties of motoneurons recorded with the perpendicular and longitudinal approaches, and cells from both methods have been included in the analysis.

Analysis of plateaus

Intracellular current pulses and slow triangular current ramps (0.5 nA/s standard, 0.4 - 3 nA/s range) were used to evoke voltage-dependent plateaus, as described previously (Bennett et al. 1998a; Hounsgaard et al. 1988). During the current ramps, the persistent inward current (PIC) producing the plateau, and sustaining the firing, was estimated from the difference in injected current at recruitment, compared to de-recruitment (I; see Results). For computing the average I for each cell, we only used responses from small, slow current ramps (0.5 nA/s as in Fig. 5*A*, unless there was a late, high-threshold plateau), optimized to avoid firing rate adaptation, as described in the Results. Also, to avoid any interactions between successive ramps (e.g., warmup Bennett et al. 1998b), we separated ramps by at least 10 s, and removed any depolarizing current between ramps.

The size of the plateau was estimated from the after-potential seen during current ramps (V in Fig. 5*A*, see Results). This was quantified by subtracting the potential at the end of firing (just before the last spike) from the potential at a matched current during the ascending ramp before the plateau and firing started. Because the potential can rise no higher than the firing level (ignoring the spike), this after-potential measure, ΔV, underestimates the plateaus size that might be seen if spiking were not present. In cells that stopped firing early, and at higher currents than at recruitment (i.e. without plateau; acute spinal), the after-potential was still computed, but by comparing the potential just before recruitment to that at a matched current level after de-recruitment (see Results). Some cells were recorded in bridge mode (not shown) instead of the usual DCC mode, and so the potential changes were corrupted by electrode rectification. However, by comparing the potential at matched currents on the ascending and descending current ramps, this electrode rectification problem was usually avoided (with a few exceptions, where rectification was sufficiently bad that we did not compute the after-potential, thus missing the points in Fig. 4*C*).

To directly test the role of voltage-dependent plateaus on spastic reflexes, we also studied the amplitude and duration of excitatory post synaptic potentials (EPSPs) evoked by dorsal root stimulation while changing the background depolarization of the cell with intracellular current bias (Bennett et al. 1998a).

The intracellular records were analysed with Axoscope (Axon Instr.), Sigmaplot (Jandel Sci.) and a custom Linux-based program (G.R. Detillieux, Winnipeg). In the text and Figures means ± standard deviations are shown. Statistical differences were assessed with a Student's t-test at the 95% confidence level ($p < 0.05$).

Histology

The spinal cords of additional rats (6) were sectioned and stained to examine the size and anatomy of the sacrocaudal cord. The animals were anaesthetized and perfused with 4% paraformaldehyde as in Bennett et al. (1999a). The spinal cord was removed, serially dehydrated in ethanol, imbedded in paraffin for 7 days and then sectioned at 10 μm on a microtome. Tissue was stained with silver nitrate (Bielschowsky) and cresyl violet (Kiernan, 1990).

RESULTS

Anatomy of the sacrocaudal ventral horn and motoneuron properties recorded in vitro

The small diameter of the sacrocaudal spinal cord (Fig. 1 *A*, *C*) was a major factor that enabled it to survive whole (unsliced) in vitro when it was acutely isolated from normal or chronic spinal adult rats, because oxygen and nutrients only diffuse about 300 μm into tissue (Nicholson & Hounsgaard, 1983). When intracellular recordings were made by passing the microelectrode into the cord directly through the ventral surface (perpendicular approach; see Methods), motoneurons were encountered at between 50 and 150 μm from the surface (>50 μm at Ca_1; > 100 μm at S_4). Despite the small size of the sacrocaudal cord, the sacrocaudal motoneuron cell bodies were not significantly smaller than motoneurons in the lumbar enlargement (Fig. 1*B*, *D*; average sacrocaudal motoneuron diameter: 35 ± 6 μm, n = 6 rats), and had similar basic electrical properties (Table 1).

In acute and chronic spinal rats, we recorded from motoneurons with a moderately wide range of input resistance (Rin; 9 - 25 MΩ), presumably relating to cell size (Binder et al. 1996). We found that Rin covaried with other cell properties, including AHP duration, recruitment threshold and rheobase (as with other motoneurons, Binder et al. 1996). Despite the marked differences in the ability of cells to maintain plateaus in acute and chronic spinal rats (see below), only slight (non- significant) differences were seen between these two populations in Rin, AHP amplitude and rheobase (Table 1), consistent

with previous studies in spinal animals (Baker & Chandler, 1987a; Cope et al. 1986; Gustafsson et al. 1982; Hochman & McCrea, 1994). There was a significant increase in AHP duration in chronic spinal rat motoneurons (Table 1).

Motoneurons in acute spinal rats lack plateaus

We studied the firing behaviour during intracellular current injection in 22 motoneurons from the acutely isolated sacrocaudal cord of normal rats (acute spinal condition) in normal CSF. In most of these cells there was no evidence of plateau activation (19/22). A brief current pulse did not trigger a sustained depolarization (Fig. 2*E*). Usually cells responded proportionally during slow triangular ramp current injections, with the membrane potential and firing rate increasing linearly during the upward portion of the ramp, and decreasing symmetrically during the downward portion of the ramp (see triangular reference lines drawn below potential in Fig. 2*A* and the overlapping frequency-current plots during the upward and downward ramps in Fig. 2*C*). Firing usually stopped at about the same current as where it started (Figs. 2*A*, *C*). Overall, 59% of cells responded linearly like in Fig. 2*A*, and we have classified these cells as Type 1 cells (i.e. linear firing and no plateau).

In another 36% of acute spinal rat motoneurons, firing slowed substantially on the downward portion of the slow current ramps (0.5 nA/s standard speed; Fig. 3*A*), and the frequency-current plots showed a clockwise shape and an early de-recruitment, characteristic of cells with late firing rate adaptation (Fig. 3*C*; Kernell & Monster; 1982).

We refer to these cells as Type 2 cells (rate adapting). Larger (or faster) ramps increased the incidence of rate adaptation, likely due to the higher firing rates achieved (not shown; Kernell & Monster, 1982).

Motoneurons of spastic chronic spinal rats have plateaus

Following the S2 sacral spinal cord transection, exaggerated long-lasting reflexes associated with a general spasticity syndrome developed in the tail musculature within a month, as in Bennett et al. (1999a). Motoneurons (n = 35) were recorded from the isolated sacrocaudal cord of these spastic rats at least one month after injury (chronic spinal; recordings in normal CSF). Prior to each experiment, the hyperreflexia was verified in vitro by recording the associated long-lasting ventral root reflexes (Bennett et al. 1999b; Li et al. 2004).

When a brief intracellular current pulse was injected into motoneurons of chronic spinal rats, a sustained depolarization (after-potential) and after-discharge was produced (Fig. 2*F*; i.e. plateau potential), lasting many seconds, and not seen in acute spinal rats (Fig. 2*E*). Symmetrical triangular current ramps also triggered a sustained after-discharge and after-potential (ΔV) due to the plateau activation, and a very asymmetrical response in relation to the current (Figs. 2*B* and 3*B*; 34/35 cells). That is, following recruitment of firing at a particular current on an upward current ramp (e.g., left vertical dashed line in Fig. 2*B*, 0.4 nA), de-recruitment only occurred when the current was reduced to a substantially lower level (right vertical dashed line; ΔI = -1 nA). Thus, firing stopped much later than expected (referred to as self-sustained firing; Bennett et al. 1998a; also

see Figs. 3*B*). The interpretation of this self-sustained firing is that the inward current PIC, associated with the plateau, was activated during the ascending current ramp, and then PIC effectively provided a depolarizing bias current, allowing the injected current to be substantially reduced before firing stopped (approximately: $\Delta I = -$ PIC ; see below). The reduction in current at de-recruitment compared to recruitment, ΔI, thus provides a measure of the inward current PIC that helped to sustain the firing.

Note that the term 'plateau' can be somewhat misleading during current ramps, since the depolarizing inward current PIC combines with the injected current to produce the final response, and the potential is not locked at a fixed level (see details in Bennett et al. 1998a).

Quantification of plateau and comparison in acute and chronic spinal rats

As mentioned above, in acute spinal rats there was little tendency for plateaus, and de-recruitment occurred at or above the current for recruitment, as summarized in Fig. 4*A* for all motoneurons ($I \geq 0$; ΔI not significantly different from zero, Fig. 4*B*). In three acute spinal rat motoneurons, there was a drop in injected current at de-recruitment ($\Delta I < 0$), indicating self-sustained firing and plateaus (3/22 cells). In contrast, in most chronic spinal motoneurons (34/35) the current dropped substantially at de-recruitment compared to recruitment (i.e., ΔI was significantly less than zero; $-\text{PIC} = \Delta I = -0.8 \pm 0.6$ nA). The average estimated PIC is summarized for acute and chronic spinal rats in Fig. 4*B*, which indicates a very significant (1.0 nA) increase in PIC with chronic injury.

Note that in chronic spinal rats both neurons with a low (< 1.75 nA) and high (> 1.75 nA) recruitment threshold had plateaus, as indicated by ΔI. Further, there was no significant difference between the plateaus (ΔI) in low and high threshold neurons (ΔI = -0.7 ± 0.5 nA compared to -1.1 ± 0.9 nA), and there was considerable scatter in ΔI (regression value r = 0.2 in Fig. 4*A*).

The depolarization produced by the plateau was most easily seen at the end of firing, and we have referred to this as the after-potential (ΔV in Fig. 2*B* and 3*B*; see Methods). In chronic spinal rats, the after-potential, and thus plateau estimate, was 5 to 10 mV (5.1 ± 6.0 mV) and was significantly greater than in acute spinal rats (Fig. 4*D*). In acute spinal rats the after-potential was not significantly different from zero.

In 12 motoneurons recorded in acute spinal rats, the ability of 5-HT to facilitate plateaus was studied (as in Hounsgaard & Kiehn, 1989; 5 cells studied before and after 5-HT, and 7 with 5-HT only). We used a concentration between 10 - 100 μM, which produced sustained activation of the ventral roots in response to dorsal root stimulation (not shown). The 5-HT usually depolarized cells, reduced the AHP and lowered their firing threshold current (by 2.2 nA, on average). Subsequent ramp current injections showed plateaus, although the estimated plateau current (PIC = - ΔI; Fig. 4*B*) and after-potential (ΔV; Fig. 4*D*) were not as large as in chronic spinal rats.

Characteristics of plateaus in chronic spinal rats

LOW-THRESHOLD PLATEAUS, INITIATED BEFORE RECRUITMENT (TYPE 3 CELLS). In the majority of chronic spinal rat motoneurons (63%, classified as Type 3 firing behaviour), the plateau activation started before or simultaneous to recruitment during the current ramp, and firing rate acceleration was either not seen (Fig. 3*D*) or only seen in the first few spikes (Figs. 5*A*, *B*, left arrows; and Fig. 6*D*). In these cells, during the slow current ramp, the membrane potential increased linearly until it was within about 5 mV of the firing threshold, after which there was a gradual acceleration in the depolarization (lasting about 0.5-1.0 sec; double arrow in Fig. 5*A*). This acceleration marked the onset of the plateau, because the current could be reduced at any time afterwards and there was still a sustained depolarization and firing (self-sustained firing). The most dramatic examples of this occurred with small current ramps, where the upward current just activated the plateau (at acceleration in potential, arrow Fig. 5*C*), and then immediately the downward current ramp started, just prior to recruitment. In this case, the plateau continued to depolarize the cell and produce sustained firing even when the current was reduced by 1 nA (i.e. at least 1 nA sustained PIC; in acute spinal rats a comparable small current ramp did not evoke any firing or a plateau [not shown]).

In some of the motoneurons with a low threshold for plateau initiation, accelerated and irregular firing occurred for about 1 sec after recruitment (Figs. 5*A*, *B* & Fig. 6*D*, mentioned above), suggesting that the plateau was being further activated during this early period. Additional evidence for this comes from comparing the plateaus evoked

with different amplitude ramps. Although a plateau could be activated with a very brief small ramp that just activated the cell (as described above, Fig. 5*C*), a slightly larger ascending ramp that caused a few seconds of firing (Fig. 5*A*) had a larger effect (ΔI = -1.4 nA, compared to -1 nA). Likely, this resulted from a more complete activation of the plateau with the larger ramp. Low-threshold plateau activation occurred in both low (Figs. 2*B* & 6*D*) and high (Figs. 3*B* & 5) recruitment threshold cells (range - 0.1 to 4.9 nA threshold).

In the chronic spinal rat motoneurons with a low plateau threshold (i.e., Type 3 cells; 63 % of chronic spinal motoneurons), the firing rate profiles after plateau activation were remarkably linear (r^2 ranged between 0.85 and 0.95; Figs. 3*D*, 5a, 6c,d) during slow current ramps, and the F-I plots on the ascending current ramp overlapped the profiles on the descending ramp (Fig. 6*C*, *D*; no counterclockwise hysteresis loop). Interestingly, the firing profile followed closely in proportion to the current, even at currents well below the initial recruitment current on the descending ramp (right of Fig. 5*A*). A simple interpretation of this is that once the PIC was activated, it provided a steady depolarizing bias current and did not produce any further accelerations in membrane potential or firing (though see complication below). Indeed, once the plateau was activated, the injected current could be repeatedly increased and decreased, above and below the current at plateau initiation (and recruitment) and the firing profile remained linear (on the same line in F-I plot; not shown).

FIRING RATE ADAPTATION (TYPE 2) AND EFFECT OF RAMP SPEED AND AMPLITUDE. In 17% of motoneurons of chronic spinal rats, there was firing rate adaptation (slowing of firing; Type 2 cells), with clockwise hysteresis in the frequency-current plots, and in these cells the self-sustained firing was weaker than average (i.e. plateau, ΔI, not as pronounced). As in acute spinal rats, this slowing of firing was accentuated with large or fast ramps. Indeed, even cells with a clear plateau and little firing rate adaptation during slow ramps showed some slowing of firing, with less after-discharge (ΔI) and less after-potential (ΔV) during faster or larger ramps (Fig. 5*B*, compared to Fig. 5*A*).

LATE-ACTIVATED PLATEAUS (TYPE 4). In some motoneurons (20%; as in Figs. 6*E* and 2*B*; classified as Type 4 cells), although firing initially increased linearly with current, there was a late acceleration in firing, which was assumed to mark the main activation of PIC and the plateau (at double arrow in Fig. 2*B*), as has been described in cat motoneurons (Bennett et al. 1998a; Hounsgaard et al. 1988). In these cells, there was a corresponding counterclockwise hysteresis loop in the F-I plot (Figs. 6*E* and 2*D*) and a marked drop in injected current at de-recruitment compared to recruitment ($\Delta I < 0$, i.e. large sustained PIC). All cells with this late plateau activation after recruitment were low recruitment threshold, presumably small, cells (7/35 cells; 0.12 - 2.5 nA recruitment thresholds).

Interestingly, the same late acceleration in firing could be seen during a steady pulse current injection (* in Fig. 2*F*), and we supposed that this acceleration was caused by the cell spontaneously moving from the lower (black) to the upper (white) branch of the F-I relation as the plateau was activated (see *'s in Fig. 2*D* at applied 0.8 nA current). Thus,

firing without full activation of the plateau was only transiently possible. Further, after the plateau was activated (when frequency acceleration complete, within a few seconds), the firing rate was modulated linearly with current ($r^2 > 0.85$).

PARTIAL DEACTIVATION OF PLATEAU BY SAHP DURING FIRING? In cells with a clear late acceleration in firing (Type 4), which we have previously taken to mark the main activation of the plateau (Figs. 2*B* and 6*E*; Bennett et al. 1998a), we were surprised to find that self-sustained firing (plateaus) could be evoked even when the current ramp was kept below the point where the frequency acceleration occurred (below main plateau threshold; compare Fig. 6*E* and Fig. 6*F*, responses from the same cell; contrast to Fig. 2 of Bennett et al. 1998b). However, on closer inspection, we found that there was also an acceleration in potential just prior to recruitment (single arrow in Fig. 2*B*), and this was likely associated with an early plateau activation. Thus, possibly there were two distinct plateau activations, one at recruitment and a second one later. We, however, favour an alternate interpretation based on two observations: (1) During the current ramps, the accumulated effect of the AHPs tended to hyperpolarize the membrane following recruitment (i.e. mean potential between spikes; e.g. Fig. 5*B*) compared to the potential just before recruitment. (2) Following the firing produced by a current pulse, there was, at times, a very slow hyperpolarization (sAHP), and pause in firing, before the after-discharge (plateau) continued (Fig. 8*G* described later; see similar effects in Figs. 7 & 8 of Russo & Hounsgaard, 1996). Thus, while the plateau may be partly activated before recruitment, with moderate firing rates the accumulated hyperpolarization from AHPs may have prevented further activation or even caused partial deactivation of the plateau.

Only when the cell was further depolarized by the increasing current ramp was the plateau fully activated (late acceleration, at high firing rate).

Even in cells with only a low threshold plateau activation (without a late frequency acceleration; Fig. 5), this partial plateau deactivation by accumulated AHP hyperpolarization during firing may have occurred. Indeed, during the downward current ramp, and as the firing slowed, there was at times evidence for a reactivation of the plateau (29% of cells). That is, the mean membrane potential transiently increased, despite the deceasing current, and at times caused a brief acceleration in firing (right arrow in Fig. 5*A*). Likely this occurred because the firing slowed sufficiently to allow the accumulated effect of the AHPs to diminish, allowing a more complete activation of the plateau.

VERY SLOW FIRING. When the current was reduced during a plateau and firing slowed, surprisingly long intervals often occurred between spikes (up to 1 sec), often many times the AHP duration and the related theoretical maximum interval (Figs. 5*A*, 8*H*; Kernell, 1999). In these cases, the plateau was just at threshold to deactivate, and thus perhaps each AHP transiently deactivated the plateau, and the plateau was then only slowly reactivated to produce a subsequent spike at a long interval. Indeed, this slow rise before each spike was similar to the slow rise in potential when the plateau was first activated just before recruitment (Fig. 5*A*, *B*). This phenomenon was not transient, because slow firing could continue for many seconds when pulses were used to evoke plateaus (Fig. 8*H* described later). The possibility of slow firing generated by voltage-dependent inward

currents with slow kinetics near firing threshold has been discussed by others (e.g. Carp et al. 1991; Hodgkin, 1948; Kernell, 1999).

Summary of firing behaviour in acute and chronic spinal rat motoneurons

F-I TYPES. The distribution of cells between the four types of firing behaviours described above (Types 1 to 4) is summarized in Fig. 7*A*; the majority of the acute and chronic spinal cells behaved linearly, as Type 1 and 3 cells, respectively. To summarize the type definitions: Type 1 cells had a linear F-I relation, with overlapping frequency points for the ascending and descending current ramps, but no self-sustained firing (no plateau, all from acute spinal rats, Fig. 6*A*; see also Fig. 2*C*). Type 2 cells showed firing rate adaptation, and usually no plateau (Fig. 6*B*; see also Fig. 3*C*). Some cells in chronic spinal rats were of this type, and they had only weak self-sustained firing, with rate adaptation countering the plateau. Type 3 cells had linear characteristics as in Type 1, but also showed self-sustained firing (plateau). Remarkably, the firing rate remained on the linear F-I regression line, even when the current was brought well below the recruitment current on the descending ramp (Figs. 6*C*, *D*, and 5*A*). Some of Type 3 cells started firing directly on the F-I linear regression line (thin line in Fig. 6*C*), and we assume that the plateau was fully activated at recruitment. Others included in this type had a few accelerating spikes just after recruitment below the linear regression for the F-I relation (Fig. 6*D*), which we supposed indicated the early activation of the plateau, continuing for a second after recruitment (see above). Type 4 cells had a late frequency acceleration, a few seconds after recruitment, followed by self-sustained firing (high-threshold plateau; Fig. 6*E*; Fig. 2*D*). As mentioned previously, Type 4 cells behaved linearly, as with Type

3 cells, when the current was kept below the level for a late frequency acceleration (Fig. 6*F*). With the exception of Type 4 cells, which were purely small, low recruitment-threshold cells, the other 3 types included both cells of low and high recruitment threshold. (see above).

INITIAL AND FINAL RATES. In previous motor unit experiments, motoneurons with presumed plateaus were found to have significantly higher firing rates at recruitment, compared to at de-recruitment (Gorassini et al. 1998, 2001a), and this was thought to be due to an early plateau activation at recruitment that boosted the initial firing rate above the minimum rate. In chronic spinal rats with plateaus, this was also found to be the case, with recruitment at about 8 Hz, and de-recruitment at half that value (significant difference; Fig. 7*B*). In contrast, the firing rates at recruitment and de-recruitment were not significantly different in motoneurons of acute spinal rats (about 8 Hz; Fig. 7*B*). The firing rate achieved at de-recruitment (minimum rate) in chronic spinal rats was significantly lower than in acute spinal rats, and, at times, as low as 1 Hz (see above).

LOWER F-I SLOPE AND SLOWER STEADY FIRING IN CHRONIC SPINAL RATS. Overall, motoneurons of chronic spinal rats fired at lower rates than in acute spinal rats, not just lower minimum rates. To further quantify this we have fit a linear regression to the F-I ramp responses. The first instantaneous firing rate point that fell on the F-I regression line after recruitment was measured, and referred to as the initial steady firing rate. This measure is not necessarily the instantaneous rate at recruitment, since there were often overshoots (early adaptation) or undershoots in firing before the rate was modulated

linearly with current (Fig. 6*D*). The initial steady firing rate was found to be significantly lower in chronic spinal rats, than in acute spinal rats (Fig. 7*C*).

The slope of the F-I linear regressions was also significantly lower in chronic spinal rats (Fig. 7*D*). This lower slope may be explained by an increased conductance provided by PIC in chronic spinal rats (see Discussion). Thus, while the plateau may have enabled recruitment at twice the minimum rate, its associated conductance change may have made it more difficult to produce further increases in rate (i.e. lower F-I gain).

Voltage-dependence of plateaus evoked with brief pulses

Although a brief current pulse in some chronic spinal cells could be readily used to evoke a plateau from rest (Fig. 2*F*), in others a plateau could only be evoked by a pulse when there was an appropriate steady depolarizing bias current. We found that, for a given cell, the parameters for producing a plateau from a pulse could be estimated from the ramp response as follows: First, the plateau threshold current was estimated, which was usually at the acceleration in potential just prior to firing (1.5 nA in Fig. 8*A*, *B*, see arrow). Second, the plateau current was estimated (PIC = - ΔI , which is 0.6 nA in Fig. 8*B*). Finally, a bias current was chosen that, when added to the plateau current, exceeded the threshold current for plateau activation (e.g. bias + 0.6 > 1.5 nA), thus allowing the plateau to remain activated after the pulse. By varying the bias level, we have been able to verify this recipe for plateau activation, as shown for a typical cell in Fig. 8*C-H*. With no bias current (Figs. 8*C-E*), a pulse could not produce a sustained after-discharge,

regardless of the pulse height, presumably because the plateau current, PIC, was only 0.6 nA, compared to the plateau threshold of 1.5 nA. (There was, however, evidence that the plateau was activated during the pulse, because a delayed onset in firing and slow rise in potential could be seen when the plateau threshold current was reached (arrow in Fig. 8*D*; see details in Fig. 9). When the bias current was increased to 0.7 nA (in Fig. 8*F*) a pulse evoked a sustained depolarization that outlasted the pulse (after-potential; right arrow Fig. 8*F*). This potential was slowly decrementing, suggesting that the bias current was set just below the plateau threshold (0.7 + 0.6 < 1.5 nA). A larger bias current (0.9 nA) produced more robust plateau activations (0.9 + 0.6 = 1.5 nA), with a greater after-potential and after-discharge (Fig. 8*G*).

Interestingly, following the pulse, a hyperpolarization and pause in firing often occurred (sAHP; Figs. 8*G*, *H*), and this was followed by an acceleration in firing as the plateau continued. Probably this occurred because the accumulated effect of AHPs (sAHP) during the pulse produced a partial deactivation of the plateau, which in this case was only reversed once the pulse ended (see Discussion). A related observation is that the plateau caused a greater after-discharge when it was evoked by a lower amplitude pulse (compare Figs. 8*F* and *H*). Thus, smaller pulses, which produced less firing during the pulse, caused less plateau inactivation and a greater after-discharge, presumably by producing less sAHP (as in Fig. 6 of Russo & Hounsgaard, 1996).

Slow and fast plateau activation

The plateau activation speed increased systematically with the depolarizing pulse amplitude (Fig. 9, bias current fixed at 0.75 nA). With a minimum pulse size (0.34 nA in Fig. 9*A*), the membrane potential only very slowly depolarized as the plateau was being activated, and firing was substantially delayed (4 s in this case). Larger pulses produced faster plateau activation and less delay in recruitment (the latter summarized in Fig. 9*C*, solid circles; note that the time scale is faster in Fig. 10*B*, compared with 9*A*). With the largest pulses, the plateau was activated simultaneously with recruitment (bottom of Fig. 9*B*, and Fig. 8*G*). In these cases, the presence of the plateau had to be verified by looking for a discharge after the pulse (not shown in fast time scale in Fig. 9, but see Fig. 8*G*).

In some cells, there was a delayed acceleration in firing associated with the plateau activation during the pulse (mentioned above in relation to Fig. 2*F*), and the delay for this acceleration also depended on the pulse amplitude. To quantify this, we have computed the time to reach steady-state firing during pulses of different amplitude (small arrows in Fig. 9*B*). For larger amplitude pulses, the firing increased to its steady state value faster, as summarized in Fig. 9*C*. The cell shown in Fig. 9 had its plateau primarily activated before recruitment, and then had about a 1.5 Hz increase in rate that resulted from the further plateau activation during firing (Fig. 9*D*).

Voltage-dependent long-lasting reflexes

Because our ultimate goal was to relate the presence of plateaus to the exaggerated long-lasting reflexes seen with spasticity, we have examined the reflex activation of the

motoneurons by dorsal root stimulation. In acute spinal rats a brief dorsal root stimulation only triggers a brief ventral root response (Bennett et al. 1999a,b). In contrast, in chronic spinal rats, a brief dorsal root stimulation triggers a sustained response in the ventral roots with a duration similar to tail reflexes in awake spastic rats, of about 2 s (stimuli 1.5 - 10 times threshold; Bennett et al. 1999a,b). Corresponding long-lasting reflex responses were seen during intracellular recording in chronic spinal rat motoneurons in response to the brief dorsal root stimulation, with an EPSP duration ranging from 2 - 5 s at rest (see Fig. 10*B*; no intracellular current bias, 2 s duration). The duration of this EPSP was always substantially reduced (to about 1 s in Fig. 10*C*) by hyperpolarizing the motoneuron with a steady bias current to eliminate any effect of the plateau. Conversely, a depolarizing current bias increased the duration of the reflex responses (EPSP; to 6 s in Fig. 10*A*), as might be expected from Fig. 8. The duration of the dorsal root stimulus could be as short as a single shock, yet still evoke the long-lasting voltage-dependent reflexes as just described (not shown; see also ventral root reflexes; Bennett et al. 1999b; Bennett & Li (unpublished data). This voltage-dependent behaviour suggests that plateaus were triggered by the dorsal root stimulation, and played a major role in amplifying and prolonging the reflex responses in chronic spinal rats. However, the plateau was not the only contributor to the sustained reflexes, because when the plateau was eliminated by hyperpolarization, the stimulus still evoked a depolarization that outlasted the stimulus by about 1 s (Fig. 10*C*).

DISCUSSION

The results demonstrate that plateau potentials are prominent in sacrocaudal motoneurons of chronic spinal rats with spasticity. Further, the plateaus contribute substantially to the exaggerated long-lasting reflexes, prolonging the synaptic input by many seconds, and thus playing an important role in spasticity (Bennett et al. 1999a). The plateaus occurred spontaneously when recorded in normal CSF in vitro, without exogenous neuromodulators added to the CSF, and thus these motoneurons become somewhat like deep dorsal horn neurons that normally exhibit plateaus and related oscillations spontaneously (Jiang et al. 1995; Morrisset & Nagy, 1999; Russo & Hounsgaard, 1996). In contrast, plateau behaviour was not usually seen in motoneurons of acute spinal rats, though exogenously applied 5-HT could enable plateaus.

Because previous studies have provided evidence for plateaus in hindlimb/leg motoneurons of intact rats (Eken et al. 1989; Gorassini et al. 1999b), decerebrate cats (Hounsgaard et al. 1988) and awake humans (Gorassini et al. 1998, 2001a), it is reasonable to assume that plateaus were also present in sacrocaudal tail motoneurons of intact rats prior to injury. In addition, the finding that 5-HT facilitates plateaus in these sacrocaudal cells after acute injury is consistent with this assumption, because such monoamines are thought to be a major facilitator of plateaus in normal animals (Eken et al. 1989). We can therefore conclude that motoneuron excitability provided by plateau behaviour is acutely removed by spinal cord injury and is recovered in chronic spinal rats that develop spasticity, thus verifying the hypothesis and results of Eken et al. (1989) and

Nielsen & Hultborn (1993), and the more recent inferences of plateau behaviour from motor unit recordings in awake spinal cord injured rats (Bennett et al. 2001) and humans (Gorassini et al. 1999a).

We have found a remarkably high incidence of plateaus in motoneurons of chronic spinal rats (from intracellular and motor unit recordings, Bennett et al. 2001). Nielsen & Hultborn (1993) found a lower incidence of plateaus in motoneurons of chronic spinal cats; however, we suggest that this was partly because of the criterion of hysteresis in firing that they used to identify plateaus. We found that, while most cells have plateaus, the plateaus are activated just before recruitment (low threshold), and thus clear counterclockwise hysteresis loops (F-I plot) with a late frequency acceleration are infrequent (Type 4; 20%), compared with linear frequency plots with self-sustained firing and no open counterclockwise hysteresis loop (Type 3; 63%).

The emergence of plateaus with chronic injury is very significant from a functional point of view because the normal descending inhibitory control is lacking, and uncontrolled long-lasting contractions may be triggered by brief stimuli (e.g., spasms and hypertonus; Bennett et al. 1999a). The threshold, amplitude and duration of the plateau is therefore important to quantify functionally, as discussed below. We suggest that spasticity associated with injury is not so much a condition related to motoneuron over-excitability (see discussion of plateau amplitude below), but instead to a recovery of relatively normal excitability and plateau behaviour without the normal inhibitory control to turn off plateaus and associated sustained firing.

Possible mechanisms for emergence of plateau in chronic spinal rats

The cause of plateaus after chronic spinal cord transection is unknown. The spinal cord has essentially no endogenous neurons that release monoamines (NE, 5-HT; only one 5-HT spinal neuron per rat, Newton & Hamill, 1988), and peripherally derived monoamines (from sympathetic terminal sprouts, McNicholas et al. 1980; or other hormones) could not play a role in producing plateaus in the explanted in vitro spinal cord preparation that we have used. However, as mentioned in the Introduction, persistent inward currents are likely present in many neurons, and a number of neuromodulators, outside of monoamines, can enable them to dominate sufficiently over outward currents to enable plateaus (Russo & Hounsgaard, 1999). Indeed, even in acute spinal animals a few motoneurons have plateaus (3/22 in our case; 1/20 in Hounsgaard et al. 1988), suggesting a latent endogenous capability for plateaus, perhaps controlled intrinsically or by interneuronal or afferent inputs (via substance-P and glutamate; Russo et al. 1997; Russo & Hounsgaard, 1999).

Plateaus may have emerged as a result of unmasking the persistent inward currents by reducing voltage- and calcium-gated outward K+ currents, many of which normally participate in the AHP (Russo & Hounsgaard, 1999). For example, 5-HT mediated plateaus are associated with a reduction in the AHP (Hounsgaard & Kiehn, 1989; Hultborn & Kiehn, 1992). However, the AHP amplitude (or duration) in chronic spinal rats was not significantly smaller than in acute spinal rats, suggesting that the plateaus

that emerged in chronic spinal rats were not facilitated by a reduction in these AHP-related K+ currents (in contrast to how 5-HT works). Further, because there was a plateau and a large AHP, the accumulated hyperpolarization from the AHPs in chronic spinal rats produced peculiar effects not seen in motoneurons of plateaus mediated by 5-HT (Hounsgaard et al. 1988; Hounsgaard & Kiehn, 1989), such as partial plateau deactivation during firing. Similar plateau deactivation has been reported following high-frequency firing in plateau-generating turtle dorsal horn neurons and was associated with a large slow AHP (sAHP) that slowed or stopped repetitive firing (Russo & Hounsgaard, 1996). Also, we found that, with low levels of injected current, the plateau was partially deactivated by each large AHP, and then only slowly reactivated, enabling a further spike and AHP, etc, thus explaining the very slow steady firing rates seen in chronic spinal rats (1-4 Hz; see Fig. 8*H* and similar discussions in Carp et al. 1991; Hodgkin, 1949 and Kernell, 1999).

Alternatively, the plateaus may have emerged after chronic injury because of a direct facilitation of the persistent inward current (PIC) by metabotropic actions (e.g. mGluR1 or muscarine receptors; Svirskis & Hounsgaard, 1998), or even a permanent upregulation of the associated channels or channel subunits (Ma et al. 1997). One prediction of a direct increase in PIC would be that the conductance should be increased in chronic spinal rats with plateaus, compared with acute spinal rats, whereas if PIC was simply unmasked by reducing the opposing outward currents, the opposite might occur (Kernell, 1999). Although we did not directly measure the conductance during the plateau (i.e. during firing), we did find that the F-I slope was lower in chronic spinal rats than in acute spinal

rats. This finding is consistent with a greater conductance resulting from PIC in chronic spinal rats (i.e. more current needed to increase firing), especially considering that the basic cell properties in acute and chronic spinal rats were otherwise similar (similar passive Rin, rheobase, AHP amplitude; Table 1). Also, an increase in F-I slope has been associated with a decrease in the AHP and associated conductances in the presence of neuromodulators (Berger et al. 1992; see Fig. 1 of Kernell, 1999).

The inward currents involved in the plateau after chronic injury remain uncertain and could, in principle, include persistent calcium (L-type), persistent sodium, NMDA and I_{CAN} currents (Russo & Hounsgaard, 1999). Considering the plateau timing and broad activation range seen in chronic spinal rats, we suggest the involvement of L-type calcium channels, as in plateaus of other motoneurons and dorsal horn neurons in turtle and young rat (Morisset & Nagy, 1999; Russo & Hounsgaard 1999). In particular, the very slow plateau onset during small current pulses (at threshold; Fig. 9*A*) is a characteristic property of plateaus mediated by L-type calcium channels of motoneurons (Hounsgaard et al. 1989; Svirskis & Hounsgaard, 1997).

Low plateau threshold

Functionally, one important characteristic of plateaus is the threshold for activation. In decerebrate cats, the threshold varies widely depending on the cell type (Lee & Heckman, 1998a) and mode of activation (intracellular vs synaptic, somatic vs dendritic; Bennett et al. 1998a,b; see also turtle motoneurons, Svirskis & Hounsgaard, 1997,1998). That is, with intracellular current ramps, some cat motoneurons have plateaus activated near the

recruitment level, but the majority have plateaus activated well after recruitment (at high firing rates). With synaptic activation, the threshold for plateau activation is lowered in cat motoneurons (Bennett et al. 1998a). In contrast, in chronic spinal rats the majority of motoneurons have plateaus that are initiated below the firing level, even during intracellular current injections (Figs. 5, 7*A*).

Low plateau thresholds are normally characteristic only of slow, early recruited motoneurons in the ('normal') decerebrate cat (Lee & Heckman, 1998a). Thus, the reason why all motoneuron types have a low threshold after chronic injury is unclear, especially considering that the tail muscles have both fast and slow twitch muscles (Steg, 1964). Interestingly, chronic spinal rats additionally have slower AHPs (Table 1), lower firing rates (Fig. 7) and longer muscle twitches (Stephens et al. 1999) than acute spinal rats, consistent with the whole motor unit behaving more slowly (see also Powers & Rymer, 1988). This occurs even though the recruitment threshold (Fig. 4*A*) and input resistance (Table 1) are similar to that of acute spinal rats (as in Baker & Chandler, 1987a; Hochman & McCrea, 1994).

Plateau amplitude and PIC

How large the plateaus are in chronic spinal rats in relation to those in normals or brainstem intact animals is another important functional question. In chronic spinal rats, the plateau is about 5-10 mV (Figs. 4 and 5). Further, our estimates of the sustained current supplied by the plateau (PIC) ranged from about 0.5 to 1.5 nA, with an average of

about 0.81 nA, which is substantial in relation to the current required to recruit the cell to steady firing (1.7 nA). That is, the plateaus provide about half the average current needed to recruit a motoneuron and maintain moderate firing rates (0.81/1.7). With 5-HT administration, the plateau effects are smaller (Fig. 4*B*, *D*), suggesting that plateaus in the chronic spinal rat may be at least as large as in the normal brainstem intact rat. Motoneurons in brainstem intact decerebrate cats have very similar plateau amplitudes to the chronic spinal rat (about 8 mV; Bennett et al. 1998a; see also: Hounsgaard et al. 1988; Lee & Heckman, 1998a,b), and the sustained PIC is on average 6 nA (sustained peak in Lee & Heckman, 1998b), which is again about half the average current to recruit the motoneurons (14 nA; Lee & Heckman, 1998a,b; cat motoneurons require 10 times more current to activate, compared to rat and turtle). Note, however, that the plateau can be further augmented in cats with additional monoaminergic agonists (PIC doubled with methoxamine; Lee & Heckman; see also Svirskis & Hounsgaard, 1998). Finally, in humans the plateau has a similar effect as in decerebrate cats, with the plateau again providing half the estimated input to maintain moderate firing rates (Gorassini et al. 1998, 2001a). Thus, the sustained depolarization and effective PIC current provided by the plateau in chronic spinal rats is comparable to that predicted in intact animals and humans.

Linear firing rate profiles with slow, low-amplitude current ramps

Considering the presence of plateau behaviour in motoneurons, it is remarkable that the firing rate profiles were usually linear, with the plateau prolonging the firing even though

the firing rate remained on the F-I regression line (Type 3 neurons, Fig. 6*C*). We suggest that this linearity occurred because the plateau was mostly activated at or before recruitment and thus did not markedly affect the linearity of firing afterwards, other than to provide a depolarizing bias that brought the cell to a relatively high rate (possibly optimal rate), compared to its minimum rate. In some cells, there was evidence that the plateau was being further activated (or deactivated) during firing, and this produced some non-linearities in firing (Type 4 neurons). However, we have primarily studied the plateaus with intracellular current injection, which should raise the plateau threshold in comparison to the threshold seen with synaptic activation (see above; Bennett et al. 1998a), and exaggerate the firing rate non-linearities. Importantly, the relative linearity of firing profiles implies that, even in motoneurons with plateaus, the firing rate profile should closely reflect the input to the motoneurons (Figs. 5*A*, 6*C*, *D*), and this profile can be used to study the input-output properties of other higher threshold motoneurons (with motor unit recordings in the awake rat; Bennett et al. 2001; Gorassini et al. 2001a,b).

The ramp profiles that we used were slow and small in amplitude, thus optimized to clearly see the sustained plateau. This avoided: 1) high firing rates that produced firing rate adaptation (Kernell & Monster, 1982) and 2) non-steady state dynamics of the cells (ramp speed-related), and thus favoured linear firing profiles. Non-linear behaviours can be seen with faster and larger inputs, where higher firing rates are achieved. Thus, the stimulus parameters are very important to consider in designing experiments to study plateaus, especially when studying motor unit firing (Bennett et al. 2001). This is not to say that plateaus are not present with fast, large amplitude inputs: only that they are

harder to study. Finally, because more firing rate adaptation occurred in motoneurons without plateaus (acute spinal rats; Figs. 6*B* & 7*A*), it is possible that the plateaus themselves may have countered firing rate adaptation (in chronic spinal rats). Thus, the presence of PIC may determine the degree of firing rate adaption and associated non-linear firing, with the most firing rate adaptation occurring in pentobarbital anesthetized animals where PIC is blocked (Kernell & Monster, 1982), less in the acute spinal unanesthetized case, and the least in the chronic spinal case where PIC is enhanced (see Lee & Heckman, 1998a,b).

Role of plateaus in spasticity

When the dorsal roots were briefly stimulated in chronic spinal rats, a long-lasting reflex was seen in the motoneurons; this reflex is the counterpart of the long-lasting reflex seen in ventral roots and in the tail muscles during spastic behaviour (Bennett et al. 1999a). The reflex was markedly reduced in duration by hyperpolarization (Fig. 10*C*), indicating that intrinsic voltage-dependent properties of the motoneurons contribute substantially to these spastic reflexes (i.e. plateaus amplify and prolong the reflexes). Further, spasticity in humans has been associated with tonic or poorly modulated motor unit discharge (Gorassini et al. 1999a; Thomas & Ross, 1997), abnormally low firing rates (Powers & Rymer, 1988; Thomas & Ross, 1997) and impaired rate modulation (Heckman, 1994; Wiegner et al. 1993); these findings are each consistent with the emergence of a plateau, as discussed above (i.e. increased PIC and associated conductance, without lower AHP). The finding that the long-lasting reflexes associated with spasticity are mediated in large

part by plateaus throws new light on the antispastic action of baclofen, which has recently been shown to inhibit L-type calcium currents and plateaus (Russo et al. 1998; Svirskis & Hounsgaard, 1998).

Our results also indicate that the exaggerated reflexes following spinal cord injury are in part produced by a relatively protracted synaptic input (EPSP lasting about 1 s in Fig. 10*C*; see also Baker and Chandler, 1987b). A single low-threshold shock to the dorsal roots is enough to evoke this long EPSP, even at hyperpolarized levels. Considering that plateaus are slow activating, we suggest that this long EPSP serves to prolong the effect of a brief afferent stimulation sufficiently to trigger a plateau, which in turn produces many seconds of firing. A similar long EPSP is seen in motoneurons during flexor-reflex-afferent (FRA) stimulation in DOPA-treated acute spinal cats, which is likewise prolonged by plateau potentials intrinsic to the motoneurons (Conway et al. 1988)

As we have described above, the plateau potential amplitude after chronic injury recovers to a level comparable to that estimated in normal intact animals, so the fact that we do not see spastic-like long-lasting reflexes in intact animals and humans likely involves major differences in inhibitory, as well as excitatory, control of motoneurons in intact and spinal states. Moderately long-lasting stimulation (1 s muscle vibration) can trigger self-sustained motor unit firing in normal humans (plateau, Gorassini et al. 1998, 2001a), but this firing can be inhibited easily by descending inhibition (e.g. reduction in volitional effort). This descending inhibition is lacking following complete spinal cord injury.

In summary, following chronic injury, three factors combine in the production of spasticity: 1) moderately long-lasting synaptic events emerge in response to brief, low-threshold afferent stimuli, 2) plateau behaviour is recovered, and prolongs these synaptic events by many seconds and 3) the normal inhibitory control is lacking, enabling firing to continue, and ultimately contribute to protracted muscle spasms and hypertonus associated with spasticity.

TABLES

	n	R_{in} (MΩ)	Rheobase (nA)	AHP amplitude (mV)	AHP duration (ms)
Acute spinal	22	13.5 ± 7.8	2.4 ± 2.2	5.1 ± 1.8	73.5 ± 25.1
Chronic spinal	35	14.6 ± 10.5	1.7 ± 1.5	5.8 ± 3.4	102.1 ± 26.1 *

TABLE 3-1. SUMMARY OF PASSIVE INPUT RESISTANCE (R_{IN}), RHEOBASE AND AHP IN SACROCAUDAL MOTONEURONS.

R_{in} measured with a hyperpolarizing current pulse or ramp (0.3 nA), starting from resting potential. AHP measured from an antidromically evoked spike. The AHP duration was significantly longer in chronic, compared to acute, spinal rats. R_{in}, rheobase, and AHP amplitude were not significantly different. * indicates significant difference in acute and chronic spinal rats.

FIGURES

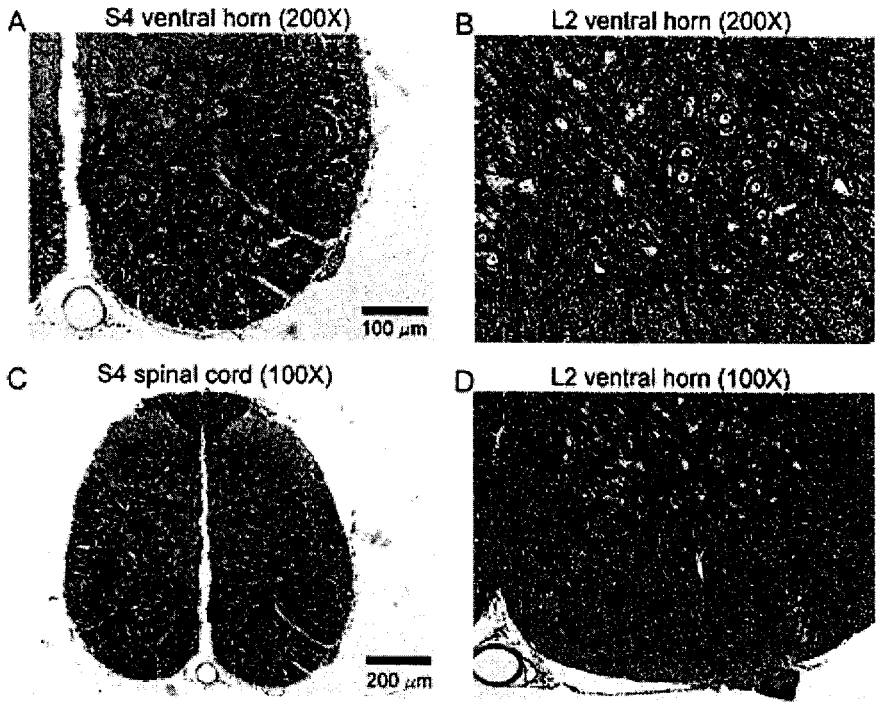

FIGURE 3-1. ANATOMY OF SACROCAUDAL SPINAL CORD.

A, C: Transverse section through the S_4 sacral spinal cord, at two magnifications. Note the motoneurons within 100 μm of the surface (arrows). Caudal spinal cord sections are even smaller (200 μm radius at Ca1; not shown). B, D: Lumbar spinal cord sections are much larger, though the lumbar and sacral motoneurons are similar in size (arrows). For orientation, note the midline ventral artery at bottom left corner in A and D. Cut axons in the white matter are seen as black dots/flecks. The S_4 section tore at midline during processing.

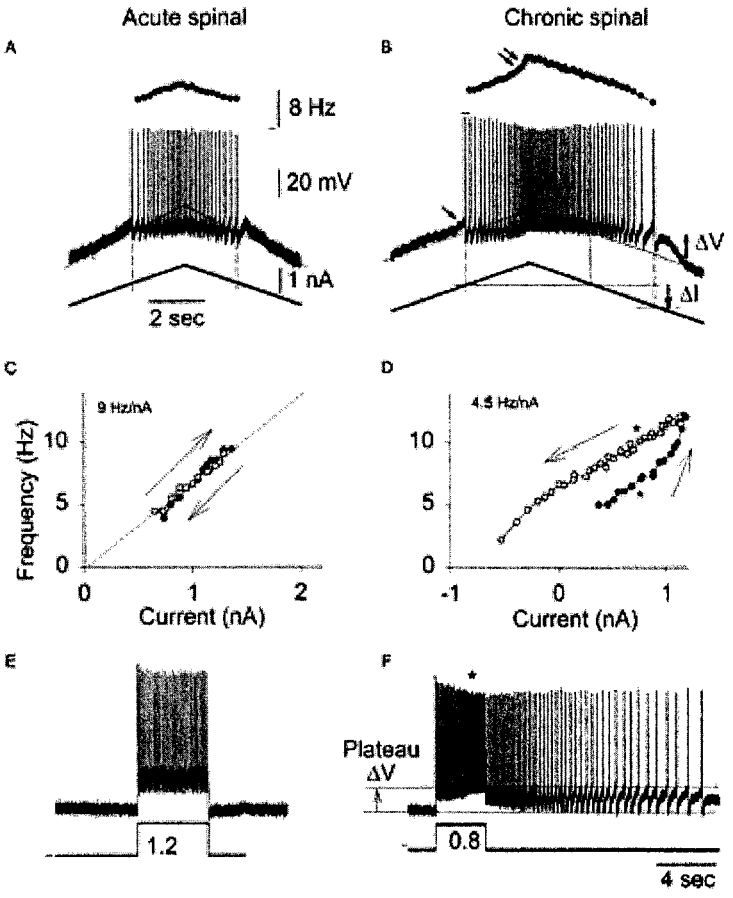
Acute spinal
Chronic spinal
A
B
8 Hz
20 mV
1 nA
2 sec
ΔV
ΔI
C
D
9 Hz/nA
4.5 Hz/nA
Frequency (Hz)
10
5
0
0
1
2
Current (nA)
-1
0
1
Current (nA)
E
F
1.2
Plateau
ΔV
0.8
4 sec

FIGURE 3-2. PLATEAU IN LOW-THRESHOLD MOTONEURON OF CHRONIC SPINAL RAT.

A: membrane potential and firing rate response to slow current ramp in low-threshold motoneuron of *acute* spinal rat. Note symmetry of response in relation to current, and thus lack of plateau. Scaled current (thin line) plotted with potential for reference. Tick marks denote 0 Hz. B: response to same current ramp in low-threshold motoneuron of *chronic* spinal rat. Note acceleration in potential (single arrow) and firing (double arrow), indicating the onset of a plateau (ie. PIC). The plateau caused a sustained depolarization (ΔV) and discharge that continued until the current was reduced by ΔI (= -PIC). C and D: frequency-current (F-I) plots for A and B. Black symbols, upward ramp; white, downward. Note the late acceleration in firing in D (chronic spinal), though overall lower F-I slope than in acute spinal rat. E and F: responses to current pulses in acute and chronic spinal rats. The plateau caused self-sustained firing in the chronic spinal rat (F, plateau onset at *). Recordings in DCC mode. Normal CSF. Same scales on A, B, E and F.

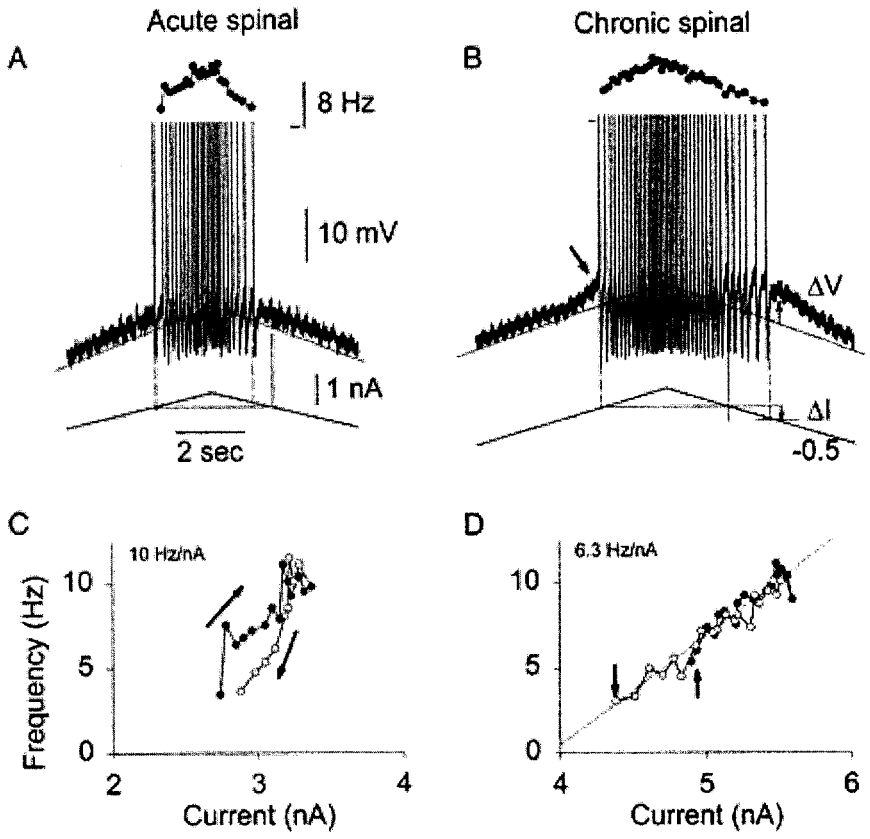

FIGURE 3-3. PLATEAU IN HIGH THRESHOLD MOTONEURON OF CHRONIC SPINAL RAT.

Same format as Fig. 2*A-D*, but motoneurons with higher recruitment threshold. A and C: motoneuron from acute spinal rat that showed no plateau and had firing rate adaptation. B: motoneuron from chronic spinal rat that had a plateau (initiated at arrow) that continued until the current was reduced by $\Delta I = -0.5$ nA. D: note linear F-I plot for same cell, with firing starting on the regression line at upward arrow.

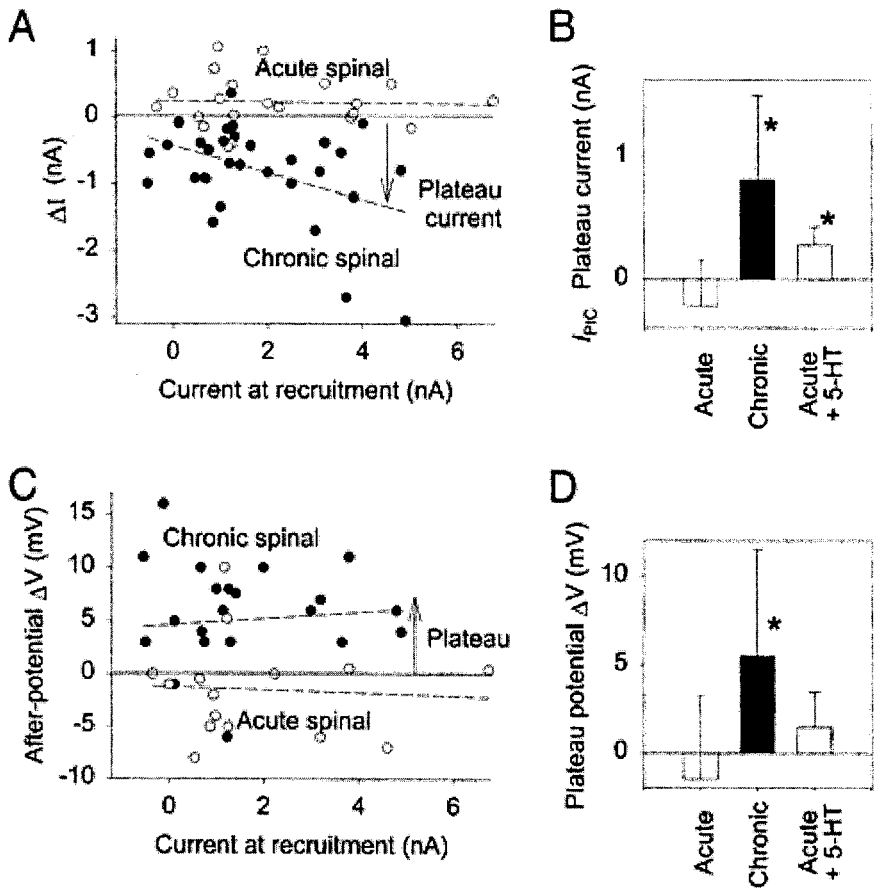

FIGURE 3-4. SUMMARY OF PLATEAU PROPERTIES OF ALL MOTONEURONS.

A: Estimation of plateau current *PIC* from the average current at de-recruitment minus current at recruitment (ΔI = - PIC). Mean value of ΔI for each acute (white symbol) and chronic (black symbol) spinal rat motoneuron is shown as a function of the recruitment current. Dashed lines show respective linear regressions, though there is considerable scatter (r^2 = 0.2 and 0.2). B: summary of average PIC (-ΔI) for acute spinal rats, chronic spinal rats and acute spinal rats with 5-HT. * indicates significant differences from zero. C: Average after-potential for each motoneuron plotted as a function of its recruitment current (same symbols as A). D: Ensemble average of after-potentials; same format as in B.

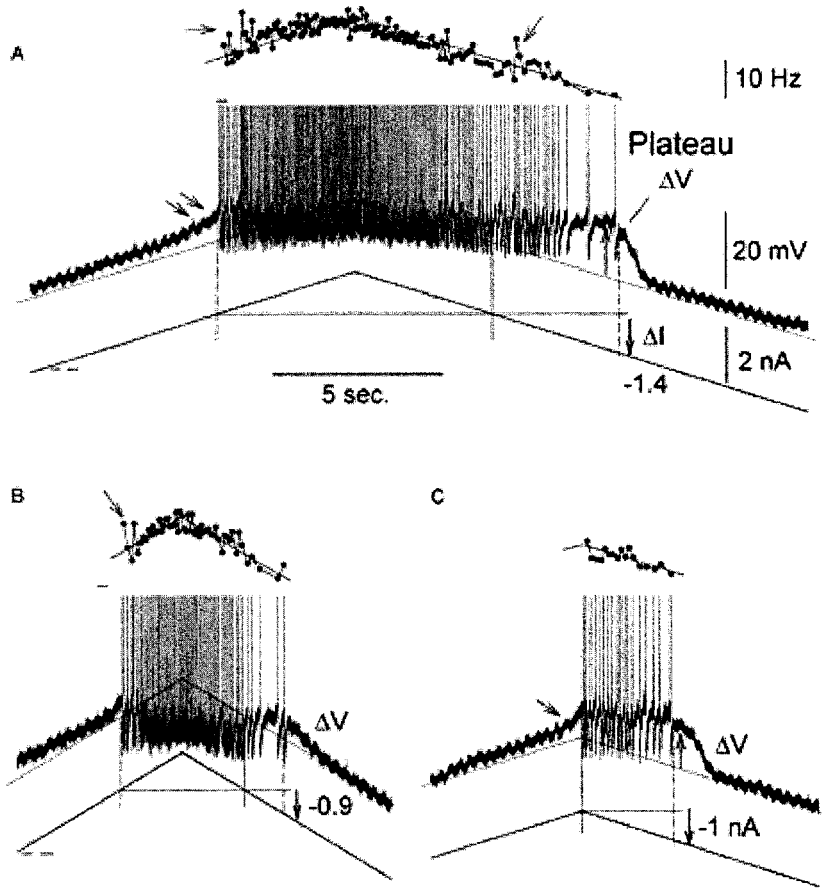

Figure 3-5. Low-threshold plateau activation in chronic spinal rat motoneuron.

Same format as Figs. 2. A: Plateau and sustained firing evoked by slow ramp. Plateau was initiated before recruitment (at double arrow), and produced a large after-potential (ΔV) and an after-discharge that continued until the current was reduced by ΔI = -1.4 nA. B: same cell with faster current ramp. Note the smaller after-potential and after-discharge (related to ΔI). In A and B there was accelerated firing just after recruitment (left arrows; plateau further activated), though afterwards the firing rate varied proportionally to

current (see thin reference line plotted with rate), except near de-recruitment (at arrow in A). C: verification of plateau initiation before recruitment (left at arrow), by using a small current ramp that was reversed just before recruitment. Same cell in A-C.

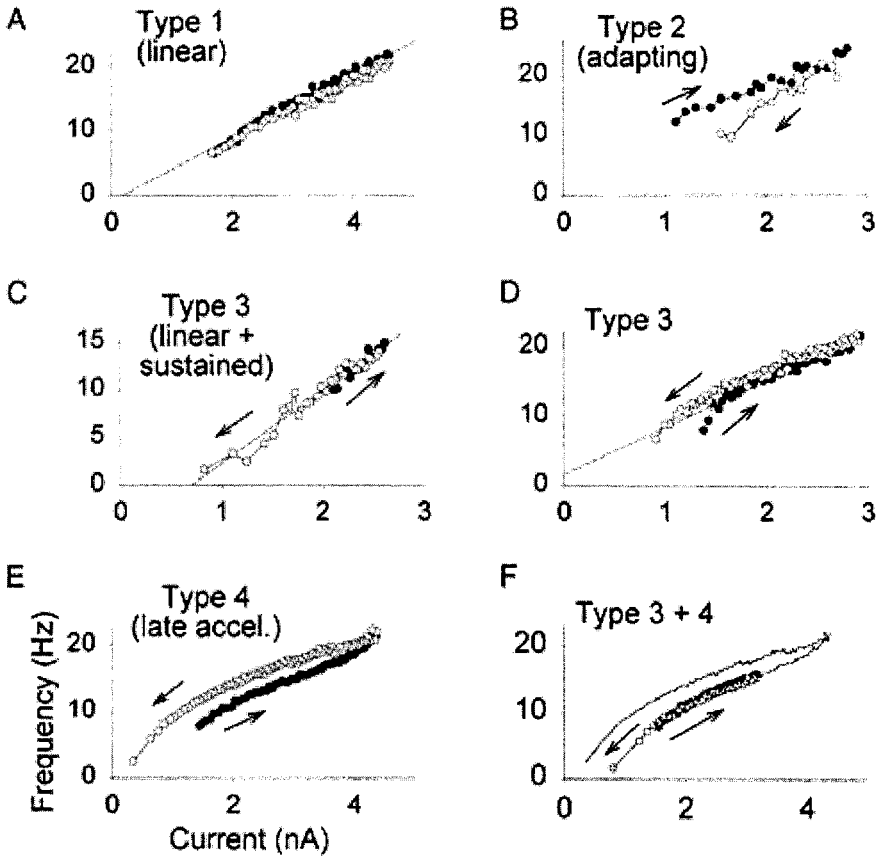

FIGURE 3-6. EXAMPLES OF 4 BASIC TYPES OF FIRING PATTERNS.

Instantaneous frequency-current (F-I) plots for upward (black symbols) and downward (white) current ramps (0.5 nA/s). A-B, two neurons from acute spinal rats. C-E, three neurons from a chronic spinal rats. F shows the response in E (line) overlayed with the response of same neuron with a smaller ramp (symbols). Regression lines shown in A, C and D. See text for details.

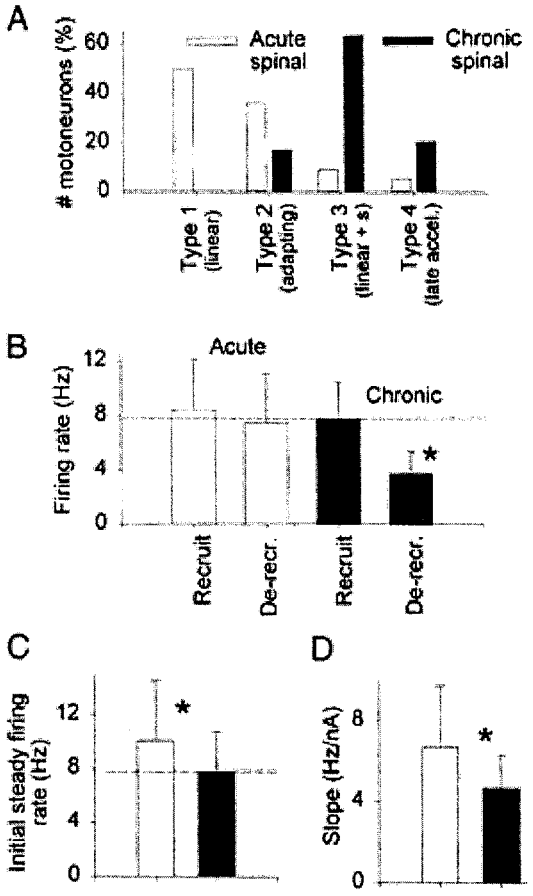

FIGURE 3-7. SUMMARY OF MOTONEURON FIRING PROPERTIES IN ACUTE AND CHRONIC SPINAL RATS.

A: distribution of motoneurons among the 4 types of firing profiles. Note that most cells had a linear F-I profile, both in acute (white bars) and chronic (black) spinal rats, though the latter also had self-sustained firing (Type 3, denoted linear + self-sustained firing). Late acceleration in firing (Type 4) and firing rate adaptation (Type 2) were less common. B: mean firing rates at recruitment and de-recruitment. C: mean initial steady firing rates during slow ramps (see text). D: mean slopes of F-I plots (regression line) in acute and chronic spinal rats. * indicates significant difference.

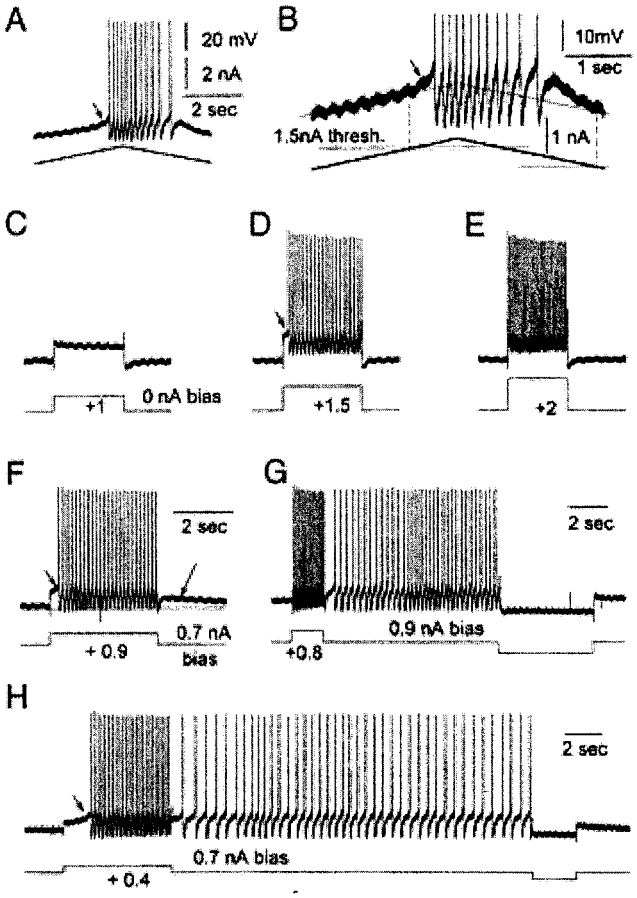

FIGURE 3-8. VOLTAGE-DEPENDENCE OF PLATEAU IN MOTONEURON OF CHRONIC SPINAL RAT.

A: plateau initiated by slow current ramp. B: same data as in A, but on different scale to showing threshold for plateau onset, and estimation of *PIC*. C-E: responses to current pulses without a bias current. Note delay in onset of firing and slow rising potential at arrow in D. F-H: responses to current pulses with a depolarizing bias current. Note plateau activation with after-potential (F) and after-discharges (G, H). Also, note the pause in firing after the pulse (G, H). Small suprathreshold pulses (H) were more effective than larger pulses (F) in evoking a plateau, at a given bias current. Plateau

stopped by hyperpolarizing pulses in G and H. Same neuron for all panels. Same vertical scales in A, C - H. Same time scale in A, C - F.

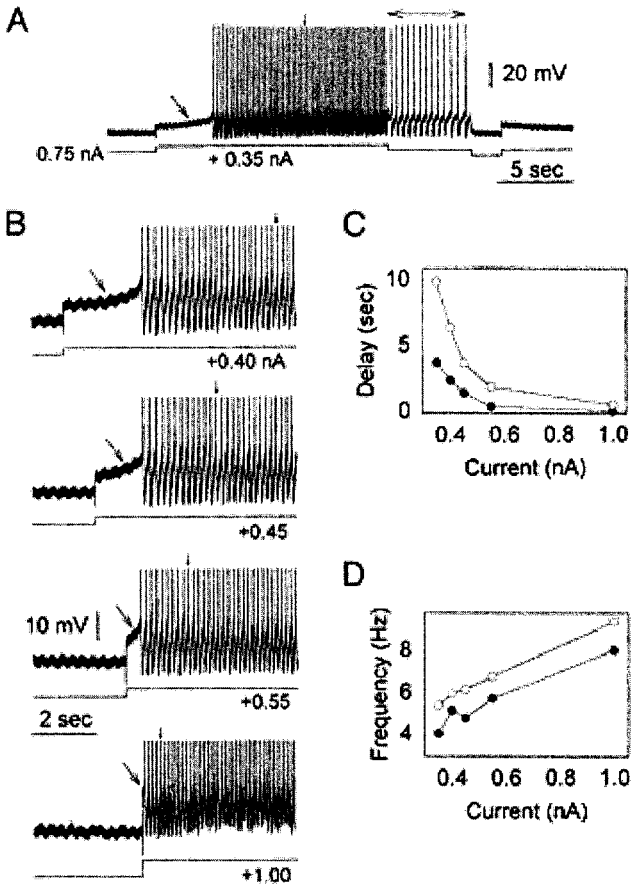

FIGURE 3-9. SLOW PLATEAU ACTIVATION IN CHRONIC SPINAL RAT MOTONEURON.

A: depolarizing current pulse just at threshold to initiate a plateau caused a very slow plateau activation (5 sec delay, at left arrow), followed by an after-discharge. B: progressively larger current pulses produced a faster plateau activation (arrows). Same bias current (0.75 nA) in A and B. Small arrows indicate time at which steady firing was achieved. Different time and voltage scales in A and B. C: delay in onset of firing (black symbols) and steady firing (white) as a function of current. Note that plateau activation was much faster for large pulses. D: initial (black) and steady state (white) firing frequency as a function of current.

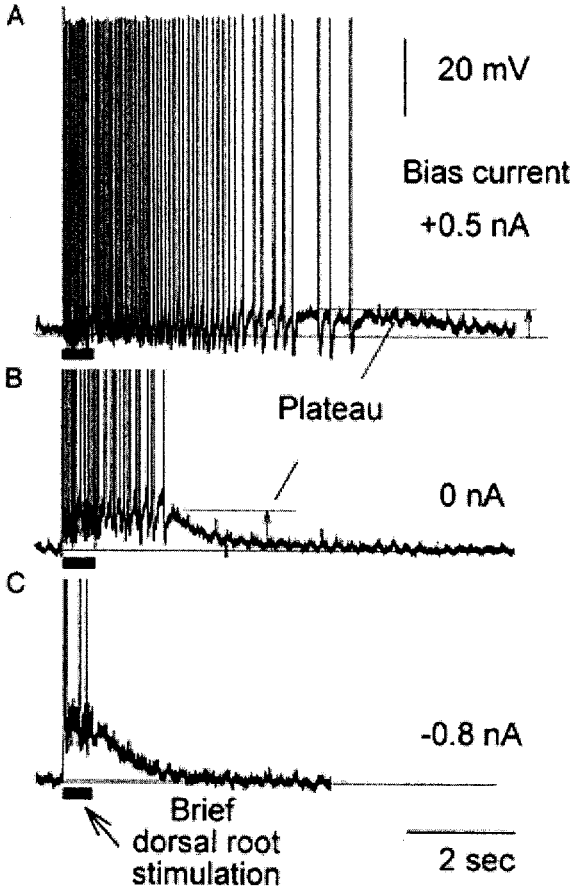

FIGURE 3-10. PLATEAUS TRIGGERED BY BRIEF DORSAL ROOT STIMULATION IN CHRONIC SPINAL RAT MOTONEURON.

A-C: voltage responses of motoneuron to brief stimulation of the Ca_1 dorsal root (20 Hz, 5xT) with various intracellular bias currents. Note the marked reduction in reflex duration as the cell was hyperpolarized and the effect of the voltage-dependent plateau was reduced. In C a sufficient hyperpolarization was applied to eliminate the plateau, and there remained a 1 sec response that outlasted the stimulation.

REFERENCES

Aghajanian, G.K. and Rasmussen, K. Intracellular studies in the facial nucleus illustrating a simple new method for obtaining viable motoneurons in adult rat brain slices. *Synapse* 3: 331_338, 1989.

Ashby, P. and McCrea, D.A. Neurophysiology of spinal spasticity. In: *Handbook of the Spinal Cord.* R.A. Davidoff (ed.), Marcel Dekker Inc., New York, 1987, p.120-143.

Baker, L.L. and Chandler, S.H. Characterization of hindlimb motoneuron membrane properties in acute and chronic spinal cats. *Brain Res.* 420: 333_339, 1987a.

Baker, L.L. and Chandler, S.H. Characterization of postsynaptic potentials evoked by sural nerve stimulation in hindlimb motoneurons from acute and chronic spinal cats. *Brain Res.* 420: 340_350, 1987b.

Bennett, D.J., Hultborn, H., Fedirchuk, B. and Gorassini, M. Synaptic activation of plateaus in hindlimb motoneurons of decerebrate cats. *J. Neurophysiol.* 80: 2023-2037, 1998a.

Bennett, D.J., Hultborn, H., Fedirchuk, B. and Gorassini, M. Short_term plasticity in hindlimb motoneurons of decerebrate cats. *J. Neurophysiol.* 80: 2038_2045, 1998b.

Bennett, D.J., Gorassini, M., Fouad, K., Sanelli, L., Han, Y. and Cheng, J. Spasticity in rats with sacral spinal cord injury. *J. Neurotrauma* 16: 69_84, 1999a.

Bennett, D.J., Gorassini, M.A., and Siu, M. In vitro preparation to study spasticity in chronic spinal rats. Soc. *Neuroscience Abst.* 25:1394, 1999b.

Bennett, D.J., Li, Y., Harvey, P.J. and Gorassini, M. Evidence for plateau potentials in tail motoneurons of awake chronic spinal rats with spasticity. *J. Neurophysiol.* 86 (4): 1955-1971, 2001.

Berger, A.J., Bayliss, D.A. and Viana, F. Modulation of neonatal rat hypoglossal motoneuron excitability by serotonin. *Neurosci. Lett.* 143: 164_168, 1992.

Binder, M.D., Heckman, C.J. and Powers, R.K. The physiological control of motoneuron activity. In: *The Handbook of Physiology.* L.B. Rowell, J.T. Sheperd (eds.), America Physiological Society, Oxford University Press, NY, 1996, sect.12, chapt.1, p.3-53.

Blaschak, M.J., Powers, R.K. and Rymer, W.Z. Disturbances of motor output in a cat hindlimb muscle after acute dorsal spinal hemisection. *Exp. Brain Res.* 71: 377_387, 1988.

Burke, D., Gillies, J.D. and Lance, J.W. The quadriceps stretch reflex in human spasticity. *J. Neurol. Neurosurg. Psychiat.* 33: 216-223, 1970.

Carp, J.S., Powers, R.K. and Rymer, W.Z. Alterations in motoneuron properties induced by acute dorsal spinal hemisection in the decerebrate cat. *Exp. Brain Res.* 83: 539_548, 1991.

Cavallari, P. and Pettersson, L.G. Tonic suppression of reflex transmission in low spinal cats. *Exp. Brain Res.* 77: 201-212, 1989.

Conway, B.A., Hultborn, H., Kiehn, O. and Mintz, I. Plateau potentials in alpha_motoneurons induced by intravenous injection of L_dopa and clonidine in the spinal cat. *J. Physiol. (Lond).* 405: 369_384, 1988.

Cope, T.C., Bodine, S.C., Fournier, M. and Edgerton V.R. Soleus motor units in chronic spinal transected cats: physiological and morphological alterations. *J. Neurophysiol.* 55: 1202-1220, 1986.

Eken, T., Hultborn, H. and Kiehn, O. Possible functions of transmitter-controlled plateau potentials in alpha-motoneurones. In: *Progress in Brain Research* (80). J.H.J. Allum and M. Hulliger (eds.), Elsevier Science Publishers (Biomedical Division), chapt. 21, p. 257-267, 1989.

Gorassini, M.A., Bennett, D.J. and Yang, J.F. Self_sustained firing of human motor units. *Neurosci. Lett.* 247: 13_16, 1998.

Gorassini, M., Bennett, D.J. and Yang, J.F. Excitability of motor units in persons with spasticity from spinal cord injury. *Soc. Neuroscience Abst.* 25:120, 1999a.

Gorassini, M.A., Bennett, D.J., Eken, T. Kiehn, O., and Hultborn, H. Activation patterns of hindlimb motoneurons in the awake rat and their relation to motoneuron intrinsic properties. *J. Neurophysiol.* 82: 709-717, 1999b.

Gorassini, M.A., Yang, J., Siu, M. and Bennett, D.J. Possible role of plateau potentials in human motoneuron discharge: sustained voluntary contractions. *J. Neurophysiol.* (in revision) 2001a.

Gorassini, M.A., Yang, J., Siu, M. and Bennett, D.J. Possible role of plateau potentials in human motoneuron discharge: short-term facilitation by repeated contractions. *J. Neurophysiol.* (in revision) 2001b.

Guertin, P.A. and Hounsgaard, J. NMDA_Induced intrinsic voltage oscillations depend on L_type calcium channels in spinal motoneurons of adult turtles. *J. Neurophysiol.* 80: 3380_3382, 1998.

Guertin, P.A. and Hounsgaard, J. Non_volatile general anaesthetics reduce spinal activity by suppressing plateau potentials. *Neuroscience* 88: 353_358, 1999.

Gustafsson, B., Katz, R. and Malmsten, J. Effects of chronic partial deafferentation on electrical properties of lumbar alpha-motoneurons in the cat. *Brain Res.* 246: 23-33, 1982.

Heckman, C.J. Alterations in synaptic input to motoneurons during partial spinal cord injury. *Med. Sci. Sports Exerc.* 26: 1480_1490, 1994. Review.

Hochman, S. and McCrea, D.A. Effects of chronic spinalization on ankle extensor motoneurons. II. Motoneuron electrical properties. *J. Neurophysiol.* 71: 1468-1479, 1994.

Hochman, S., Jordan, L.M. and Schmidt, B.J. TTX_resistant NMDA receptor_mediated voltage oscillations in mammalian lumbar motoneurons. *J. Neurophysiol.* 72: 2559_2562, 1994.

HODGKIN, A.L. The local electric changes associated with repetitive action in a non-medullated nerve. *J. Physiol. (Lond).* 107: 165-181, 1948.

HOUNSGAARD, J., HULTBORN, H., JESPERSEN, B. AND KIEHN, O. Bistability of alpha_motoneurones in the decerebrate cat and in the acute spinal cat after intravenous 5_hydroxytryptophan. *J. Physiol. (Lond).* 405: 345_367, 1988.

HOUNSGAARD, J. AND KIEHN, O. Serotonin_induced bistability of turtle motoneurones caused by a nifedipine_sensitive calcium plateau potential. *J. Physiol. (Lond).* 414: 265_282, 1989.

HULTBORN, H. AND MALMSTEN, J. Changes in segmental reflexes following chronic spinal cord hemisection in the cat. I. Increased monosynaptic and polysynaptic ventral root discharges. *Acta Physiol. Scand.* 119: 405-422, 1983a.

HULTBORN, H. AND MALMSTEN, J. Changes in segmental reflexes following chronic spinal cord hemisection in the cat. II. Conditioned monosynaptic test reflexes. *Acta Physiol. Scand.* 119: 423-433, 1983b.

HULTBORN, H. AND KIEHN, O. Neuromodulation of vertebrate motor neuron membrane properties. *Current Opinion in Neurobiology* 2: 770_775, 1992.

JANKOWSKA, E., JUKES, M.G.M., LUND, S. AND LUNDBERT, A. The effect of DOPA on the spinal cord. 6. Half_centre organization of interneurones transmitting effects from the flexor reflex afferents. *Acta Physiol. Scand.* 70: 389_402, 1967.

JIANG, M.C., CLELAND, C.L. AND GEBHART, G.F. Intrinsic properties of deep dorsal horn neurons in the L6_S1 spinal cord of the intact rat. *J. Neurophysiol.* 74: 1819_1827, 1995.

KERNELL, D. Repetitive impulse firing in motoneurons: facts and perspectives. *Prog. Brain Res.* 123: 31_37, 1999. Review.

KERNELL, D. AND MONSTER, A.W. Time course and properties of late adaptation in spinal motoneurones of the cat. *Exp. Brain Res.* 46: 191_196, 1982.

KIEHN, O. AND EKEN, T. Prolonged firing in motor units - evidence of plateau potentials in human motoneurons? *J. Neurophysiol.* 78: 3061-3068, 1997.

KIEHN, O., JOHNSON, B.R. AND RAASTAD, M. Plateau properties in mammalian spinal interneurons during transmitter_induced locomotor activity. *Neurosci.* 75: 263_273, 1996.

KIERNAN, J.A. Histological and Histochemical Methods: Theory and Practice. Pergamon Press: Elmsford, New York, 1990.

KRENZ, N.R. AND WEAVER, L.C. Sprouting of primary afferent fibers after spinal cord transection in the rat. *Neurosci.* 85: 443_458, 1998.

KUHN, R.A. AND MACHT, M.B. Some manifestations of reflex activity in spinal man with particular reference to the occurrence of extensor spasm. *Bull. Johns Hopkins Hosp.* 84: 43-75, 1948.

LEE, R.H. AND HECKMAN, C.J. Bistability in spinal motoneurons in vivo: systematic variations in rhythmic firing patterns. *J. Neurophysiol.* 80: 572_582, 1998a.

LEE, R.H. AND HECKMAN, C.J. Bistability in spinal motoneurons in vivo: systematic variations in persistent inward currents. *J. Neurophysiol.* 80: 583_593, 1998b.

LI, Y., HARVEY, P.J. AND BENNETT, D.J. Spastic long-lasting reflexes in the chronic spinal rat, studied in vitro. *J. Neurophysiol. (in press),* 2004.

LONG, S.K., EVANS, R.H., CULL, L., KRIJZER, F. AND BEVAN, P. IN VITRO mature spinal cord preparation from the rat. *Neuropharmacology* 27: 541-546, 1988.

MA, J.Y., CATTERALL, W.A. AND SCHEUER, T. Persistent sodium currents through brain sodium channels induced by G protein betagamma subunits. *Neuron.* 19: 443_452, 1997.

MAILIS, A. AND ASHBY, P. Alterations in group Ia projections to motoneurons following spinal lesions in humans. *J. Neurophysiol.* 64: 637_647, 1990.

MCNICHOLAS, L.F., MARTIN, W.R., SLOAN, J.W. AND NOZAKI, M. Innervation of the spinal cord by sympathetic fibers. *Exp. Neurol.* 69: 383_394, 1980.

McQUISTON, A.R. AND MADISON, D.V. Muscarinic receptor activity induces an afterdepolarization in a subpopulation of hippocampal CA1 interneurons. *J. Neurosci.* 19: 5703_5710, 1999.

MORISSET, V. AND NAGY, F. Ionic basis for plateau potentials in deep dorsal horn neurons of the rat spinal cord. *J. Neurosci.* 19: 7309_7316, 1999.

NEWTON, B.W. AND HAMILL, R.W. The morphology and distribution of rat serotoninergic intraspinal neurons: an immunohistochemical study. *Brain Res. Bull.* 20: 349_360, 1988.

NICHOLSON, C. AND HOUNSGAARD, J. Diffusion in the slice microenvironment and implications for physiological studies. *Fed. Proc.* 42: 2865_2868, 1983.

NIELSEN, J. AND HULTBORN, H. Regulated properties of motoneurons and primary afferents: new aspects on possible spinal mechanisms underlying spasticity. In: *Spasticity: Mechanisms and Management.* Thilmann et al. (eds.), Springer-Verlag Berlin, 1993, p. 177-191.

NOTH, J. Trends in the pathophysiology and pharmacotherapy of spasticity. *J. Neurol.* 238: 131-139, 1991.

POWERS, R.K. AND RYMER, W.Z. Effects of acute dorsal spinal hemisection on motoneuron discharge in the medial gastrocnemius of the decerebrate cat. *J. Neurophysiol.* 59: 1540-1556, 1988.

POWERS R.K., CAMPBELL D.L., RYMER W.Z. Stretch reflex dynamics in spastic elbow flexor muscles. Ann Neurol. 25: 32-42, 1989.

REKLING, J.C., FUNK, G.D., BAYLISS, D.A., DONG, X.W. AND FELDMAN, J.L. Synaptic control of motoneuronal excitability. *Physiological Rev.* 80: 767-852, 2000.

REMY-NERIS, O., BARBEAU, H., DANIEL, O., BOITEAU, F. AND BUSSEL, B. Effects of intrathecal clonidine injection on spinal reflexes and human locomotion in incomplete parapalegic subjects. *Exp. Brain Res.* 129: 433-440, 1999.

RUSSO, R.E. AND HOUNSGAARD, J. Plateau_generating neurones in the dorsal horn in an in vitro preparation of the turtle spinal cord. *J. Physiol. (Lond.)* 493: 39_54, 1996.

RUSSO, R.E. AND HOUNSGAARD, J. Dynamics of intrinsic electrophysiological properties in spinal cord neurones. *Prog. Biophys. Mol. Biol.* 72: 329_365, 1999.

RUSSO, R.E., NAGY, F. AND HOUNSGAARD, J. Modulation of plateau properties in dorsal horn neurones in a slice preparation of the turtle spinal cord. *J. Physiol. (Lond.)* 499: 459-474, 1997.

RUSSO, R.E., NAGY, F. AND HOUNSGAARD, J. Inhibitory control of plateau properties in dorsal horn neurones in the turtle spinal cord *in vitro*. *J. Physiol. (Lond.)* 506: 795-808, 1998.

SCHWINDT, P.C. AND CRILL, W.E. Membrane properties of cat spinal motoneurons. In: *Handbook of the spinal cord.* R.A. Davidoff (ed.), Marcel Dekker Inc., New York, 1984, p. 199-242.

SCHWINDT, P.C. AND CRILL, W.E. Amplification of synaptic current by persistent sodium conductance in apical dendrite of neocortical neurons. *J. Neurophysiol.* 74: 2220-2224, 1995.

STEG, G. Efferent muscle innervation and rigidity. *Acta Physiol. Scand.* 61: 1-53, 1964.

STEERS, W.D. Rat: overview and innervation. *Neurourol. Urodyn.* 13: 97_118, 1994. Review.

STEPHENS, M., BOBET, J., HAN, L., SANELLI, L. AND BENNETT, D.J. Changes in muscle mechanical properties following chronic sacral spinal cord injury in rats. *Soc. Neuroscience Abst.* 25:1145, 1999.

SVIRSKIS, G. AND HOUNSGAARD J. Depolarization_induced facilitation of a plateau_generating current in ventral horn neurons in the turtle spinal cord. *J. Neurophysiol.* 78: 1740_1742, 1997.

SVIRSKIS, G. AND HOUNSGAARD, J. Transmitter regulation of plateau properties in turtle motoneurons. *J. Neurophysiol.* 79: 45_50, 1998.

TAYLOR, J.S., FRIEDMAN, R.F., MUNSON, J.B. AND VIERCK JR., C.J. Stretch hyperreflexia of triceps surae muscles in the conscious cat after dorsolateral spinal lesions. *J. Neurosc.* 17: 5004-5015, 1997.

THILMANN, A.F., FELLOWS, S.J. AND GARMS, E. The mechanism of spastic muscle hypertonus. Variation in reflex gain over the time course of spasticity. *Brain* 114: 233_244, 1991.

THOMAS, C.K. AND ROSS, B.H. Distinct patterns of motor unit behavior during muscle spasms in spinal cord injured subjects. *J. Neurophysiol.* 77: 2847_2850, 1997.

THOMPSON, F.J., PARMER, R. AND REIER, P.J. Alteration in rate modulation of reflexes to lumbar motoneurons after midthoracic spinal cord injury in the rat. I. contusion injury. *J. Neurotrauma* 15: 495_508, 1998.

WIEGNER, A.W., WIERZBICKA, M.M., DAVIES, L. AND YOUNG, R.R. Discharge properties of single motor units in patients with spinal cord injuries. *Musc. Nerve* 16: 661_671, 1993.

YOUNG, R.R. Spasticity: A review. *Neurol.* 44: S12-S20, 1994.

Chapter 4: Persistent sodium and calcium current cause plateau potentials in motoneurons of chronic spinal rats

(Revised from Li and Bennett, J. Neurophysiol. 90: 857-869, 2003)

INTRODUCTION

Motoneurons can produce plateau potentials that amplify and sustain their motor output (Bennett et al. 1998a, b; Hounsgaard and Kiehn 1989; Hultborn 2002; Kiehn and Eken 1997; Lee and Heckman 1998b; Schwindt and Crill 1982). That is, in motoneurons there are voltage-dependent persistent inward currents (PICs) that are regeneratively activated once the membrane is depolarized beyond a critical threshold (about -45 to -55 mV) by a brief stimulus (~ 1 sec). These currents can remain active for many seconds afterwards, and produce a sustained depolarization (plateau) and after-discharge (self-sustained firing). In motoneurons these PICs underlying the plateau are mainly mediated by calcium currents from low threshold L-type calcium channels (Cav1.3 type, Carlin et al. 2000b; Hounsgaard and Kiehn 1985, 1993), though persistent sodium currents may also play a role (Hsiao et al. 1998; Lee and Heckman 2001), and outward voltage- and calcium-dependent K^+ currents can oppose the inward calcium current (Hounsgaard and Kiehn 1989). Thus the PIC is considered to be the net persistent current from the combined inward and outward current sources.

The ability to activate plateaus in normal motoneurons relies on the facilitation of PICs by neuromodulators such as 5-HT (Hounsgaard and Kiehn 1989; Hsiao et al. 1998), NE (Foehring et al. 1989), or glutamate (through mGluR1 receptors, Svirskis and Hounsgaard 1998), and this occurs both by a direct facilitation of L-type calcium channels (Hounsgaard and Kiehn 1989) or by reduction of opposing outward K^+ currents (Hounsgaard and Kiehn 1989; Hultborn and Kiehn 1992). Evidence from awake humans

(Gorassini et al. 1998; Kiehn and Eken 1997) and animals (Gorassini et al. 1999), and brainstem intact decerebrate cats (Hounsgaard et al. 1984) indicates that there is normally an adequate supply of neuromodulators to enable plateaus and associated self-sustained firing in motoneurons. Following an *acute spinal cord transection*, these brainstem-derived neuromodulors are lost, and motoneurons caudal to the injury lose their ability to produce plateaus. However, these motoneurons regain their ability to produce plateaus with externally applied neuromodulators, such as 5-HT_2, NE α_1, $mGluR_1$ and muscarine receptor agonists (Conway et al. 1988; Hounsgaard and Kiehn 1985, 1989; Svirskis and Hounsgaard 1998), or with stimulation activating neuromodulator release (Delgado-Lezama et al. 1999).

Although *acute* spinal cord transection can eliminate plateaus in motoneurons, recent evidence indicates that these motoneurons somehow regain their ability to produce plateaus over the months that follow the injury (Bennett et al. 2001a,b; Eken et al. 1989). For example, following chronic sacral spinal transection, the motoneurons below the injury spontaneously exhibit plateaus, even though they were completely isolated from the brainstem and there was no externally applied neuromodulators or facilitated neuromodulator release (Bennett et al. 2001a,b). Ultimately, these plateaus cause an enhanced intrinsic excitability that leads to spasms in affected muscles (Bennett et al. 2001a), and thus are of major clinical significance.

The purpose of the present paper was to examine the ionic mechanisms underlying these spontaneous plateaus that emerge in *chronic spinal rats* despite the lack of brainstem

control or externally applied neuromodulators. Considering the involvement of the L-type calcium channels in plateaus generation in other preparations, we first examined whether blocking calcium currents could eliminate the plateaus. Surprisingly, the PIC and plateaus could only be reduced to about half their initial values with a calcium channel blockade. The remaining PIC was found to be mediated by TTX-sensitive persistent sodium currents. Part of this work has been previously published in abstract form (Li et al. 2001).

METHODS

Both normal adult female Sprague-Dawley rats (> 60 days old, n = 5) and spastic rats with chronic spinal cord injury (> 90 days old, n = 35) were included in the present study. For the spastic rat, a complete spinal cord transection was made at the S_2 sacral level when the rat was 40 to 50 days old (Bennett et al. 1999a; Bennett et al. 2001a,b). Usually, within 30 days dramatic spasticity developed in the tail muscles, which are innervated by motoneurons below the level of the injury. Only rats more than 50 days post injury with clear spasticity were included in the present study (see Bennett et al. 1999 for details of the animal model). All experimental procedures were approved by the University of Alberta animal welfare committee (HSAPWC).

In vitro preparation

The detailed *in vitro* procedures have been described previously (Bennett et al. 2001c). Briefly, normal and chronic spinal rats were anaesthetized with urethane (0.9 mg/100 g), and the whole cord caudal to the L_{12} vertebrate (which is above the S_2 injury level in chronic spinal rats) with the attached ventral and dorsal roots was exposed and wetted with modified artificial cerebral spinal fluid (mACSF). The rat was then given pure oxygen with a mask until the dorsal vein turned bright red and then the cord was quickly removed to the dissection chamber, and immersed in mACSF. In contrast to the previous paper, the dorsal roots attached to the cord were cut off (except the Ca_1 caudal dorsal roots, which were kept together with the caudal equina), and the cord was glued (super glue; RP 1500, Adhesive Systems Inc.) onto a small piece of nappy paper (with the

ventral side facing up) to increase stability. After an hour's rest in the dissection chamber maintained at room temperature (20°C), the cord was transferred to the recording chamber, where it was immersed in continuously flowing (at a rate of 5 ml/min) normal ACSF (nACSF), which was maintained at 25°C. The cord was then secured at the bottom of the recording chamber by pinning the nappy paper onto the Sylgard base of the chamber.

Intracellular recording

The long ventral roots (usually sacral S_4 and caudal Ca_1) and caudal equina were mounted on silver-chloride wires supported above the recording chamber fluid and covered with high vacuum grease. Sharp intracellular recording electrodes were made from thick wall glass capillaries (Warner GC 150F-10, 1.5 mm OD) with a micropipette puller (Sutter P-87 puller), filled with a 1:1 mixture of 2 M KAcetate and 2 M KCl to give an initial impedance of 40 to 60MΩ, and beveled down to 20 to 30 MΩ on a rotary grinder (Sutter, BV-10, fine 006 beveling stone). Electrodes had a short bee-stinger shape for maximum current passing capability to enable good voltage clamp. Electrodes were advanced perpendicularly into the ventral surface of the cord with a stepper-motor micromanipulator (660, Kopf), initially with fast 30 μm steps to pass the pia and white matter, and then with 2 μm steps. Ventral roots were stimulated with 0.1 ms, 0.015 mA (2xT) pulses at 1 Hz to evoke an antidromic field during the search for motoneurons. Brief capacitance over compensation was applied to produce a high frequency current to break the cell membrane. Motoneurons were identified by antidromic spikes from ventral root stimulation. Only motoneurons with a stable penetration, resting potential < -60 mV,

spike amplitude >60 mV, and reliable repetitive firing were included in the study. An Axoclamp2b intracellular amplifier (Axon Instruments) running in either discontinuous current-clamp modes (DCC, switching rate 7 to 10 kHz, output bandwidth 3.0 kHz) or discontinuous voltage-clamp modes (gain 1 to 2.5 nA/mV) were used to collect the data.

Drugs and solution

Two kinds of ACSF were used in the experiments: nACSF in the recording chamber and mACSF in the dissection chamber prior to recording. The composition of nACSF was (in mM): 122 NaCl, 24 $NaHCO_3$, 2.5 $CaCl_2$, 3 KCl, 1 $MgSO_4$ and 12 D-glucose. The composition of mACSF was (in mM): 118 NaCl, 24 $NaHCO_3$, 1.5 $CaCl_2$, 3 KCl, 5 $MgCl_2$, 1.4 NaH_2PO_4, 1.3 $MgSO_4$, 25 D-glucose and 1 μM Kynurenic acid; the latter is a non-specific blocker of glutamate transmission (Kekesi et al. 2002). Both kinds of ACSF were saturated with 95% O_2 - 5% CO_2, and maintained at pH 7.4. Drugs added to the nACSF in the experiments included: 0.5 to 2 μM TTX (RBI), 3 to 20 μM nimodipine (Sigma), 400 μM Cd^{++} (Sigma) and 2 μM conotoxin GVIA (RBI) and 1 μM conotoxin MVIIC (RBI). TTX and Cd^{++} were dissolved in high concentrations (x100) as stocks; nimodipine was dissolved in DMSO before each experiment (100 to 200mM). These drugs were then diluted to the desired concentration in nACSF. The DMSO concentration was < 0.02% in the final nASCF solution (DMSO had no effect on plateaus, n = 5). The conotoxins were directly dissolved in the nACSF before each experiment.

Persistent inward current in current and voltage clamp recording

Slow triangular current ramps (ramp speed 0.4 nA/s) and voltage ramps (standard ramp speed 3.5 mV/s, varied from 2 to 5 mV/s) were applied to the motoneurons to evoke the plateaus and the associated PIC. During the current ramps (in current-clamp), the persistent inward current that contributed to the plateau and sustained firing was estimated from the difference in injected current required to terminate a plateau (I_{end}), compared to the current required to start the plateau ($\Delta I = I_{end} - I_{start}$, see Fig. 2A or 3A and Bennett et al, 2001b for detail). During voltage ramps (in voltage-clamp), the amplitude of PIC was measured directly, as shown in Fig. 1. That is, when the voltage was increased in a slow ramp the measured current initially increased proportionally, due to linear subthreshold leak currents. However, above the PIC threshold the current deviated negatively from following the applied current (at I_{on} in Fig. 1), and ultimately decreased dramatically despite the continued increase in voltage, and thus formed a negative-slope region in the current-voltage relation (N-shaped V-I relation). When the voltage ramp turned downward, the inward current continued, but was ultimately deactivated (at I_{off} in Fig. 1) and thus produced another negative-slope region in V-I relation. To obtain an estimation of the passive leak currents that sum with the PIC to give the recorded current, a linear relation was fit to the subthreshold current response in the linear region 10 mV below the PIC threshold (to give a leak conductance) and extrapolated to more positive voltages (*leak current*, thin triangular line overlaying current; Fig. 1). The PIC amplitude was then estimated by subtracting this leak current from the recorded current. The PIC revealed after leak subtraction demonstrated a clear initial peak and sustained peak (Fig. 1, lower trace). There was at times an error in the voltage-clamp when the PIC was activated (deviation from triangular shape), and this

was compensated for by scaling the actual voltage recorded by the leak conductance and using this as the leak current.

Following the terminology of Lee and Heckman (Lee and Heckman 1998a), the first zero slope point on the up ramp in the recorded current was defined as the *onset current* (I_{on}) of the PIC, and the corresponding voltage was defined as the *onset voltage* (V_{on}); the second zero slope point of the recorded current in the up-ramp was defined as the *initial peak current* (I_i) of the PIC; the first zero slope point on the down ramp of the recorded current was defined as the *sustained peak current* (I_s) of the PIC; the second zero slope point on the down ramp of the recorded current was defined as the *offset current* (I_{off}) of the PIC and the corresponding voltage was defined as the *offset voltage* (V_{off}). Since the recorded current went down at the negative slope region, and then went up again during the upward ramp, it always passed the onset current level line twice (the onset current point itself and the later one); the voltage corresponding to this latter point was defined as the *jump-voltage* (Vj; see Results associated with Fig. 9). In some of the motoneurons, the offset of the inward current was very gradual, so it was hard to choose the sustained peak; in these cases, the point on the down ramp corresponding to the same voltage as the onset voltage was defined as the sustained peak. Initial and sustained peak amplitudes after leak subtraction in voltage clamped ramps were measured to quantify the size of the persistent inward currents (as shown in Fig. 1).

The basic properties of the motoneurons, such as cell resistance, firing threshold, firing level were measured during current ramps in DCC mode. The resistance of the

motoneurons was obtained by measuring the slope of the V-I plot at the sub-threshold region during a current-clamp ramp. The spike threshold for each cell was measured from the first spike elicited by the current ramp, at the potential where there first began a rapid acceleration in the rate of depolarization to > 10 V/s (Brownstone et al. 1992; Krawitz et al. 2001).

To better understand the dynamics of the inward currents, a series of voltage steps/pulses were also applied to some of the motoneurons. Each series consisted of 10 consecutive pulses (2.5 mV increases between each pulse), lasting 4.5 seconds.

Data analysis

To avoid warm-up or inactivation between ramps (Bennett et al. 1998a; Bennett et al. 2001a), only ramp responses measured >10 sec after a previous ramp were included in the analysis. Data were analyzed in Clampfit 8.0 (Axon Inst.). Data are shown as averages $\pm$ standard deviation. A Student's *t*-test was used to test for statistical differences, with a significance level of $P < 0.05$.

RESULTS

A total of 35 motoneurons from below a chronic S_2 sacral spinal transection were included in the present study, mostly recorded from the S_4 sacral and Ca_1 caudal segments. These cells had a resistance between 5 to 15 mΩ, resting membrane potential of -66.2 ± 8.5 mV, firing threshold of 1.78 ± 1.51 nA, firing level of -46.1 ± 4.5 mV and spike height of 82.5 ± 10.6 mV.

Plateaus were caused by L-type calcium and TTX-sensitive persistent sodium currents

As we found previously (Bennett et al. 2001b), all motoneurons of chronic spinal rats were able to spontaneously exhibit plateaus (onset at arrow in Fig. 2*A*) and self-sustained firing (that continued at currents below the recruitment current) in response to slow triangular current ramps (Fig. 2*A* and 3*A*). The maintained depolarizations (plateaus) underlying the self-sustained firing were clearly revealed in the presence of TTX (0.5 to 2 μM, n = 16, Fig. 2*B*), where the potential deviated markedly from a linear increase with the current ramp (at arrow), and continued for many seconds as the current was reduced. Either Cd^{++} (400 μM, n = 4), a non-specific calcium channel blocker, or nimodipine (10 to 20 μM, n = 8), a specific L-type calcium channel blocker, completely abolished this TTX-resistant plateau (Fig. 2*C*), indicating that it was mediated by L-type calcium channels. However, when nimodipine (20 μM, n = 9) was added into the nACSF first, although the self-sustained firing was shortened (Fig. 3*A*,*B*), it was not completely eliminated. After nimodipine, the application of 2 μM TTX (n = 7, Fig. 3*C*) completely blocked the remaining plateaus. This result suggested that part of the PIC underlying the

plateau was sensitive to TTX, probably due to a TTX-sensitive persistent sodium current (Hsiao et al. 1998), as shown below. Thus, we estimated the effects of TTX on the PIC itself, as follows.

Previously we have shown that the amplitude of the PIC that produces the plateau and self-sustained firing can be indirectly estimated during current ramps from the reduction in injected current required to terminate the plateau (and self-sustained firing), compared to the current required to initiate the plateau (i.e., PIC $\cong \Delta I = I_{end} - I_{start}$, Figs. 2*A* and 3*A*, also see Fig. 2*B* in Bennett et al. 2001b for detail). Oddly enough, when we compare Fig. 2*A* with Fig. 2*B*, the PIC estimated from ΔI increased when TTX was added, as it did for most other motoneurons when TTX was added (8/10, with an average increase from 0.67 nA to 1.41 nA; see later section). This occurred because TTX has two major effects: it blocks any TTX-sensitive persistent sodium current and it also blocks the spikes; the later eliminates a substantial outward current caused by the spike afterhyperpolarization (AHP), and thus, on balance the estimated PIC increased with TTX. Thus, to directly study the persistent sodium current without the effect of spiking and AHPs, we voltage-clamped the motoneurons to eliminate fast sodium spikes, and this gave a direct measurement of the slow PIC before and after TTX, as follows.

When a slow depolarizing voltage ramp was applied under voltage-clamp conditions, the measured current initially increased linearly (left of Fig. 2*D*, lower trace), but deviated from linear about 10 mV below the spike threshold (dotted line) as the PIC was activated. For these slow ramps the spikes were usually blocked by the voltage-clamp as in Fig. 2*D*

(n = 30 / 35 cells; the remaining 5 cells had 1 or 2 unblocked spikes), and the spike threshold was measured separately during the current clamp, as in Fig. 2A. Eventually the current decreased, even though the voltage continued to increase (at arrow in Fig. 2*D*). This formed a characteristic negative-slope region in the current response (N-shaped V-I relation; see Fig. 1 in Methods for detail), with a drop in current of 1.5 nA in Fig. 2*D* (initial depth of negative-slope region). However, this depth of the negative-slope region is less than the total PIC, because the membrane potential was being ramped up continuously, which caused a proportional increase in current that is estimated by the leak current drawn as a thin line overlaying the current in Fig. 2*D* (see Methods). The difference between the measured current and the leak current represents the total PIC (length of arrow in Fig. 2*D*; 3.25 nA). After TTX the PIC was smaller (arrow in Fig. 2*E*, 1.73 nA) compared to before TTX (Fig. 2*D*, see Table 1 for summary). Also, after TTX the negative-slope region occurred at a higher threshold (above the spike threshold; dotted line). Together, these results indicate that part of the PIC was caused by a TTX-sensitive persistent inward current. The remaining PIC and negative-slope region after TTX (Fig. 2*E*) was completely eliminated by nimodipine (Fig. 2*F*), indicating that it was mediated by L-type calcium channels, in this case (Fig. 2) with a slightly higher threshold than the TTX-sensitive portion of the PIC (near spike threshold).

When nimodipine was applied by itself, the PIC and associated negative-slope region was reduced (Fig. 3*D*,*E*, Table 1), as was the plateau, further confirming the role of L-type calcium channels in plateau production. The remaining PIC after nimodipine was

completely eliminated by TTX (Fig. 3*E* and Fig. 3*F*), again indicating that part of the PIC was sensitive to TTX.

Because TTX not only blocked the postsynaptic sodium channels, but also the presynaptic spike-mediated neurotransmitter release, there remained a question of whether the TTX-sensitive PIC was mediated by this synaptic activity, rather than by a TTX-sensitive persistent sodium current. For example, basal levels of synaptic activity could release glutamate that could induce a PIC either directly (via NMDA receptors) or indirectly (via metabotropic glutamate receptor facilitation of L-type calcium channels, Delgado-Lezama et al. 1999). To answer this question, 400 μM Cd^{++} was added into the nACSF (n= 5; compare PIC and plateaus before and after Cd^{++} in Figs. 4*A*,*D* and 4*B*,*E*). Cd^{++} at this concentration completely blocks pre- and postsynaptic calcium currents, including the L-type calcium currents (as shown above; see also Chow 1991). Thus, Cd^{++} blocks normal presynaptic transmitter release, and indeed we found that Cd^{++} rapidly eliminated both spontaneous and reflex evoked postsynaptic potentials (EPSPs, not shown). After Cd^{++} blocked the calcium channels, there was still a substantial PIC (and plateau) that remained (Fig. 4*B*, *E*), which was completely eliminated by TTX (Fig. 4*C*, *F*; n = 4). This result proves that the TTX-sensitive PIC was indeed mediated by a *TTX-sensitive persistent sodium current*, because with Cd^{++} present TTX can have no effects other than on postsynaptic sodium channels, with all the synaptic activity already blocked and only sodium inward currents remaining. All together, our results demonstrate that the plateaus and self-sustained firing in motoneurons after chronic

spinal cord transection were mediated by both an L-type calcium current *(calcium PIC)* and a persistent sodium current (*sodium PIC*).

Characteristics of the sodium and calcium PIC

AMPLITUDE OF THE SODIUM AND CALCIUM PIC. The amplitude of the PIC in voltage-clamp recordings was quantified by measuring the initial and sustained peak amplitudes of the PIC after subtraction of the leak current (see Methods and Fig. 1 for detail). On average the initial peak was 2.88 $\pm$ 0.95 nA, and the sustained peak was 1.64 $\pm$ 0.52 nA (n = 23). These large PICs occurred in all cells, with no correlation to the leak conductance ($r < 0.5$). When TTX was added into the nACSF (n = 12, Fig. 5*A*), the amplitude of the initial and sustained peak of PIC decreased by 57.6 $\pm$ 22.2% (from 2.95 $\pm$ 0.83 nA to 1.21 $\pm$ 0.60nA) and 36.8 $\pm$ 28.7% (from 1.54 $\pm$ 0.50 nA to 1.03 $\pm$ 0.55 nA) respectively and thus the TTX-sensitive PIC contributed these proportions to the total PIC. The PIC that remained after TTX (white bars in Fig. 5*A*) represented the calcium PIC by itself, because this current was completely eliminated by nimodipine or Cd^{++} (not significantly different from zero; gray bars in Fig. 5*A*, *B*). Thus the calcium PIC contributed 42.4% (1.21 $\pm$ 0.60 nA) of the initial peak and 63.2% (1.03 $\pm$ 0.56 nA) of the sustained peak of the total PIC.

When Cd^{++} was added into the nACSF first (n = 4, Fig. 5*B*), the amplitude of the initial and sustained peak decreased by 61.4 $\pm$ 8.0% (from 2.31 $\pm$ 0.65 nA to 0.89 $\pm$ 0.31 nA) and 63.0 $\pm$ 19.4% (from 1.64 $\pm$ 0.46 nA to 0.57 $\pm$ 0.30 nA), respectively. The PIC that remained after Cd^{++} (white bars in Fig. 5*B*) represented the sodium PIC by itself, because this current was completely eliminated by TTX (not significantly different from zero;

gray bars in Fig. 5*B*). This sodium PIC measured this way (as opposed to with direct application of TTX) contributed 38.6% (0.89 ± 0.31 nA) of the initial peak and 37.0% (0.57 ± 0.30 nA) of the sustained peak of the total PIC. When nimodipine was added into the nACSF (n = 7, Fig. 5*C*), the amplitude of the initial and sustained peak of PIC deceased by 45.2 ± 22.6% (from 3.10 ± 1.25nA to 1.75 ± 0.99 nA) and 45.7 ± 23.3% (from 1.83 ± 0.60nA to 1.01 ± 0.58 nA), respectively. Nimodipine did not block the synaptic transmission in our preparation (data not shown), thus these numbers represent the amplitude of calcium PIC and are similar to the numbers obtained from the experiments adding TTX first, just described. In summary, these results indicate that while sodium and calcium PIC contributed almost equally in generating the initial part of the total PIC, sodium PIC only contributed to ~ 1/3 of the sustained peak and calcium PIC contributed to ~ 2/3 of the sustained peak of the total PIC. The small discrepancies in sodium and calcium PIC estimates with different drug combinations may represent a portion of the PIC that is blocked by the presynaptic actions of TTX or Cd^{++}, as quantified further in the Discussion.

VOLTAGE THRESHOLD OF THE SODIUM AND CALCIUM PIC. In all the motoneurons (20/20 in Fig. 6), the voltage threshold of the PIC (-54.2 ± 4.76 mV) was lower than the firing threshold (-46.1 ± 4.5 mV). Because the voltage threshold of the total PIC is determined by the current with lower voltage threshold, we blocked one of the inward currents to reveal the threshold of the other current. When TTX was added into the nACSF (n = 10, Fig. 6*A*), the voltage threshold of the remaining current (calcium PIC) was on average – 48.7 ± 6.42 mV, significantly higher than before. With TTX the threshold increased in

7/10 motoneurons (by > 2.5 mV), suggesting that in these cells the calcium PIC had a clearly higher voltage threshold than the sodium PIC. In the remainder (3/10), there was only a small change in threshold, suggesting that in these cells calcium PIC either had a lower or similar threshold compared to the sodium PIC. In addition, of the 10 cells studied, 2 cells had a calcium PIC threshold (after TTX) higher than the voltage threshold of the spike (prior to TTX), and the remainder had a calcium PIC threshold below the spike threshold. Thus the voltage threshold of calcium PIC could be either below or above the firing threshold or the sodium PIC threshold.

When Cd^{++} (n = 3) or nimodipine (n = 7, Fig. 6*B*) was added into the nACSF first, the threshold of the remaining current (TTX-sensitive sodium PIC) was -52.8 ± 3.95 mV, not significantly different from before (-54.1 ± 4.48 mV). In most of the cells (8/10) the PIC threshold did not increase (< 2.5 mV change), suggesting that the sodium PIC had a voltage threshold lower or similar to the calcium PIC in these cells. In the other cells (2/10) there was an increase in threshold > 2.5 mV with calcium blockade, suggesting that the calcium PIC had a lower threshold than sodium PIC. However, no matter how the threshold changed with calcium blockade, it never exceeded the firing threshold of these cells, suggesting that sodium PIC was always activated sub-threshold to the spike. In conclusion, our results indicate that: 1) the sodium PIC was activated about 7 mV sub-threshold to the spike; whereas the calcium PIC was activated either lower, or higher (by 5 mV) than the spike threshold; and 2) in most of the motoneurons, the calcium PIC had a higher voltage threshold than the sodium PIC, while in a few of them, calcium PIC had a similar or lower threshold than the sodium PIC The activation voltages of these PICs

were measured at the electrode, which may be different from the actual gating voltages for the channels mediating these currents, considering that these channels may be on distal dendrites (Bennett et al. 1998b; Powers and Binder 2003).

KINETICS OF THE SODIUM AND CALCIUM PIC. As shown above, the sodium PIC decreased significantly during the approximately 8-second long standard voltage ramp (from an average of 0.82 nA initial peak to 0.39 nA sustained peak); in contrast, most of the calcium PIC persisted during the same ramp (from an average of 1.19 nA initial peak to 1.01 nA sustained peak; not significant reduction). These results indicate that the sodium PIC inactivated significantly, while calcium PIC did not. To further study the kinetics of these two different PICs, a series of 4.5 sec voltage steps/pulses of increasing size were applied to the motoneurons (n = 7). With small voltage steps (sub-threshold to the PIC), the current responded simply in proportion to the voltage step, with a step-like shape and amplitude that increased with applied voltage (leak current). When the threshold of the PIC was reached, instead of increasing, the amplitude of the recorded current decreased with increasing pulse size (PIC activated, thick lines in Fig. 7*A*). When the negative peak of the recorded current was plotted against the voltage applied (Fig. 7*B*), an N-shaped V-I relation was formed, with a negative-slope region corresponding to the PIC activation (just as for the slow ramps described in Figs. 1 to 4). This series of voltage steps were applied before (squares in Fig. 7*B*) and after each drug application, and the PIC components were eliminated in succession as expected of blocking the sodium PIC (with TTX, circles) and calcium PIC (with Cd^{++} and TTX, triangles), leaving a linear V-I relation.

Currents recorded from the same supra-threshold depolarizing step/pulse with different drugs applied are overlaid in Fig. 7*C*. With a complete block of the PICs with TTX and Cd^{++} the current response was step-like, and represented the passive leak current (trace-c in Fig. 7*C*). With just TTX present (trace-b, sodium blocked) the current response to the step was initially the same as in trace-c, but after about 1 sec the current dropped, as the calcium PIC was activated. The actual calcium PIC was estimated from subtracting trace-b from c (lower part of Fig. 7*C*). Likewise, the sodium PIC was estimated from subtracting trace-a in normal ACSF from trace-b in TTX. The calcium PIC had a slow onset (~ 1 sec in Fig. 7*C*) that was highly voltage-dependent. That is, the time to activate half of the PIC ($T_{1/2}$) was 250 to 500 ms with high voltage steps, whereas the $T_{1/2}$ was more than 1 second with voltage steps just above threshold (Fig. 7*D*). The slow onset of the calcium PIC is also seen in the raw data in Fig. 7*A* (at vertical lines for traces 5 to 7) recorded in TTX when only the calcium PIC remained. Interestingly, the lowest voltage step (trace 5) evoked a calcium PIC that took more than 2 sec to start and was activated in *two* discrete steps. Once activated, the calcium PIC usually did not inactivate with time (Fig. 7*A*,*C*). Finally, corresponding to its slow activation, the calcium PIC also turned off slowly following the depolarizing step (deactivated slowly). That is, there was usually a tail current following the pulse (5/7, Fig. 7*A*, arrow), which was on average about 1 nA and lasted for about 500 ms. The tail current was not significantly affected by TTX, and completely blocked by nimodipine or Cd^{++}, which indicated that it was mediated by an L-type calcium current; and thus, it serves as a useful positive indicator of the presence of a calcium PIC in normal CSF (Fig. 7*C*, trace-a).

The activation of the sodium PIC (Fig. 7*C*) was in general much more rapid than the calcium activation. However, it was more difficult to study since in normal ACSF there was usually an unclamped sodium spike at the start of the voltage step (not shown), followed by a voltage-clamped outward current corresponding to the AHP currents and lasting ~ 80 ms (brief outward current at onset of step in trace-a of Fig. 7*C*). Nevertheless, following this brief unclamped behavior the sodium PIC was immediately visible, as the current crossed below the dotted zero-line in the lower part of Fig. 7*C* (at 80 ms), and thus the sodium PIC was likely activated in < 80 ms. The sodium PIC reached its peak rapidly (at arrow in Fig. 7*C*), partly inactivated over about 1 sec, and there was usually a steady sodium current that persisted throughout the voltage step. Sometimes, at voltages just below the spike threshold of the cell, we saw a slow onset of sodium PIC (~ 1 sec; data not shown), indicating that just at threshold the sodium PIC could come on slowly. This was a threshold phenomenon, unlike the slow onset of calcium PIC over a wide voltage range (Fig. 7*D*), and it was difficult to study because of the unclamped spikes at higher voltages, as mentioned. The deactivation of the sodium current was rapid (< 50 ms), like its onset, and produced no tail current after the pulse.

Other calcium currents?

Plateaus and the associated PICs were usually completely blocked by nimodipine and TTX, and thus, it was unlikely that other types of calcium currents could play a major role in plateau activation. However, in few cells with nimodipine and TTX added (2/15), there was a low-threshold transient inward current that remained, which produced a brief

depolarization during the current ramps, and was sensitive to Cd^{++}, suggesting that significant low-voltage activated T-type calcium current might exist in these cells (Russo and Hounsgaard 1996), though this needs further investigation. The nimodipine-sensitive persistent calcium current in our preparation was low-voltage activated (around -50 mV), and was probably associated with the Cav1.3 Ca channel with low voltage behavior (see Discussion). This current was usually fully activated at < -40 mV, and indeed we usually did not voltage-clamp our cells above this -40 mV level, suggesting that high-voltage activated calcium channels do not play a major role. However, to directly rule out the involvement of high-voltage activated calcium channels (i.e. N, P, Q-type, etc) in the activation of the PIC, conotoxin GVIA and MVIIC, high-voltage activated calcium channel blockers, were added into the nACSF. Conotoxin GVIA and MVIIC partially blocked the EPSPs and the AHP, but did *not* block plateau or the associated PIC (n = 3, data not shown); and thus, these high-voltage activated calcium currents were not involved in the low threshold PIC studied here.

Sensitivity of the PIC to TTX and nimodipine

In the above results we used standard doses of TTX, Cd^{++} and nimodipine that produced a complete block in about 10 mins (steady state effect). We also tested lower doses to determine these standard doses and judge the sensitivity of the PIC to these drugs. When TTX was applied at the standard dose of 2 μM, it usually blocked the fast sodium spikes in 3 to 5 mins, and at this time the TTX-sensitive portion of the PIC was also nearly completely blocked. Lower doses of TTX (0.5 to 1 μM) gave longer times to block the spike (6 to 14 mins), but the TTX-sensitive portion of the PIC was again blocked at the

same time as the spikes. These results suggest that, at least in the 0.5 to 2 μM range, the fast spike and the PIC have a similar sensitivity to TTX.

When nimodipine was applied at the standard 20 μM dose there was a steady state reduction in the PIC in 8 to 15 mins. This moderately high dose had no effect on the sodium spike, and thus was unlikely to affect the sodium channels. A 10 μM dose took 20 to 30 mins to take effect. Nimodipine doses as low as 3 μM only partly blocked the calcium portion of the PIC (with TTX present), and a further full block required 10 to 20 μM.

Acute spinal rats motoneurons have a small PIC

Consist with the previous studies, motoneurons from acute spinal rats did not produce plateaus in current-clamp recording (Fig. 8*A*), and corresponding to this, they usually (4/5) did not produce a negative-slope region during voltage-clamped ramps (Fig. 8*B*). However, during these voltage ramps there was a small PIC (seen with leak subtraction, arrows in Fig. 8*B*), and this produced an inflection (left arrow) in the current response. The mean initial and sustained peaks of the PIC are 0.59 ± 0.44 and 0.54 ± 0.32 nA respectively, significantly smaller than the PIC in chronic spinal rats (Fig. 8*D*). This PIC is TTX and Cd^{++} sensitive, though we have not quantified the respective sodium and calcium PICs.

Role of PICs in activation of plateaus

In the present section we examine how the PICs measured from voltage-clamp experiments are involved in producing plateaus, similarly to the analysis of Booth et al. (1997) and Lee and Heckman (1998a), but specifically examining the roles of the sodium and calcium PICs. This issue is initially addressed in cells with spikes blocked with TTX (Fig. 9*B*), by replotting the data recorded in current-clamp (plateau; Fig. 9*B*) and voltage-clamp (PIC; Fig. 9*C*) in a voltage-current format (V-I plot; Fig. 9*E* and Fig. 9*F*). In current-clamp (thick line in Fig. 9*E*), when the current was increased between the levels labeled 1 and 2 (horizontal lines in Fig. 9*E*) the voltage increased and followed closely to the V-I plot of the voltage-clamp data (thin line in Fig. 9*E*), as expected of this region sub-threshold to the plateau activation. However, when the current was increased further (in current-clamp) from levels 2 to 3, the membrane potential response (thick line) could no longer continuously follow the V-I plot of the voltage-clamp current response (thin line), but instead the voltage jumped rapidly across the negative-slope region to rejoin the voltage-clamp V-I plot at a current corresponding to the current level 3 (bistable point; Vj). This jump corresponds to the onset of the plateau, and thus: the width of the valley formed by the negative-slope region in the V-I plot corresponds to the amplitude of the plateau that would be produced by the PICs alone, without spikes present (width: Vj - Von, thick arrow in Fig. 9*E*). Interestingly, this width measured in TTX (Table 1) is not significantly different from the corresponding width measured in nimodipine; and thus the respective calcium and sodium PICs must contribute equally to the onset of a plateau (prior to drug applications). Also, either TTX or nimodipine only reduced the width of the negative-slope region marginally from control conditions (only significant reduction

in nimodipine; Table 1), and thus either current is sufficient to activate a large plateau. The primary requirement for a plateau is a negative-slope region of adequate width.

Role of PICs in current-clamp hysteresis, ΔI

During a triangular ramp under current-clamp, when the current was decreased after the PIC activation the voltage response (thick line in Fig. 9*F*; downward ramp) initially followed closely to the associated downward voltage-clamp V-I plot (thin line, covered by thick line from current-clamp; upper right corner of Fig. 9*F*; levels 1 –to 4). However, when the current was decreased further in current-clamp (to level 0 in Fig. 9*F*), the PIC was deactivated, and the potential (thick line) jumped from the bottom of the negative-slope region to the lower-left branch of the voltage-clamp V-I plot (at level 0; bottom left of Fig. 9*F*), as the plateau was terminated. Thus, the relative depth of the negative-slope region on the downward ramp (sustained depth) compared with the onset of the PIC (Ion – Is, sustained depth shown as thick arrow in Fig. 9*C*) corresponds to the current-clamp hysteresis ΔI (Fig. 9*B*). In fact, the mean ΔI measured in current-clamp after TTX (1.41 + 1.13 nA; e.g., 2nA in Fig. 9*B*) was indeed close to the sustained depth (Ion – Is in Fig. 9*C*) of the negative-slope region after TTX (mean 1.12 + 0.66 nA; see Table 1). However, the ΔI measured in current-clamp before TTX (mean 0.67 + 0.36 nA; 1.2 nA in Fig. 9*A*) was significantly smaller than the sustained depth of the negative-slope region before TTX (mean 0.99 + 0.49 nA; see Ion – Is in Fig. 1), due to AHPs associated with spikes in current-clamp, as mentioned earlier. The sustained depth measured in normal ACSF was significantly reduced by nimodipine, but not TTX, indicating that the calcium

PIC plays a primary role in the current-clamp hysteresis and self-sustained firing during long slow ramps. However, the initial depth of the negative slope region (Ion – Ii) was significantly reduced by TTX (Table 1), indicating that the sodium PIC should play a role in the self-sustained firing during short ramps that turn around just after activating the PIC (e.g. Fig. 3).

Voltage-clamp hysteresis

Hysteresis in voltage-clamp PIC response was associated with additionally prolonged plateaus and sustained firing, and we demonstrate next that this PIC hysteresis was mainly caused by the calcium PIC. The voltage-clamp hysteresis is in general seen as a clockwise loop in the V-I plot (Fig. 9*D*). The size of this loop was quantified as the difference between the current or voltage at the onset of the PIC (Ion or Von) and offset of the PIC (Ioff or Voff). This hysterisis (Ion – Ioff or Von – V0ff) was significantly reduced by the application of nimodipine (Table 1), as was the ΔI. In contrast, when the TTX was added the hysteresis (Ion – Ioff or Von – Voff) was not significantly reduced (Table 1), and the ΔI was also not reduced. Thus, most of the voltage-clamp hysteresis was mediated by the calcium PIC (seen with TTX in Fig. 9*D*), while the sodium PIC produced little voltage-clamp hysteresis. Indeed the sodium PIC, seen directly in Cd++ or nimodipine, was usually not hysteretic (see symmetric response in Fig. 4*E*).

DISCUSSION

Our results demonstrate that after *chronic* spinal transection motoneurons exhibit large PICs. These PICs (and associated negative-slope regions) produce large plateaus that have been demonstrated to cause sustained muscle spasms associated with spasticity after chronic spinal cord injury (Bennett et al. 2001a, b). The PICs occur spontaneously, that is, without the application of neuromodulators or facilitation of neurotransmitter release, and remain even after possible spike-mediated transmitter/neuromodulator release is completely blocked by TTX or Cd^{++}. Acute spinal transection is only associated with small PICs, consistent with the lack of plateaus or spastic behavior (Bennett et al. 2001a, b). The large PIC in chronic spinal rats is mediated by both persistent sodium and calcium currents. The *sodium* PIC is activated sub-threshold, inactivates partly, and de-activates rapidly, and thus contributes to almost half of the initial part of the PIC, but only a third of the sustained part. In contrast, the *calcium* PIC (L-type) can be activated above or below the firing threshold of the motoneurons, does not show much inactivation, and de-activates slowly, and thus contributes to about half of the initial part of the PIC and two thirds of the sustained PIC. The calcium PIC is clearly hysteretic, even during slow voltage ramps (Fig. 9D), suggesting that these calcium currents are of dendritic origin, and thus not fully voltage-clamped (Lee and Heckman 1998a). In contrast, the sodium PIC is not hysteretic, likely due to its partial inactivation with time.

Role of voltage-clamp recordings

The present experiments examined the persistent inward currents underlying plateaus, using voltage-clamp methods. The main objective of the voltage-clamp was to clamp the membrane potential of the soma, and thus stop the spikes (and the associated AHPs) to make it possible to quantify the effect of TTX on the PICs underlying the plateaus. As mentioned in the Results, when spiking occurs during current-clamp experiments the outward potassium current during AHPs reduces the net PIC, and thus when TTX is applied it is difficult to infer whether it blocks the persistent sodium current because it also blocks the AHP current, with often a net increase, rather than decrease, in inferred PIC (ΔI). This difficulty indeed might explain why a prominent role of TTX-sensitive persistent sodium currents has not been previously described in motoneurons (Hounsgaard and Kiehn 1985), though see Hsiao et al. (1998). Thus, the main objective of the voltage-clamp experiments was to block the spikes and the associated AHPs, without blocking the TTX-sensitive persistent sodium current, so that this persistent sodium current could be measured prior to TTX application. A good voltage-clamp of the soma was sufficient for this purpose and a clamp of the dendrites was neither necessary nor possible, due to the large dendritic trees of motoneurons (Ritz et al. 1992). In fact, it is probable that unclamped channels on the dendrites produced most of the hysteresis of the PIC in voltage-clamp recording (Bennett et al. 1998a; Hounsgaard and Kiehn 1993; Lee and Heckman 1996).

Ionic mechanisms underlying the persistent inward current

An important finding of the present study is that a major part of the plateau is mediated by a TTX-sensitive persistent sodium current. Although TTX-sensitive persistent sodium

currents mediating plateaus in motoneurons have not been extensively studied, persistent sodium currents have been proposed to exist in normal spinal motoneurons (Lee and Heckman 2001), and they have been suggested to play a role in plateau activation in hamster trigeminal motoneurons (Hsiao et al. 1998) and many other neurons (Angstadt and Choo 1996; Elson and Selverston 1997; Rekling and Laursen 1989; Sandler et al. 1998; Schwindt and Crill 1995; Stafstrom et al. 1985; Stafstrom et al. 1982). According to these studies, the persistent sodium currents are sensitive to TTX, have a voltage threshold a few millivolts below the spike threshold, activate and de-activate rapidly, and demonstrate considerable inactivation following activation. In our experiments, Cd^{++} was used to block calcium channels and thus reveal the persistent sodium current in isolation. This PIC that remained after Cd^{++} was completely eliminated by TTX, and its characteristics (low threshold, fast kinetics, inactivation) closely resemble the persistent sodium current seen in other preparations, and thus it is mediated by a similar TTX-sensitive persistent sodium current (see review, Crill 1996).

The other major part of the PIC in chronic spinal rats was found to be mediated by L-type calcium channels, consist with data shown in many other preparations (Hounsgaard and Kiehn 1989; Hsiao et al. 1998; Mills and Pitman 1997; Morisset and Nagy 1999). Although L-type calcium channels are conventionally considered as high-voltage gated channels, activated at above –30 mV (Fox et al. 1987; Tsien et al. 1988), our results demonstrate that the threshold of L-type calcium channels is around the firing threshold of the motoneurons, which is similar to the low threshold obtained in other studies of plateaus in neurons (i.e. -45 to -55mV, Hounsgaard and Kiehn 1989; Mills and Pitman

1997; Morisset and Nagy 1999; Voisin and Nagy 2001; Zhang and Harris-Warrick 1995). In addition, these L-type calcium channels involved in plateau activation require a higher concentration of dihydropyridines (10 μM nimodipine in our experiments, 15 μM nifedipine in Hounsgaard and Kiehn, 1989; 10 μM nifedipine in Voisin and Nagy, 2001; and 50 μM nifedipine in Mills and Pitman, 1997) to be completely blocked than do conventional L-type calcium channels (< 1 μM, Fanelli et al. 1994; McCarthy and TanPiengco 1992). Two subtypes of L-type calcium channels, Cav1.3 and Cav1.4 have recently been found. Cav1.3 subtype has a lower activation threshold and a much lower sensitivity to the dihydropyridines (Koschak et al. 2001; Xu and Lipscombe 2001); thus it is very likely that the plateaus found in ours and others' preparations are mediated by the Cav1.3 subtype L-type calcium channels. While higher threshold calcium channels (N- and P-type) are not involved in plateaus under physiological conditions (nimodipine blocks plateaus, Carlin et al. 2000b; Hounsgaard and Kiehn 1989), they can produce large plateaus and PICs (above –30 mV) when K+ currents and intracellular Ca++ are artificially reduced (our unpublished data and Carlin et al. 2000a; Powers and Binder 2003).

Although our results demonstrate that part of the PIC in chronic spinal rats is *mediated* by L-type calcium channels (nimodipine-sensitive), it does not mean that this calcium current acts simply by directly depolarizing the cell membrane and producing the plateaus. Calcium from the L-type calcium channels may trigger many intracellular cascades and affect the activity of other channels and receptors that ultimately contribute to the PIC and plateau. For example, in rat deep dorsal horn interneurons, after L-type

calcium currents initiate plateaus, these plateaus are further prolonged by a calcium-activated non-selective cation current (I_{CAN}) (Morisset and Nagy 1999; Zhang et al. 1995); however, see Perrier and Hounsgaard (1999). Also, in turtle motoneurons, calcium facilitates plateaus by activating a calmodulin pathway, which may ultimately facilitate the L-type calcium channel itself (Perrier et al. 2000). Recent experiments have shown that the calmodulin levels in motoneurons of chronic spinal rats are increased compared to in normal rats (Anelli et al. 2001); therefore, it is possible that calmodulin is also involved in the large PICs and plateaus seen after injury. Finally, the inflow of calcium can activate Ca^{++} dependent K^+ currents, which oppose the inward current; thus, the amplitude of inward current recorded in the present experiments may be underestimated. However, it is unlikely that the emergence of large inward currents in chronic spinal rats is simply caused by a reduction in the AHP-related K^+ currents, because the AHP itself is not reduced in chronic spinal rats (Bennett et al. 2001c).

Possible origin of persistent inward currents after chronic injury

There may be several reasons why after chronic spinal cord injury motoneurons are spontaneously able to produce such large persistent inward currents and plateaus. First, after spinal cord injury, synaptic transmission below the level of injury is no longer controlled by descending inhibitory tracts (Baldissera et al. 1981; Jankowska 1992a), and thus, there might be more neurotransmitter released from certain afferent terminals or interneurons (Thor et al. 1994). However, while this may be important, its actions are clearly only relevant in the long-term, since large PICs and plateaus are not present immediately after acute spinal cord transection, presumably due to the acute loss of

brainstem derived transmitters such as 5-HT or NE (Conway et al. 1988; Hounsgaard et al. 1988). With long-term injury additional changes may occur that make the residual transmitters more effective in facilitating PICs. For example, metabotropic receptors that facilitate PICs may become supersensitive to the released neurotransmitters (Hains et al. 2002) or the receptors may be up regulated after chronic spinal cord injury (Mills and Hulsebosch 2002). If a supersensitivity does occur, then even lower than normal levels of transmitters might be important; for example, up to 12% of normal 5-HT remains chronically below a complete spinal transection (Newton and Hamill 1988; Shapiro 1997). Thus, enhanced metabotropic receptor action (via glutamate, 5-HT, etc) might contribute to the exaggerated PICs and associated plateaus after chronic injury. It is noteworthy that sodium currents should be modulated by metabotropic receptor actions (via cyclic AMP and protein kinase C pathways, Astman et al. 1998; Crill 1996; Li et al. 1992; Mittmann and Alzheimer 1998), just as persistent calcium currents are (Russo and Hounsgaard 1999).

This possible involvement of metabotropic receptor action may appear to be at odds with our present finding that calcium or sodium PICs survive synaptic blockade with TTX or Cd^{++} respectively. However, in our studies we measured the calcium PIC (or sodium PIC) within 10 to 15 mins after TTX (or Cd^{++}) application, a time that may not be long enough for the long-lasting intracellular actions of metabotropic receptors to be reversed. For example, $5\text{-}HT_{2c}$ receptor activation can have effects that last for 1 hour after 5-HT agonist have been removed (Machacek et al. 2001) see also (Miller et al. 1996). In contrast, metabotropic glutamate receptor facilitation of PICs has a shorter lasting action,

and is reversed within a few minutes of removal of receptor activation (Delgado-Lezama et al. 1999). Thus, part but not all of the PIC might be reduced by the 10 to15 min synaptic blockade in our experiments, and this might explain why about 15 % of the total PIC is unaccounted for by the sum of the individual sodium and calcium PICs that remain after either Cd++ or TTX (see Results).

The exaggerated PICs after chronic injury might also be related to an upregulation in the number of L-type calcium channels. Expression of more calcium channels has been shown after peripheral nerve trauma in dorsal root ganglion cells (Kim et al. 2001; Luo et al. 2001). At the present time, there is no evidence of increase expression of calcium channels after central nervous system trauma. However, increased expression of calcium channels does occur after ischemia or hypoxia (Chung et al. 2001; Duffy and MacVicar 1996; Westenbroek et al. 1998a).

In summary, large persistent inward currents can be activated in motoneurons of chronically transected rat spinal cord, without the application of neuromodulators, or stimulated neuromodulator release. These PICs are mediated by low-threshold persistent sodium (TTX-sensitive) and calcium (L-type) currents. Ultimately, these PICs cause the large plateaus that have been shown to underlie muscle spasms after injury (Bennett et al. 2001c). The detailed involvement of persistent sodium and calcium inward currents in abnormal firing and spasticity after spinal cord injury is addressed in a companion paper (Li et al., 2004).

TABLE

Negative-slope region	Normal ACSF	+ 2 μM TTX	Normal ACSF	+ 20 μM nimodipine
$V_j - V_{on}$, mV (width)	11.46 ± 4.25	9.99 ± 5.87	13.77 ± 3.14	9.30 ± 3.47*
$I_{on} - I_i$, nA (initial depth)	1.51 ± 0.66	0.69 ± 0.43*	1.78 ± 0.73	0.65 ± 0.30*
$I_{on} - I_s$, nA (sustained depth)	0.99 ± 0.46	1.12 ± 0.66	1.50 ± 0.72	0.28 ± 0.39*
V_{on} - V_{off}, mV (hysteresis)	4.98 ± 4.26	4.34 ± 2.92	6.12 ± 3.85	0.02 ± 4.82*
I_{on} - I_{off}, nA (hysteresis)	0.58 ± 0.31	0.63 ± 0.29	0.97 ± 0.44	0.17 ± 0.55*
$I_i - I_s$, nA	-0.51 ± 0.65	0.50 ± 0.86*	-0.44 ± 0.68	-0.43 ± 0.67

TABLE 4-1. SUMMARY OF THE CHARACTERISTICS OF THE NEGATIVE-SLOPE REGION AND HYSTERESIS IN VOLTAGE-CLAMP.

N = 12 cells for TTX application, n = 7 cells for nimodipine application; values are means ± SD. * indicates significant difference before and after drug application. Abbreviations V_j, etc. described in Fig. 1.

FIGURES

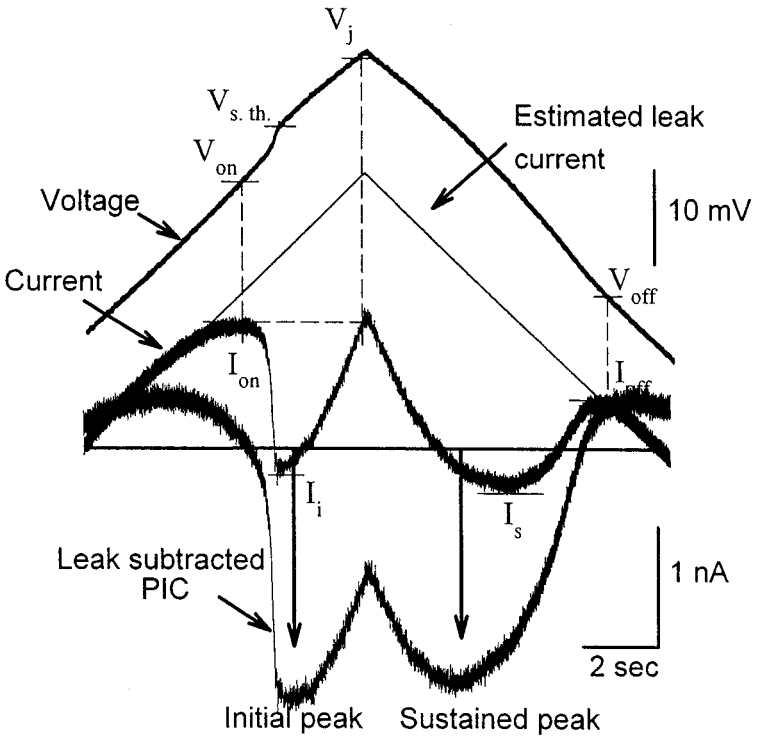
V_j
$V_{s.\,th.}$
V_{on}
Estimated leak
current
Voltage
10 mV
Current
V_{off}
I_{on}
I_{off}
I_i
I_s
Leak subtracted
PIC
1 nA
2 sec
Initial peak
Sustained peak

Figure 4-1. PERSISTENT INWARD CURRENT MEASUREMENT DURING A SLOW TRIANGULAR VOLTAGE RAMP UNDER DISCONTINUOUS SINGLE ELECTRODE VOLTAGE-CLAMP CONDITIONS. Current (middle trace) recorded intracellularly from a motoneuron of a chronic spinal rat recorded in normal ACSF during the slow voltage ramp (top trace). Note that the voltage-clamp blocks the fast sodium spikes above the spike threshold ($V_{S.\ Th.}$, -41mV). In the subthreshold region the current increases linearly with voltage (passive leak current) and a linear regression is used to extrapolate this leak current to higher voltages (thin triangular line). When the PIC is initiated (at V_{on}, I_{on}) the current drops despite the increasing voltage (negative-slope region). The PIC is quantified as the deviation from the estimated leak current (leak-current subtracted in lower trace). The onset, peak and offset of the PIC are marked by abbreviations described in the Methods (V_{on}, I_{on}, etc). Current-clamp recording from same cell is described later in Fig. 9A.

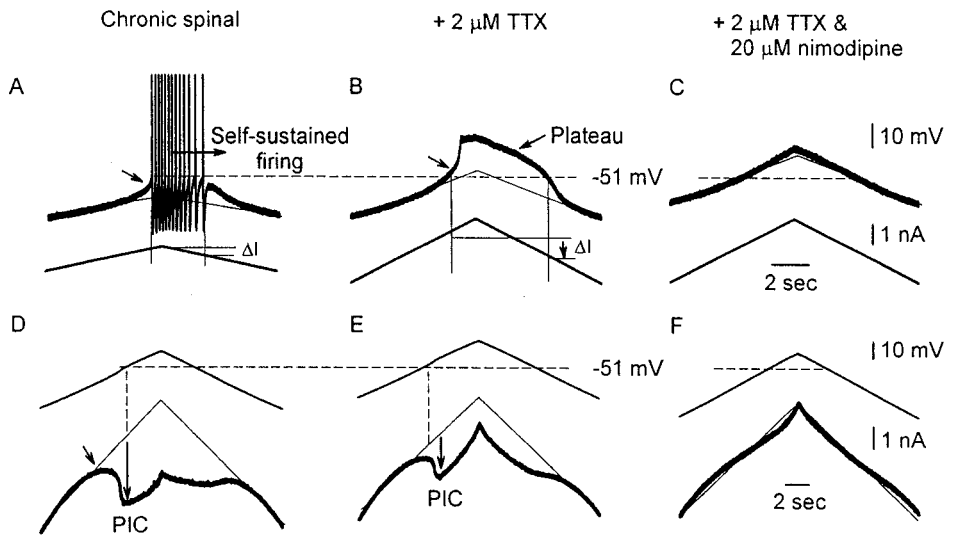

Figure 4-2. PLATEAU AND PIC IS PARTLY MEDIATED BY AN L-TYPE CALCIUM CURRENT. A: Voltage response in motoneuron of chronic spinal rat during slow ramp current injection, under discontinuous current-clamp conditions. Note the onset of a plateau at the acceleration in potential just before recruitment (left arrow) and associated self-sustained firing (quantified by ΔI). Dashed line indicates spike threshold (-51 mV). B: Response to current ramp after TTX application, which blocked sodium spikes and synaptic activity (latter not shown). Note the clear plateau not obscured by spikes (blocked by TTX), though its onset (at left arrow) was at a higher threshold than prior to TTX (arrow in A). C: Nimodipine, a specific L-type calcium channel blocker, abolished the plateau in B. D: Response of the same motoneuron prior to drug application during a slow voltage ramp under voltage-clamp conditions (as in Fig. 1; taken 30 sec after A). Note the large PIC (arrow), and associated negative-slope region that starts below the spike threshold (dashed lines at –51mV). E: Response to a voltage ramp after TTX. Note the decreased

magnitude and increased voltage threshold (negative-slope above original spike threshold) of the PIC (arrow), indicating that part of the PIC is mediated by a TTX-sensitive current. F: Further application of nimodipine eliminated the remaining PIC, consistent with response in C. Tops of spikes in A - C clipped.

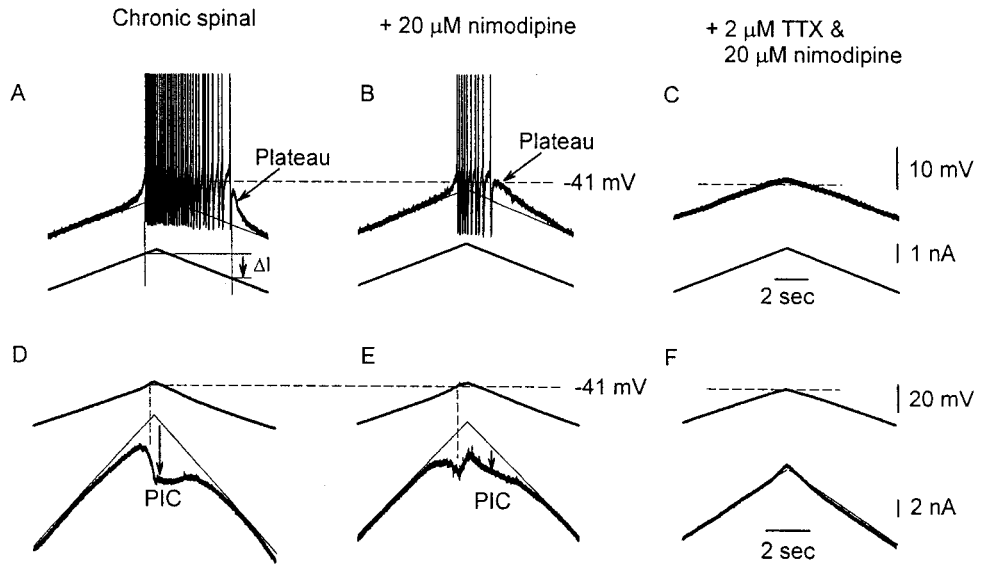

Figure 4-3. NIMODIPINE CANNOT COMPLETELY ELIMINATE PLATEAU AND PIC; THE REMAINING PLATEAU AND PIC ARE SENSITIVE TO TTX.

Same format as Fig. 2. A: Plateau and associated self-sustained firing (ΔI) evoked in motoneuron of chronic spinal rat in current-clamp recording. B: Nimodipine reduced, but did not eliminate, the plateau and self-sustained firing. C: Remaining plateau abolished by TTX. D: PIC (arrow) and negative-slope region in voltage-clamp recording. E: Nimodipine reduced the PIC (arrow). F: TTX eliminated the remaining PIC. Dash line indicates spike threshold of -45 mV.

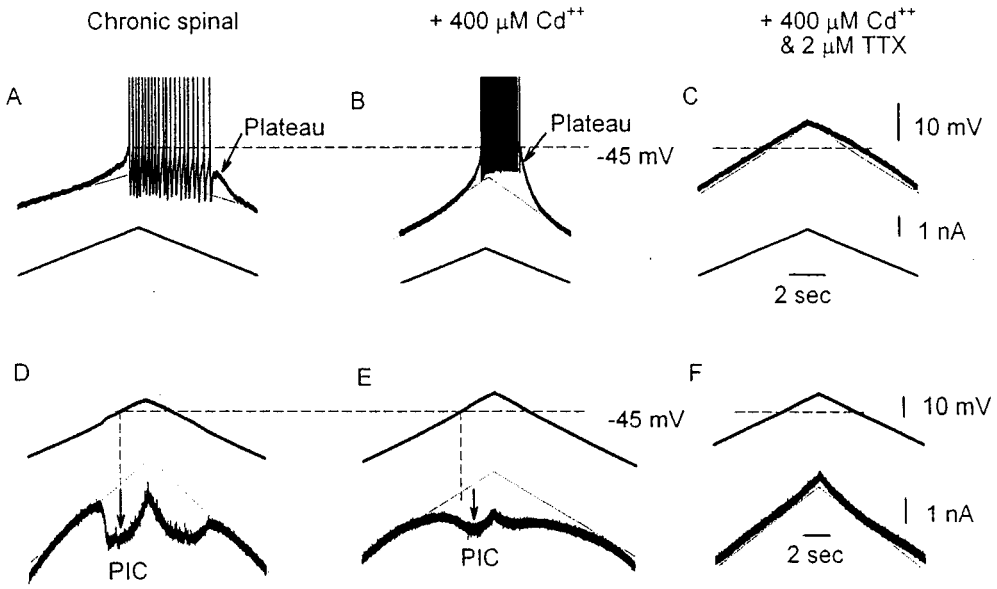

Figure 4-4. PLATEAU AND PIC IS PARTLY MEDIATED BY A PERSISTENT SODIUM CURRENT. Same format as in Figs. 2 and 3. A: Plateau and self-sustained firing evoked by a current ramp under current-clamp conditions. B: A substantial plateau remained in a general calcium channel blockade with Cd^{++}, though note the shortened self-sustained firing and increased firing frequency (Cd^{++} eliminated the slow AHP). Cd^{++} also blocked all synaptic inputs (not shown). C: TTX blocked the remaining plateau, leaving a linear voltage-response to the current ramp. D: PIC and negative-slope region in voltage-clamp recording prior to drug application. E: Cd^{++} reduced the magnitude and increased the threshold of the PIC, consistent with the block of a low threshold persistent calcium current (as in Figs. 2 and 3). F: TTX blocked the remaining Cd^{++}-resistant PIC. Because Cd^{++} blocked presynaptic activity and all calcium currents, the PIC blocked by TTX must be a postsynaptic persistent sodium current. Dash line indicates spike threshold of -49 mV.

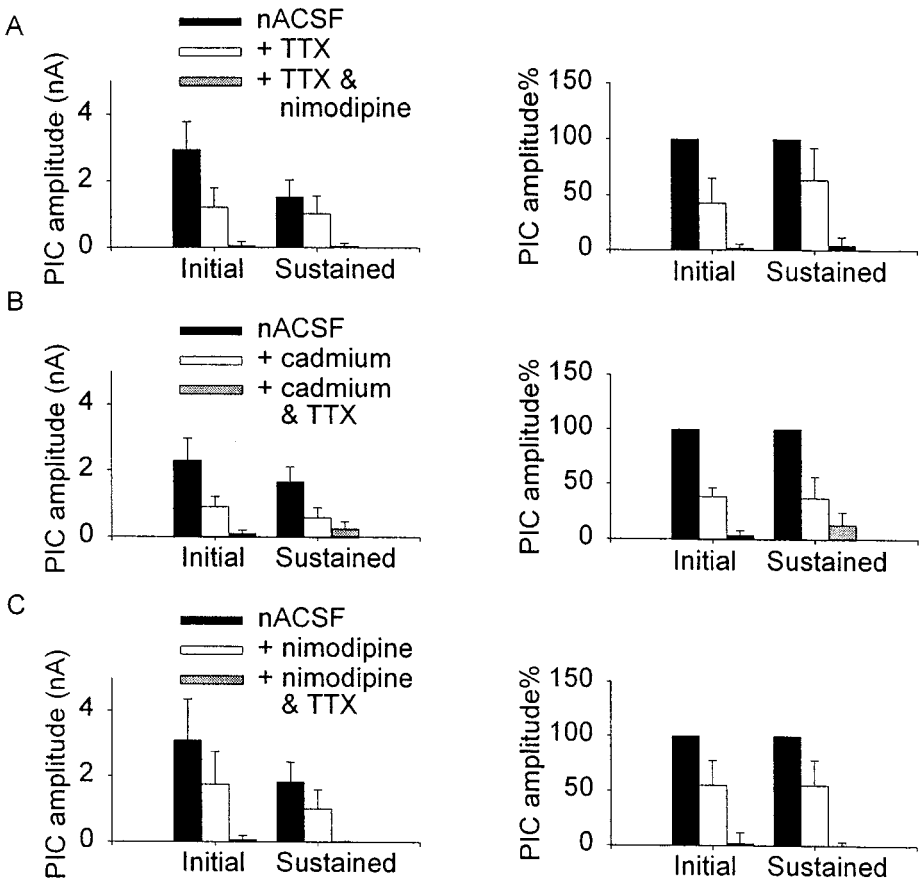
A
nACSF
+ TTX
+ TTX &
nimodipine
PIC amplitude (nA)
4
2
0
Initial
Sustained
PIC amplitude%
150
100
50
0
Initial
Sustained
B
nACSF
+ cadmium
+ cadmium
& TTX
PIC amplitude (nA)
4
2
0
Initial
Sustained
PIC amplitude%
150
100
50
0
Initial
Sustained
C
nACSF
+ nimodipine
+ nimodipine
& TTX
PIC amplitude (nA)
4
2
0
Initial
Sustained
PIC amplitude%
150
100
50
0
Initial
Sustained

Figure 4-5. SUMMARY OF INITIAL AND SUSTAINED PEAK AMPLITUDE OF THE PIC AFTER LEAK SUBTRACTION.

A: Averaged magnitude of *initial* and *sustained* peak of PIC in normal nACSF (black bar), after TTX (white bar) and after TTX plus nimodipine (gray bar, small). Left, amplitude of PIC in nA. Right, amplitude as percentage of original PIC. B-C: Same format as A. B: Average initial and sustained PIC in nACSF (black bar), after Cd^{++} (white bar) and after Cd^{++} plus TTX (gray bar). C: Average initial and sustained PIC in nACSF (black bar), after nimodipine (white bar) and after nimodipine plus TTX (gray bar). All changes with drug applications in A-C are significant, and the PIC remaining after TTX plus Cd^{++} (B) or TTX plus nimodipine (A, C) are not significantly different from zero (some gray bars too small to be visible).

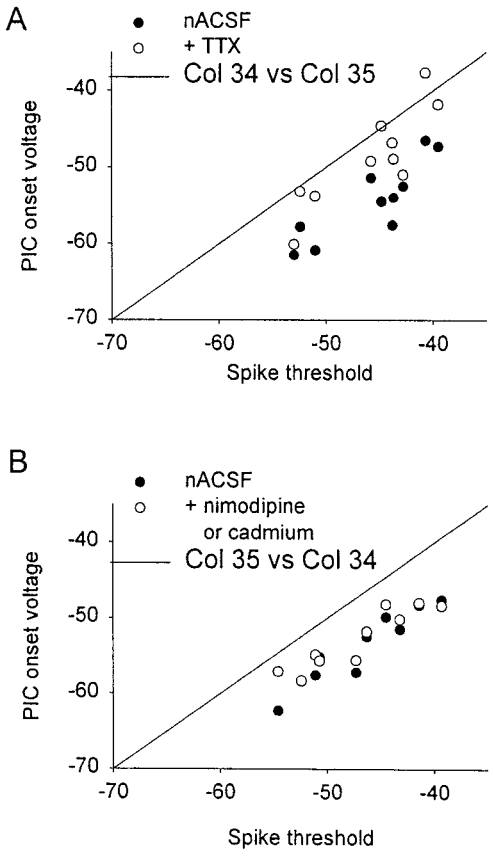

Figure 4-6. SUMMARY OF THE VOLTAGE THRESHOLD OF THE PIC.

A: Onset voltage of the PIC (V_{on}) shown as a function of the spike threshold for each cell in nACSF (black dot) and after the sodium PIC is blocked with TTX (white dot). The solid line indicates where the onset voltage equals the spike threshold. B: Same format as in A, but black dot indicates PIC threshold in nACSF and white dot indicates PIC threshold after calcium PIC blocked with nimodipine or Cd^{++}.

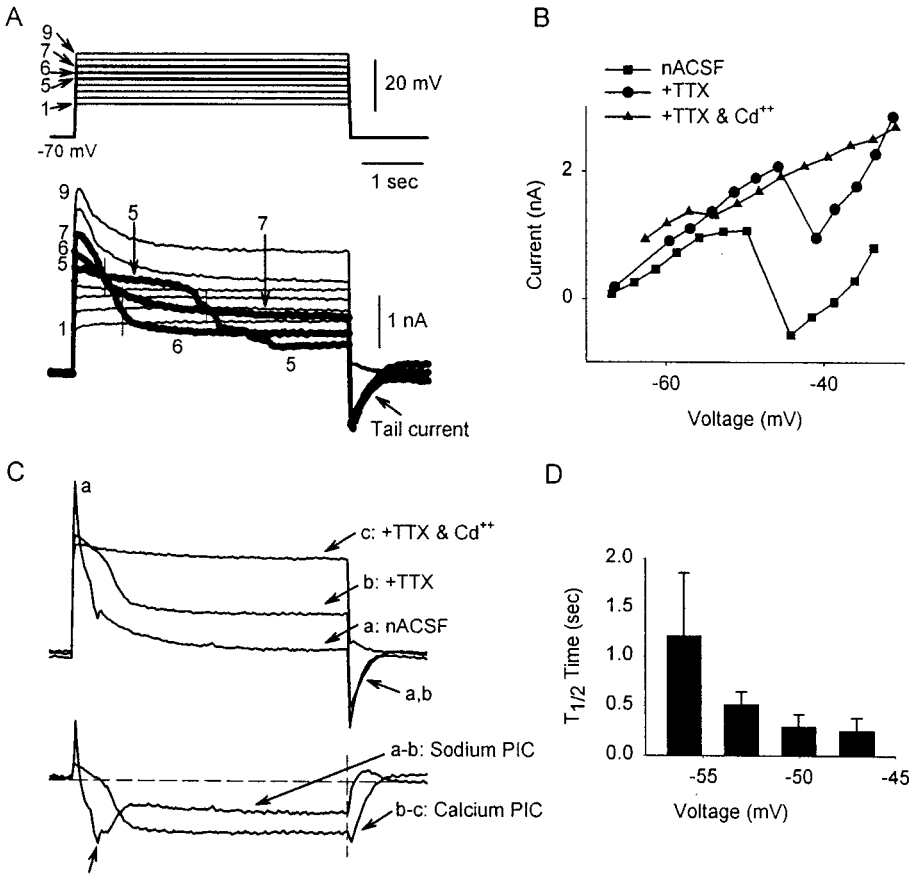
A
9
7
6
5
1
20 mV
-70 mV
1 sec
9
7
6
5
1
5
7
6
5
1 nA
Tail current
B
nACSF
+TTX
+TTX & Cd++
Current (nA)
2
0
-60
-40
Voltage (mV)
C
a
c: +TTX & Cd++
b: +TTX
a: nACSF
a,b
a-b: Sodium PIC
b-c: Calcium PIC
D
T1/2 Time (sec)
2.0
1.5
1.0
0.5
0.0
-55
-50
-45
Voltage (mV)

Figure 4-7. INWARD CURRENT ACTIVATION DURING LONG VOLTAGE PULSES (STEPS) UNDER VOLTAGE-CLAMP CONDITIONS.

A: Current recorded from a motoneuron of a chronic spinal rat when a series of increasing voltage steps were applied, each starting from -70mV (all steps shown in B, but not A). As the voltage step increased the current initially increased proportionally (traces 1- 4). Above -50 mV (thickened lines, 5 to 7) the PIC was activated with a delay (half activation at vertical ticks) and caused a reduction in the current. Recorded in 2 μM TTX, and thus only calcium PIC present. Note the tail current after the pulse when a calcium PIC was activated (traces > 5). B: Peak negative deflection in current during the steps shown as a function of the voltage of the step, in nACSF (square), in TTX (circle) and in TTX plus Cd^{++} (triangular). Note the negative-slope region as PIC is activated (N-shaped V-I plot). C: Overlay of the current recorded in nACSF (a), TTX (b) and TTX plus Cd^{++}(c) in response to the same suprathreshold voltage pulse. The lower Figure shows reduction in current with TTX (a – b, sodium PIC) and Cd^{++} (b – c, calcium PIC). Note the slow onset and offset (tail current) of the calcium PIC, and rapid onset and offset of the sodium PIC. Same scale as A. D: Average half activation time ($T_{1/2}$) for the calcium PIC. Data binned at 3 mV intervals for averaging, n = 4.

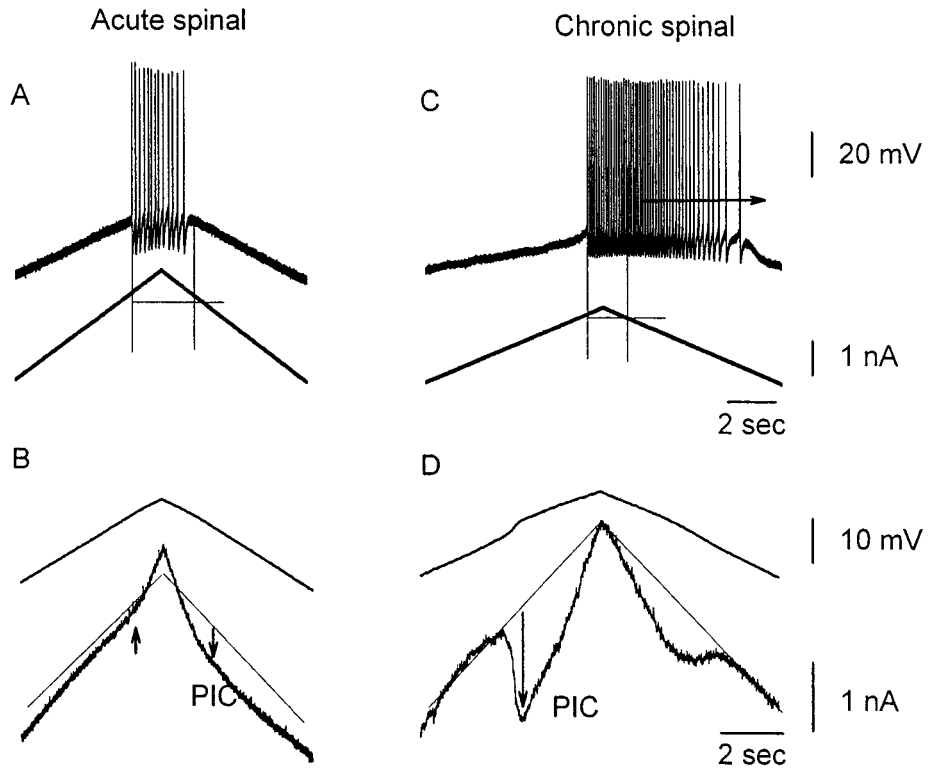

Figure 4-8. MOTONEURONS FROM ACUTELY TRANSECTED SPINAL RATS DO NOT HAVE PLATEAUS, BUT HAVE SMALL PICS, SEEN BY LEAK CURRENT SUBTRACTION.

A: Current-clamp recording from a motoneuron of an acute spinal rat with no plateau or self-sustained firing. B: Voltage-clamp recording from the same cell as in A. Note the small PIC (arrows) that was not large enough to produce a negative slope region. C: Current-clamp recording from a motoneuron of a chronic spinal rat. Note the long self-sustained firing (arrow). D: Voltage-clamp recording from the same cell as in C. Note the large PIC and negative slope region (arrow).

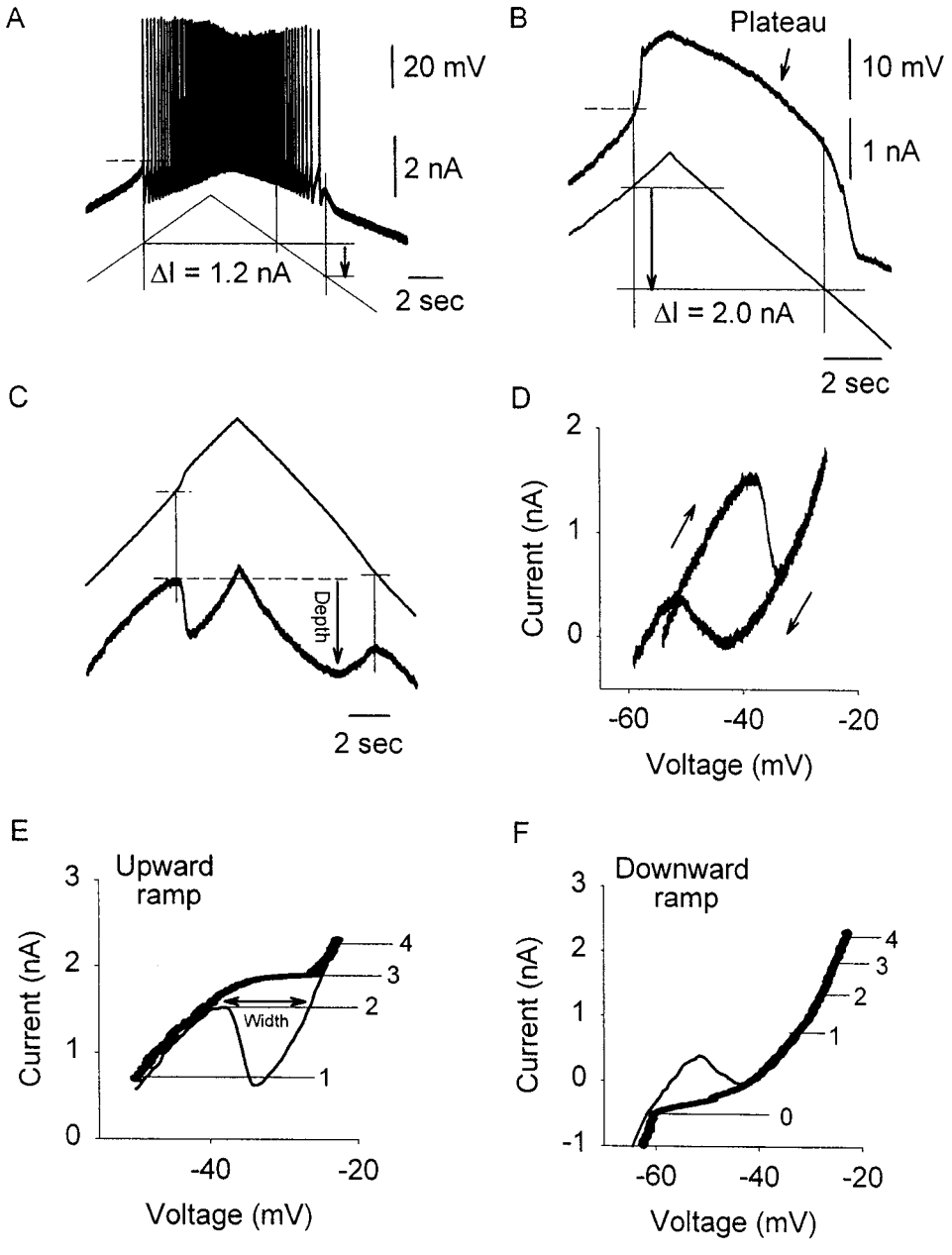
A
20 mV
2 nA
ΔI = 1.2 nA
2 sec
B
Plateau
10 mV
1 nA
ΔI = 2.0 nA
2 sec
C
Depth
2 sec
D
Current (nA)
2
1
0
-60
-40
-20
Voltage (mV)
E
Upward ramp
Current (nA)
3
2
1
0
Width
4
3
2
1
-40
-20
Voltage (mV)
F
Downward ramp
Current (nA)
3
2
1
0
-1
4
3
2
1
0
-60
-40
-20
Voltage (mV)

Figure 4-9. RELATION BETWEEN VOLTAGE- AND CURRENT-CLAMP RECORDINGS.

A: Current-clamp recording from a motoneuron of a chronic spinal rat with plateau and self-sustained firing (ΔI). Voltage-clamp for same cell shown in Fig. 1. B: Current-clamp recording from the same cell after TTX application. C: Voltage-clamp recording from the same cell after TTX application. D: Voltage-clamp current response plotted as a function of the voltage applied (V-I plot), derived from C. Note the N-shaped relation, and clockwise hysteresis on the downward ramp (down arrow) compared to the upward ramp (up arrow) E: Overlay of the upward ramp V-I plots from current-clamp (thick line) and voltage-clamp (thin line) recordings of B and C. Note the close overlay of the data, except in the valley formed by the negative-slope region. Horizontal lines indicate current levels discussed in the text. F: Overlay of the downward ramp responses of B and C. Short dash lines in A, B and C indicate the firing threshold of the cell before TTX application. B and C, same vertical scale.

REFERENCES

Akatani J, Wada N, and Kanda K. Intersegmental neuronal pathways in sacrococcygeal spinal cord (S3-Co3) activated by electrical stimulation of tail muscle nerves with low threshold in low spinal cats. *Brain Res* 924: 30-38, 2002.

Alvarez F, Pearson J, Harrington D, Dewey D, Torbeck L, and Fyffe R. Distribution of 5-hydroxytryptamine-immunoreactive boutons on alpha- motoneurons in the lumbar spinal cord of adult cats. *J Comp Neurol* 393: 69-83, 1998.

Anderson RJ, Brigham P, Cady WJ, and Kellar KJ. Role of alpha-2 adrenergic affinity in the action of a non-sedative antispasticity agent. *Acta Neurol Scand* 66: 248-258, 1982.

Anelli R, Sanelli L, Johnson M, Bennett D, and Heckman CJ. Changes in calcium binding proteins expression following spinal cord injury. *American Society of Neuroscience*, 2001.

Angstadt JD and Choo JJ. Sodium-dependent plateau potentials in cultured Retzius cells of the medicinal leech. *J Neurophysiol* 76: 1491-1502, 1996.

Ashby P and McCrea DA. Neurophysiology of spinal spasticity. In: *Handbook of the Spinal Cord*, edited by Davidoff RA. New York: Marcel Dekker Inc., 1987, p. 120-143.

Ashby P, Verrier M, and Lightfoot E. Segmental reflex pathways in spinal shock and spinal spasticity in man. *J Neurology, Neurosurgery, and Psychiatry* 37: 1352-1360, 1974.

Ashby P and Wiens M. Reciprocal inhibition following lesions of the spinal cord in man. *J Physiol* 414: 145-157, 1989.

Astman N, Gutnick MJ, and Fleidervish IA. Activation of protein kinase C increases neuronal excitability by regulating persistent Na+ current in mouse neocortical slices. *J Neurophysiol* 80: 1547-1551, 1998.

Baker LL and Chandler SH. Characterization of postsynaptic potentials evoked by sural nerve stimulation in hindlimb motoneurons from acute and chronic spinal cats. *Brain Res* 420: 340-350, 1987.

Baldissera F, Hultborn H, and Illert M. Integration in spinal neuronal systems. In: *Handbook of Physiology. The Nervous system. Motor Control*, edited by VB B. Bethesda: American Physiological Society, 1981, p. 509-595.

Barbeau H and Bedard P. Denervation supersensitivity to 5-hydroxytryptophan in rats following spinal transection and 5,7-dihydroxytryptamine injection. *Neuropharmacology* 20: 611-616, 1981.

Barron DH and Matthews BHC. Dorsal root reflexes. *J Physiol* 94: 26-29P, 1938.

Bennett DJ, Gorassini M, Fouad K, Sanelli L, Han Y, and Cheng J. Spasticity in rats with sacral spinal cord injury. *J Neurotrauma* 16: 69-84, 1999a.

Bennett DJ, Gorassini MA, and Siu M. In vitro preparation to study spasticity in chronic spinal rats. *Soc Neuroscience Abst* 25: 1394, 1999b.

Bennett DJ, Hultborn H, Fedirchuk B, and Gorassini M. Short-term plasticity in hindlimb motoneurons of decerebrate cats. *J Neurophysiol* 80: 2038-2045, 1998a.

Bennett DJ, Hultborn H, Fedirchuk B, and Gorassini M. Synaptic activation of plateaus in hindlimb motoneurons of decerebrate cats. *J Neurophysiol* 80: 2023-2037, 1998b.

Bennett DJ, Li Y, Harvey PJ, and Gorassini M. Evidence for plateau potentials in tail motoneurons of awake chronic spinal rats with spasticity. *J Neurophysiol* 86: 1972-1982, 2001a.

Bennett DJ, Li Y, and Sanelli L. Role of NMDA in spasticity following sacral spinal cord injury in rats. *Soc Neurosci Abstr* 31: 933.11, 2001b.

Bennett DJ, Li Y, and Siu M. Plateau potentials in sacrocaudal motoneurons of chronic spinal rats, recorded in vitro. *J Neurophysiol* 86: 1955-1971, 2001c.

Bennett DJ, Sanelli L, and Cooke C. Spastic long-lasting reflexes in the awake rat after sacral spinal cord injury. *J Neurophysiol*: submitted, 2003.

Björklund A and Skagerberg G. Descending monoaminergic projections to the spinal cord. In: *Brain Stem Control of Spinal Mechanisms*, edited by Sjolund B and Bjorklund A. Amsterdam: Elsevier Biomedical Press, 1982, p. 55-88.

Booth V, Rinzel J, and Kiehn O. Compartmental model of vertebrate motoneurons for Ca2+-dependent spiking and plateau potentials under pharmacological treatment. *J Neurophysiol* 78: 3371-3385, 1997.

Brooks CM, Koizumi K, and Malcolm JL. Effects of changes in temperature on reactions of the spinal cord. *J Neurophysiol* 18: 205-216, 1955.

Brownstone RM, Jordan LM, Kriellaars DJ, Noga BR, and Shefchyk SJ. On the regulation of repetitive firing in lumbar motoneurones during fictive locomotion in the cat. *Exp Brain Res* 90: 441-455, 1992.

Burke D, Gillies JD, and Lance JW. The quadriceps stretch reflex in human spasticity. *J Neurol Neurosurg Psychiatry* 33: 216-223, 1970a.

Burke D, Gillies JD, and Lance JW. The quadriceps stretch reflex in human spasticity. *J Neurol Neurosurg Psychiat* 33: 216-223, 1970b.

Carlin KP, Jiang Z, and Brownstone RM. Characterization of calcium currents in functionally mature mouse spinal motoneurons. *Eur J Neurosci* 12: 1624-1634, 2000a.

Carlin KP, Jones KE, Jiang Z, Jordan LM, and Brownstone RM. Dendritic L-type calcium currents in mouse spinal motoneurons: implications for bistability. *Eur J Neurosci* 12: 1635-1646, 2000b.

Chau C, Barbeau H, and Rossignol S. Effects of intrathecal alpha1- and alpha2-noradrenergic agonists and norepinephrine on locomotion in chronic spinal cats. *J Neurophysiol* 79: 2941-2963, 1998.

Chung YH, Shin CM, Kim MJ, and Cha CI. Enhanced expression of L-type Ca2+ channels in reactive astrocytes after ischemic injury in rats. *Neurosci Lett* 302: 93-96, 2001.

Clarke RW, Eves S, Harris J, Peachey JE, and Stuart E. Interactions between cutaneous afferent inputs to a withdrawal reflex in the decerebrated rabbit and their control by descending and segmental systems. In: *Neuroscience*, 2002, p. 555-571.

Cleland CL and Rymer WZ. Neural mechanisms underlying the clasp-knife reflex in tha cat. I. Characteristics of the reflex. In: *Journal of Neurophysiology*, 1990, p. 1303-1318.

Conway BA, Hultborn H, Kiehn O, and Mintz I. Plateau potentials in alpha-motoneurones induced by intravenous injection of L-dopa and clonidine in the spinal cat. *J Physiol* 405: 369-384, 1988.

Crill WE. Persistent sodium current in mammalian central neurons. *Annu Rev Physiol* 58: 349-362, 1996.

Delgado-Lezama R, Perrier JF, and Hounsgaard J. Local facilitation of plateau potentials in dendrites of turtle motoneurones by synaptic activation of metabotropic receptors. *J Physiol* 515 (Pt 1): 203-207, 1999.

Delwaide PJ. Electrophysiological testing of spastic patients: its potential usefulness and limitations. In: *Clinical neurophysiology in spasticity. Restorative neurology*, edited by Delwaide PJ and Young RR. Amsterdam: Elsevier, 1985, p. 186-203.

Delwaide PJ and Oliver E. Short-latency autogenic inhibition (IB inhibition) in human spasticity. *J Neurology, Neurosurgery, and Psychiatry* 51: 1546-1550, 1988.

Duffy S and MacVicar BA. In vitro ischemia promotes calcium influx and intracellular calcium release in hippocampal astrocytes. *J Neurosci* 16: 71-81, 1996.

Eken T, Hultborn H, and Kiehn O. Possible functions of transmitter-controlled plateau potentials in alpha motoneurones. *Prog Brain Res* 80: 257-267; discussion 239-242, 1989.

Elson RC and Selverston AI. Evidence for a persistent Na+ conductance in neurons of the gastric mill rhythm generator of spiny lobsters. *J Exp Biol* 200 (Pt 12): 1795-1807, 1997.

Fanelli RJ, McCarthy RT, and Chisholm J. Neuropharmacology of nimodipine: from single channels to behavior. *Ann N Y Acad Sci* 747: 336-350, 1994.

Fox AP, Nowycky MC, and Tsien RW. Kinetic and pharmacological properties distinguishing three types of calcium currents in chick sensory neurones. *J Physiol* 394: 149-172, 1987.

Giroux N, Rossignol S, and Reader TA. Autoradiographic study of alpha1- and alpha2-noradrenergic and serotonin1A receptors in the spinal cord of normal and chronically transected cats. *J Comp Neurol* 406: 402-414, 1999.

Gorassini M, Bennett DJ, Kiehn O, Eken T, and Hultborn H. Activation patterns of hindlimb motor units in the awake rat and their relation to motoneuron intrinsic properties. *J Neurophysiol* 82: 709-717, 1999.

Gorassini MA, Bennett DJ, and Yang JF. Self-sustained firing of human motor units. *Neurosci Lett* 247: 13-16, 1998.

Hains BC, Everhart AW, Fullwood SD, and Hulsebosch CE. Changes in serotonin, serotonin transporter expression and serotonin denervation supersensitivity: involvement in chronic central pain after spinal hemisection in the rat. *Exp Neurol* 175: 347-362, 2002.

Harvey PJ, Gorassini MA, Yakovenko S, Gritsenko V, and Bennett DJ. Contralateral presynaptic inhibition of the monosynaptic reflex in the sacral spinal cord. *Soc Neuroscience Abst* 25: 1394, 1999.

Heckman CJ. Alterations in synaptic input to motoneurons during partial spinal cord injury. *Med Sci Sports Exerc* 26: 1480-1490, 1994.

Hounsgaard J, Hultborn H, Jespersen B, and Kiehn O. Bistability of alpha-motoneurones in the decerebrate cat and in the acute spinal cat after intravenous 5-hydroxytryptophan. *J Physiol* 405: 345-367, 1988.

Hounsgaard J, Hultborn H, Jespersen B, and Kiehn O. Intrinsic membrane properties causing a bistable behaviour of alpha-motoneurones. *Exp Brain Res* 55: 391-394, 1984.

Hounsgaard J and Kiehn O. Ca++ dependent bistability induced by serotonin in spinal motoneurons. *Exp Brain Res* 57: 422-425, 1985.

Hounsgaard J and Kiehn O. Calcium spikes and calcium plateaux evoked by differential polarization in dendrites of turtle motoneurones in vitro. *J Physiol* 468: 245-259, 1993.

Hounsgaard J and Kiehn O. Serotonin-induced bistability of turtle motoneurones caused by a nifedipine-sensitive calcium plateau potential. *J Physiol* 414: 265-282, 1989.

Hsiao CF, Del Negro CA, Trueblood PR, and Chandler SH. Ionic basis for serotonin-induced bistable membrane properties in guinea pig trigeminal motoneurons. *J Neurophysiol* 79: 2847-2856, 1998.

Hultborn H. Plateau potentials and their role in regulating motoneuronal firing. *Adv Exp Med Biol* 508: 213-218, 2002.

Hultborn H and Kiehn O. Neuromodulation of vertebrate motor neuron membrane properties. *Curr Opin Neurobiol* 2: 770-775, 1992.

Hultborn H and Malmsten J. Changes in segmental reflexes following chronic spinal cord hemisection in the cat. I. Increased monosynaptic and polysynaptic ventral root discharges. *Acta Physiol Scand* 119: 405-422, 1983a.

Hultborn H and Malmsten J. Changes in segmental reflexes following chronic spinal cord hemisection in the cat. II. Conditioned monosynaptic test reflexes. *Acta Physiol Scand* 119: 423-433, 1983b.

Jankowska E. Interneuronal relay in spinal pathways from proprioceptors. *Prog Neurobiol* 38: 335-378, 1992a.

Jankowska E. Interneuronal relay in spinal pathways from proprioceptors. In: *Progress in Neurobiology*, 1992b, p. 335-378.

Jankowska E, Jukes MG, Lund S, and Lundberg A. The effect of DOPA on the spinal cord. 5. Reciprocal organization of pathways transmitting excitatory action to alpha motoneurones of flexors and extensors. *Acta Physiol Scand* 70: 369-388, 1967.

Jankowska E, Padel Y, and Zarzecki P. Crossed disynaptic inhibition of sacral motoneurones. *J Physiol* 285: 425-444, 1978.

Jiang C, Agulian S, and Haddad GG. O2 tension in adult and neonatal brain slices under several experimental conditions. *Brain Res* 568: 159-164, 1991.

Katz R, Pierrot-Deseilligny E, and Hultborn H. Recurrent inhibition of motoneurones prior to and during ramp and ballistic movements. *Neurosci Lett* 31: 141-145, 1982.

Kekesi G, Joo G, Csullog E, Dobos I, Klimscha W, Toth K, Benedek G, and Horvath G. The antinociceptive effect of intrathecal kynurenic acid and its interaction with endomorphin-1 in rats. *Eur J Pharmacol* 445: 93-96, 2002.

Kerkut GA and Bagust J. The isolated mammalian spinal cord. *Prog Neurobiol* 46: 1-48, 1995.

Kiehn O and Eken T. Prolonged firing in motor units: evidence of plateau potentials in human motoneurons? *J Neurophysiol* 78: 3061-3068, 1997.

Kim DS, Yoon CH, Lee SJ, Park SY, Yoo HJ, and Cho HJ. Changes in voltage-gated calcium channel alpha(1) gene expression in rat dorsal root ganglia following peripheral nerve injury. *Brain Res Mol Brain Res* 96: 151-156, 2001.

Koschak A, Reimer D, Huber I, Grabner M, Glossmann H, Engel J, and Striessnig J. alpha 1D (Cav1.3) subunits can form l-type Ca2+ channels activating at negative voltages. *J Biol Chem* 276: 22100-22106, 2001.

Krawitz S, Fedirchuk B, Dai Y, Jordan LM, and McCrea DA. State-dependent hyperpolarization of voltage threshold enhances motoneurone excitability during fictive locomotion in the cat. *J Physiol* 532: 271-281, 2001.

Kuhn RA and Macht MB. Some manifestations of reflex activity in spinal man with particular reference to the occurrence of extensor spasm. *Bull Johns Hopkins Hosp* 84: 43-75, 1948.

Lance JW and Burke D. Mechanisms of spasticity. *Arch Phys Med Rehabil* 55: 332-337, 1974.

Lee RH and Heckman CJ. Bistability in spinal motoneurons in vivo: systematic variations in persistent inward currents. *J Neurophysiol* 80: 583-593, 1998a.

Lee RH and Heckman CJ. Bistability in spinal motoneurons in vivo: systematic variations in rhythmic firing patterns. *J Neurophysiol* 80: 572-582, 1998b.

Lee RH and Heckman CJ. Enhancement of bistability in spinal motoneurons in vivo by the noradrenergic alpha1 agonist methoxamine. *J Neurophysiol* 81: 2164-2174, 1999.

Lee RH and Heckman CJ. Essential role of a fast persistent inward current in action potential initiation and control of rhythmic firing. *J Neurophysiol* 85: 472-475, 2001.

Lee RH and Heckman CJ. Influence of voltage-sensitive dendritic conductances on bistable firing and effective synaptic current in cat spinal motoneurons in vivo. *J Neurophysiol* 76: 2107-2110, 1996.

Levi R, Hultling C, and Seiger A. The Stockholm Spinal Cord Injury Study: 2. Associations between clinical patient characteristics and post-acute medical problems. *Paraplegia* 33: 585-594, 1995.

Li M, West JW, Lai Y, Scheuer T, and Catterall WA. Functional modulation of brain sodium channels by cAMP-dependent phosphorylation. *Neuron* 8: 1151-1159, 1992.

Li Y and Bennett DJ. Effect of baclofen on spinal reflexes and persistent inward currents in motoneurons of acute and chronic spinal rats. *J Neurophysiology* (submitted), 2004.

Li Y and Bennett DJ. Persistent sodium and calcium currents cause plateau potentials in motoneurons of chronic spinal rats. *J Neurophysiol* 90: 857-869, 2003.

Li Y, Gorassini M, and Bennett D. Role of persistent sodium and calcium currents in motoneuron firing and spasticity in chronic spinal rats. *J Neurophysiology* (in press), 2004a.

Li Y, Gorassini MA, and Bennett DJ. Role of peristent sodium and calcium currents in motoneuron firing and spasticity in chronic spinal rats. *J Neurophysiol*: in press, 2003.

Li Y, Harvey PJ, and Bennett DJ. Spastic long-lasting reflexes in the chronic spinal rat, studied in vitro. *J Neurophysiology* (accepted), 2004b.

Li Y, Sanelli L, and Bennett DJ. Ionic mechanisms for plateau potentials in motoneurons of chronic spinal spastic rats. *Soc Neurosci 31* 933.10, 2001.

Little JW, Micklesen P, Umlauf R, and Britell C. Lower extremity manifestations of spasticity in chronic spinal cord injury. *Am J Phys Med Rehabil* 68: 32-36, 1989.

Long SK, Evans RH, Cull L, Krijzer F, and Bevan P. An in vitro mature spinal cord preparation from the rat. *Neuropharmacology* 27: 541-546, 1988.

Luo ZD, Chaplan SR, Higuera ES, Sorkin LS, Stauderman KA, Williams ME, and Yaksh TL. Upregulation of dorsal root ganglion (alpha)2(delta) calcium channel subunit and its correlation with allodynia in spinal nerve-injured rats. *J Neurosci* 21: 1868-1875, 2001.

Machacek DW, Garraway SM, Shay BL, and Hochman S. Serotonin 5-HT(2) receptor activation induces a long-lasting amplification of spinal reflex actions in the rat. *J Physiol* 537: 201-207, 2001.

Masson RL, Jr., Sparkes ML, and Ritz LA. Descending projections to the rat sacrocaudal spinal cord. *J Comp Neurol* 307: 120-130, 1991.

Matthews PB. Relationship of firing intervals of human motor units to the trajectory of post-spike after-hyperpolarization and synaptic noise. *J Physiol* 492 (Pt 2): 597-628, 1996.

Maxwell L, Maxwell D, Neilson M, and Kerr R. Confocal microscopic survey of serotoninergic axons in the lumbar spinal cord of the rat: co-localization with glutamate decarboxylase and neuropeptides. *Neuroscience* 75: 471-480, 1996.

McCarthy RT and TanPiengco PE. Multiple types of high-threshold calcium channels in rabbit sensory neurons: high-affinity block of neuronal L-type by nimodipine. *J Neurosci* 12: 2225-2234, 1992.

McNicholas L, Martin W, Sloan J, and Nozaki M. Innervation of the spinal cord by sympathetic fibers. *Exp Neurol* 69, 1980.

Miller JF, Paul KD, Lee RH, Rymer WZ, and Heckman CJ. Restoration of extensor excitability in the acute spinal cat by the 5-HT2 agonist DOI. *J Neurophysiol* 75: 620-628, 1996.

Miller JF, Paul KD, Rymer WZ, and Heckman CJ. 5-HT1B/1D agonist CGS-12066B attenuates clasp knife reflex in the cat. In: *J. Neurophysiol.*, 1995, p. 453-456.

Mills CD and Hulsebosch CE. Increased expression of metabotropic glutamate receptor subtype 1 on spinothalamic tract neurons following spinal cord injury in the rat. *Neurosci Lett* 319: 59-62, 2002.

Mills JD and Pitman RM. Electrical properties of a cockroach motor neuron soma depend on different characteristics of individual Ca components. *J Neurophysiol* 78: 2455-2466, 1997.

Mittmann T and Alzheimer C. Muscarinic inhibition of persistent Na+ current in rat neocortical pyramidal neurons. *J Neurophysiol* 79: 1579-1582, 1998.

Morisset V and Nagy F. Ionic basis for plateau potentials in deep dorsal horn neurons of the rat spinal cord. *J Neurosci* 19: 7309-7316, 1999.

Nacimiento W and Noth J. What, if anything, is spinal shock? *Arch Neurol* 56: 1033-1035, 1999.

Naftchi N, Schlosser W, and Horst W. Correlation of changes in the GABA-ergic system with the development of spasticity in paraplegic cats. *Adv Exp Med Biol*: 431-450, 1979.

Nance PW, Sheremata WA, Lynch SG, Vollmer T, Hudson S, Francis GS, O'Connor P, Cohen JA, Schapiro RT, Whitham R, Mass MK, Lindsey JW, and Shellenberger K. Relationship of the antispasticity effect of tizanidine to plasma concentration in patients with multiple sclerosis. *Arch Neurol* 54: 731-736, 1997.

Newton BW and Hamill RW. The morphology and distribution of rat serotoninergic intraspinal neurons: an immunohistochemical study. *Brain Res Bull* 20: 349-360, 1988.

Nielsen J, Petersen N, and Crone C. Changes in transmission across synapses of Ia afferents in spastic patients. *Brain* 118: 995-1004, 1995.

Noth J. Trends in the pathophysiology and pharmacotherapy of spasticity. *J Neurol* 238: 131-139, 1991.

Patel R, Kerr R, and Maxwell D. Absence of co-localized glutamic acid decarboxylase and neuropeptides in noradrenergic axons of the rat spinal cord. *Brain Res* 749: 164-169, 1997.

Penn RD. Medical and surgical treatment of spasticity. *Neurosurg Clin N Am* 1: 719-727, 1990.

Perrier JF and Hounsgaard J. Ca(2+)-activated nonselective cationic current (I(CAN)) in turtle motoneurons. *J Neurophysiol* 82: 730-735, 1999.

Perrier JF, Mejia-Gervacio S, and Hounsgaard J. Facilitation of plateau potentials in turtle motoneurones by a pathway dependent on calcium and calmodulin. *J Physiol* 528 Pt 1: 107-113, 2000.

Pierau FR, Klee MR, and Klussmann FW. Effect of temperature on postsynaptic potentials of cat spinal motoneurones. *Brain Res* 114: 21-34, 1976.

Powers RK and Binder MD. Persistent sodium and calcium currents in rat hypoglossal motoneurons. *J Neurophysiol* 89: 615-624, 2003.

Powers RK and Binder MD. Summation of effective synaptic currents and firing rate modulation in cat spinal motoneurons. *J Neurophysiol* 83: 483-500, 2000.

Powers RK, Campbell DL, and Rymer WZ. Stretch reflex dynamics in spastic elbow flexor muscles. *Ann Neurol* 25: 32-42, 1989.

Rekling JC and Feldman JL. Calcium-dependent plateau potentials in rostral ambiguus neurons in the newborn mouse brain stem in vitro. *J Neurophysiol* 78: 2483-2492, 1997.

Rekling JC and Laursen AM. Evidence for a persistent sodium conductance in neurons from the nucleus prepositus hypoglossi. *Brain Res* 500: 276-286, 1989.

Remy-Neris O, Barbeau H, Daniel O, Boiteau F, and Bussel B. Effects of intrathecal clonidine injection on spinal reflexes and human locomotion in incomplete paraplegic subjects. *Exp Brain Res* 129: 433-440, 1999.

Richmond FJ and Loeb GE. Electromyographic studies of neck muscles in the intact cat. II. Reflexes evoked by muscle nerve stimulation. *Exp Brain Res* 88: 59-66, 1992.

Richmond FJ, Thomson DB, and Loeb GE. Electromyographic studies of neck muscles in the intact cat. I. Patterns of recruitment underlying posture and movement during natural behaviors. *Exp Brain Res* 88: 41-58, 1992.

Ritz LA, Bailey SM, Carter RL, Sparkes ML, Masson RL, and Rhoton EL. Crossed and uncrossed projections to cat sacrocaudal spinal cord: II. Axons from muscle spindle primary endings. *J Comp Neurol* 304: 316-329, 1991.

Ritz LA, Bailey SM, Murray CR, and Sparkes ML. Organizational and morphological features of cat sacrocaudal motoneurons. *J Comp Neurol* 318: 209-221, 1992.

Ritz LA, Brown PB, and Bailey SM. Crossed and uncrossed projections to cat sacrocaudal spinal cord: I. Axons from cutaneous receptors. *J Comp Neurol* 289: 284-293, 1989.

Ritz LA, Murray CR, and Foli K. Crossed and uncrossed projections to the cat sacrocaudal spinal cord: III. Axons expressing calcitonin gene-related peptide immunoreactivity. *J Comp Neurol* 438: 388-398, 2001.

Robert R and Young MD. Spasticity: a review. *Neurology* 44(Suppl 9): 12-20, 1994.

Russo RE and Hounsgaard J. Burst-generating neurones in the dorsal horn in an in vitro preparation of the turtle spinal cord. *J Physiol* 493 (Pt 1): 55-66, 1996.

Sandler VM, Puil E, and Schwarz DW. Intrinsic response properties of bursting neurons in the nucleus principalis trigemini of the gerbil. *Neuroscience* 83: 891-904, 1998.

Schwindt PC and Crill WE. Amplification of synaptic current by persistent sodium conductance in apical dendrite of neocortical neurons. *J Neurophysiol* 74: 2220-2224, 1995.

Schwindt PC and Crill WE. Factors influencing motoneuron rhythmic firing: results from a voltage-clamp study. *J Neurophysiol* 48: 875-890, 1982.

Schwindt PC and Crill WE. Properties of a persistent inward current in normal and TEA-injected motoneurons. *J Neurophysiol* 43: 1700-1724, 1980.

Shapiro S. Neurotransmission by neurons that use serotonin, noradrenaline, glutamate, glycine, and gamma-aminobutyric acid in the normal and injured spinal cord. *Neurosurgery* 40: 168-176; discussion 177, 1997.

Stafstrom CE, Schwindt PC, Chubb MC, and Crill WE. Properties of persistent sodium conductance and calcium conductance of layer V neurons from cat sensorimotor cortex in vitro. *J Neurophysiol* 53: 153-170, 1985.

Stafstrom CE, Schwindt PC, and Crill WE. Negative slope conductance due to a persistent subthreshold sodium current in cat neocortical neurons in vitro. *Brain Res* 236: 221-226, 1982.

Stauffer E. Trauma. In: *Spinal Deformity in Neurological and Muscular Disorders*, edited by Hardy J. St, Louis: C.V. Mosby, 1974, p. 219 - 239.

Stone LS, Broberger C, Vulchanova L, Wilcox GL, Hokfelt T, Riedl MS, and Elde R. Differential distribution of alpha2A and alpha2C adrenergic receptor immunoreactivity in the rat spinal cord. *J Neurosci* 18: 5928-5937, 1998.

Svirskis G and Hounsgaard J. Transmitter regulation of plateau properties in turtle motoneurons. *J Neurophysiol* 79: 45-50, 1998.

Taylor JS, Friedman RF, Munson JB, and Vierck CJ, Jr. Stretch hyperreflexia of triceps surae muscles in the conscious cat after dorsolateral spinal lesions. *J Neurosci* 17: 5004-5015, 1997.

Thilmann AF, Fellows SJ, and Garms E. The mechanism of spastic muscle hypertonus. Variation in reflex gain over the time course of spasticity. *Brain* 114 (Pt 1A): 233-244, 1991.

Thompson FJ, Parmer R, and Reier PJ. Alteration in rate modulation of reflexes to lumbar motoneurons after midthoracic spinal cord injury in the rat. I. Contusion injury. *J Neurotrauma* 15: 495-508, 1998.

Thor KB, Roppolo JR, Kawatani M, Erdman S, and deGroat WC. Plasticity in spinal opioid control of lower urinary tract function in paraplegic cats. *Neuroreport* 5: 1673-1678, 1994.

Tsien RW, Lipscombe D, Madison DV, Bley KR, and Fox AP. Multiple types of neuronal calcium channels and their selective modulation. *Trends Neurosci* 11: 431-438, 1988.

Voisin DL and Nagy F. Sustained L-type calcium currents in dissociated deep dorsal horn neurons of the rat: characteristics and modulation. *Neuroscience* 102: 461-472, 2001.

Wada N, Miyata H, and Tokuriki M. Histochemical fiber composition of cat's tail muscles. *Arch Ital Biol* 132: 53-58, 1994a.

Wada N, Nakata A, Koga T, and Tokuriki M. Anatomical structure and action of the tail muscles in the cat. *J Vet Med Sci* 56: 1107-1112, 1994b.

Wada N and Shikaki N. Neuronal pathways for spinal reflexes activated by group I and group II muscle afferents in the spinal segment (Co1) innervating the tail in the low spinalized cat. *Exp Brain Res* 125: 129-138, 1999.

Wada N, Sugita S, Jouzaki A, and Tokuriki M. Descending projections to coccygeal spinal segments in the cat. *J Anat* 182 (Pt 2): 259-265, 1993.

Westenbroek RE, Bausch SB, Lin RC, Franck JE, Noebels JL, and Catterall WA. Upregulation of L-type Ca2+ channels in reactive astrocytes after brain injury, hypomyelination, and ischemia. *J Neurosci* 18: 2321-2334, 1998a.

Westenbroek RE, Hoskins L, and Catterall WA. Localization of Ca2+ channel subtypes on rat spinal motor neurons, interneurons, and nerve terminals. *J Neurosci* 18: 6319-6330, 1998b.

Xu W and Lipscombe D. Neuronal Ca(V)1.3alpha(1) L-type channels activate at relatively hyperpolarized membrane potentials and are incompletely inhibited by dihydropyridines. *J Neurosci* 21: 5944-5951, 2001.

Young RR. Spasticity: a review. *Neurol* 44: S12-S20, 1994.

Zhang B and Harris-Warrick RM. Calcium-dependent plateau potentials in a crab stomatogastric ganglion motor neuron. I. Calcium current and its modulation by serotonin. *J Neurophysiol* 74: 1929-1937, 1995.

Zhang B, Wootton JF, and Harris-Warrick RM. Calcium-dependent plateau potentials in a crab stomatogastric ganglion motor neuron. II. Calcium-activated slow inward current. *J Neurophysiol* 74: 1938-1946, 1995.

Zijdewind I and Thomas CK. Motor unit firing during and after voluntary contractions of human thenar muscles weakened by spinal cord injury. *J Neurophysiol* 89: 2065-2071, 2003.

Zijdewind I and Thomas CK. Spontaneous motor unit behavior in human thenar muscles after spinal cord injury. *Muscle Nerve* 24: 952-962, 2001.

Chapter 5: Role of persistent sodium and calcium currents in motoneuron firing and spasticity in chronic spinal rats

(Revised from Li et al. J. Neurophysiol. 91: 767-783, 2004)

INTRODUCTION

In the months following a spinal cord injury a spasticity syndrome develops that is characterized by hyperactive tendon jerks, increased muscle tone, clonus and involuntary flexor withdrawal and extensor spasms. These symptoms are very debilitating as they can interfere with residual motor function, produce pain, disrupt sleep and at times, produce skin breakage (Little et al. 1989). Although studies have shown that exaggerated cutaneous/flexor reflexes (Bennett et al. 1999; Remy-Neris et al. 1999) and increased tonic stretch reflexes are involved in the production of this syndrome (Burke et al. 1970; Powers et al. 1989; Thilmann et al. 1991), the exact mechanisms underlying spasms and spasticity are still not fully understood. Increased excitatory spinal reflex pathways (Barbeau and Norman 2003; Schmit et al. 2002), decreased descending and segmental inhibition (Cavallari and Pettersson 1989; Crone et al. 2003; Mailis and Ashby 1990; Thompson et al. 1998), newly-formed neuronal circuitry due to the sprouting after injury (Krenz and Weaver 1998), and increased neuronal excitability, including interneurons and motoneurons (Bennett et al. 2001c; Eken et al. 1989), may all contribute.

Our recent studies from spinal cord injured adult rats have shown that the development of muscle spasms is caused by large voltage-dependent persistent inward currents (PICs; e.g. calcium currents) that develop in motoneurons weeks to months after injury (chronic spinal, Li and Bennett 2003). These PICs produce sustained depolarizations of the motoneuron (plateau potentials; lasting seconds) in response to brief depolarizing stimulations, resulting in sustained firing that outlasts the stimulation (self-sustained firing). Thus, the PICs amplify and prolong the response of motoneurons to transient

sensory inputs and ultimately generate exaggerated and sustained reflex responses characteristic of the spastic syndrome. Further study indicates that the PICs in these motoneurons are mediated by a sub-threshold TTX-sensitive persistent sodium current (sodium PIC) and a low-threshold nimodipine-sensitive persistent calcium current (calcium PIC; Cav1.3 L-type calcium channel; Li and Bennett, 2003). One goal of the present study was to examine how these two currents contribute to the long-lasting reflexes associated with muscle spasms.

Plateaus and PICs are also activated in motoneurons of animals with intact spinal cord and brainstem (Bennett et al. 1998; Gorassini et al. 1999b; Lee and Heckman 1998a) and uninjured humans (Gorassini et al. 2002; Gorassini et al. 1998; Kiehn and Eken 1997), and thus amplify and prolong synaptic inputs in normal behavior. Normally PICs depend critically on descending facilitation from brainstem-derived serotonin (5-HT) or noradrenaline (Hounsgaard et al. 1988a; Hsiao et al. 1998; Lee and Heckman 1998a, b), and thus, plateaus are eliminated with acute spinal cord injury. Surprisingly, the redevelopment of PICs in motoneurons after chronic spinal cord injury occurs even though the monoamines that normally facilitate PICs, such as 5-HT, are greatly diminished below the injury site (Newton and Hamill 1988). The recovered PICs after chronic injury have amplitudes comparable to those recorded in spinal cord/ brainstem intact animals (Bennett et al. 1998; Lee and Heckman 1998a, b) and normal awake humans (Gorassini et al. 2002). However, due to the loss of proper descending inhibitory control after spinal cord injury, even a brief stimulation is sufficient to trigger plateaus and produce very long-lasting reflexes and spasms (Bennett et al. 2001b).

The activation of the PICs may also contribute to the abnormally slow firing of motor units observed in humans with spasticity following chronic spinal cord injury. For example, the activated PICs may increase the conductance of the motoneurons (Bennett et al. 2001c), thus making it more difficult to increase the firing rate, which could contribute to the lower maximum firing rates reached during volitional contractions in humans following spinal cord injury (Zijdewind and Thomas 2003). Another interesting phenomenon seen in these injured humans is very slow clockwork-like motor unit firing, either occurring spontaneously or triggered following an innocuous stimulation (Gorassini et al., in preparation; see also Zijdewind and Thomas 2001). Interspike intervals during this firing are up to half a second and are much longer than expected from normal motoneurons (Matthews 1996). A similar phenomenon has also been recorded directly in motoneurons of rats after chronic injury (Bennett et al. 2001c). It can be triggered by intracellular stimulation, and thus is an intrinsic property of the motoneurons. Likely, it is mediated by repetitive re-activation of the voltage-dependent PICs with slow kinetics near firing threshold (as suggested by Bennett et al. 2001c; Carp et al. 1991; Hodgkin 1948; Kernell 1999). Thus, the second goal of the present study was to specifically examine the role of PICs in this and other abnormal slow firing behaviors seen after injury.

Aside from abnormally slow firing, the firing behavior of motoneurons of chronic spinal rats is very much like that in normal motoneurons, in the spinal cord intact state (i.e., in unanesthetized decerebrate cats, Bennett et al. 1998; Hounsgaard et al. 1988a; Lee and

Heckman 1998b). Both exhibit self-sustained firing produced by large PICs (see above), and both exhibit classic input-output properties with primary and secondary range firing responses to injected current (piecewise linear frequency-current, F-I, relations). However, with the chronic spinal rat preparation recordings are made *in vitro* (Bennett et al. 2001c), making it possible to directly block the PICs pharmacologically and examine their role in the classic input-output firing properties of motoneurons. This was our third goal. We found that the activation voltage of the calcium PIC critically determines the firing behavior. When the calcium PIC is activated subthreshold to the initial firing level at recruitment (in about half the cells) then it assists in producing self-sustained firing, but this firing is linearly modulated with current, with a single F-I slope. However, when the calcium PIC is activated above the initial firing level, then it does not assist in low frequency firing (in primary range), but causes a steep acceleration in firing when it is being activated (secondary range F-I slope). In all cells, after the calcium PIC is steadily activated then it produces a paradoxically lower F-I slope (denoted as tertiary range), which we argue is due to the increased conductance provided by this calcium PIC. These results lead to the suggestion that steady state firing in the primary, secondary and tertiary ranges can be directly defined in terms of the state of the calcium PIC (see Discussion).

METHODS

Both normal adult female Sprague-Dawley rats (> 60 days old, n = 5) and spastic rats with chronic spinal cord injury (> 90 days old, n = 27) were included in the present study. For the spastic rat, a complete spinal cord transection was made at the S_2 sacral level when the rat was 40 to 50 days old (Bennett et al. 1999; Bennett et al. 2001b,c). Usually, within 30 days dramatic spasticity developed in the tail muscles, which are innervated by sacrocaudal motoneurons below the level of the injury. Only rats more than 50 days (also usually less than 120 days) post injury with clear spasticity were included in the present study. See Bennett et al. (1999) for details of the chronic spinal transection and spasticity assessment. All experimental procedures were approved by the University of Alberta animal welfare committee (HSAPWC).

In vitro preparation

The experimental procedure has been previously described in detail (Li and Bennett 2003), and is only briefly summarized here. Normal and chronic spinal rats were deeply anaesthetized with urethane (0.18 g/100 g; with a maximum of about 0.45 g for rats > 250 g), and the whole sacrocaudal spinal cord was removed and placed in a dissection chamber filled with modified ACSF (mACSF) maintained at 20°C. After an hour's rest in the dissection chamber, the cord was transferred to the recording chamber where it was immersed in continuously flowing (5 ml/min) normal ACSF (nACSF), maintained at 25°C. The long ventral roots (usually sacral S_4 and caudal Ca_1) and caudal equina (which

had attached caudal dorsal roots) were mounted on silver-chloride wires above the nACSF and covered with high vacuum grease (Dow Corning). Sharp intracellular recording electrodes were made from thick wall glass capillaries (Warner GC 150F-10, 1.5 mm OD) with a micropipette puller (Sutter P-87 puller), filled with a 1:1 mixture of 2 M KAcetate and 2 M KCl and beveled down to 20 to 30 MΩ on a rotary grinder (Sutter, BV-10, fine 006 beveling stone). Electrodes were advanced perpendicularly into the ventral surface of the cord with a stepper-motor micromanipulator (660, Kopf) to penetrate motoneurons. Motoneurons were identified by antidromic ventral root stimulation. Only motoneurons with stable a penetration, resting potential < -60 mV, spike amplitude > 60 mV and reliable repetitive firing were included in the study. An Axoclamp2b intracellular amplifier (Axon Instruments) running in either discontinuous current-clamp modes (DCC, switching rate 7 to 10 kHz, output bandwidth 3.0 kHz) or discontinuous voltage-clamp modes (gain 1 to 2.5 nA/mV) were used to collect the data. The basic properties of the motoneurons, such as cell resistance, firing threshold, firing level were measured during current ramps in DCC mode, as described in Li and Bennett (2003).

Drugs and solution

Two kinds of ACSF were used in the experiments: nACSF in the recording chamber and mACSF in the dissection chamber prior to recording. The composition of nACSF was (in mM): 122 NaCl, 24 $NaHCO_3$, 2.5 $CaCl_2$, 3 KCl, 1 $MgSO_4$ and 12 D-glucose. The composition of mACSF was (in mM): 118 NaCl, 24 $NaHCO_3$, 1.5 $CaCl_2$, 3 KCl, 5 $MgCl_2$, 1.4 NaH_2PO_4, 1.3 $MgSO_4$, 25 D-glucose and 1 Kynurenic acid. Both kinds of

ACSF were saturated with 95% O_2 - 5% CO_2, and maintained at pH 7.4. Drugs added to the nACSF in the experiments included: 0.5 to 2 μM TTX (RBI), 3 to 20 μM nimodipine (Sigma) and 400 μM Cd^{++} (Sigma), as detailed in Li and Bennett, 2003.

Plateau and PIC activation in current and voltage clamp recording

Slow triangular current ramps (0.4 nA/s) and voltage ramps (standard speed 3.5 mV/s, varied from 2 to 5 mV/s) were applied to the motoneurons to evoke the plateaus and the associated PIC. During the current ramps (in current-clamp), the PIC that contributed to a subthreshold plateau and sustained firing was estimated from the difference in injected current required to terminate a plateau (I_{end}), compared to the current required to start the plateau ($\Delta I = I_{end} - I_{start}$, see Fig. 1*A* and Bennett et al, 2001c). Also, the subthreshold plateau is quantified by extrapolating the linear subthreshold voltage-current relation to just prior to the first spike (thin line in Fig. 1*A*), and subtracting this linear response from the actual depolarization (measured 5 ms prior to the first spike to avoid rapid upswing of the spike). The term plateau is used to denote any relatively sustained depolarization produced by a PIC. As discussed in Bennett et al. (1998), it does not imply a fixed depolarization. Instead, the depolarization produced by the PIC (plateau) can summate with other depolarizations, such as the passive depolarization during a current ramp, and thus a plateau can essentially ride on top of a passive current ramp response (Fig. 1A and Fig. 4*B*). A plateau is inherently a bistable phenomena, and near threshold can be triggered on or off repeatedly (Hounsgaard, 1988), and thus can have a variable duration.

During the voltage ramps (in voltage-clamp), the PIC caused a negative-slope region in the I-V relation, and this negative slope region caused the plateau seen in current clamp (Li and Bennett, 2003). To obtain an estimation of the passive leak current that summed with the PIC to give the total recorded current, a linear relation was fit to the subthreshold current response in the linear region 10 mV below the negative slope region onset, and extrapolated to more positive voltages (*leak current*, thin triangular line overlaying current; Fig. 1*B*). The PIC amplitude was then estimated by subtracting this leak current from the recorded current, and this difference is indicated by the arrow in Fig. 1*B* (see details in Fig. 1 of Li and Bennett 2003). In the previous paper (Li and Bennett, 2003), we defined the first zero slope point on the up ramp in the recorded current as the onset current (I_{on}) of the PIC, and the corresponding voltage as the onset voltage (V_{on}); the second zero slope point of the recorded current in the up-ramp as the initial peak current (I_i) of the PIC. In the present paper, we measured the half-activation voltage ($V_{1/2}$) of the PIC because this point corresponded well to when the plateau was activated in current-clamp (see Fig. 9 in Li and Bennett, 2003; $V_{1/2}$ is voltage at which half PIC activated, at I_{on} - (I_{on} – I_i)/2). Also, the PIC was activated over a broad range, and the onset voltage V_{on} underestimates the voltage at which the PIC and plateau were functional, compared to $V_{1/2}$. The slope of the subthreshold leak current was denoted S_1. The slope of the I-V relation was also computed at suprathreshold voltages, above the negative slope region and denoted S_2. The S_2 slope was measured over a small 1mV range and at a common voltage when the PIC was fully activated (at Vj in Fig. 1 of Li and Bennett, 2003), to minimize time dependent activation effects. Thus, the S_1 and S_2 approximate the membrane conductance.

Instantaneous firing frequency as a function of injected current (F-I) was computed using a custom Linux-based program (G. R. Detillieux, Winnipeg). The F-I slope was computed for piecewise linear regions of the F-I relation with a regression. To compare the difference in firing frequency before and after drug applications (nimodipine), only ramps with matched amplitude and speed were employed, and thus some cells were discarded because we did not have matched ramps. This was particularly important for cells with significant rate adaptation (Bennett et al. 2001c), which were very sensitive to ramp speed amplitude and speed. In some cells, there were significant changes in sub-threshold input resistance after drug application, presumably due to leakage or electrode blockage, and such cells were also discarded from the F-I analysis. The initial firing level (spike threshold) for each cell was measured from the first spike elicited by the current ramp, at the potential where there first began a rapid acceleration in the rate of depolarization to > 10 V/s (Li and Bennett, 2003).

Dorsal root reflexes

A single electrical stimulation pulse was applied to the dorsal caudal root (Ca_1; 0.02 to 0.1nA, 0.1ms, 10 sec minimum interval between stimuli) while the motoneuron membrane was held at different potentials, and reflex responses were recorded in the motoneurons. This single shock was usually enough to elicit a long-lasting reflexes. However, in a few cells, 2 to 3 shocks at 200 ms intervals had to be given to evoke a long-lasting reflex.

Data analysis

Data were analyzed in Clampfit 8.0 (Axon Inst.). Data are shown as averages $\pm$ standard deviation. A Student's *t*-test was used to test for statistical differences, with a significance level of $P < 0.05$.

RESULTS

A total of 27 motoneurons from chronic spinal rats and 5 motoneurons from acutely transected normal rats were included in the present study. Previously, we have described the basic properties and persistent inward currents (PICs) in these same neurons (26 of them; Li and Bennett, 2003), and the purpose of the present paper was to determine how these PICs affected firing behavior. The PICs were measured with slow triangular voltage ramps, in voltage-clamp mode, as shown in Fig. 1*B*. During an upward voltage ramp the current initially increased linearly due to the passive leak current (shown extrapolated with thin triangular line, middle trace in Fig. 1*B*), but after the onset of the PIC the current deviated negatively and caused a negative-slope region in the I-V relation. The difference between the measured current and the extrapolated leak current was used as an estimate of the net PIC (vertical arrow in Fig. 1*B*; see Methods). The half activation voltage of the PIC ($V_{1/2}$; vertical thin line in Fig. 1*B*) was used to quantify the location of the negative-slope region, which we have previously shown corresponds to the point at which a plateau is activated during a current ramp (see Fig. 9 in Li and Bennett, 2003). In all motoneurons of chronic spinal rats (n = 27) the $V_{1/2}$ was on average -50.1 ± 4.72 mV, which was 3.79 ± 1.72 mV below the firing level (i.e. spike threshold, dashed line in Fig. 1*B*; significant difference), where the subthreshold plateau occurred (left arrow in Fig. 1*A*).

There are only two major currents that make up the PIC: a TTX-sensitive persistent sodium current (sodium PIC) and a nimodipine-sensitive persistent calcium current

(calcium PIC; Li and Bennett, 2003). With the application of nimodipine only the sodium PIC remains, and this current is shown in Fig. 1*F* (upper trace), after leak current subtraction (see Methods). The reduction in current with nimodipine represents the calcium PIC, and this is also shown in Fig. 1*F* (lower trace). Nimodipine blocks the calcium PIC without affecting the fast sodium spike (Figs. 2 and 9, described latter), and was thus particularly useful in studying the effects of PICs on firing as shown below.

Firing behavior classification (LLS and LAS type cells)

Previously, we have shown that motoneurons of chronic spinal rats can be divided into two distinct types based on their unique firing patterns (Bennett et al. 2001c), and these were again found in the present population of motoneurons, as shown in Figs. 1 and 2. In the first type of motoneuron (Fig. 1; n = 16/27 cells), there was initially a linear increase in potential during a current ramp, but about 5 mV below the firing level the potential accelerated relatively steeply. This acceleration marked the onset of a subthreshold plateau (left arrow in Fig. 1*A*; Bennett et al. 2001c; Li and Bennett, 2003), because if the current was reduced shortly afterwards, there was a maintained depolarization and associated firing that continued even when the current was reduced far below the current that initiated firing (self-sustained firing). This self-sustained firing was quantified by $\Delta I = I_{start} - I_{end}$, where I_{start} and I_{end} are the currents at the start and end of plateau and firing. The ΔI was on average 1.13 ± 0.19 nA for this cell type. The plateau stopped just after firing ceased, as seen by the after-potential at the end of the descending current ramp (right arrow in Fig. 1*A*). In this type of cell the plateau was as fully activated as possible shortly after recruitment, because larger ramps did not produce more self-sustained firing

(not shown, though see Fig. 5 in Bennett et al, 2001c). Furthermore, shortly after recruitment there was no further evidence of plateau activation (no firing rate jumps) and the firing changed linearly with the current, even during repeated current ramps, and during self-sustained firing (at currents below the plateau activation threshold; Fig. 1*C*). Thus, we refer to this type of cell as Low-threshold Linear Self-sustained firing cells (LLS type).

In the second type of motoneuron, shown in Fig. 2 (n = 11/27 cells), during a slow current ramp there was also a subthreshold plateau (and PIC) activation like in LLS cells (left arrow in Fig. 2*A* and *B*). However, this plateau/PIC was *not* fully activated at recruitment, because only a small degree of self-sustained firing was produced when the ramp was turned around shortly after recruitment ($\Delta I = 0.6$ in Fig. 2*A*; mean $\Delta I = 0.34 \pm 0.15$ nA for all cells). In contrast, larger ramps evoked a late acceleration in firing (labeled '*s*' in Fig. 2*B*) that marked the further onset of a PIC, because this extra firing was sustained despite reduced current (F-I hysteresis) and there was significantly more self-sustained firing ($\Delta I = 1.2$ in Fig. 2*B*; mean $\Delta I = 0.98 \pm 0.15$ nA). These cells we refer to a Late-Accelerating Self-sustained firing cells (LAS type). LAS type cells were on average lower rheobase cells (1.29 + 1.53 nA) than LSS cells (2.53 + 0.69 nA; see Bennett et al. 2001c).

The linear increase in firing with current prior to the late acceleration we refer to as primary range firing (*p* in Fig. 2*B*) and the firing during the late acceleration we refer to as ramp-evoked secondary range firing (*s* in Fig. 2*B*), similar to the classic steady-state

firing responses (Bennett et al. 1998; Kernell 1965a; Schwindt and Crill 1982). The firing after the late acceleration we refer to as tertiary range firing (*t* in Fig. 2*B*). Classically, the steady-state primary and secondary range firing is obtained from an increasing sequence of 1 sec current steps, and measured in the last half second of each step (Kernell 1965a). We instead used very slowly increasing current ramps (lasting 10 – 20 sec), but for the primary and tertiary ranges, the firing obtained at a particular current was similar to the steady-state firing during a classic current step (data not shown). In the secondary range during a current ramp, the firing was not quite in steady-state, because the Calcium PIC is likely being activated at this time (see below, Calcium PIC activation takes about 0.5 sec, Li and Bennett, 2003c), and thus we denote this the ramp-evoked secondary range. While the F-I slope in this range is steep compared to the primary slope, the firing still increases over a 2 sec period (Fig. 2), and thus is approximately comparable to the classic secondary range response to two 1 sec current steps.

Sub-threshold sodium and calcium PIC contributions to LLS-type cells

In LLS type cells the subthreshold plateau activation was caused by both sodium and calcium PICs, because nimodipine significantly reduced it (from 9.49 ± 3.53 to 3.17 ± 2.09 mV), but blocking it required both nimodipine and TTX (see details in Li and Bennett, 2003). Furthermore, direct measurements of these two PICs in voltage-clamp (described above) indicate that they were both activated subthreshold, and thus should indeed produce a subthreshold plateau. That is, in LLS cells the half activation voltage $V_{1/2}$ of the calcium PIC (-44.2 mV in Fig. 1*F*) and sodium PIC (-43.7 mV in Fig. 1*F*) were always less than the firing level (-41.4 mV in Fig. 1*F*; n = 7/7 cells with

nimodipine), and not significantly different from each other. Nimodipine significantly increased the current required to initiate firing (from 2.53 $\pm$ 0.69 nA to 3.26 $\pm$ 0.55 nA), and in most cells lowered the initial firing rate (in 4/7 cells; lowered from 7.73 $\pm$ 1.34 Hz to 6.38 $\pm$ 1.53 Hz, though not quite significantly; P = 0.13), so the calcium PIC was involved in initiating firing. Both the sodium and calcium PICs were nearly fully activated by the time the firing level at recruitment was reached (Fig. 1*F*), and this is consistent with the above conclusion that the PICs and plateau were as fully activated as possible at recruitment, and subsequently did not contribute to accelerations in firing rate during the ascending current ramp (unlike LAS cells). Nimodipine also significantly reduced the after-potential after de-recruitment (from 6.39 ± 1.33 to 3.01 ± 2.14 mV; right arrows in Fig. 1*A* and *D*), and eliminated the brief accelerations in firing that are sometimes seen just prior to de-recruitment (* in Fig. 1*A* and *C*, but not 1*D*; also see Fig. 5 of Bennett et al. 2001c), and thus these were Calcium PIC mediated.

The characteristic self-sustained firing evoked even by small current ramps in LLS cells was in large part caused by the low threshold calcium PIC, because this self-firing was markedly reduced by nimodipine (ΔI significantly lowered from 1.15 $\pm$ 0.22 nA to 0.26 $\pm$ 0.26 nA). A subthreshold calcium PIC occurred in all LLS cells, and thus is a primary requirement for LLS type firing behavior. However, there did remain significant self-sustained firing in nimodipine, and this was due to slow firing caused by the sodium PIC, that under some conditions could last for very long periods (see Figs. 6-8 described below).

Calcium PIC causes the late acceleration in LAS-type cells

In contrast, when nimodipine was applied to LAS-type cells (n = 5), there was no significant effect on the subthreshold plateau activation, the recruitment current (1.29 $\pm$ 1.53 nA before and 1.40 $\pm$ 2.25 nA after), or low frequency firing (see details in Fig. 5*B*, described later) and thus only the sodium PIC was involved in subthreshold plateau behavior and low frequency firing. However, when these cells were brought to fire at higher frequencies with a larger current ramp, there was a characteristic late acceleration in firing that was always blocked by nimodipine (5/5 cells), and thus this non-linearity in the F-I relation (*s* range in Fig. 2*B*) was caused by the calcium PIC. In LAS type cells the calcium PIC (seen in Fig. 2) was activated at a potential ($V_{1/2}$ = -44.8 $\pm$ 5.3 mV; right arrow in Fig. 2*F*) significantly higher than the firing level at recruitment (-47.2 $\pm$ 4.3 mV; dashed line in Fig. 2*F*), and much higher than the subthreshold sodium PIC ($V_{1/2}$ = -50.0 $\pm$ 4.7 mV; left arrow in Fig. 2*F*). Thus, this higher threshold calcium PIC was only activated after recruitment when the membrane potential was sufficiently depolarized during higher frequency firing. At this time the calcium PIC activation produced the late acceleration in firing rate (firing level at this time indicated by * in Fig. 2*F*).

The self-sustained firing after the late acceleration was significantly reduced by nimodipine in LAS cells (from ΔI = 0.97 $\pm$ 0.15 to 0.24 $\pm$ 0.31 nA), indicating that the calcium PIC played a major role in sustaining the firing, as for LSS cells. In summary, in LAS cells the sodium and calcium PICs were distinctly separated in their activation voltages and respectively produced two distinct effects: an early subthreshold plateau and a late acceleration in firing respectively followed by self-sustained firing.

Variations in calcium PIC determines firing behavior

In many cells (n = 13) we added TTX first, rather than nimodipine, and in these cells we could not study the firing since the spikes were blocked together with the sodium PIC. However, in these cells the calcium PIC could be observed directly as the PIC remaining in TTX (Fig. 3*C,D*), and compared to the firing level at recruitment prior to TTX. The half activation potential of the calcium PIC ($V_{1/2}$ calcium) clearly separated all these cells into two groups corresponding to the LLS and LAS classification of their firing behavior (prior to TTX application), as expected from the nimodipine experiments described above. This is shown in Fig. 3*F* where the degree of self-sustained firing (ΔI) is plotted as a function of the $V_{1/2}$ calcium relative to the firing level. When the $V_{1/2}$ calcium was below firing level (n = 7; Fig. 3*C*), pronounced sustained firing occurred ($\Delta I = 1.12 \pm 0.16$ nA) even for small ramps reaching just above the recruitment threshold (as in Fig. 3*A*; solid circles at left of vertical zero line in Fig. 3*F*), and these cells all corresponded to LLS type cells (n = 7/7), as described above. When the $V_{1/2}$ calcium was above the firing level (n = 6; Fig. 3*D*) significantly less self-sustained firing occurred ($\Delta I = 0.35 \pm 0.16$ nA) for the same small current ramps (Fig. 3*B* and solid circles at right of vertical line in Fig. 3*F*), even though these cells had as large PICs (Fig. 3*D*) as the LLS cells (Fig. 3*C*). However, with larger ramps (like in Fig. 2*B*; open circles in Fig. 3*E*) pronounced self-sustained firing ($\Delta I = 1.02 \pm 0.11$ nA) could usually be evoked after a late acceleration in firing (n = 4/6), and these cells corresponded to LAS type cells (upper open circles at right of Fig. 3*E*).

There were however a few cells with the $V_{1/2}$ calcium above the firing level that always had weak self-sustained firing and did not have a firing rate acceleration regardless of the ramp amplitude (lower open circles at right of Fig. 3*E*; n = 2/6 cells tested with TTX). These cells had large calcium PICs, but the calcium PIC threshold was too high to produce a late acceleration during firing evoked with a current ramp (due to accumulated AHP effects; see Li and Bennett 2003). Interestingly, in these cells the calcium PIC and firing rate acceleration could be activated by synaptic input (described below), suggesting a difference due to dendritic location of the synaptic inputs and calcium PIC (Bennett et al. 1998b).

Low F-I slope in chronic spinal rats results from Ca^{++} mediated conductance

As we have shown previously, motoneurons from chronic spinal rats fired with a significantly shallower frequency-current (F-I) slope (mean 4.56 Hz/nA, see below) than the motoneurons of acute spinal rats, 6.7 Hz/nA (acute data from Bennett et al. 2001c), when tested with current ramps as in Fig. 2. We proposed that the main reason for this lower slope was the activation of the large PICs in chronic spinal rats, which should have increased the conductance of the cells and thus increased the difficulty in depolarizing the cells with injected current and ultimately decreased the F-I slope (Bennett et al. 2001c). To examine this issue we first verified that the membrane conductance increased after the PIC activation, by estimating the conductance from the slope of the I-V relation during the ramp voltage-clamp experiments (see Methods). Indeed as shown in Fig. 4*A* (lower trace), at voltages below the negative-slope region, prior to PIC activation, the

conductance (I-V slope S_1) was much shallower than above the negative-slope region with the PIC activated (S_2, measured at common potential at vertical line). In motoneurons of chronic spinal rats, the ratio of these two slopes (S_2/S_1) was significantly greater than 1 ($S_2/S_1 = 5.28 \pm 3.42$, n = 13), whereas in motoneurons of acute spinal rats, the ratio was not significantly different from 1 (since there was usually a linear I-V relationship, with no PIC activation; S_2 slopes measured at same voltage as in chronic spinal rats; see Li and Bennett 2003). This increased conductance in chronic spinal rats was mediated by both sodium and calcium PICs, because the ratio of $S_2/S_1$was significantly decreased when TTX or nimodipine were added to the bath (TTX shown in Fig. 4*A*, middle trace), and it was decreased to 1 after both drugs were applied (Fig. 4*A*, upper linear trace). Importantly, the increased conductance following PIC activation was not caused by a voltage-dependent potassium conductance in the voltage range studied (< -30 mV), because TTX and nimodipine eliminated the increased conductance when measured at a common voltage (see linear responses in top trace of Fig. 4*A*). Thus, persistent sodium and calcium PICs mediated the increased conductance. The calcium PIC mediated increase in conductance (S2) likely includes a Ca++ -activated K+ current (unpublished data).

The increased conductance after calcium PIC activation was also seen during current-clamp experiments where TTX was present (Fig. 4*B*), and a calcium-mediated plateau occurred without spiking. That is, on the plateau with the calcium PIC activated, the slope of the voltage curve (resistance, R_2 = 1/ conductance) was only 48% of the slope before the plateau started (R_1; significantly lower; $R_1/R_2 = 2.10 \pm 0.83$; n = 12),

suggesting that the conductance of the membrane was doubled by the activated calcium PIC.

Finally, to prove that the presence of the calcium PIC contributed to the shallow F-I slope seen in motoneurons of chronic spinal rats, we blocked this current with nimodipine (Fig. 5), which again, had no direct affect on the sodium spikes or AHPs. As expected, the F-I slope was found to be significantly steeper after nimodipine compared to before (7.37 $\pm$ 3.32 Hz/nA compared to 4.56 $\pm$ 1.19 Hz/nA, n = 9, Fig. 5*A*), provided that the slope before nimodipine application was measured in a region where the calcium PIC was known to be active (above calcium PIC threshold). The cell in Fig. 5*A* is an LLS cell with the calcium PIC activated subthreshold to firing, and the F-I slope was clearly affected throughout by nimodipine. Whereas, the cell in Fig. 5*B* is an LAS cell with the calcium PIC only activated after the late acceleration in firing, and the slope was only increased by nimodipine after this late acceleration, in the tertiary range, as described next.

Secondary and tertiary range firing caused by calcium PIC

In LAS type cells (Fig. 5*B*), nimodipine had no significant effect on the F-I slope when the cell fired in the primary range subthreshold for late acceleration in firing (Fig. 5*B* and *C;* mean slope 3.04 $\pm$ 1.02 Hz/nA in the primary range before nimodipine, *p*, and 3.70 $\pm$ 1.02 Hz/nA after nimodipine, p'), as would be expected of the lack of calcium PIC in this range. In contrast, after the late acceleration in firing, and thus calcium PIC activation, the F-I slope (in tertiary range, *t* in Fig. 5*B*; mean 2.10 $\pm$ 1.31 Hz/nA) was significantly less than the slope in nimodipine, even at matched frequency ranges (Fig. 5*C;* mean 3.70

± 1.02 Hz/nA), consistent with the activated calcium PIC reducing the F-I slope. Also consistent with this interpretation, the slope with the calcium PIC fully activated, in tertiary range (Fig. 5*B*; *t;* mean 2.10 Hz/nA, as above), was significantly less than the slope measured prior the calcium PIC activation, in the primary range (*p* in Fig. 5*B*; mean 3.04 Hz/nA). Of course, during the late acceleration in firing (ramp-evoked secondary range) the F-I slope was very steep (*s* in Fig. 5*B;* mean 6.32 ± 3.63 Hz/nA), and this steep secondary range firing was eliminated with nimodipine (as discussed above), leaving only simple linear primary range firing for all currents (Fig. 5*C;* mean 3.70 ± 1.02 Hz/nA). This is consistent with the idea that the secondary range firing is caused by the calcium PIC onset (Schwindt and Crill 1982).

Very slow firing caused by persistent sodium currents

When a current ramp was applied to a motoneuron of a chronic spinal rat, the last few spikes of firing were usually very slow (mean 2.28 ± 0.67 Hz; Figs. 1*A*, 2*A*, 3*A*, and 5*B*), and less than half the minimum repetitive firing rate that occurs in motoneurons of acute spinal rats (7.51 ± 3.53 Hz, Bennett et al. 2001c; significant difference). We demonstrate in this section that this unusually slow firing is mediated by a subthreshold oscillation of the large sodium PIC seen in motoneurons of chronic spinal rats.

Very slow firing was most clearly studied when evoked by a brief current pulse in a cell held close to its firing threshold with a bias current (Fig. 6*A*). Following the pulse, there was usually a pause in firing during which a plateau was slowly activated (at arrow in upper trance of Fig. 6*A*) and then very slow self-sustained firing began. This self-

sustained firing continued for many seconds, or even minutes, and then either stopped spontaneously or was terminated by a hyperpolarizing pulse (Fig. 6*A*). Typically, the firing rate was very low (mean 2.82 $\pm$ 1.21 Hz) and extremely regular (standard deviation in firing 0.26 $\pm$ 0.13 Hz), unlike the variable slow firing that can be driven by synaptic noise (Matthews 1996; Powers and Binder 2000). In some cells we did see transient rate changes during the long periods of slow self-sustained firing (stars in Fig. 7 described latter), but these were due to spontaneous synaptic events, because EPSPs of a similar duration could be seen prior to firing (not shown). The minimum firing rates corresponded to inter-spike intervals of 300 - 800 ms, which were much longer than the duration of the usual AHP (50 – 100 ms), measured in response to antidromic stimulation at rest (indicated by length of the open bar in the expanded section of data in Fig. 6*A*). Thus, these cells fired like clockwork at much lower rates than predicted by the AHP duration.

In contrast, in motoneurons of acute spinal rats the minimum repetitive firing rate during a depolarizing pulse was 7.51 $\pm$ 3.53 Hz (Bennett et al. 2001c; 7.68 Hz in Fig. 6*B*), which corresponds to an inter-spike interval of 133 ms, and this is close to the AHP duration (100 ms in Fig. 6*B*), as would be expected for motoneurons with small PICs that fire in the absence of synaptic noise (Kernell 1965b). Also, self-sustained firing could not be evoked in acute spinal rats (Fig. 6*B* and Bennett et al 2001c), consistent with the small PICs and lack of negative-slope region in the I-V relation in these cells (Li and Bennett 2003).

During slow firing in chronic spinal rats the trajectory of the membrane potential between spikes was very much like the subthreshold onset of a plateau prior to the first spike following a brief current pulse (left arrow in upper trace of Fig. 6*A*) or during a current ramp (left arrows in Figs. 1*A*-3*A*). That is, on the expanded time scale in Fig. 6*A*, after the current pulse a plateau was activated that depolarized the cell initially with a slow ramp up and then with a faster acceleration that ultimately triggered a spike (ramp&accelerate trajectory; left of expanded plot). Following the 100 ms AHP from this first spike (region of bar), the membrane potential rose again with the same ramp&accelerate trajectory as though a plateau was again being activated, and this triggered a second spike (second arrow; see also Fig. 7). Thus, it appeared that a plateau was being activated prior to each spike and then deactivated by the AHP that followed that spike, and this process was repeated to cause slow firing.

Because the sodium PIC is rapidly deactivated by a hyperpolarization (in < 10 - 50 ms, Lee and Heckman 2001, Li and Bennett 2003), whereas the calcium PIC is not (remains on for > 500 ms), it stands to reason that only the sodium portion of the plateau could be deactivated during each 100ms AHP, and thus only the sodium PIC could participate in this slow firing. Indeed, in cells where the calcium PIC was activated far above the firing threshold and was only involved in high frequency firing (LAS type; Fig. 6 shows such a cell), slow self-sustained firing was just as easily evoked as in other cells (LLS type).

Also, slow firing persisted when the calcium PIC was blocked with nimodipine (n = 4) or Cd^{++} (n = 2), with the same slow steady rate (3.37 $\pm$ 0.49 Hz before and 2.60 $\pm$ 0.67 Hz

after nimodipine; Fig. 7) and the same characteristic subthreshold plateau activation and associated ramp&accelerate interspike trajectory (arrows in Fig. 7*B*). Thus, this very slow firing did not involve the calcium PIC. In contrast, in cells that had a poor persistent sodium PIC, which did not by itself produce a negative slope region (Fig. 10*D*; described latter), very slow firing could not be evoked (Fig. 10*A*). Instead the minimum firing rate corresponded to an inter-spike interval similar in duration to the AHP, as for motoneurons of acute spinal rats described above. Thus, a negative-slope region produced by the sodium PIC is the primary requirement for slow firing.

Finally to directly demonstrate that the sodium PIC caused slow firing and related subthreshold plateau activation, nimodipine was given together with a low dose of TTX (0.5 μM; Fig. 8). During low dose TTX application there was a brief window in time (5 mins) when the spike was unaffected (see insets in Fig. 8), but the sodium PIC was reduced (not shown). Because this window in time was only brief, we in this case studied slow firing with brief current ramps rather than pulses (pulse protocols are time consuming requiring the PIC threshold to be determined). Prior to drug applications, on the upward current ramp there was the characteristic acceleration in potential as a plateau started (left arrow in Fig. 8*A*), and this as usual did not require the calcium PIC, since it was not blocked by nimodipine (Fig. 8*B*; LAS cell described above). Likewise, just prior to de-recruitment on the downward current ramp there was the usual very slow firing (mean rate 2.31 $\pm$ 1.04 Hz), with one very long interval, with a characteristic ramp&accelerate trajectory similar to the plateau onset (Fig. 8*A*, right arrow). This slow firing again did not depend on the calcium PIC, because it was not significantly altered

by nimodipine (Fig. 8*B;* mean rate 2.28 $\pm$ 0.67 Hz). When low dose TTX was added, with nimodipine present, the characteristic subthreshold acceleration/plateau onset was eliminated (left of Fig. 8*C* and *D*), and likewise the slow firing on the downward ramp and characteristic ramp&accelerate interspike trajectory were eliminated. Thus, the subthreshold plateau onset and slow firing are both mediated by the TTX-sensitive sodium PIC.

The firing became very erratic and failed on the downward current ramp in low dose TTX, even when the spike was unaffected. Long irregular firing intervals were seen on the upward ramp, but with a very different interspike trajectory, without the ramp&accelerate shape (Fig. 8*C,D*). Instead, long intervals occurred on the upward ramp simply because a spike failed to be produced by the end of the AHP, and then was only produced as the cell was further depolarized by the increasing current. Furthermore, it appears that this sodium PIC is critical in enabling the cell to generate rhythmic firing at all, because when this current was disrupted firing became irregular (Fig. 8*C, D*), as has been previously reported (Lee and Heckman 2001).

Long-lasting spastic reflexes evoked by brief low-threshold afferent stimulation

In chronic spinal rats a single low threshold dorsal root stimulation shock produced a very long-lasting reflex response that we observed in most motoneurons during intracellular recording (stimulation 2 x afferent threshold, T in Fig. 9*B* and typically 2 – 10xT; n = 11/13), as described previously (Bennett et al. 2001c). This is consistent with the exaggerated reflexes recorded extracellularly from ventral roots of these chronic

spinal rats with the same dorsal root stimulation (Li et al. 2003), and the associated tail spasms recorded with EMG in awake chronic spinal rats (Bennett et al. 1999; Bennett et al. 2001b).

To examine the role of plateaus/PICs in long-lasting reflexes we have blocked the plateau with two separate methods: 1) hyperpolarization and 2) application of nimodipine. The first method relies on the voltage-dependence of the PIC that underlies the plateaus (Bennett et al. 2001c), as demonstrated in a motoneuron of a chronic spinal rat in Fig. 9*A*. That is, although a brief depolarizing current pulse activated a large plateau and long-lasting self-sustained firing when the cell was held at rest, the same pulse could not activate a plateau when the cell was hyperpolarized (i.e. hyperpolarization abolished the plateau). Similarly, while a brief dorsal root stimulation triggered a long-lasting reflex in a motoneuron (upper part of Fig. 9*B*), no long-lasting reflex could be evoked when the motoneuron was held hyperpolarized (Fig. 9*B*). Therefore, the long-lasting reflex was mediated by a PICs/plateaus intrinsic to the motoneurons that was blocked by hyperpolarization (just as in Fig. 9*A*).

Hyperpolarization of the motoneuron did not block the synaptic input caused by the dorsal root stimulation, and this input produced a 0.5 to 1 sec long excitatory postsynaptic potential (EPSP; lower panel of Fig. 9*B*). It is this unusually long EPSP that triggered the slowly activating PICs and reflex when the cell was not hyperpolarized. This can be clearly seen in Fig. 9*B*, where the onset of spiking was delayed because the cell was very near threshold, and the EPSP could be observed first, followed by a PIC/plateau onset (at

arrow) and then self-sustained firing. Also, cells without a clear long polysynaptic EPSP (n = 2/13) did not have long-lasting reflexes to a single low threshold stimulation even though they had large PICs. They could however produce a long-lasting reflex (seconds) in response to repeated high frequency stimulation (100 Hz, for 0.5 sec), by the summated monosynaptic reflex (see below) triggering a plateau/PIC.

Calcium PIC alone produces the long-lasting reflex in some motoneurons

In addition to the sodium and calcium PICs, any other voltage-dependent current facilitated by the dorsal root stimulation (i.e. NMDA receptors) could also be involved in the plateau and associated long-lasting reflex. In general, proving that only sodium and calcium PICs are involved is difficult, because the sodium PIC cannot be easily blocked without blocking the synaptic input involved in triggering the long-lasting reflex (EPSP; TTX blocks the dorsal roots rapidly). Fortunately, there were some motoneurons (n = 2/9) that had clear long-lasting reflexes (Fig. 10*A*) and only weak sodium PICs (Fig. 10*D*). In these motoneurons, 20 μM nimodipine blocked the long-lasting reflex, regardless of the holding potential (Fig. 10*C*), and thus the calcium PIC mediated these long-lasting reflexes. Furthermore, nimodipine did not block the EPSP evoked by the dorsal root stimulation (Fig. 10*C*) and thus nimodipine's primary effect was to block the L-type Ca^{++} channels and associated self-sustained firing postsynaptically. In these cells nimodipine also blocked the plateaus evoked with intracellular current injection (not shown), and this is consistent with the elimination of the calcium mediated negative-slope regions in the I-V plot during voltage-clamp (compare Fig. 10*C* and *D*). There was a small TTX-sensitive sodium PIC that remained in nimodipine (Fig. 10*D*) though not

large enough to produce a plateau, as mentioned above (no negative slope region). In summary, in these cells with weak sodium PICs, the long-lasting portion of the spastic reflexes were entirely due to calcium PICs on the motoneurons mediated by L-type calcium currents, and sustained postsynaptic NMDA-like currents were thus not involved in the long-lasting reflexes.

Sodium and calcium PICs produce long-lasting reflexes in other motoneurons

In other motoneurons (n = 7/9) persistent sodium currents were also involved in the long-lasting reflex. Again these cells had a long-lasting reflex mediated by a large PIC and self-sustained firing that was triggered by dorsal root stimulation and this was blocked by hyperpolarization (Fig. 11*A*). However, this dorsal root evoked PIC and long-lasting reflex was not blocked by nimodipine. It was however reduced in amplitude and there was slower firing and no acceleration in firing, presumably due to the block of the calcium PIC (compare Figs. 11*A* and *D*). This PIC and long-lasting reflex that remained in nimodipine was due to the sodium PIC currents, because there remained a large PIC in voltage-clamp ramps (Fig. 11*F* compared to *C*), there was characteristic very slow firing (upper trace in Fig. 11*D*), and this sodium PIC was blocked by TTX (not shown). Thus, in this cell both sodium and calcium PICs produced the long-lasting reflexes.

Dendritic origin of calcium PICs

Interestingly, reflex evoked calcium PICs and plateaus were more easily triggered (at a lower potentials) than PICs evoked by intracellular current injection, perhaps related to

the dendritic location of the Ca^{++} channels and synaptic inputs (Bennett et al. 1998). That is, with intracellular current injection the calcium PIC was only activated in LAS type cells with a substantial depolarization well above the initial firing level at recruitment (after frequency acceleration at left arrow in upper part of Fig. 9*A*; LAS type cell). Whereas, with dorsal root stimulation a subthreshold plateau and subsequent long-lasting reflex could be activated (e.g. left arrow in upper part of Fig. 9*B*). In the extreme case, there were cells that had high threshold calcium PICs that could not be activated during firing evoked by intracellular current injection (described above), but subthreshold calcium PICs and long-lasting firing could be evoked by dorsal root stimulation (n = 3/3).

Unusually long polysynaptic EPSPs in acute and chronic spinal rats

As mentioned above, in chronic spinal rats the low threshold dorsal root stimulation evoked unusually long EPSPs that were clearly seen when the motoneurons were hyperpolarized to block the plateau and associated PICs (Figs. 11*A*, *B*; 10*A*, *B*; 9*B*). These hyperpolarized EPSPs were on average 9.8 $\pm$ 4.8 mV in amplitude and lasted 960 $\pm$ 270 ms. Typically, the reflex response also had a monosynaptic component, and this was on average14.4 $\pm$ 8.3 mV (Fig. 11 *B*). The long EPSP followed in the tail of the monosynaptic EPSP and thus was of short latency. However, the long EPSP was definitely of polysynaptic origin, because when the monosynaptic reflex was not present, then the long EPSP had a latency of 3.3 ms beyond the monosynaptic latency. Both the mono- and polysynaptic EPSPs were not blocked by nimodipine (Figs. 10 and 11), and thus did not depend on pre- or postsynaptic L-type calcium channels (calcium PICs).

Interestingly, in acute spinal rats there were also very similar long polysynaptic EPSPs (Fig. 9*C*), and thus these must have emerged acutely with injury, because indirect evidence from EMG recordings suggest that this EPSP is not present prior to injury in the awake rat (Bennett and Cooke, in preparation). When these EPSPs were measured with the cell hyperpolarized (lower trace in Fig. 9*C*), as above, they were found to have a long duration (740 $\pm$ 190 ms) and short latency not significantly different from in chronic spinal rats. However, the amplitude of the long EPSP was significantly smaller (4.2 $\pm$ 1.6 mV) in acute compared to chronic spinal rats, as was the monosynaptic reflex (3.2 $\pm$ 4.6 mV). Further, when the cell was held at rest these long EPSPs never evoked firing (no reflex), though at times the monosynaptic EPSP evoked a spike (Fig. 9*C*). Further, there was never a plateau or long-lasting reflex triggered by these long EPSPs, and the EPSP was not amplified by depolarization (unlike in chronic, see below), consistent with the lack of plateaus and small PICs seen in acute spinal rats (Bennett et al. 2001c; Li and Bennett, 2003).

DISCUSSION

Motoneuron firing activated by injected current

Our results indicate that motoneuron firing is dramatically altered by the presence of large intrinsic sodium and calcium PICs in chronic spinal rats, and thus, these currents play a major role in the input-output properties of motoneurons. When activated with intracellular current injection, the sodium PIC causes the activation of a subthreshold plateau potential (TTX-sensitive, and nimodipine resistant) that helps recruit the motoneuron and contributes to sustained firing that outlasts the current injection (self-sustained firing; Figs. 1, 2 and 8). The sodium PIC is also critical in maintaining regular repeated firing (Fig. 8 and Lee and Heckman 2001) and can, by itself, produce very slow self-sustained firing (Fig. 7).

The calcium PIC also helps recruit and sustain firing in cells where it is activated subthreshold to firing, and these effects are clearly demonstrated with a nimodipine block of the calcium PIC (Fig. 1; LSS type cells, Low-threshold Linear Self-sustained firing type). However, in other cells where the calcium PIC has a higher threshold above the initial firing level, it does not participate in recruitment or low frequency primary range firing (Figs. 2 and 5*B;* LAS, Late-Accelerating Self-sustained firing type). Instead, the calcium PIC causes a late acceleration in firing during its activation (causing the steep secondary range firing). After the late acceleration in firing, the calcium PIC helps sustain the firing (in tertiary range). The activation of the calcium PICs dramatically increases the conductance of the cell, likely through the activation of calcium activated

conductances (potassium, Krnjevic et al. 1975; Viana et al. 1993), as well as directly through its own L-type calcium channel conductance (Li and Bennett, 2003). This makes it harder to depolarize the cell and to increase the firing rate with further injected current. This causes a lower F-I slope, or tertiary range, in all cells (LSS and LAS type); LSS type cells are especially interesting, because they fire only in the tertiary range and have no primary or secondary range. Thus, while PICs may help recruit and sustain the firing of a motoneuron, after they are activated they make it harder for subsequent inputs to influence the cell, ultimately lowering the input-output gain (F-I slope; see also Bennett et al. 1998b).

Large PICs also occur in spinal cord intact animals (Hounsgaard et al. 1984; Lee and Heckman 1998a; Schwindt and Crill 1982) and thus, some of the present results likely extend to normal motoneurons in the intact state, or motoneurons modulated by transmitters such as 5-HT (Hounsgaard and Kiehn 1989). We know that during intracellular current injection steady state primary range firing occurs below the activation level of the calcium PIC or plateau (Schwindt and Crill, 1982; Bennett et al. 1998b) and thus, the calcium PIC is likely not involved in this firing. Further, the steady state secondary range firing in intact animals coincides with the onset of the calcium PIC (Schwindt and Crill, 1982), and changes in the activation threshold of the PIC induces associated changes in the secondary range firing (Bennett et al. 1998b). Thus, the onset of the calcium PIC likely causes the secondary range firing in the intact state, like we have directly demonstrated for the chronic spinal rat using nimodipine (Fig. 5, ramp-evoked secondary range). With full PIC activation the firing moves into what we call the tertiary

range, above the secondary range, and the F-I slope is often lower than the slope in the primary range (Fig. 2 in Bennett et al. 1998b with spinal cord intact animals), again like in the chronic spinal rat (Fig. 5). In some motoneurons, especially high threshold cells, the calcium PIC slowly inactivates and this further slows the firing, contributing to rate adaptation (Lee and Heckman, 1998b; Bennett et al. 1998b; Bennett et al. 2001c).

Motoneurons firing activated by synaptic inputs

The calcium PIC arises largely from the dendrites (Carlin et al. 2000; Hounsgaard and Kiehn 1993). Thus, synaptic inputs that arrive at the dendrites more easily activate the calcium PIC, compared to intracellular current injection which is usually in the soma (see Results and Bennett et al. 1998b). This leads to a dramatically altered input-output relation during synaptic input, because the synaptic current can more readily activate the nearby calcium PIC and plateau compared to the somatic sodium spike. Thus, the calcium PIC and plateau are always activated subthreshold to firing, even in cells where the opposite occurs during intracellular current injection (which is somatic) with firing prior to PIC activation (LAS type cells; Bennett et al. 1998b). That is, during graded synaptic excitation when cells begin firing the calcium PIC is already being activated.

If we consider the present results that demonstrate that primary range firing occurs before the calcium PIC activation, and secondary range firing occurs during the calcium PIC activation (Fig. 5), we are led to the conclusion that primary range firing cannot occur during synaptic excitation, because the calcium PIC is activated prior to recruitment (Fig. 9*B*; see also Bennett et al. 1998b). Indeed if we re-define the secondary range as firing

during the onset of the calcium PIC, then it is clear that secondary range firing can only occur just after recruitment, if at all, because the calcium PIC is mostly activated prior to the first spike and only continues to be activated during the first few spikes (like Fig. 9*B*; see also Fig. 8 in Bennett et al. 1998b). After this the calcium PIC is tonically activated, which corresponds to the tertiary range. Thus, during synaptic excitation the firing moves quickly into the tertiary range, where the calcium PIC is tonically activated and the frequency increases slowly with current (corresponding to low F-I slope). Indeed, in many motoneurons the calcium PIC is fully activated prior to recruitment, even with current injection, and firing only occurs in the tertiary range (LSS cells; Fig. 1). Interestingly, in this tertiary range the firing increases linearly with current (Fig. 1*C*; Bennett et al. 2001), and likely synaptic currents summate linearly (Prather et al. 2001), and so the original concept of linear summation proposed by (Granit et al. 1966a) still holds, but functionally occurs in the tertiary, not primary range. These conclusions are consistent with the relatively linear rate modulation and lack of firing rate accelerations seen in motor unit recordings of awake animals and humans (Gorassini et al. 1999b; Gorassini et al. 2002).

Very slow firing in motoneurons after chronic spinal cord injury

One special characteristic of firing in chronic spinal rats is very slow firing, and this also occurs in other animal models of spinal cord injury (Powers and Rymer 1988) and humans with spinal cord injury (Gorassini et al., in preparation, Zijdewind and Thomas 2001). Slow firing can occur in non-injured humans briefly just prior to de-recruitment, but the long periods of low frequency, low variability firing seen with injury are not

common (Gorassini et al. 2002). The reason for the prominence of very slow firing with injury is unclear, but may relate to the particular combination of large sodium PICs and large AHPs seen with injury (Bennett et al. 2001c, Li and Bennett 2003). We have shown in the Results that a subthreshold oscillation of the sodium PIC and AHP mediates very slow firing. Although the concept of a subthreshold PIC oscillation has been suggested by others (Carp et al. 1991; Hodgkin 1948; Kernell 1999), it has not been directly demonstrated before for motoneurons. Similar oscillations of persistent currents underlie other important physiological functions, with pacemaker activity of the heart being the classic example (Irisawa et al. 1993; Zhang et al. 2002).

In motoneurons of chronic spinal rats the large sodium PIC is activated a few milivolts subthreshold to the spike (Figs. 1 and 2), as seen in other neurons (Elson and Selverston 1997; Sandler et al. 1998; Schwindt and Crill 1995). The sodium PIC by itself produces a TTX-sensitive plateau potential (provided that the sodium PIC has a negative-slope region, Li and Bennett, 2003) and this sodium plateau is very different from the classic calcium-mediated plateau described in motoneurons (Hounsgaard et al. 1984), because it is rapidly deactivated by a hyperpolarization, and thus, deactivated by a single brief (100 ms) AHP that follows a spike. This is because the sodium PIC is deactivated very rapidly (in < 10 - 50 ms, Lee and Heckman 2001; Li and Bennett 2003) in relation to the much slower calcium PIC, which can take a second to turn on or off (Li and Bennett 2003).

The sodium PIC can also activate rapidly with moderate depolarizations, but when the potential is near threshold the sodium PIC activates very slowly (Li and Bennett 2003). Thus, near threshold for the sodium PIC a brief disturbance (current pulse or EPSP)

causes the sodium plateau to be slowly activated (ramp-up before left arrow in upper trace of Fig. 7*B*). This plateau activation accelerates as the potential is more depolarized (at left arrow in Fig. 7*B*), presumably due to fast sodium PIC dynamics for larger depolarizations, and this ultimately triggers a spike. The AHP that follows the spike brings the potential far below the sodium PIC threshold for about 100ms (expanded trace in Fig. 7*B*), which is adequate time to fully deactivate the sodium PIC (Fig. 6*C* in Li and Bennett 2003) and thus the sodium plateau is fully deactivated. However, when the AHP finishes (in 100ms) the sodium plateau/PIC is reactivated by the same process and this triggers a second spike and so on. In this way a subthreshold oscillation of the sodium PIC, with repeated sodium plateau activation and deactivation, causes very slow firing.

The very slow firing does not involve the calcium PIC and is exclusively produced by the sodium PIC, because it is not affected by nimodipine (Fig. 7) and blocked by a low dose of TTX that reduces the sodium PIC without affecting the sodium spikes. The characteristic acceleration before the spike during slow firing (ramp&accelerate; arrows in Figs. 7 and 8) is also mediated by the sodium PIC and not by the classic I_A potassium current that can cause similar effects (Conner and Stevens 1971), because it is blocked by low dose TTX (Fig. 8*D*) and is much slower than occurs with I_A. A depolarization after the AHP can be caused by other mechanisms than the sodium PIC, such as the hyperpolarization activated Ih current(Russo and Hounsgaard 1999) and the classic late afterdepolarization following a single spike and AHP (Kernell 1965b). However, such late afterdepolarizations are very small in motoneurons (< 1mV), only last about 100 ms after the AHP, and are activated well below the sodium PIC threshold (our unpublished

results and Kernell 1965b), and thus cannot account for the much larger (many mV) and slower depolarizations between AHPs during slow firing.

Presumably, the sodium PIC is transiently activated prior to each spike even during moderately fast firing, but this is difficult to distinguish from the termination of the AHP from the prior spike. During very fast firing the sodium PIC may not fully deactivate with each AHP, and thus only provides a steady depolarization, similar to the calcium PIC. However, this issue and the relation of the sodium PIC to fast firing need further investigation.

Interspike intervals as long as 1 s can occur by the sodium PIC mediated slow firing (right of Fig. 7*B*), much longer than can be produced by normal motoneurons in acute spinal or anesthetized preparations (Bennett et al. 2001c; Hounsgaard et al. 1988b; Kernell 1965b). Theoretically, slow firing with interspike intervals somewhat longer than the 100ms AHP duration can be obtained by synaptic noise superimposed on a subthreshold depolarization. However, this sort of firing is characteristically variable (Matthews 1996) and decreases in variability as the cell is depolarized closer to threshold, where the AHP then determines firing rate. In contrast, the slow firing produced by the sodium PIC is extremely regular, and depolarizing synaptic excitation/noise only serves to increase its variability (*'s in Fig. 7). Further, the slow firing does not require synaptic noise at all, because it persists in drugs that produce a complete ionotropic synaptic blockade (Harvey and Bennett; unpublished results).

The sodium PIC is particularly prone to inactivation that occurs after a few seconds (Li and Bennett 2003), and thus, a single sodium plateau also inactivates over a few seconds. However, when the sodium PIC is fully deactivated and then reactivated with each AHP, as occurs during slow firing, then the sodium plateau is essentially recharged following each AHP and sodium inactivation does not play a major role in this slow firing. Thus, slow self-sustained firing can continue for many minutes or hours, without stopping, as we have seen during intracellular recordings (minutes) and in motor unit recordings in the awake chronic spinal rats (hours; Bennett et al. 2001b, unpublished findings). Long-lasting very slow firing is also seen in spontaneously active (involuntary) motor units in humans with spinal cord injury (Gorassini et al., in preparation; Zijdewind and Thomas 2001) and this is likely mediated by the same subthreshold sodium PIC oscillation, especially considering the lack of variability in this firing, which is a special characteristic of the slow sodium PIC mediated firing.

Long lasting reflexes and spasms in chronic spinal rats

Both spinal cord intact and chronic spinal animals (but not acute spinal) have large PICs that produce self-sustained firing (as discussed above), and evidence for this is even seen in intact and injured humans (Gorassini et al. 1999a; Gorassini et al. 2002; Gorassini et al. 1998; Kiehn and Eken 1997). However, uncontrolled muscle spasms only occur after chronic spinal cord injury. In the intact state there must be numerous inhibitory control mechanisms that help to terminate PICs, and avoid uncontrolled muscle contractions. These include control of volitional supraspinal inputs to motoneurons and segmental reflexes (Baldissera et al. 1981), control of brainstem monoaminergic systems that

modulate motoneuron PICs (Hounsgaard et al. 1988a) and descending inhibition of segmental reflexes (Baker and Chandler 1987; Clarke et al. 2002; Jankowska 1992; Thompson et al. 1992). With chronic injury this inhibitory control is lost: there is no volitional control, motoneurons exhibit plateaus/PICs spontaneously without the need for brainstem monoamines (Bennett et al. 2001c), and segmental reflexes become disinhibited. Interestingly, the segmental reflexes become disinhibited immediately after injury, leading to unusually long low-threshold polysynaptic EPSPs (Fig. 9C, see also Bennett and Cook, in preparation; Baker and Chandler, 1987). However, these EPSPs do not trigger long-lasting reflexes until the motoneuron excitability is raised by the recovery of PICs with chronic injury (weeks after injury; Fig. 9*B*). Thus, PICs must play a central role in the generation of long-lasting reflexes and associated spasms seen in the awake rat (Bennett et al. 1999), and this is discussed next.

Long-lasting spasms are caused by PICs on the motoneurons

Because PICs and plateaus are voltage-dependent, their activation can be stopped by hyperpolarizing the motoneurons, and the contribution of the PIC to long-lasting reflexes directly quantified. Interestingly, with hyperpolarization the many second long portion of the reflex is completely blocked, leaving only a half second long EPSP (Figs. 9 – 11). This demonstrates that the long-lasting reflex results almost entirely from voltage-dependent PIC activation intrinsic to the motoneurons, with only a half second long contribution from synaptic input (EPSP). This leads to the surprising conclusion that spasms, which we know are closely associated with these long-lasting reflexes (Bennett et al. 1999), are caused by PICs intrinsic to the motoneurons and are *not* caused by many

second long polysynaptic inputs to the motoneurons. The PICs and plateaus are triggered by polysynaptic EPSPs, which are exaggerated with injury (see below), but the long-lasting discharge during spasms must result entirely from motoneuron PICs that far outlast these EPSPs.

In most motoneurons nimodipine partly reduced, but did not eliminate, the long-lasting reflex response to a brief low threshold dorsal root stimulation (slowed firing; Fig. 10), indicating that both the calcium and sodium PICs contributed to long-lasting reflexes and spasms. Nimodipine did not affect the EPSP that triggered the PICs/plateaus (seen with hyperpolarization) and thus acted primarily by blocking the postsynaptic calcium PIC. With nimodipine present, the sodium PIC alone caused a long-lasting reflex by producing slow self-sustained firing (see slow firing section and Fig. 10*C*). This slow reflex induced firing (2 – 3 Hz) thus likely produces slow unfused contractions in the awake rat (twitches are < 100ms for these tail muscles, unpublished data), and thus likely contributes to clonus seen during muscle spasms (Bennett et al. 1999). With calcium PICs, together with the sodium PICs (prior to nimodipine), the firing rate accelerated during long-lasting reflexes, and thus the calcium PICs likely contribute to more powerful muscle contractions during spasms. In a few motoneurons, the sodium PIC was too weak to by itself produce a plateau, and nimodipine blocked the long-lasting reflex (Fig. 10). Thus, in these motoneurons the calcium PIC alone produced the long-lasting reflex.

The hyperpolarization used to block the sodium and calcium PICs should theoretically also block any voltage-dependent component of the EPSP, such as that mediated by NMDA receptors. This component could contribute to the plateau and long-lasting reflex in addition to the sodium and calcium PICs. However, postsynaptic NMDA receptors are not likely involved in the many second long reflex response, because in cells without large sodium PICs (just mentioned) nimodipine blocks the long-lasting reflex, and the EPSP that remains in nimodipine is not longer than the EPSP seen with hyperpolarization. Further, a block of the NMDA receptors with APV (Bennett et al. 2001a) or a complete block of all ionotropic transmission does not block the PICs or plateaus (Harvey and Bennett, unpublished results). Interestingly, APV does block the polysynaptic EPSP (Bennett et al. 2001a), and these EPSPs must therefore be mediated by NMDA receptors on interneurons.

EPSPs that trigger PICs and spasms

Any long depolarizing synaptic input, lasting about half a second, can activate the full PIC (Bennett et al. 2001c; Li and Bennett 2003), causing self-sustained firing and ultimately the long-lasting reflex associated with muscle spasms. Shorter depolarizations, such as from the monosynaptic EPSP, cannot evoke a plateau or long-lasting reflexes (see Results). However, repeated monosynaptic stimulation or tendon vibration is effective in evoking PICs/plateaus (see Results and Lee and Heckman, 1998b), and thus should trigger spasms. The reduction in the amount of presynaptic inhibition/depression of monosynaptic and polysynaptic reflexes seen with spinal cord injury (Ashby et al. 1987) is thus functionally very important. In spinal cord injured humans (Dimitrijevic and

Nathan 1968; Hornby et al. 2003; Kuhn and Macht 1948) and animals (Bennett et al. 2001b), cutaneous inputs are especially effective in evoking muscle spasms, and this is consistent with the emergence of unusually long EPSPs evoked by single low or high threshold cutaneous stimulation after spinal cord injury (Baker and Chandler 1987; Clarke et al. 2002). The long EPSPs in our sacral spinal cord preparation (Figs. 9 – 11) are also likely mediated by cutaneous afferents, because they are best evoked by the most caudal dorsal roots that innervate the skin at the tip of the tail (Bennett et al. 1999).

In summary, muscle spasms after spinal cord injury are produced primarily by sodium and calcium PICs on the motoneurons, triggered by any moderately long synaptic excitation. However, the increased afferent transmission and prolonged EPSPs, especially through cutaneous pathways, allows PICs and thus spasms to be triggered by brief non-noxious afferent stimulation, as is commonly seen in injured humans (Delwaide 1987; Kuhn and Macht 1948).

FIGURES

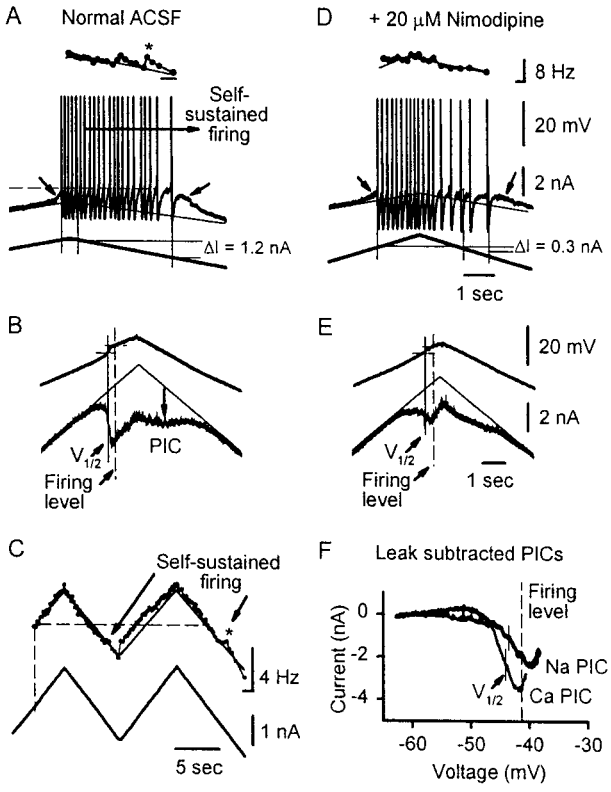

FIGURE 5-1. LOW THRESHOLD SODIUM AND CALCIUM PIC ACTIVATION IN LSS TYPE MOTONEURONS.

A: voltage and firing rate response of an LLS type cell to a slow triangular current ramp. Note the acceleration in potential just before recruitment (early plateau activation, left

arrow), the long self-sustained firing (ΔI) and the prominent after potential (right arrow). Firing level shown with dashed line. B: response of the same motoneuron to a slow triangular voltage ramp, recorded in voltage-clamp mode. PIC taken as difference between leak current (thin line) and recorded current (vertical arrow). Note the negative-slope-region produced by the PICs was almost fully formed at the firing level (dashed line), and thus the PIC was activated well before firing. The solid vertical line indicates the PIC half-activation voltage ($V_{1/2}$). C: firing rate of another LLS cell during a double triangular current ramp. Note the relative linearity of firing in relation to current, except the small acceleration at the end (*), also seen at * in A. D-F: same cell as in A and B. D: after nimodipine blocked the calcium PIC, during a current ramp a subthreshold plateau remained (left arrow), though decreased in amplitude, the long self-sustained firing was shortened (ΔI reduced) and the after potential greatly reduced. E: blockade of calcium PIC with nimodipine seen during voltage-clamp and leaving only effects of sodium PIC. F: sodium PIC computed from E by leak subtraction, and calcium PIC computed by subtracting E from B. Note that both PICs are activated at voltages lower than the firing level of the cell. A and D same scale; B and E same scale.

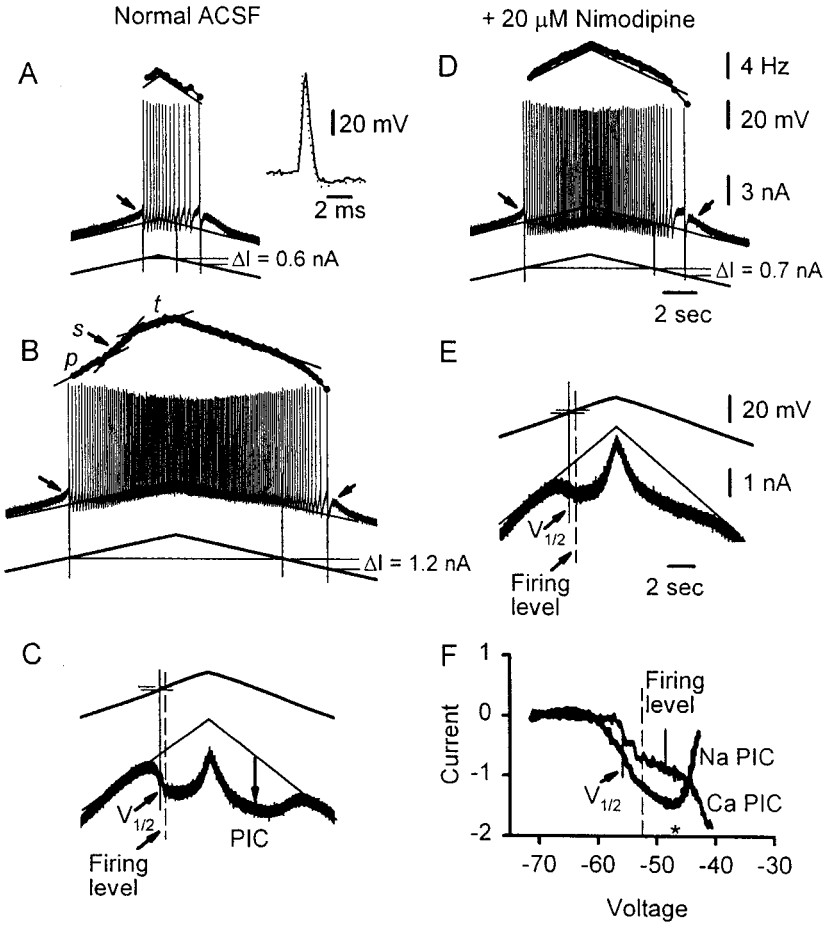
Normal ACSF
+ 20 μM Nimodipine
A
20 mV
2 ms
ΔI = 0.6 nA
D
4 Hz
20 mV
3 nA
ΔI = 0.7 nA
2 sec
B
s
t
p
ΔI = 1.2 nA
E
20 mV
1 nA
V1/2
Firing level
2 sec
C
V1/2
PIC
Firing level
F
Firing level
Na PIC
Ca PIC
V1/2
Current
1
0
-1
-2
-70 -60 -50 -40 -30
Voltage

FIGURE 5-2. HIGH THRESHOLD CALCIUM PIC ACTIVATION IN LAS TYPE CELLS.

Same format as Fig. 1. A: response of a LAS cell to a small current ramp. Inset shows first spike in A (dotted) and D (solid) overlaid to demonstrate that nimodipine had no effect on the spike threshold or shape. B: response of the same cell to a larger current ramp. Note that the self-sustained firing was greatly prolonged (larger ΔI), compared to in A, and also note the acceleration in firing rate during the upward ramp (at region marked with 's'). C: response of the cell to a slow voltage-ramp. D: after nimodipine blocked the calcium PIC, the late acceleration in firing during a large ramp was eliminated, and the self-sustained firing reduced to similar to that in A (ΔI). E: voltage-clamp response with nimodipine application. F: calcium and sodium PIC, computed by subtraction as in Fig. 1 The irregularities in the Ca PIC trace are likely due to inherent errors in subtracting data before and after drug applications. Note that the sodium PIC was activated sub-threshold ($V_{1/2}$ < firing level), whereas the calcium PIC was mostly activated *above* the initial firing level ($V_{1/2}$ > firing level). A, B and D, same scale; C and E, same scale.

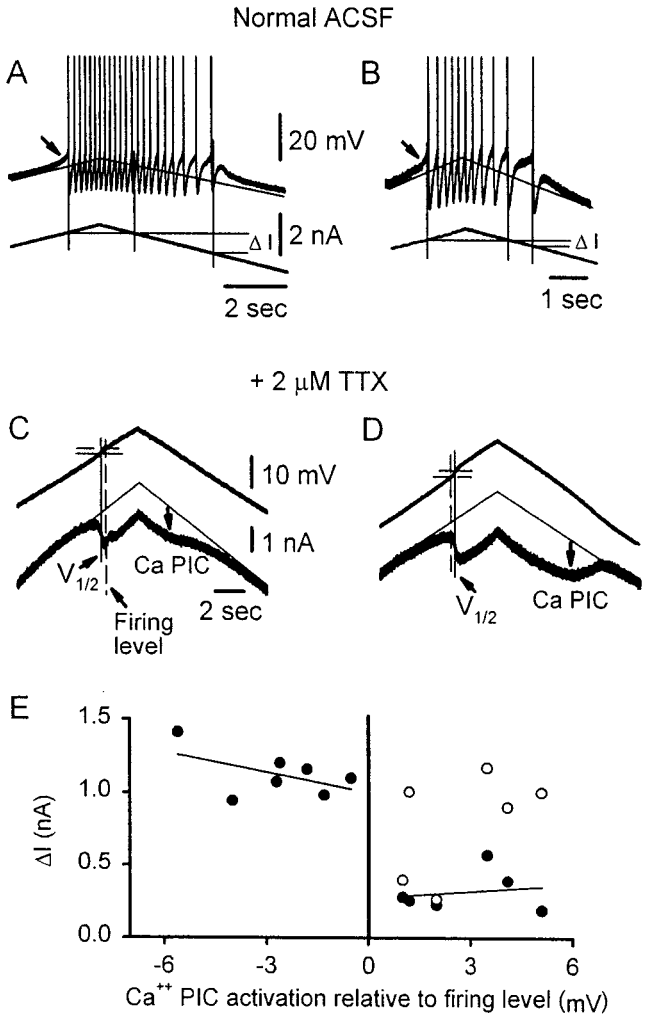

FIGURE 5-3. SEPARATION OF LLS AND LAS CELLS BY TTX APPLICATION.

A and B: responses of two chronic spinal motoneurons to small current ramps with similar small amplitude. A and B are from LSS and LAS type cells respectively. Note the much longer self-sustained firing elicited in A (ΔI), compared to B. C and D: calcium

PIC revealed in isolation after TTX application. Note that the LSS cell in E had a calcium PIC activation ($V_{1/2}$, solid line) below the firing level (dashed line), whereas the LAS cell in F had a calcium PIC activated above firing level. E: degree of self-sustained firing produced by the PIC in current-clamp recording ($\Delta I = I_{end} - I_{start}$) shown as a function of the difference between calcium PIC activation voltage ($V_{1/2}$) and spike threshold (firing level). Solid symbols indicate the response to small current ramps that turned around shortly after recruitment, as in Fig. 3. The vertical line indicates where the calcium activation voltage equals the firing level at recruitment. These responses cleanly separated the cells into two groups: all the cells to the left of the vertical line had large ΔI values and were LSS cells. Those to the right had small ΔI values and were mostly LAS cells. That is, when larger ramps were applied to the latter cells (as in Fig. 2*B*) the ΔI was usually increased (open symbols). A and B, same scale, C and D, same scale.

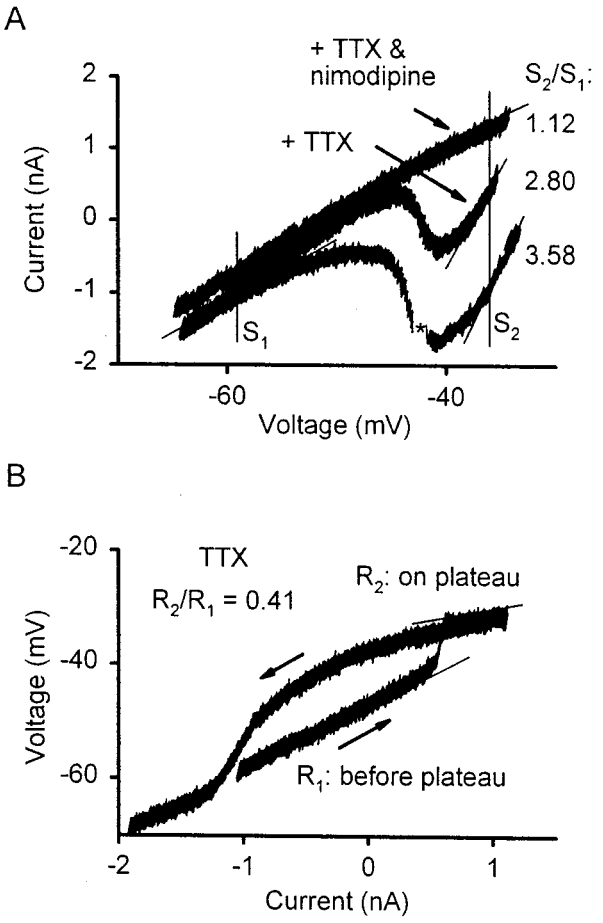

FIGURE 5-4. INCREASE IN CONDUCTANCE MEDIATED BY ACTIVATED PICS.

A: current response of a motoneuron to a slow voltage ramp (as in Fig. 3*B*) plotted against the applied voltage, recorded in normal ACSF, after TTX, and after TTX & nimodipine application. Diagonal lines indicate conductances measured before (S_1) and after (S_2) PIC activation, and vertical lines indicate voltage where S_1 and S_2 were measured. Note the marked decreases in the conductance S_2 after TTX and nimodipine application. The star indicates a transient unclamped spike, which was removed for clarity. B: in TTX, voltage response from a motoneuron, plotted against the current applied during a standard slow upward ramp (upward arrow) and slow downward ramp

(downward arrow). Note the resistance measured after plateau activation (R_2) was much smaller than before plateau activation (R_1).

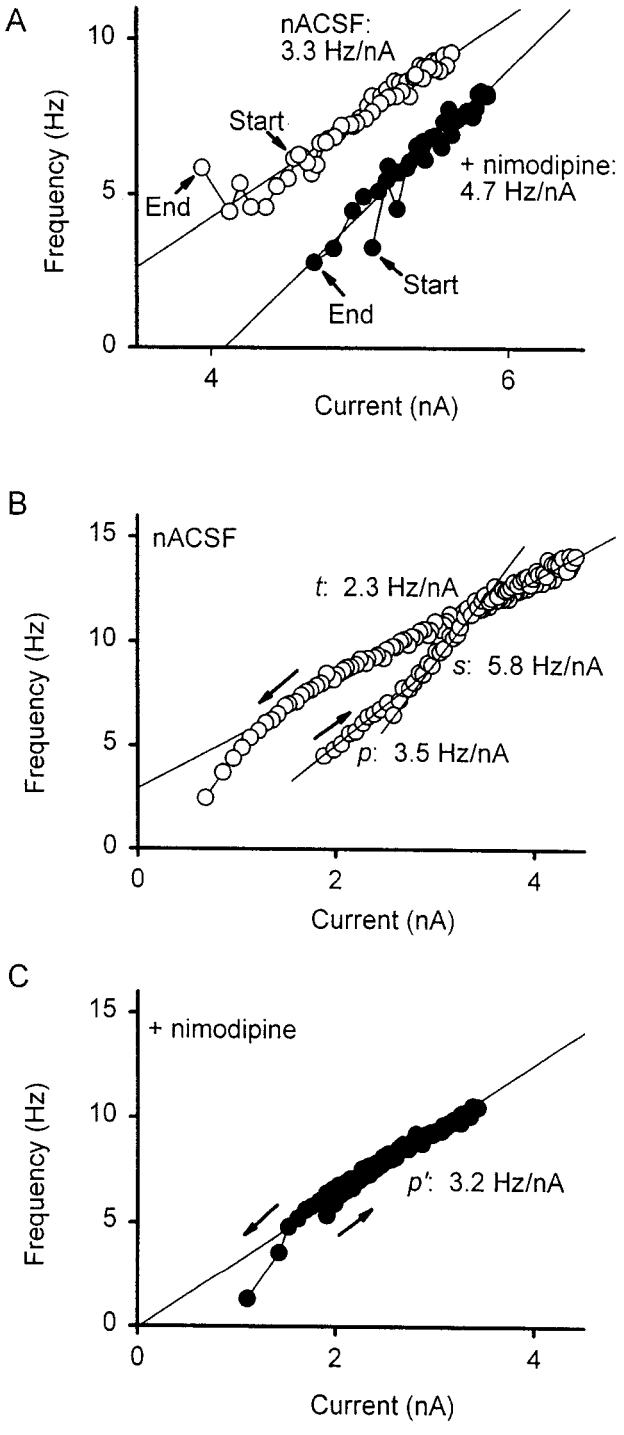
A
nACSF:
3.3 Hz/nA
Start
End
+ nimodipine:
4.7 Hz/nA
Start
End
Frequency (Hz)
Current (nA)
B
nACSF
t: 2.3 Hz/nA
s: 5.8 Hz/nA
p: 3.5 Hz/nA
Frequency (Hz)
Current (nA)
C
+ nimodipine
p': 3.2 Hz/nA
Frequency (Hz)
Current (nA)

FIGURE 5-5. EFFECTS OF CALCIUM PIC ON F-I RELATION IN MOTONEURONS OF CHRONIC SPINAL RATS.

A: F-I plots of a LLS cell obtained from a slow triangular ramp (like Fig. 1*C*), in nACSF (white symbols) and in nimodipine (black symbols). Note simple linear F-I relation and self-sustained firing ($I_{start} - I_{end}$) prior to nimodipine. Nimodipine increased the F-I slope and threshold current (at start) and decreased the initial firing rate and self-sustained firing. B: F-I plot of a LAS cell in respond to a slow triangular ramp (same cell as in Fig. 2). Note on the upward ramp (upward arrow) the initial linear F-I slope (primary range, *p*), then late acceleration to a steeper slope (ramp-evoked secondary range, *s*), followed by firing with a very shallow slope (tertiary range, *t*). On the downward ramp (down arrow) the shallow tertiary range slope continued, and there was marked self-sustained firing. C: same motoneuron in B, after nimodipine. Note that the F-I slope was similar to the primary range prior to nimodipine. Thus the secondary and tertiary range firing resulted from the calcium PIC.

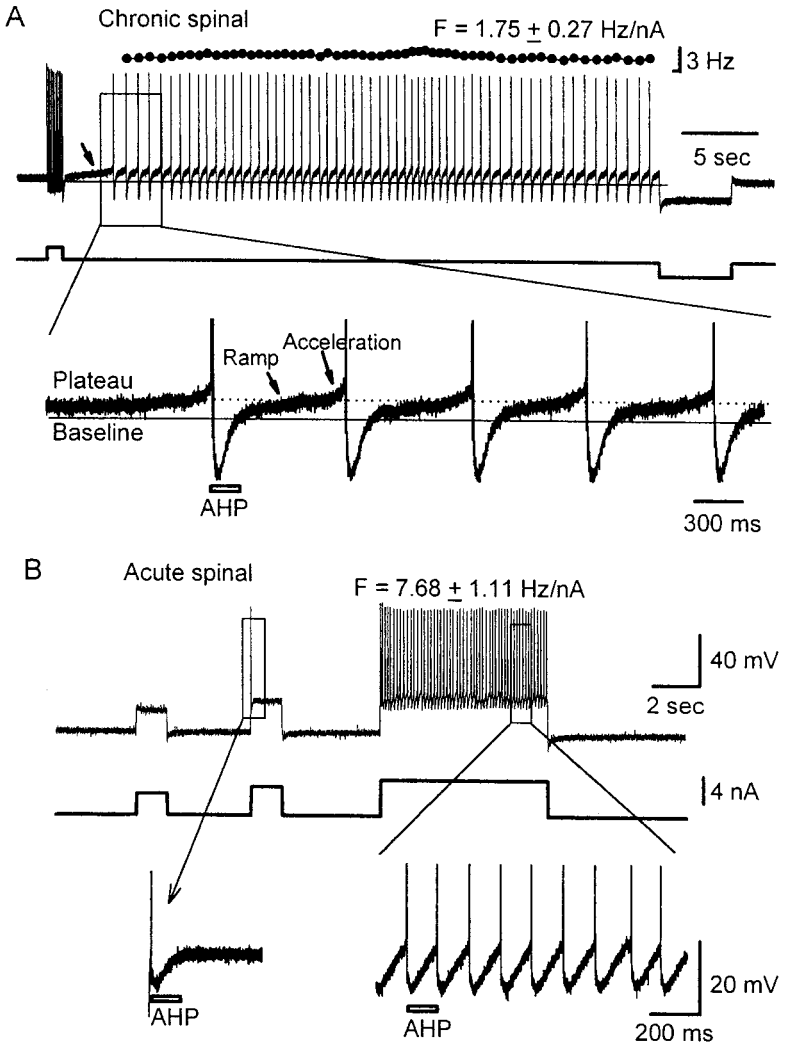
A
Chronic spinal
F = 1.75 ± 0.27 Hz/nA
3 Hz
5 sec
Ramp
Acceleration
Plateau
Baseline
AHP
300 ms
B
Acute spinal
F = 7.68 ± 1.11 Hz/nA
40 mV
2 sec
4 nA
AHP
AHP
20 mV
200 ms

FIGURE 5-6. VERY SLOW FIRING IN MOTONEURONS OF CHRONIC SPINAL RATS.

A: upper trace: plateau and self-sustained firing in a chronic spinal motoneuron, induced by a brief current pulse, and terminated by a hyperpolarizing pulse. Motoneuron held near threshold with a 1.7 nA bias current. Note the remarkably low firing rate (1.75 Hz), and the small variation (SD = 0.27 Hz). Lower trace: amplification of part of the upper trace. Note the characteristic acceleration in potential before each spike (arrows) and interspike interval much longer than the AHP duration (indicated by length of open box, measured during antidromic spike, not shown). B: upper trace: motoneuron of acute spinal rat without plateau. Firing only occurs during the current pulses and the minimum repetitive firing frequency (right pulse, 7.68 Hz) is much higher than in A. Also, the interspike interval is very close to the AHP duration (open box in lower trace).

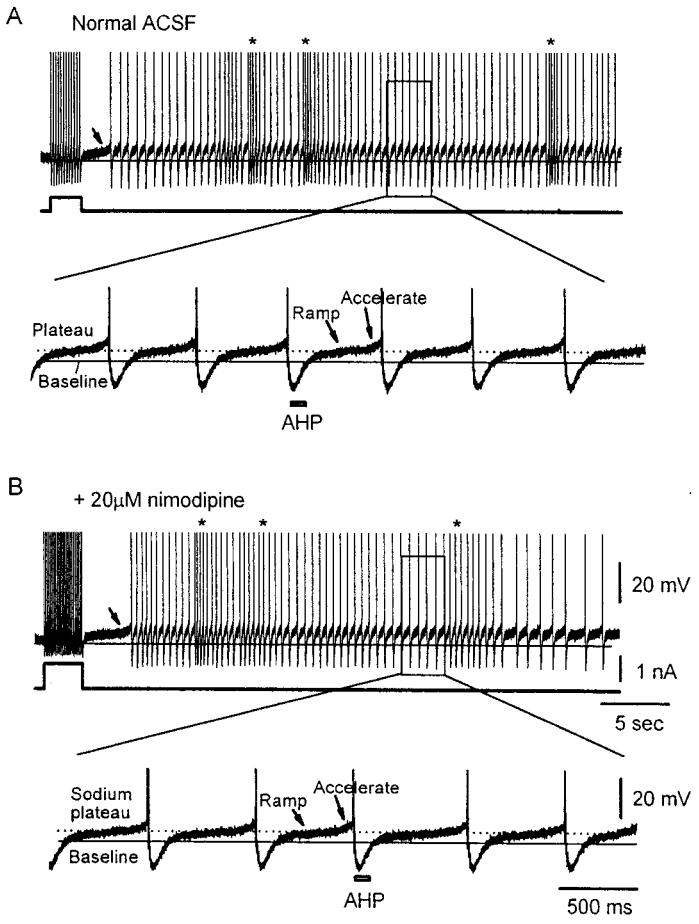

FIGURE 5-7. VERY SLOW FIRING DOES NOT DEPEND ON THE CALCIUM PIC.

A: long-lasting slow firing caused by a brief current pulse in a chronic spinal motoneuron, as in Fig. 6*A*. Note again plateau onset, at left arrow, and very slow self-sustained firing with a characteristic interspike trajectory similar to a plateau onset, seen in insert. B: after calcium PIC block with nimodipine, a plateau (sodium plateau) and very slow firing were again triggered by a brief current pulse. There were transit accelerations in firing frequency caused by synaptic noise (at *'s) in this cell, before and after nimodipine.

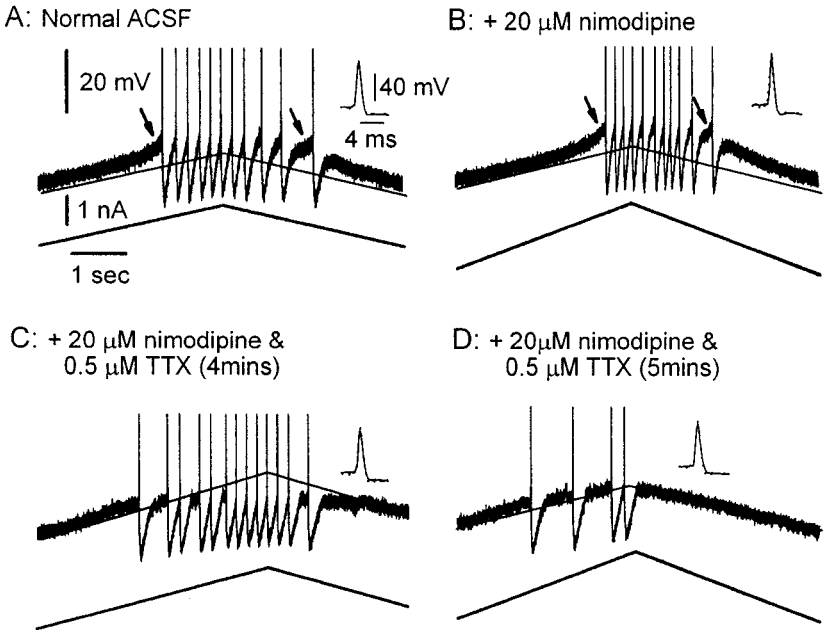

FIGURE 5-8. SODIUM PIC PRODUCES VERY SLOW FIRING AND MAINTAINS NORMAL RHYTHMIC FIRING.

A: voltage response of a chronic spinal motoneuron in current clamp. Note the characteristic ramp&acceleration in potential just before recruitment (plateau onset, left arrow) and slow firing prior to de-recruitment (the last spike, right arrow). B: ramp&acceleration in potential and slow firing remained in nimodipine (arrows). Note nimodipine did not affect the spike threshold or amplitude (inserts in A, B; spike from A overlaid with B as dotted line). C and D: when low dose TTX was applied the spike amplitude/threshold were unaffected (inserts in C and D, with A overlaid again). However, the characteristic ramp&accelerate (plateau onset) prior to the first and last spike was abolished, as was associated slow firing. Also, the cell was unable to generate

rhythmic firing. Thus, the sodium PIC and sodium plateau mediates very slow firing and helps maintain rhythmic firing.

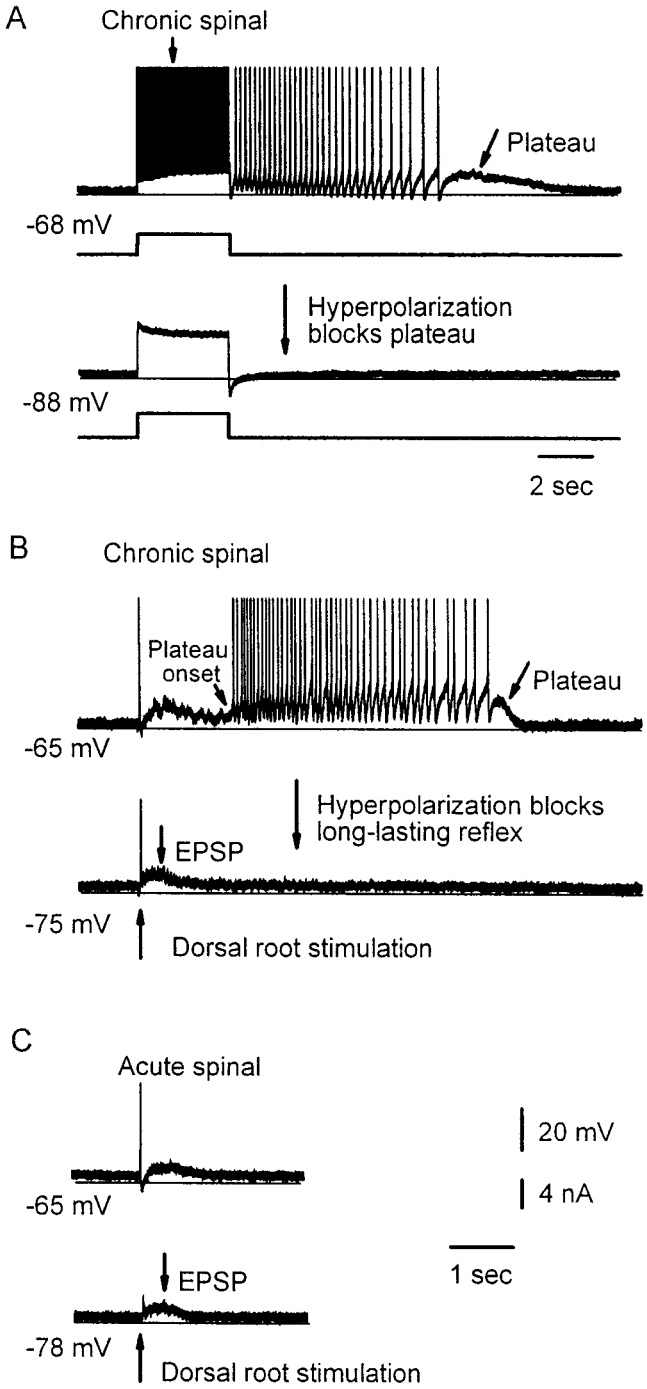
A
Chronic spinal
Plateau
-68 mV
Hyperpolarization
blocks plateau
-88 mV
2 sec
B
Chronic spinal
Plateau
onset
Plateau
-65 mV
Hyperpolarization blocks
long-lasting reflex
EPSP
-75 mV
Dorsal root stimulation
C
Acute spinal
20 mV
4 nA
-65 mV
1 sec
EPSP
-78 mV
Dorsal root stimulation

FIGURE 5-9. LONG-LASTING REFLEX IS CAUSED BY VOLTAGE-DEPENDENT PIC, AND TRIGGERED BY LONG EPSP.

A: upper trace: self-sustained firing and plateau activated by a current pulse in a chronic spinal motoneuron. LAS type cell, with late firing rate acceleration, and thus late calcium PIC activation, that occurred a couple seconds after the pulse onset (as small arrow). Lower trace: hyperpolarizing the cell with a bias current completely abolished self-sustained firing and plateau activation, for the same current pulse. B: same cell, upper trace: long-lasting reflex triggered by a brief dorsal root stimulation (single shock, 2xT). Lower trace: hyperpolarizing the membrane, to block the plateau/PICs (as in A), abolished the long-lasting reflex to the same stimulation, and thus the reflex was caused by the PICs. In this cell an EPSP and then slow plateau onset (at upper left arrow in upper trace) occurred prior to firing. The initial half-second of this EPSP remained after hyperpolarization; the rest was eliminated and must have resulted from the PICs. C: motoneuron from an acute spinal rat. Upper trace: the same dorsal root stimulation produced a smaller, though similar long duration EPSPs to that in B, but this did not trigger long-lasting firing. Lower trace: the EPSPs remained unchanged after hyperpolarization, and thus were not amplified by PICs, unlike in B.

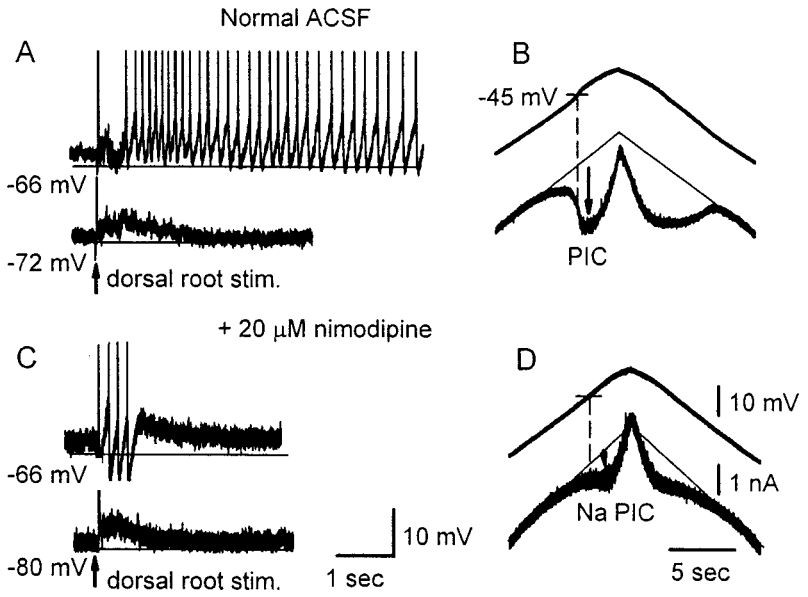

FIGURE 5-10. LONG-LASTING REFLEXES MEDIATED BY CALCIUM PIC.

A: long-lasting reflexes triggered by a brief dorsal root stimulation (single shock, 2xT; as in Fig. 9*B*). Note the EPSPs revealed by hyperpolarization, that again was much shorter than the long-lasting reflex discharge. B: large PIC activated by a voltage ramp in the same cell. Same format as Fig. 1*B*. C: after nimodipine application to block the calcium PIC, no long-lasting reflex could be evoked, no matter what the holding potential, although the EPSP remained. D: voltage clamp recording demonstrating the loss of the calcium PIC in nimodipine and the small sodium PIC in this particular cell.

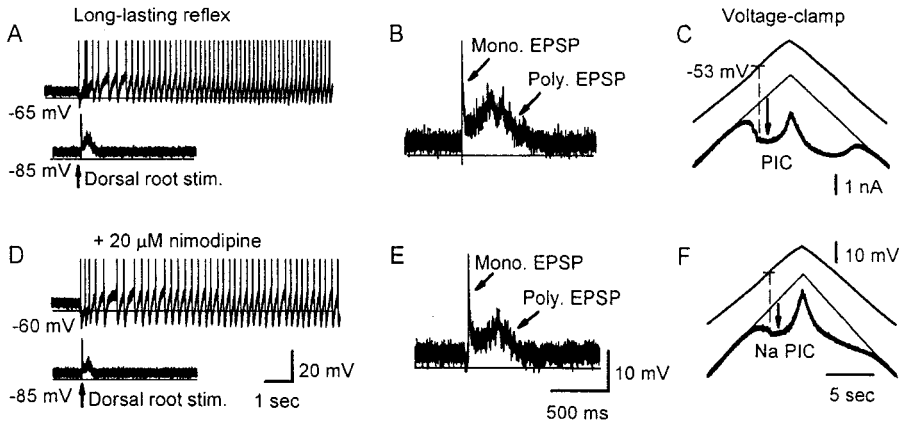

FIGURE 5-11. LONG-LASTING REFLEXES MEDIATED BY SODIUM PIC.

A: long-lasting reflexes recorded in a chronic spinal motoneuron triggered by a brief dorsal root stimulation (single shock, 2xT). B: amplification of lower trace in A to show the hyperpolarized mono- and polysynaptic EPSPs. C: large PIC activation in voltage-clamp recording in the same cell. D-E: after nimodipine application, the long-lasting reflexes and the EPSPs remained. However, the firing frequency decreased markedly with nimodipine, and had the characteristics of slow sodium PIC mediated firing. F: voltage-clamp recording revealing a large sodium PIC in nimodipine that produced a large negative-slope-region, and must have caused the slow firing and long-lasting reflexes in D.

REFERENCES

Ashby P, Stalberg E, Winkler T, and Hunter JP. Further observations on the depression of group Ia facilitation of motoneurons by vibration in man. *Exp Brain Res* 69: 1-6, 1987.

Baker LL and Chandler SH. Characterization of postsynaptic potentials evoked by sural nerve stimulation in hindlimb motoneurons from acute and chronic spinal cats. *Brain Res* 420: 340-350, 1987.

Baldissera F, Hultborn H, and Illert M. Integration in spinal neuronal systems. In: *Handbook of Physiology. The Nervous system. Motor Control*, edited by VB B. Bethesda: American Physiological Society, 1981, p. 509-595.

Barbeau H and Norman KE. The effect of noradrenergic drugs on the recovery of walking after spinal cord injury. *Spinal Cord* 41: 137-143, 2003.

Bennett D, Li Y, and Sanelli L. Role of NMDA in spasticity following sacral spinal cord injury in rats. *Soc Neurosci Abstr* 31: 933.11, 2001a.

Bennett DJ, Gorassini M, Fouad K, Sanelli L, Han Y, and Cheng J. Spasticity in rats with sacral spinal cord injury. *J Neurotrauma* 16: 69-84, 1999.

Bennett DJ, Hultborn H, Fedirchuk B, and Gorassini M. Synaptic activation of plateaus in hindlimb motoneurons of decerebrate cats. *J Neurophysiol* 80: 2023-2037, 1998.

Bennett DJ, Li Y, Harvey PJ, and Gorassini M. Evidence for plateau potentials in tail motoneurons of awake chronic spinal rats with spasticity. *J Neurophysiol* 86: 1972-1982, 2001b.

Bennett DJ, Li Y, and Siu M. Plateau potentials in sacrocaudal motoneurons of chronic spinal rats, recorded in vitro. *J Neurophysiol* 86: 1955-1971, 2001c.

Burke D, Gillies JD, and Lance JW. The quadriceps stretch reflex in human spasticity. *J Neurol Neurosurg Psychiatry* 33: 216-223, 1970.

Carlin KP, Jones KE, Jiang Z, Jordan LM, and Brownstone RM. Dendritic L-type calcium currents in mouse spinal motoneurons: implications for bistability. *Eur J Neurosci* 12: 1635-1646, 2000.

Carp JS, Powers RK, and Rymer WZ. Alterations in motoneuron properties induced by acute dorsal spinal hemisection in the decerebrate cat. *Exp Brain Res* 83: 539-548, 1991.

Cavallari P and Pettersson LG. Tonic suppression of reflex transmission in low spinal cats. *Exp Brain Res* 77: 201-212, 1989.

Clarke RW, Eves S, Harris J, Peachey JE, and Stuart E. Interactions between cutaneous afferent inputs to a withdrawal reflex in the decerebrated rabbit and their control by descending and segmental systems. *Neuroscience* 112: 555-571, 2002.

Conner JA and Stevens CF. voltage clamp studies of a transient outward membrane current in gastropod neural somata. *J Physiology* 213: 21-30, 1971.

Crone C, Johnsen LL, Biering-Sorensen F, and Nielsen JB. Appearance of reciprocal facilitation of ankle extensors from ankle flexors in patients with stroke or spinal cord injury. *Brain* 126: 495-507, 2003.

Delwaide PJ. Spasticity: from pathophysiology to therapy. *Acta Neurochir Suppl (Wien)* 39: 91-95, 1987.

Dimitrijevic MR and Nathan PW. Studies of spasticity in man. 3. Analysis of reflex activity evoked by noxious cutaneous stimulation. *Brain* 91: 349-368, 1968.

Eken T, Hultborn H, and Kiehn O. Possible functions of transmitter-controlled plateau potentials in alpha motoneurones. *Prog Brain Res* 80: 257-267; discussion 239-242, 1989.

Elson RC and Selverston AI. Evidence for a persistent Na+ conductance in neurons of the gastric mill rhythm generator of spiny lobsters. *J Exp Biol* 200 (Pt 12): 1795-1807, 1997.

Gorassini M, Bennett D, and Yang JF. Excitability of motor units in persons with spasticity from spinal cord injury. *Soc Neurosci Abstr 25:120*, 1999a.

Gorassini M, Bennett DJ, Kiehn O, Eken T, and Hultborn H. Activation patterns of hindlimb motor units in the awake rat and their relation to motoneuron intrinsic properties. *J Neurophysiol* 82: 709-717, 1999b.

Gorassini M, Yang JF, Siu M, and Bennett DJ. Intrinsic activation of human motoneurons: possible contribution to motor unit excitation. *J Neurophysiol* 87: 1850-1858, 2002.

Gorassini MA, Bennett DJ, and Yang JF. Self-sustained firing of human motor units. *Neurosci Lett* 247: 13-16, 1998.

Hodgkin A. The local electric changes associated with repetitive action in a non-medullated nerve. *J Physiology (Lond)* 107: 165-181, 1948.

Hornby TG, Rymer WZ, Benz EN, and Schmit BD. Windup of flexion reflexes in chronic human spinal cord injury: a marker for neuronal plateau potentials? *J Neurophysiol* 89: 416-426, 2003.

Hounsgaard J, Hultborn H, Jespersen B, and Kiehn O. Bistability of alpha-motoneurones in the decerebrate cat and in the acute spinal cat after intravenous 5-hydroxytryptophan. *J Physiol* 405: 345-367, 1988a.

Hounsgaard J, Hultborn H, Jespersen B, and Kiehn O. Intrinsic membrane properties causing a bistable behaviour of alpha-motoneurones. *Exp Brain Res* 55: 391-394, 1984.

Hounsgaard J and Kiehn O. Calcium spikes and calcium plateaux evoked by differential polarization in dendrites of turtle motoneurones in vitro. *J Physiol* 468: 245-259, 1993.

Hounsgaard J and Kiehn O. Serotonin-induced bistability of turtle motoneurones caused by a nifedipine-sensitive calcium plateau potential. *J Physiol* 414: 265-282, 1989.

Hounsgaard J, Kiehn O, and Mintz I. Response properties of motoneurones in a slice preparation of the turtle spinal cord. *J Physiol* 398: 575-589, 1988b.

Hsiao CF, Del Negro CA, Trueblood PR, and Chandler SH. Ionic basis for serotonin-induced bistable membrane properties in guinea pig trigeminal motoneurons. *J Neurophysiol* 79: 2847-2856, 1998.

Irisawa H, Brown HF, and Giles W. Cardiac pacemaking in the sinoatrial node. *Physiol Rev* 73: 197-227, 1993.

Jankowska E. Interneuronal relay in spinal pathways from proprioceptors. *Prog Neurobiol* 38: 335-378, 1992.

Kernell D. High frequency repetitive firing of cat lumbosacral motoneurones stimulated by long-lasting injected currents. *Acta Physiol Scand* 65: 74-86, 1965a.

Kernell D. The limits of firing frequency in cat lumbosacral motoneurones possessing different time course of afterhyperpolarization. *Acta Physiol Scand* 65: 87-100, 1965b.

Kernell D. Repetitive impulse firing in motoneurons: facts and perspectives. *Prog Brain Res* 123: 31-37, 1999.

Kiehn O and Eken T. Prolonged firing in motor units: evidence of plateau potentials in human motoneurons? *J Neurophysiol* 78: 3061-3068, 1997.

Krenz N and Weaver L. Sprouting of primary afferent fibers after spinal cord transection in the rat. *Neuroscience* 85: 443-458, 1998.

Krnjevic K, Puil E, and Werman R. Evidence for Ca2+-activated K+ conductance in cat spinal motoneurons from intracellular EGTA injections. *Can J Physiol Pharmacol* 53: 1214-1218, 1975.

Kuhn RA and Macht MB. Some manifestations of reflex activity in spinal man with particular reference to the occurrence of extensor spasm. *Bull Johns Hopkins Hosp* 84: 43-75, 1948.

Lee RH and Heckman CJ. Bistability in spinal motoneurons in vivo: systematic variations in persistent inward currents. *J Neurophysiol* 80: 583-593, 1998a.

Lee RH and Heckman CJ. Bistability in spinal motoneurons in vivo: systematic variations in rhythmic firing patterns. *J Neurophysiol* 80: 572-582, 1998b.

Lee RH and Heckman CJ. Essential role of a fast persistent inward current in action potential initiation and control of rhythmic firing. *J Neurophysiol* 85: 472-475, 2001.

Li Y and Bennett DJ. Persistent sodium and calcium currents cause plateau potentials in motoneurons of chronic spinal rats. *J Neurophysiol* 90: 857 - 869, 2003.

Li Y, Harvey PJ, and Bennett DJ. Spastic long-lasting reflexes in the chronic spinal rat, studied in vitro. *J Neurophysiol*: submitted, 2003.

Little JW, Micklesen P, Umlauf R, and Britell C. Lower extremity manifestations of spasticity in chronic spinal cord injury. *Am J Phys Med Rehabil* 68: 32-36, 1989.

Mailis A and Ashby P. Alterations in group Ia projections to motoneurons following spinal lesions in humans. *J Neurophysiol* 64: 637-647, 1990.

Matthews PB. Relationship of firing intervals of human motor units to the trajectory of post-spike after-hyperpolarization and synaptic noise. *J Physiol* 492 (Pt 2): 597-628, 1996.

Newton BW and Hamill RW. The morphology and distribution of rat serotoninergic intraspinal neurons: an immunohistochemical study. *Brain Res Bull* 20: 349-360, 1988.

Powers RK and Binder MD. Relationship between the time course of the afterhyperpolarization and discharge variability in cat spinal motoneurones. *J Physiol* 528 Pt 1: 131-150, 2000.

Powers RK, Campbell DL, and Rymer WZ. Stretch reflex dynamics in spastic elbow flexor muscles. *Ann Neurol* 25: 32-42, 1989.

Powers RK and Rymer WZ. Effects of acute dorsal spinal hemisection on motoneuron discharge in the medial gastrocnemius of the decerebrate cat. *J Neurophysiol* 59: 1540-1556, 1988.

Prather JF, Powers RK, and Cope TC. Amplification and linear summation of synaptic effects on motoneuron firing rate. *J Neurophysiol* 85: 43-53, 2001.

Remy-Neris O, Barbeau H, Daniel O, Boiteau F, and Bussel B. Effects of intrathecal clonidine injection on spinal reflexes and human locomotion in incomplete paraplegic subjects. *Exp Brain Res* 129: 433-440, 1999.

Russo RE and Hounsgaard J. Dynamics of intrinsic electrophysiological properties in spinal cord neurones. *Prog Biophys Mol Biol* 72: 329-365, 1999.

Sandler VM, Puil E, and Schwarz DW. Intrinsic response properties of bursting neurons in the nucleus principalis trigemini of the gerbil. *Neuroscience* 83: 891-904, 1998.

Schmit BD, Benz EN, and Rymer WZ. Reflex mechanisms for motor impairment in spinal cord injury. *Adv Exp Med Biol* 508: 315-323, 2002.

Schwindt PC and Crill WE. Amplification of synaptic current by persistent sodium conductance in apical dendrite of neocortical neurons. *J Neurophysiol* 74: 2220-2224, 1995.

Schwindt PC and Crill WE. Factors influencing motoneuron rhythmic firing: results from a voltage-clamp study. *J Neurophysiol* 48: 875-890, 1982.

Thilmann AF, Fellows SJ, and Garms E. The mechanism of spastic muscle hypertonus. Variation in reflex gain over the time course of spasticity. *Brain* 114 (Pt 1A): 233-244, 1991.

Thompson FJ, Parmer R, and Reier PJ. Alteration in rate modulation of reflexes to lumbar motoneurons after midthoracic spinal cord injury in the rat. I. Contusion injury. *J Neurotrauma* 15: 495-508, 1998.

Thompson FJ, Reier PJ, Lucas CC, and Parmer R. Altered patterns of reflex excitability subsequent to contusion injury of the rat spinal cord. *J Neurophysiol* 68: 1473-1486, 1992.

Viana F, Bayliss DA, and Berger AJ. Multiple potassium conductances and their role in action potential repolarization and repetitive firing behavior of neonatal rat hypoglossal motoneurons. *J Neurophysiol* 69: 2150-2163, 1993.

Zhang H, Holden AV, and Boyett MR. Sustained inward current and pacemaker activity of mammalian sinoatrial node. *J Cardiovasc Electrophysiol* 13: 809-812, 2002.

Zijdewind I and Thomas CK. Motor unit firing during and after voluntary contractions of human thenar muscles weakened by spinal cord injury. *J Neurophysiol* 89: 2065-2071, 2003.

Zijdewind I and Thomas CK. Spontaneous motor unit behavior in human thenar muscles after spinal cord injury. *Muscle Nerve* 24: 952-962, 2001.

Chapter 6: Effect of baclofen on spinal reflexes and persistent inward currents in motoneurons of acute and chronic spinal rats

(Revised from Li et al. J. Neurophysiol. 2004 in press)

INTRODUCTION

Baclofen has been used widely as an anti-spasticity drug since the 1970s (Hudgson and Weightman 1971; Hudgson et al. 1972). Because it reduces muscle tone and spasms with similar efficacy in patients with spasticity caused by complete or incomplete spinal cord injury, or from cerebral origin (Albright et al. 1991; Davidoff 1985; Metz 1998; Meythaler et al. 2001), it is assumed to act mainly at the spinal cord level. This assumption has been confirmed by the recent finding that the effect of baclofen is more potent when applied intrathecally than orally (Azouvi et al. 1996; Kamensek 1999; Ochs et al. 1989). $GABA_B$ receptors are distributed extensively in the spinal cord, especially presynaptically on the primary sensory afferent terminals (Price et al. 1984; Yang et al. 2001). Baclofen, as a potent $GABA_B$ receptor agonist, has been shown in many studies to decrease synaptic transmission by binding to the presynaptic $GABA_B$ receptors at the afferent terminal, through a second messenger pathway, ultimately decreasing the calcium influx and neurotransmitter release (Batueva et al. 1999; Bussieres and El Manira 1999; Curtis et al. 1997; Miller 1998). In addition, baclofen's binding to the presynaptic $GABA_B$ receptors can also decrease the neurotransmitter release by activating potassium channels (Gage 1992), thus contributing to its presynaptic inhibitory effect.

Recently, major postsynaptic effects of baclofen have also been reported in motoneurons and interneurons (Russo et al. 1998; Svirskis and Hounsgaard 1998; Voisin and Nagy 2001), which could also contribute to baclofen's antispastic action. In motoneurons of normal animals (or humans) with intact spinal cord and brainstem, there are voltage-

dependent persistent inward currents (PICs) that, once activated, can remain active for many seconds after stimulation, producing sustained depolarizations (plateau potentials) and firing (self-sustained firing), thus greatly increasing their excitability (Bennett et al. 1998b; Gorassini et al. 2002; Hounsgaard et al. 1984; Lee and Heckman 1998a, b; Schwindt and Crill 1984). The PICs are composed of a low-threshold persistent calcium current, carried by Cav1.3 L-type calcium channels, and a TTX-sensitive persistent sodium current (Chandler et al. 1994; Hounsgaard and Kiehn 1989; Lee and Heckman 2001; Li and Bennett 2003; Schwindt and Crill 1995). Large PICs are not present in motoneurons immediately after spinal cord injury because of the massive loss of brainstem-derived monoamines that normally facilitate PICs (Hounsgaard et al. 1988a). Exogenous application of metabotropic receptor agonists (such as 5-HT, NE, and muscarine receptors) can enhance PICs and thus recover plateaus and self-sustained firing after acute spinal transection or *in vitro* slice injury (Hounsgaard and Kiehn 1989; Lee and Heckman 1998a, b; Svirskis and Hounsgaard 1998). Baclofen has been shown recently to decrease the amplitude of these enhanced PICs in motoneurons of turtle spinal cord slices (Svirskis and Hounsgaard 1998), and to decrease spontaneously occurring PICs in deep dorsal horn neurons of turtles and rats (Russo et al. 1998; Voisin and Nagy 2001), raising the interesting possibility that baclofen's clinical action may be partly postsynaptic by decreasing the PICs, which are recovered in motoneurons after chronic spinal cord injury and play an important role in the production of spasticity (Bennett et al. 2001b; Bennett et al. 2001d; Li et al. 2004a).

Weeks after spinal cord transection in rats (chronic spinal rats), for some unknown reason, the plateaus and PICs in motoneurons below the injury recover spontaneously,

without exogenous application of metabotropic receptor agonists (Bennett et al. 2001b; Bennett et al. 2001d; Li and Bennett 2003). With these recovered PICs (and thus recovered motoneuron excitability) combined with a loss of descending inhibition over spinal reflexes after spinal cord injury, a brief dorsal root stimulation can produce long-lasting exaggerated reflexes or spasms, which reflect an essential characteristic of spasticity (Bennett et al. 2001b; Bennett et al. 2001d; Li et al. 2004a). The recovered PICs in chronic spinal rats are mediated by a low threshold L-type calcium current (Ca PIC, as in the turtle motoneurons and rat deep dorsal horn neurons) and a persistent sodium current (Na PIC, Li and Bennett 2003). Considering that baclofen can inhibit the PIC mediated by L-type calcium currents in normal motoneurons, we examined in the present paper whether baclofen acts similarly in chronic spinal rats. Surprisingly, we found that baclofen did not decrease the PICs, even at high doses, and instead somewhat increased the PICs.

Spasticity is usually absent in acutely injured animal preparations, and it only gradually develops with chronic injury (>1 month, Bennett et al. 1999a). However, much of our understanding of baclofen's mechanisms of action comes from normal or acutely injured animal preparations that do not exhibit the hyper-excitability of the chronic spinal spastic state. Thus, in the present paper we studied how baclofen reduced spastic reflexes in adult rat spinal cords following *chronic* spinal cord transection when spasticity had become prominent. We found that baclofen blocked the monosynaptic and the exaggerated long-lasting spastic reflexes at low doses ($\leq$ 1 μM) that did not change the basic motoneuron membrane properties or PICs, suggesting that its primary anti-spastic action was mediated by reducing synaptic input to the motoneurons, as expected from previous

studies in normal animals (see above). However, the dose of baclofen required to inhibit the monosynaptic reflex of chronic spinal rats was moderately higher than that of the acute spinal rats, suggesting changes in receptor number/sensitivity or endogenous GABA level after chronic injury. Parts of this work have been presented in abstract form (Li et al. 2002).

METHODS

Both normal adult female Sprague-Dawley rats (> 60 days old, n = 17) and spastic rats with chronic spinal cord injury (> 90 days old, n = 16) were included in the present study. For the spastic rat, a complete spinal cord transection was made at the S_2 sacral level when the rat was 50 days old (Bennett et al. 1999a). Usually, within 30 days, dramatic spasticity developed in the tail muscles, which were innervated by sacrocaudal motoneurons below the level of the injury. Only rats more than 50 days (50 - 120 days) post injury with clear spasticity were included in the present study. The details of the chronic transection and spasticity assessment are described in Bennett et al. (1999a; 2003b). All experimental procedures were approved by the University of Alberta animal welfare committee (HSAPWC).

In vitro preparation

Two *in vitro* preparations were employed in the present study: one for intracellular recording and one for root reflex recording. For both preparations, normal and chronic spinal rats were deeply anaesthetized with urethane (0.18 g/100 g; with a maximum of 0.45 g for rats > 250 g), and the whole sacrocaudal spinal cord was removed and placed in a dissection dish filled with modified artificial cerebrospinal fluid (mACSF) at 20 - 21°C. For the root reflex preparation, all the dorsal and ventral roots below the S_3 level were kept, and gently separated (see details in Li et al. 2004b). After an hour's rest in the dissection chamber, the cord was transferred to the recording chamber, where it was immersed in continuously flowing (5 ml/min) normal ACSF (nACSF), maintained at 24 -

25°C (see Li et al. 2004b for procedure details). In the recording chamber, the cord was supported on a nappy paper mesh and secured by passing pins through the end of the cord and through the lateral vasculature and connective tissue and into the Sylgard base below the nappy paper. For the intracellular recording preparation, everything was the same as the root reflex preparation, except that all the dorsal roots attached to the cord were cut off except the main caudal dorsal root (i.e., Ca_1, which was attached to the caudal equina), and the cord was glued (super glue; RP 1500, Adhesive Systems Inc.) on its dorsal surface to a small piece of nappy paper (with the ventral side facing up) to increase stability (see Li and Bennett 2003 for details).

Root reflex recording

Each dorsal and ventral root (usually S_3, S_4 and Ca_1 ventral and dorsal) was mounted on a silver-chloride wire above the ASCF of the recording chamber and covered with a 1:1 mixture of Vaseline and mineral oil for monopolar stimulation and recording (Li et al. 2004b). To record the monosynaptic reflex in the ventral root, the dorsal roots were stimulated at 0.05 Hz, 0.1 ms, 0.1 mA (≈ 10x Threshold, 10xT; T = 0.01 mA), i.e., a 20-sec delay existed between each stimulation to avoid reflex depression. To record the polysynaptic reflex, the dorsal roots were stimulated similarly, except sometimes with a higher repetition rate (0.5 Hz, 0.1 ms, 0.1 mA) to facilitate the long-lasting polysynaptic reflexes (Li et al. 2004b). This stimulation intensity was chosen to be supramaximal to evoke mono- and polysynaptic reflexes reliably. The ventral root reflexes were amplified by 5000x with a custom-built preamplifier, low-pass filtered at 3 kHz, high-pass filtered

at 100 Hz and recorded with a data acquisition system sampling at 6 kHz (Axonscope 8; Axon Instr., USA). The monosynaptic reflex was recognized by its large amplitude and short delay (around 3 ms, including peripheral delay), and the peak amplitude was measured with Axonscope 8. The polysynaptic reflex was quantified by rectifying the data and averaging over a 1-sec window starting 50 ms after the stimulus using Matlab (Mathworks, USA).

Intracellular recording

The same intracellular recording procedures described previously were employed (Li and Bennett 2003) and are only briefly summarized here. The long ventral roots (usually sacral S_4 and caudal Ca_1) and caudal equina (which had attached caudal dorsal roots, Ca_1) were mounted on silver-chloride wires above the nACSF and covered with high vacuum grease (Dow Corning). Sharp intracellular recording electrodes were made from thick wall glass capillaries (Warner GC 150F-10, 1.5 mm OD) with a micropipette puller (Sutter P-87 puller), filled with a 1:1 mixture of 2 M K-Acetate and 2 M KCl and beveled down to 20 to 30 MΩ on a rotary grinder (Sutter, BV-10, fine 006 beveling stone). Electrodes were advanced perpendicularly into the ventral surface of the cord with a stepper-motor micromanipulator (660, Kopf) to penetrate motoneurons. Motoneurons were identified by antidromic ventral root stimulation. Only motoneurons with a stable penetration, resting potential < -60 mV, spike amplitude > 60 mV and reliable repetitive firing were included in the study. An Axoclamp2b intracellular amplifier (Axon Instruments) running in either discontinuous current-clamp modes (DCC, switching rate

7 to 10 kHz, output bandwidth 3.0 kHz) or discontinuous voltage-clamp modes (gain 1 to 2.5 nA/mV) was used to collect the data. The basic properties of the motoneurons, such as cell resistance, firing threshold and firing level were measured during current ramps in DCC mode, as described in Li and Bennett (2003).

Slow triangular current ramps (0.4 nA/s) and voltage ramps (standard speed 3.5 mV/s, varied from 2 to 5 mV/s) were applied to the motoneurons to evoke firing and quantify the PICs. During the current ramps (in current-clamp), the PICs that contributed to sustained firing (self-sustained firing) were estimated from the difference between the injected current required to terminate firing (I_{end}) and the current required to start firing ($\Delta I = I_{end} - I_{start}$, see Fig. 4*A* and Bennett et al. 2001b). During the voltage ramps (in voltage-clamp), the PICs caused a negative-slope region in the current-voltage (I-V) relation, and this negative-slope region caused the plateau behavior and self-sustained firing seen in current clamp (Li and Bennett 2003). To obtain an estimation of the passive leak current that summed with the PICs to give the total recorded current, a linear relation was fit to the subthreshold current response in the linear region 10 mV below the negative-slope region onset, and extrapolated to more positive voltages (*leak current*, thin triangular line overlaying current; Fig. 4*E*). The PIC amplitude was then estimated by subtracting this leak current from the recorded current; this difference is indicated by the arrow in Fig. 4*E* (see details in Fig. 1 of Li and Bennett 2003).

Reflexes and excitatory postsynaptic potentials (EPSPs) were also recorded during intracellular recordings, in response to brief stimulation of the Ca_1 dorsal root.

Drugs and solutions

Two kinds of ACSF were used in the experiments: normal ACSF (nACSF) in the recording chamber and modified ACSF (mACSF) in the dissection chamber. The composition of nACSF was (in mM): 122 NaCl, 24 $NaHCO_3$, 2.5 $CaCl_2$, 3 KCl, 1 $MgSO_4$ and 12 D-glucose. The composition of mACSF was (in mM): 118 NaCl, 24 $NaHCO_3$, 1.5 $CaCl_2$, 3 KCl, 5 $MgCl_2$, 1.4 NaH_2PO_4, 1.3 $MgSO_4$, 25 D-glucose and 1 Kynurenic acid; the latter is a non-specific blocker of glutamate transmission (Kekesi et al. 2002). Both kinds of ACSF were saturated with 95% O_2-5% CO_2, and maintained at pH 7.4. Drugs added to the nACSF in the experiments included: 0.01 - 30 μM (±) baclofen (Sigma), 1 - 2 μM TTX (RBI), 10 - 20 μM nimodipine (Sigma), 400 μM Cd^{++} (Sigma) and 10 μM 5-HT (Sigma). Baclofen was mixed in 1 mM as stock; TTX, 5-HT and Cd^{++} were dissolved at high concentrations (x100 of final concentration) as stock. Nimodipine was dissolved in DMSO before each experiment (100 – 200 mM). These drugs were then diluted to the desired concentration in nACSF. The DMSO concentration was < 0.02% in the final nACSF solution and had no effect on PICs/plateaus (Li and Bennett 2003).

Data analysis

Data were analyzed in Clampfit 8.0 (Axon Instr., USA) and Matlab (Mathworks, USA). Figures were made in Sigmaplot (Jandel Scientific, USA). The effective concentration of baclofen to reduce the reflex by 50% (EC50) in each rat was obtained by fitting a sigmoid

curve to the relation between the percentage inhibition of reflex amplitude and the drug concentration (log). Data were shown as average $\pm$ standard deviation. A Student's *t*-test was used to test for statistical differences, with a significance level of $P < 0.05$.

RESULTS

A total of 17 acute spinal rats and 16 chronic spinal rats were included in the present study. For the 17 acute spinal rats, 6 were used to record the root reflexes and 11 were used for intracellular recording. For the 16 chronic spinal rats, 7 were used for the root reflex recording and 9 were used for intracellular recording.

The motoneurons of chronic spinal rats had a input resistance of 7.70 $\pm$ 4.14 MΩ, resting membrane potential of -75.9 $\pm$ 7.1 mV, firing level of -44.6 $\pm$ 4.6 mV (during the slow current ramp) and spike height of 71.7 $\pm$ 8.85 mV (with antidromic ventral root activation). Motoneurons of acute spinal rats had an input resistance of 4.67 $\pm$ 1.58 MΩ, resting membrane potential of -74.9 $\pm$ 8.7 mV, firing level of -47.2 $\pm$ 9.8 mV and spike height of 66.1 $\pm$ 2.59 mV. No significant differences were found between acute and chronic spinal rats in these membrane properties.

Effect of baclofen on root reflexes of chronic spinal rats

In chronic spinal rats, when a single stimulation pulse was applied to the dorsal roots (10xT), the ventral roots usually responded with a large monosynaptic reflex (3 - 5 ms latency, depending on root lengths, Fig. 1*C*) followed by a long-lasting polysynaptic reflex (usually about 2 seconds long, Fig. 1*A*), which is the counterpart of the long-lasting spastic reflex and spasms seen in these spinal rats when they were awake (Bennett et al. 1999, 2003). The monosynaptic reflex in chronic spinal rats was on average 3.85 $\pm$ 2.37 mV in amplitude (peak amplitude) and the polysynaptic reflex was about 0.48 $\pm$ 0.31 mV

(mean rectified response in a 1-sec window; see Methods; n = 7). When increasing concentrations (0.01, 0.03, 0.1, 0.3, 1 μM) of baclofen were applied to the bath, the monosynaptic and the long-lasting polysynaptic reflexes were reduced almost simultaneously. For example, at a concentration of 0.3 μM, the monosynaptic reflex was inhibited by 67.81 ± 21.86%, and the long-lasting polysynaptic reflexes were inhibited by 69.99 ± 19.59% (Fig. 2*A*, *B*). Both the monosynaptic reflex and the long-lasting reflexes of these chronic spinal rats were completely eliminated at 1 μM (Fig. 1*B*, *D*). The EC50 of baclofen for the monosynaptic reflex was 0.26 ± 0.07 μM, and the EC50 of baclofen for the polysynaptic reflexes was 0.25 ± 0.09 μM (n = 7, Figure 2*B*, *C*). There was no significant statistical difference between these numbers, suggesting the blockades of both reflexes were mediated by the same underlying mechanisms, most probably through decreased presynaptic neurotransmitter release.

Effect of baclofen on EPSPs and membrane properties of motoneurons of chronic spinal rats

To further determine whether baclofen blocked the reflexes by decreasing neurotransmitter release presynaptically or by changing motoneuron membrane properties postsynaptically, we recorded intracellularly from the motoneurons while stimulating the dorsal roots (n = 6). A single stimulation pulse to the dorsal roots triggered a long-lasting reflex discharge similar to that recorded from the ventral roots (Fig. 3*A*). Hyperpolarization of the motoneuron membrane, to eliminate the action of voltage-dependent PICs and spiking, reduced the duration of the response substantially,

indicating that the motoneuron PICs produced the many-second-long response, as described previously (Bennett et al. 2001d; Li et al. 2004a). However, under these hyperpolarized conditions, a 0.5-sec-long response (hyperpolarized EPSPs, Fig. 3*B*) remained that represented the synaptic input unaffected by postsynaptic PICs. Without hyperpolarization, this synaptic input normally triggered the PICs that ultimately caused the long-lasting reflex discharge (Fig. 3*A,* for details see Li et al. 2004a; Bennett et al. 2001). The hyperpolarized EPSPs had mono- and polysynaptic components as indicated in Fig. 3*B*. Application of 1 μM baclofen eliminated these mono- and polysynaptic EPSPs (Fig. 3*D*, cell hyperpolarized), and accordingly eliminated the long-lasting reflexes (Fig. 3*C*; cell not hyperpolarized), consistent with the finding that this dose of baclofen eliminated the ventral root reflexes (Fig. 1 described above). Thus, baclofen's major antispastic action is to block the synaptic input to the motoneurons. Higher doses of baclofen (20 - 30 μM) also completely eliminated the EPSPs.

Postsynaptically, baclofen had only weak effects that could not contribute to its antispastic action. That is, in chronic spinal rats baclofen (1 - 30 μM, n = 6) did not significantly change the motoneuron resting membrane potential (change of 0.06 $\pm$ 1.92 mV), input resistance (change of -0.81 $\pm$ 1.78 MΩ) or the current threshold to evoke firing (change of 0.07 $\pm$ 1.19 nA). Baclofen did significantly decrease the spike threshold (by 4.05 $\pm$ 3.09 mV) and increase the PIC amplitude (see details below), but these effects increased the motoneuron excitability. Thus, baclofen's antispastic action is not to decrease the motoneuron excitability, but to block the synaptic inputs to the motoneurons.

Effect of baclofen on root reflexes of acute spinal rats

In acute spinal rats, following a dorsal root stimulation pulse, only a monosynaptic reflex could be recorded on the ventral roots (Fig. 1*E*), consistent with the lack of spastic reflexes seen in the acute spinal state (Bennett et al. 1999a; Li et al. 2004b). This monosynaptic reflex had a latency of 3 - 5 ms, and an average amplitude of 0.72 $\pm$ 0.48 mV (n = 6), significantly smaller than of chronic spinal rats. During baclofen application, the amplitude of this monosynaptic reflex started to decrease at the low 0.1 μM concentration and was completely eliminated at 1 μM (Fig. 1*F*). At a concentration of 0.3 μM, 92.92 $\pm$ 11.31% of the monosynaptic reflex was eliminated, a significantly larger decrease than that of chronic spinal rats at this dose (which was 68%, Fig. 2*A*, *B*). In addition, the EC50 of baclofen for the monosynaptic reflex was 0.18 $\pm$ 0.02 μM (n = 6, Fig. 2*A*), significantly lower than that of the chronic spinal rats (0.26 μM). These results suggest that chronic spinal rats have a moderately lower (30%) sensitivity to baclofen than do acute spinal rats, which might be due to a down regulation/desensitization of $GABA_B$ receptors or decreased background GABA levels after chronic spinal cord injury (see Discussion).

Effect of baclofen on EPSPs and membrane properties of motoneurons of acute spinal rats

When recorded intracellularly, long mono- and polysynaptic EPSPs in acute spinal rats were, as in chronic spinal rats, triggered by a single stimulation pulse. Therefore, these

long EPSPs emerged acutely with injury (data not shown, see Fig. 9*C* of Li et al. 2004a for detail). Unlike in chronic spinal rats, these long EPSPs never triggered any long-lasting reflexes, nor were they amplified by depolarization, consistent with the small PICs seen in acute spinal rats. Low doses of baclofen (1 μM) eliminated the EPSPs, as did higher doses (20 - 30 μM), indicating that baclofen, as in the chronic spinal rats, eliminated the monosynaptic reflex mainly by decreasing presynaptic neurotransmitter release in the acute spinal rats.

Baclofen did not have an obvious effect on the basic membrane properties of motoneurons of acute spinal rats. That is, baclofen (1 - 30 μM, n = 6) did not significantly change the motoneuron resting membrane potential ($\Delta V = -0.35 \pm 4.02$ mV), the input resistance ($\Delta R = -0.12 \pm 0.46$ MΩ), the spike threshold ($\Delta V = -0.93 \pm 0.64$ mV) or the current threshold ($\Delta I = 0.12 \pm 0.45$ nA) in acute spinal rats.

There was an inhibitory effect of baclofen on the PICs, described below. However, since these PICs are too slow to play a major role in monosynaptic reflexes (Li et al. 2004a), the reduction in monosynaptic reflexes in acute spinal rats is not mediated by postsynaptic actions.

Effect of baclofen on the PICs in chronic spinal rats

As reported previously for motoneurons of chronic spinal rats, a subthreshold plateau potential followed by self-sustained firing could be activated with slow triangular current ramps without any exogenous neuromodulator application (Fig. 4*A*; see Bennett et al. 2001a for detail). The PIC that caused this plateau and self-sustained firing was

quantified with slow voltage ramps, under voltage-clamp conditions (Fig. 4*E*; peak of the leak subtracted PICs indicated by arrow; thin line indicates leak current). The PICs were always large enough to generate a negative-slope region in the current-voltage relation (at downward deflection during upward ramp in Fig. 4*E*). Unexpectedly, application of doses of baclofen sufficient to block the spastic reflexes (1 - 30 μM) never decreased the total PIC, even though these doses had previously been shown to be effective in reducing PIC in turtle motoneurons and dorsal horn neurons (Russo et al. 1998; Svirskis and Hounsgaard 1998).

Furthermore, 20 - 30 μM baclofen increased, rather than decreased, the total PIC as follows (n = 6; opposite of Svirskis & Hounsgaard 1998; 1 μM had no effect on the PICs). First of all, the amplitude of the initial peak of the PIC (peak PIC on upward ramp, after leak subtraction; arrow in Fig. 4*E*) increased significantly with baclofen from an average of 2.52 ± 1.52 nA to 3.20 ± 1.70 nA. The sustained peak of the PIC (peak PIC on downward current ramp, Li and Bennett 2003) also increased significantly from 2.06 ± 1.34 nA to 2.65 ± 1.48 nA. Thus, there was a 31.6 ± 12.4% increase in the initial peak and 40.5 ± 24.6% increase in the sustained peak (summarized in Fig. 6*A*). Also, the width of the classic N-shaped dip in current formed by the negative-slope region (width of valley; see double arrow in Fig. 4*G* and details in Li and Bennett 2003) significantly increased from 12.51 ± 4.22 mV to 18.73 ± 5.57 mV.

Even though the PIC was increased, this did not lead to increased self-sustained firing, as quantified by the difference between the current to start and stop firing ΔI (see Methods)

on the triangular current injections. That is, ΔI did not significantly increase with baclofen, though it did increase somewhat, from 0.90 ± 0.41 nA to 1.02 ± 0.31 nA. This discrepancy may be because the total PIC is made up of both an L-type calcium current (Ca PIC) and a TTX-sensitive persistent sodium current (Na PIC). The Ca PIC is primarily responsible for the long-lasting self-sustained firing, whereas the Na PIC produces less self-sustained firing (Li and Bennett 2003; Harvey and Bennett in preparation). Thus, it is possible that baclofen may increase the total PIC by increasing *only* the Na PIC, and thus not markedly increasing the self-sustained firing. This idea is also supported by the fact that the voltage spike threshold of motoneurons deceased significantly, by 4.05 mV ± 3.09 mV, after high doses of baclofen, and we have previously shown the spike threshold to be linked with the Na PIC (see Discussion for detail).

To directly examine how baclofen affected the Ca PIC, we studied this current in isolation by blocking the Na PIC with TTX (2 uM, Li and Bennett, 2003). In these TTX treated cells the Ca PIC was *reduced* markedly by baclofen, with significant reductions in both the initial (52 ± 20%) and sustained (58 ± 17 %) components of the Ca PIC (n = 3). Thus, the considering that the total PIC, without TTX present, was increased by baclofen, these results indicate that baclofen increased the Na PIC and decreased the Ca PIC, but the Na PIC increase must have been larger, to outweigh the Ca PIC decrease and give a net increase in total PIC.

The increase in Ca PIC with baclofen could also be deduced indirectly without the use of TTX, from data such as in Fig. 4, by assessing the hysteresis of in total PIC, which we

have previously shown to result almost exclusively from the Ca PIC (Li and Bennett 2003). In voltage-clamp, this hysteresis is in general seen by a clockwise loop in the current-voltage (I-V) relation (see Fig. 9*D* in Li and Bennett 2003) and is quantified by the difference between the current or voltage at the onset of the PIC (I_{on} or V_{on}, the first zero slope point on the up ramp in the recorded current, see Li and Bennett 2003) and offset of the PIC (I_{off} or V_{off}, the first zero slope point on the down ramp in the recorded current). Prior to baclofen, a significant hysteresis existed in the total PIC, as assessed either by $I_{on} - I_{off}$ (0.61 $\pm$ 0.13 nA) or $V_{on} - V_{off}$ (6.93 $\pm$ 3.20 mV). This hysteresis was significantly reduced by the application of baclofen (from 0.61 $\pm$ 0.13 nA to 0.26 $\pm$ 0.27 nA and from 6.93 $\pm$ 3.20 mV to 2.30 $\pm$ 1.91 mV, respectively), without significant change of the onset voltage of PICs, again suggesting that baclofen actually decreased the Ca PIC portion of the total PIC, as shown in the other neurons (Russo et al. 1998; Svirskis and Hounsgaard 1998; Voisin and Nagy 2001).

We also tested the application of TTX (2 μM) *after* baclofen application (Fig. 4). In TTX and balcofen, a large calcium plateau potential could be revealed during a current ramp because the spikes were also blocked (Fig. 4*C*, see details in Li and Bennett 2003). However, the underlying PIC was smaller than before TTX application because of the block of the TTX-sensitive Na PIC (Fig. 4*F*, *G*; see Li and Bennett 2003). The remaining PIC and plateau were eliminated by 20 μM nimodipine (Fig. 4*D*, *H*), and thus were mediated by L-type calcium channels. These results indicate that both Na and Ca PICs persist with baclofen. Thus, while baclofen likely increases the Na PIC and decreases the Ca PIC (see above), it does not completely block the Ca PIC.

Effect of baclofen on PICs induced by 5-HT in acute spinal rats

In acute spinal rats there was usually no subthreshold plateau or self-sustained firing (Fig. 5*A*); accordingly, there was no PIC large enough to produce a negative-slope region in the voltage-current relation (Fig. 5*E*) (as in Li and Bennett 2003). That is, in current-clamp recording, when a triangular current ramp was applied to the motoneuron, the motoneuron usually started and stopped firing at the same current level; in voltage-clamp recording, when a triangular voltage ramp was applied, the recorded current response was nearly linear (Fig. 5*A*, *E*). To facilitate PICs in these motoneurons, 10 – 30 μM 5-HT was added to the bath (n = 6). This induced self-sustained firing, a plateau (see ΔI) during a current ramp (Fig. 5*B*) and a moderate PIC (leak subtracted PIC, arrow of Fig. 5*F*) measured under voltage-clamp.

When baclofen (20 – 30 μM) was added to these 5-HT treated cells (n = 6), the PICs were decreased: the opposite action to that seen in chronic spinal rats, but consistent with Svirskis and Hounsgaard (1998). That is, the initial peak amplitude of the PICs decreased significantly with baclofen from an average of 2.83 ± 0.97 nA to 1.93 ± 1.32 nA, and the sustained peak amplitude decreased significantly from 2.91 ± 1.08 nA to 2.19 ± 1.32 nA respectively, which was about a 38.8 ± 25.8 % decrease in the initial peak amplitude and a 29.3 ± 24.3% decrease in the sustained peak amplitude (Fig. 5*C*, *G*, summarized in Fig. 6*B*). The PIC onset voltage, V_{on}, did not change significantly with baclofen (changed by 1.41 ± 2.65 %). Lower doses of baclofen (1 μM, n = 4) had no effect on the PICs. For the cell shown in Fig. 5, the remaining small PIC after baclofen was almost completely

eliminated by TTX (Fig. 5*D*, *H*), suggesting that it was a Na PIC that remained in baclofen, and that any Ca PIC was inhibited by baclofen prior to the TTX. However, in other cells where TTX was added first to block the Na PIC, to leave only a pure Ca PIC (see below), baclofen often only partly blocked this Ca PIC, suggesting that baclofen only incompletely blocked the calcium mediated portion of the PICs (see below, n = 4). Together, these results suggest that in acute spinal rats baclofen acts to reduce the total PIC by reducing the Ca PIC.

The 3 cells with the largest PICs induced by 5-HT (of 6 cells total) exhibited very slow firing at de-recruitment (Fig. 5*B*, *C*), which we have previously shown to result from subthreshold oscillations of a large Na PIC (Li et al. 2004a). Interestingly, these cells with the presumably largest Na PICs showed the least percent reduction in total PICs with baclofen, with one cell showing no effect of baclofen. We suspected, therefore, that baclofen might selectively inhibit the Ca PIC, and facilitate the Na PIC (as mentioned above for chronic spinal rats; also see Discussion). To test this idea, PICs were induced by 5-HT (10 μM) in 4 additional cells and then TTX (2 μM) was added to block the Na PIC prior to baclofen application (and also to block any spike mediated transmission), thus leaving the Ca PIC in isolation (Li and Bennett 2003). In all these cells, there was a clear calcium-mediated plateau and Ca PIC with characteristic hysteresis (not shown, Li and Bennett 2003). The application of baclofen (20 - 30 μM) decreased these Ca PICs markedly. That is, the initial peak amplitude of the PICs decreased significantly with baclofen from an average of 1.74 $\pm$ 0.59 nA to 0.97 $\pm$ 0.32 nA, and the sustained peak amplitude decreased significantly from 1.69 $\pm$ 0.65 nA to 1.01 $\pm$ 0.40 nA respectively,

which was about a 57.2 $\pm$ 16.4% decrease in the initial peak amplitude and 60.5 $\pm$ 13.8% decrease in the sustained peak amplitude (Fig. 5*C*, *G*, summarized in Fig. 6*B*). The remaining PIC in TTX/5HT/baclofen was eliminated by a calcium blockade with Cd^{++}, showing that it was indeed a Ca PIC. Importantly, the absolute reduction of the PIC by baclofen after TTX (0.77 nA initial PIC) was not significantly different from the reduction of the total PIC in cells not treated with TTX (0.90 nA, see above) and was, on average, smaller, suggesting that baclofen's inhibitory action is primarily to reduce the Ca PIC and that baclofen moderately increased the Na PIC. Furthermore, the percent reduction in PIC by baclofen was significantly larger after TTX application (almost doubled), also consistent with the suggestion that baclofen primarily inhibits the Ca PIC, and thus removing the Na PIC with TTX reveals a much larger direct effect of baclofen on the Ca PIC.

DISCUSSION

Our results demonstrate that very low concentrations of baclofen (≤1 μM) are sufficient to block both monosynaptic and long-lasting spastic reflexes in chronic spinal rats, and the underlying EPSPs recorded intracellularly. These same low concentrations of baclofen have no major inhibitory effect on postsynaptic motoneuron properties and, in particular do not reduce the PICs that are known to play a major role in producing long-lasting spastic reflexes. Thus, at doses where the reflexes are inhibited (similar to the clinical dose range, see below), baclofen's antispastic action is purely presynaptic. Considering that long-lasting spastic reflexes are mediated by postsynaptic PICs in the motoneurons that are triggered by polysynaptic EPSPs (Fig. 2 and Li et al. 2004a), baclofen must act to block these spastic reflexes by simply blocking the polysynaptic EPSPs so that the PICs are not triggered, rather than blocking the PICs directly. The polysynaptic reflex decreased at similar doses to the monosynaptic reflex (similar dose-response curve slope and EC50), suggesting similar mechanisms underlying the two blockades, most probably by reducing neurotransmitter release. Interestingly, the monosynaptic reflex of acute spinal rats was inhibited at a lower dose than that of the chronic spinal rats, suggesting there might be decreased sensitivity/number of $GABA_B$ receptors or less background GABAergic inhibition after chronic injury. Baclofen did have postsynaptic effects (significant at 20 - 30 μM), but these were unexpectedly excitatory in chronic spinal rats, increasing the PICs and decreasing the spike threshold voltage. In normal motoneurons of acute spinal rats, baclofen decreased the PICs induced by 5-HT, consistent with baclofen's inhibitory action in normal turtle motoneurons and

deep dorsal horn neurons (Russo et al. 1998; Svirskis and Hounsgaard 1998; Voisin and Nagy 2001).

The different effects of baclofen on acute and chronic spinal rats in both root reflexes and PICs were unexpected. The reasons for such effects are discussed below, in addition to their possible implications in treating spasticity with baclofen in spinal cord injured humans.

Decreased GABAergic inhibition after chronic spinal cord injury

It has been shown that there are abundant $GABA_B$ receptors in the primary afferent terminal in many vertebrates (Price et al. 1984; Yang et al. 2001). Baclofen can strongly activate these receptors, and through the second messenger system, coupled to the calcium and potassium channels, substantially decrease the neurotransmitter release; in some preparations, as in the present study, this blockade can be complete (Jimenez et al. 1991; Kangrga et al. 1991). Since the blockade of the monosynaptic and polysynaptic EPSPs occurs at a low baclofen concentration (≤ 1 μM) where there are no major changes in postsynaptic motoneuron properties (Edwards et al. 1989; Lev-Tov et al. 1988), this blockade is likely mediated primarily by decreased presynaptic neurotransmitter release from the primary afferents terminals (Dolphin et al. 1990; Miller 1998; Takahashi et al. 1998). The fact that the monosynaptic and polysynaptic long-lasting reflexes are inhibited by identical doses of baclofen (EC50 = 250 - 260 nM) suggests that baclofen acts with equal efficacy in the mono- and polysynaptic pathways. Thus, polysynaptic pathways are

likely also inhibited by presynaptic inhibition of the afferent terminals, like the monosynaptic reflex. However, we cannot rule out baclofen's action on interneurons in the polysynaptic reflex pathway.

Interestingly, the doses of baclofen needed to inhibit the monosynaptic reflex in chronic spinal rats were moderately higher than in acute spinal rats (i.e., the dose-response curve was shifted to the right in chronic spinal rats, EC50 was 40% higher). The reason for this decreased sensitivity of chronic spinal rats to baclofen is still uncertain, though there may be less background GABA available and thus less GABAergic inhibition in chronic spinal rats, so that more baclofen would be needed to reach a similar level of inhibition. This idea is consistent with the decreased presynaptic inhibition of the monosynaptic reflex in the lower limbs of patients with upper motoneurons disease (Ashby and McCrea 1987; Iles and Roberts 1986; Nielsen et al. 1995). The decreased GABAergic inhibition may also explain why the monosynaptic reflex increases in amplitude in chronic spinal rats (see Results) and could also contribute to triggering the exaggerated long-lasting reflexes. Indeed, our unpublished data suggest that there are GABAergic interneurons in both the ipsilateral and contralateral sacral spinal cord that provide a strong inhibition of the monosynaptic reflex in normal rats, because the size of the ipsilateral monosynaptic reflex increases dramatically after removal of the contralateral cord with a sagittal hemisection (publication in preparation). Similar decreases in GABA levels have also been observed in the superficial dorsal horn after chronic peripheral nerve injury (Moore et al. 2002). In addition, fewer GABA receptors after chronic spinal cord injury due to receptor degeneration (Castro-Lopes et al. 1995; Price et al. 1987) or changes in $GABA_B$-

coupled second messenger systems after chronic injury may also explain the decreased efficacy of baclofen after chronic injury.

Paradoxical effect of baclofen on PICs in acute and chronic spinal motoneurons

One unexpected finding of the present study is that baclofen increased the amplitude of the PICs in chronic spinal rats (at 20 - 30 μM). By contrast, in normal motoneurons of acute spinal rats, baclofen decreased the PICs induced by 5-HT, consistent with baclofen's inhibitory action in normal turtle motoneurons and in turtle and rat deep dorsal horn neurons (Russo et al. 1998; Svirskis and Hounsgaard 1998; Voisin and Nagy 2001). In turtle neurons, baclofen hyperpolarizes the membrane and decreases the membrane conductance; however, it has been proposed that baclofen exerts its effect mainly by intracellularly inhibiting the L-type calcium channels, which mediate the activation of PICs and the associated plateau potentials in these neurons (Russo et al. 1998; Svirskis and Hounsgaard 1998).

L-type calcium currents also mediate PICs and plateau potentials in motoneurons of chronic spinal rats. However, this Ca PIC makes up only about half of the initial peak of the total PIC; the other half is mediated by a persistent sodium current, Na PIC (Li and Bennett 2003). By contrast, in turtle motoneurons and deep dorsal horn interneurons, a Na PIC has not been reported to play a major role (Hounsgaard and Kiehn 1989; Russo and Hounsgaard 1996b). We have found that baclofen increases PICs in chronic spinal rats by facilitating the Na PIC more than it decreases the Ca PIC. This idea is supported

by several facts. First, balcofen *decreases* the Ca PIC (measured in TTX or inferred from hysteresis), even though it *increases* the total net PIC (measured without TTX present), which we know is composed of just two currents: Na PIC and Ca PIC. Second, although baclofen increases the PIC amplitude, the self-sustained firing (indicated by ΔI) measured in current-clamp recording is not significantly increased. L-type calcium currents play a major role in producing the self-sustained firing while persistent sodium currents play a smaller role (Li and Bennett 2003; Li et al. 2004a); therefore, increased PICs without large changes in ΔI are more consistent with an increased Na PIC. Third, the spike threshold decreases by about 4.05 mV with high concentration of baclofen (see Results). The persistent sodium current appears to be tightly linked to the spike threshold, with a threshold that is always a few milivolts lower than the spike threshold, and it is important in initiating firing (Lee and Heckman 2001; Li and Bennett 2003). Thus, the lowering of the spike threshold may result from a facilitation of the persistent sodium current by baclofen.

In summary, the net effect of baclofen depends on the balance of two opposite effects: a facilitation of the Na PIC and an inhibition of the Ca PIC. A large portion of the PIC is mediated by Na PICs in motoneurons of chronic spinal rats, and thus, the facilitatory effect of baclofen on the Na PIC dominates. In contrast, in motoneurons of acute spinal rats the PIC induced by 5-HT often has a larger Ca PIC than the Na PIC, and therefore, the inhibitory effect of baclofen on the Ca PIC dominates, and the net PIC is reduced by baclofen.

Anti-spasticity effect of baclofen on rats and humans

The dose-response relation for baclofen is very steep. That is, the dose of baclofen to inhibit 50 % of the mono- and polysynaptic reflexes (EC50 0.26 μM and 0.25 μM, respectively) is very close to the concentration of baclofen that blocks all the reflexes (mono- and polysynaptic reflexes, 1 μM, about 4 times that of the EC50). This very steep, dose-response curve is consistent with our *in vivo* studies in chronic spinal rats, where we found it difficult to increase the dose to an effective antispastic dose without producing a total loss of all reflexes and side effects such as loss of bladder control (unpublished results). A similar phenomenon has been observed in humans. In spastic patients, the therapeutic plasma baclofen concentration is around 100 – 650 ng/ml (i.e. 0.47 - 3.04 μM, Aisen et al. 1992; Knuttson et al. 1974), and the maximal safe dose should not exceed 1 μg/ml (4.68 μM). At a concentration of 2 μg/ml, which is also about 4 times the therapeutic concentration of baclofen, serious toxicity including muscle flaccidity occurs (Flanagan 1998). Finally, with a plasma-to-cerebrospinal fluid concentration ratio of approximately 8:1 (Knuttson et al. 1974), the therapeutic concentration of orally administered baclofen in the CSF is in the low nanomolar range (0.06 – 0.38 μM), very close to the effective baclofen concentration in our ACSF.

Various researchers have demonstrated that baclofen relieves spasticity at the spinal cord level, and mainly decreases the neurotransmitter release by presynaptic inhibition (Abbruzzese 2002; Davidoff 1985). In our experiments, the low concentrations of baclofen, equivalent to the clinical doses (less than 1 μM), do not have obvious effects on the postsynaptic motoneuron properties, even though baclofen blocks mono- and long-

lasting reflexes at these low doses. Thus, baclofen likely blocks spasticity in the chronic spinal rats by the same presynaptic mechanisms proposed in humans. The similarity between the effect of baclofen in chronic spinal rats and spastic patients with chronic spinal cord injury suggests a similarity in the mechanisms of spasticity in the two systems and provides another piece of evidence that chronic sacral spinal rats may be a good model to develop new anti-spasticity drugs (Bennett et al. 1999a; Li et al. 2004a). For example, drugs that effectively inhibit the motoneuron PICs involved in spasticity (Li and Bennett 2003), without blocking the presynaptic neurotransmitter release (unlike baclofen), might be more effective antispastic agents.

FIGURES

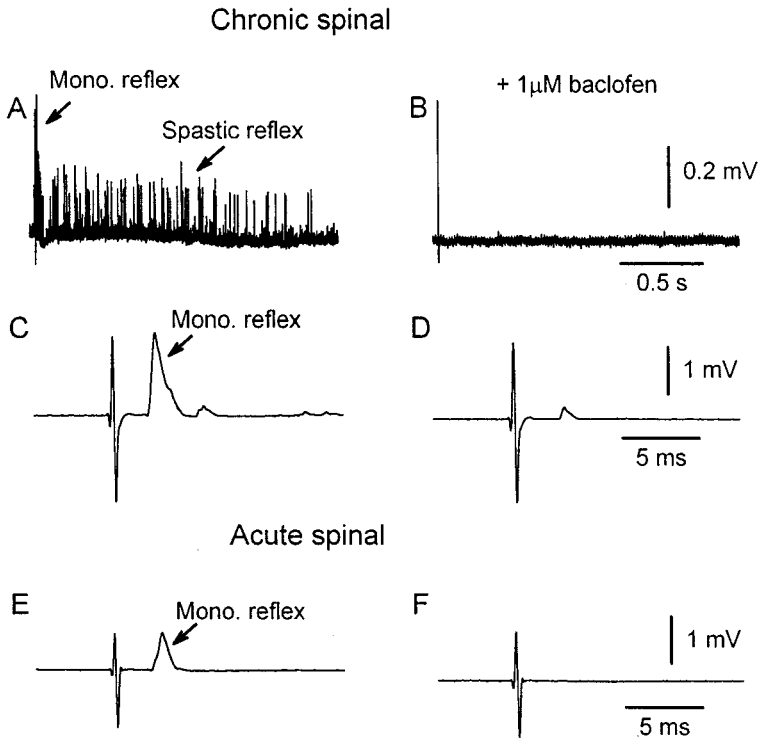

FIGURE 6-1. A LOW CONCENTRATION OF BACLOFEN (1 μM) WAS SUFFICIENT TO BLOCK MONO- AND POLYSYNAPTIC LONG-LASTING SPASTIC REFLEXES IN CHRONIC SPINAL RATS.

A: long-lasting spastic reflex recorded from the ventral roots of a chronic spinal rat, triggered by a single dorsal root stimulation pulse (0.1 mA, 0.1 ms). Note the length of the reflex (approx. 2s). B: 1 μM baclofen completely eliminated the long-lasting reflex. C and D: expanded version of A and B to show the exaggerated monosynaptic reflex in chronic spinal rats, which is also completely eliminated by 1 μM baclofen. E: only a small monosynaptic reflex was recorded from the ventral root of an acute spinal rat by

the same stimulation in A. F: 1 μM of baclofen completely eliminated the monosynaptic reflex.

A: Monosynaptic reflex in acute spinal rats

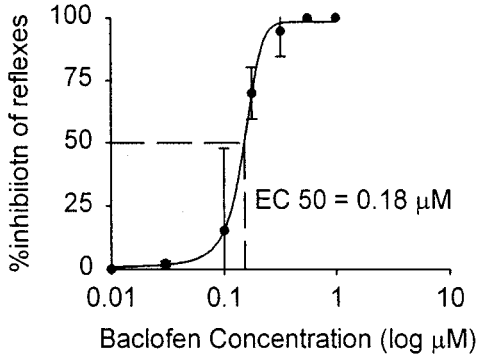

B: Monosynaptic reflex in chronic spinal rats

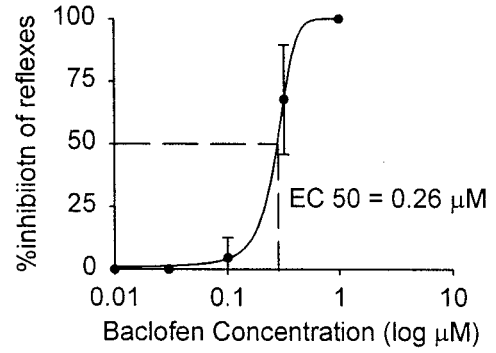

C: Polysynaptic reflex in chronic spinal rats

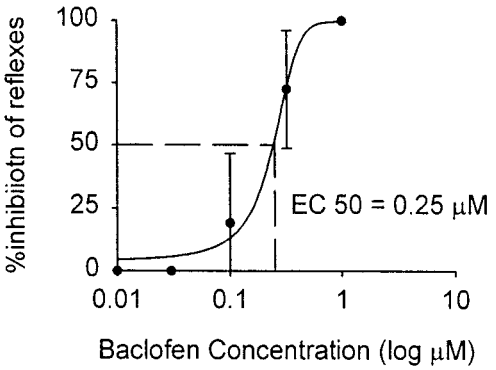

FIGURE 6-2. DOSE-RESPONSE CURVES OF BACLOFEN IN ACUTE AND CHRONIC SPINAL RATS. A: average dose-response curve for the monosynaptic reflex in acute spinal rats. The average EC50 was obtained for each rat by fitting a sigmoid curve to the response, computing the EC50, and averaging across rats. B: average dose-response curve for the monosynaptic reflex in chronic spinal rats. Note the significantly larger EC 50 compared with that in acute spinal rats. C: average dose-response curve for the polysynaptic reflex in chronic spinal rats. Note that the EC 50 for the polysynaptic reflex is very close to that for the monosynaptic reflex in chronic spinal rats.

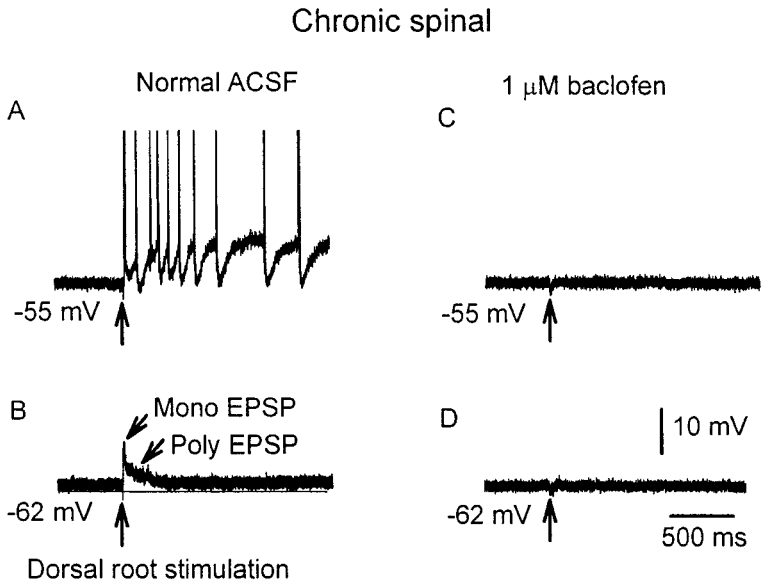

FIGURE 6-3. LOW CONCENTRATION OF BACLOFEN (1 μM) BLOCKED THE LONG EPSPS THAT TRIGGERED THE LONG-LASTING REFLEXES.

A: long-lasting reflex recorded intracellularly from a motoneuron of a chronic spinal rat, triggered by a single dorsal root stimulation pulse (0.1 mA, 0.1 ms). B: when PICs were blocked by hyperpolarizing the membrane, long EPSPs that triggered the PICs (and thus the long-lasting reflexes) were revealed. C and D: both the EPSPs and the long-lasting reflex were blocked by 1 μM baclofen.

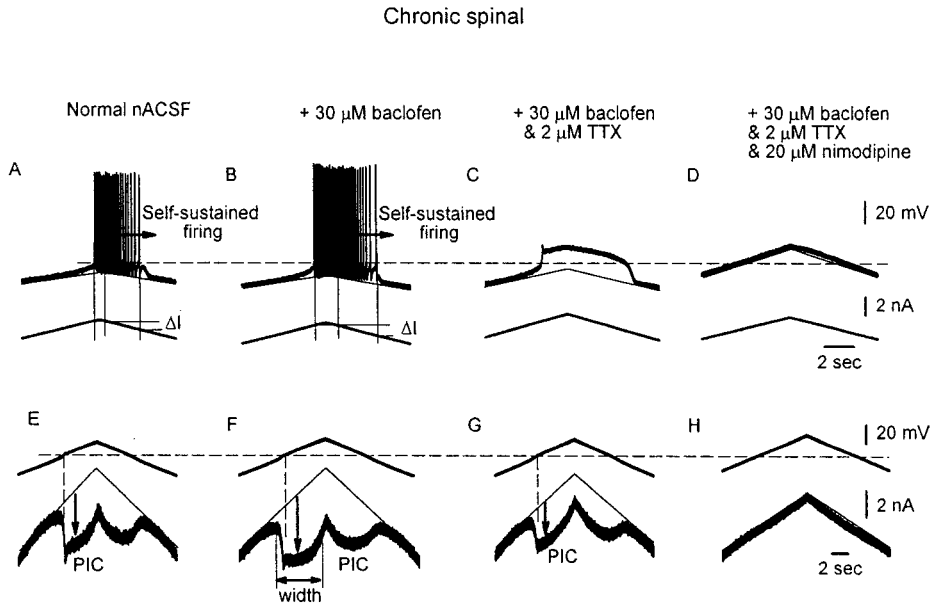

FIGURE 6-4. BACLOFEN (30 μM) INCREASED THE AMPLITUDE OF PICS IN MOTONEURONS OF CHRONIC SPINAL RATS.

A: voltage response in a motoneuron of a chronic spinal rat during slow ramp current injection, under discontinuous current-clamp conditions. Note the long self-sustained firing (quantified by ΔI). Dashed line indicates spike threshold (-55 mV). B: response to a similar current ramp after baclofen application. Note the slightly increased ΔI. C: after TTX blocked sodium spikes and synaptic activity (latter not shown), a plateau was revealed. D: nimodipine, a specific L-type calcium channel blocker, abolished the plateau in C, proving that it was calcium mediated. E: current response of the same motoneuron prior to drug application during a slow voltage ramp under voltage-clamp conditions,

with thin line indicating the estimated leak current. Note the large leak-subtracted PICs (initial peak indicated by vertical arrow) and associated negative-slope region (width indicated by double arrows in F). Dashed lines indicate spike threshold at -55mV. F: response to a similar voltage ramp after baclofen application. Note the deepened and widened negative-slope region after baclofen application and the larger leak subtracted PICs (arrow). G: TTX decreased the magnitude of the negative-slope region produced by PICs (arrow), indicating that parts of the PICs were mediated by a TTX-sensitive current. H: further application of nimodipine eliminated the remaining PICs, consistent with the response in D.

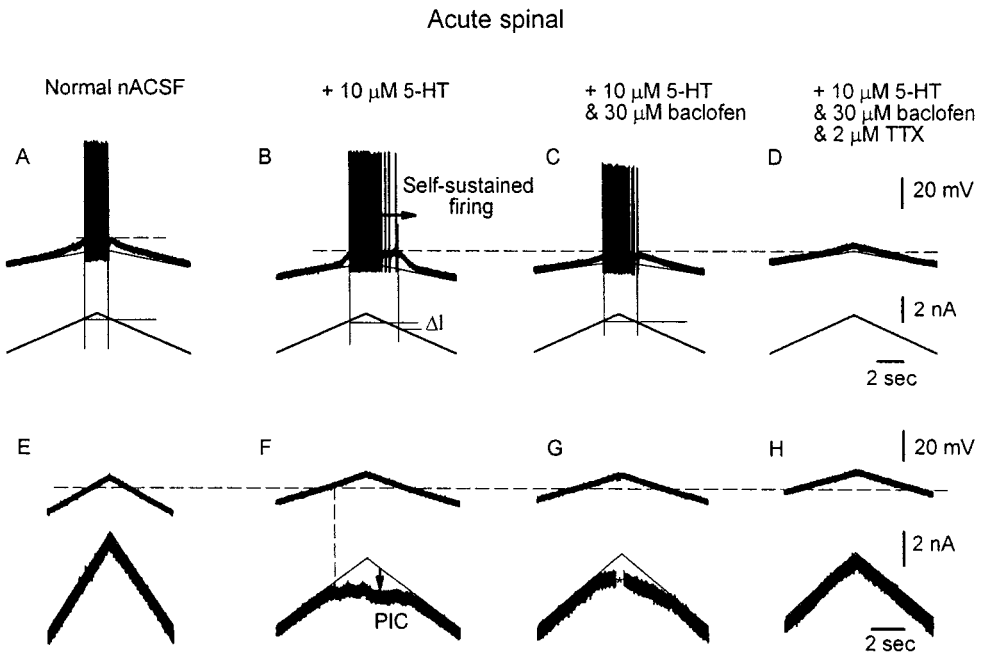

FIGURE 6-5. BACLOFEN (30 μM) DECREASED THE AMPLITUDE OF PICS INDUCED BY 10 μM 5-HT IN MOTONEURON OF ACUTE SPINAL RAT.

Similar format to Figure 4. A: current-clamp recording from a motoneuron of an acute spinal rat with no plateau or self-sustained firing. B: 10 μM 5-HT induced a self-sustained firing in the same motoneuron, indicated by ΔI. C: 30 μM baclofen greatly decreased the amplitude of ΔI. D: the remaining self-sustained firing and the underlying sustained depolarization were completely blocked by TTX. E: voltage-clamp recording from the same cell. No PIC was activated by a slow voltage ramp prior to 5-HT. F: 10 μM 5-HT induced a small negative-slope region in voltage-clamp and a small PIC (arrow). G: 30 μM baclofen greatly decreased the amplitude of the PICs induced by 5-

HT. The asterisk indicates a transient unclamped spike, which was removed for clarity. H: the remaining PIC was completely blocked by TTX.

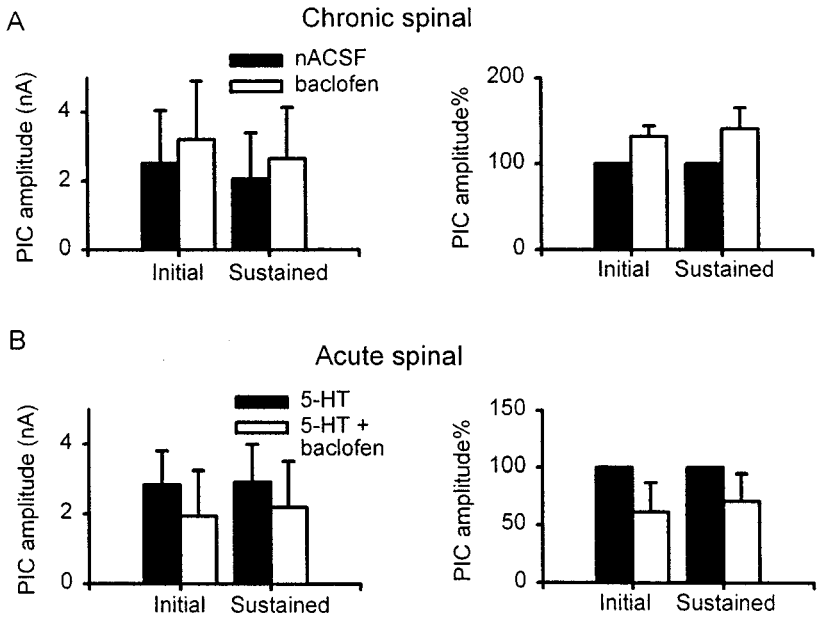
A
Chronic spinal
nACSF
baclofen
PIC amplitude (nA)
4
2
0
Initial
Sustained
PIC amplitude%
200
100
0
Initial
Sustained
B
Acute spinal
5-HT
5-HT +
baclofen
PIC amplitude (nA)
4
2
0
Initial
Sustained
PIC amplitude%
150
100
50
0
Initial
Sustained

FIGURE 6-6. SUMMARY OF THE INITIAL AND SUSTAINED PEAK AMPLITUDE OF THE PICS.

A: averaged magnitude of the initial and sustained peak of PICs in motoneurons of chronic spinal rats in nACSF (black bar) and after 20 - 30 μM baclofen (white bar). Left, amplitude of PICs in nA. Right, amplitude as percentage of the PIC prior to baclofen. B: same format as A. Averaged magnitude of the initial and sustained peak of PICs in motoneurons of acute spinal rats after 10 μM 5-HT (black bar) and after 20 - 30 μM baclofen (white bar). All changes with drug applications are significant.

REFERENCES

Abbruzzese G. The medical management of spasticity. Eur J Neurol 9 Suppl 1: 30-34; discussion 53-61, 2002.

Aisen ML, Dietz MA, Rossi P, Cedarbaum JM, and Kutt H. Clinical and pharmacokinetic aspects of high dose oral baclofen therapy. J Am Paraplegia Soc 15: 211-216, 1992.

Albright AL, Cervi A, and Singletary J. Intrathecal baclofen for spasticity in cerebral palsy. Jama 265: 1418-1422, 1991.

Ashby P and McCrea DA. Neurophysiology of spinal spasticity. In: Handbook of the Spinal Cord, edited by Davidoff RA. New York: Marcel Dekker Inc., 1987, p. 120-143.

Azouvi P, Mane M, Thiebaut JB, Denys P, Remy-Neris O, and Bussel B. Intrathecal baclofen administration for control of severe spinal spasticity: functional improvement and long-term follow-up. Arch Phys Med Rehabil 77: 35-39, 1996.

Batueva I, Tsvetkov E, Sagatelyan A, Buchanan JT, Vesselkin N, Adanina V, Suderevskaya E, Rio JP, and Reperant J. Physiological and morphological correlates of presynaptic inhibition in primary afferents of the lamprey spinal cord. Neuroscience 88: 975-987, 1999.

Bennett DJ, Gorassini M, Fouad K, Sanelli L, Han Y, and Cheng J. Spasticity in rats with sacral spinal cord injury. J Neurotrauma 16: 69-84, 1999.

Bennett DJ, Hultborn H, Fedirchuk B, and Gorassini M. Synaptic activation of plateaus in hindlimb motoneurons of decerebrate cats. J Neurophysiol 80: 2023-2037, 1998.

Bennett DJ, Li Y, Harvey PJ, and Gorassini M. Evidence for plateau potentials in tail motoneurons of awake chronic spinal rats with spasticity. J Neurophysiol 86: 1972-1982, 2001a.

Bennett DJ, Li Y, and Siu M. Plateau potentials in sacrocaudal motoneurons of chronic spinal rats, recorded in vitro. J Neurophysiol 86: 1955-1971, 2001b.

Bennett DJ, Sanelli L, Cooke CL, Harvey PJ, and Gorassini MA. Spastic long-lasting reflex in the awake rat after sacral spinal cord injury. J Neurophysiol submitted, 2003.

Bussieres N and El Manira A. GABA(B) receptor activation inhibits N- and P/Q-type calcium channels in cultured lamprey sensory neurons. Brain Res 847: 175-185, 1999.

Castro-Lopes JM, Malcangio M, Pan BH, and Bowery NG. Complex changes of GABAA and GABAB receptor binding in the spinal cord dorsal horn following peripheral inflammation or neurectomy. Brain Res 679: 289-297, 1995.

Chandler SH, Hsaio CF, Inoue T, and Goldberg LJ. Electrophysiological properties of guinea pig trigeminal motoneurons recorded in vitro. J Neurophysiol 71: 129-145, 1994.

Curtis DR, Gynther BD, Lacey G, and Beattie DT. Baclofen: reduction of presynaptic calcium influx in the cat spinal cord in vivo. Exp Brain Res 113: 520-533, 1997.

Davidoff RA. Antispasticity drugs: mechanisms of action. Ann Neurol 17: 107-116, 1985.

Dolphin AC, Huston E, and Scott RJ. GABAB-mediated inhibition of calcium currents: a possible role in presynaptic inhibition. In: GABAB receptors in mammalian function, edited by Bowery NG, Bittinger H and Olpe HR. New York: Wiley, 1990, p. 259-271.

Edwards FR, Harrison PJ, Jack JJ, and Kullmann DM. Reduction by baclofen of monosynaptic EPSPs in lumbosacral motoneurones of the anaesthetized cat. J Physiol 416: 539-556, 1989.

Flanagan RJ. Guidelines for the interpretation of analytical toxicology results and unit of measurement conversion factors. Ann Clin Biochem 35 (Pt 2): 261-267, 1998.

Gage PW. Activation and modulation of neuronal K+ channels by GABA. Trends Neurosci 15: 46-51, 1992.

Gorassini M, Yang JF, Siu M, and Bennett DJ. Intrinsic activation of human motoneurons: possible contribution to motor unit excitation. J Neurophysiol 87: 1850-1858, 2002.

Hounsgaard J, Hultborn H, Jespersen B, and Kiehn O. Bistability of alpha-motoneurones in the decerebrate cat and in the acute spinal cat after intravenous 5-hydroxytryptophan. J Physiol 405: 345-367, 1988.

Hounsgaard J, Hultborn H, Jespersen B, and Kiehn O. Intrinsic membrane properties causing a bistable behaviour of alpha-motoneurones. Exp Brain Res 55: 391-394, 1984.

Hounsgaard J and Kiehn O. Serotonin-induced bistability of turtle motoneurones caused by a nifedipine-sensitive calcium plateau potential. J Physiol 414: 265-282, 1989.

Hudgson P and Weightman D. Baclofen in the treatment of spasticity. Br Med J 4: 15-17, 1971.

Hudgson P, Weightman D, and Cartlidge NE. Clinical trial of baclofen against placebo. Postgrad Med J 48: Suppl 5:37-40, 1972.

Iles J and Roberts R. Presynaptic inhibition of monosynaptic reflexes in the lower limbs of subjects with upper motoneuron disease. Journal of Neurology, Neurosurgery, and Psychiatry 49: 937-944, 1986.

Jimenez I, Rudomin P, and Enriquez M. Differential effects of (-)-baclofen on Ia and descending monosynaptic EPSPs. Exp Brain Res 85: 103-113, 1991.

Kamensek J. Continuous intrathecal baclofen infusions. An introduction and overview. Axone 20: 67-72, 1999.

Kangrga I, Jiang MC, and Randic M. Actions of (-)-baclofen on rat dorsal horn neurons. Brain Res 562: 265-275, 1991.

Kekesi G, Joo G, Csullog E, Dobos I, Klimscha W, Toth K, Benedek G, and Horvath G. The antinociceptive effect of intrathecal kynurenic acid and its interaction with endomorphin-1 in rats. Eur J Pharmacol 445: 93-96, 2002.

Knuttson E, Lindblom U, and Martensson A. Plasma and cerebrospinal fluid level of baclofen (Lioresal) at optimal therapeutic responses in spastic paresis. J Neurol Sci 23: 473-484, 1974.

Lee RH and Heckman CJ. Bistability in spinal motoneurons in vivo: systematic variations in persistent inward currents. J Neurophysiol 80: 583-593, 1998a.

Lee RH and Heckman CJ. Bistability in spinal motoneurons in vivo: systematic variations in rhythmic firing patterns. J Neurophysiol 80: 572-582, 1998b.

Lee RH and Heckman CJ. Essential role of a fast persistent inward current in action potential initiation and control of rhythmic firing. J Neurophysiol 85: 472-475, 2001.

Lev-Tov A, Meyers DE, and Burke RE. Activation of type B gamma-aminobutyric acid receptors in the intact mammalian spinal cord mimics the effects of reduced presynaptic Ca2+ influx. Proc Natl Acad Sci U S A 85: 5330-5334, 1988.

Li Y and Bennett DJ. Persistent sodium and calcium currents cause plateau potentials in motoneurons of chronic spinal rats. J Neurophysiol 90: 857-869, 2003.

Li Y, Gorassini MA, and Bennett DJ. Role of persistent sodium and calcium currents in motoneuron firing and spasticity in chronic spinal rats. J Neurophysiology 91: 767-783, 2004a.

Li Y, Harvey PJ, and Bennett DJ. Baclofen does not block plateau potentials in motoneurons of chronic spinal rats. Soc Neurosci Abstr, 2002.

Li Y, Harvey PJ, Li X, and Bennett DJ. Spastic long-lasting reflexes in the chronic spinal rat, studied in vitro. J Neurophysiology (in press), 2004b.

Metz L. Multiple sclerosis: symptomatic therapies. Semin Neurol 18: 389-395, 1998.

Meythaler JM, Guin-Renfroe S, Brunner RC, and Hadley MN. Intrathecal baclofen for spastic hypertonia from stroke. Stroke 32: 2099-2109, 2001.

Miller RJ. Presynaptic receptors. Annu Rev Pharmacol Toxicol 38: 201-227, 1998.

Moore KA, Kohno T, Karchewski LA, Scholz J, Baba H, and Woolf CJ. Partial peripheral nerve injury promotes a selective loss of GABAergic inhibition in the superficial dorsal horn of the spinal cord. J Neurosci 22: 6724-6731, 2002.

Nielsen J, Petersen N, and Crone C. Changes in transmission across synapses of Ia afferents in spastic patients. Brain 118: 995-1004, 1995.

Ochs G, Struppler A, Meyerson BA, Linderoth B, Gybels J, Gardner BP, Teddy P, Jamous A, and Weinmann P. Intrathecal baclofen for long-term treatment of spasticity: a multi-centre study. J Neurol Neurosurg Psychiatry 52: 933-939, 1989.

Price G, Kelly J, and Bowery N. The location of GABAb receptors binding sites in mammalian spinal cord. Synapse 1: 530-538, 1987.

Price GW, Wilkin GP, Turnbull MJ, and Bowery NG. Are baclofen-sensitive GABAB receptors present on primary afferent terminals of the spinal cord? Nature 307: 71-74, 1984.

Russo RE and Hounsgaard J. Plateau-generating neurones in the dorsal horn in an in vitro preparation of the turtle spinal cord. J Physiol 493 (Pt 1): 39-54, 1996.

Russo RE, Nagy F, and Hounsgaard J. Inhibitory control of plateau properties in dorsal horn neurones in the turtle spinal cord in vitro. J Physiol 506 (Pt 3): 795-808, 1998.

Schwindt P and Crill W. Membrane properties of cat spinal motoneurons. In: Handbook of the spinal cord, edited by Davidoff RA. New York: Marcel Dekker, 1984, p. 199-242.

Schwindt PC and Crill WE. Amplification of synaptic current by persistent sodium conductance in apical dendrite of neocortical neurons. J Neurophysiol 74: 2220-2224, 1995.

Svirskis G and Hounsgaard J. Transmitter regulation of plateau properties in turtle motoneurons. J Neurophysiol 79: 45-50, 1998.

Takahashi T, Kajikawa Y, and Tsujimoto T. G-Protein-coupled modulation of presynaptic calcium currents and transmitter release by a GABAB receptor. J Neurosci 18: 3138-3146, 1998.

Voisin DL and Nagy F. Sustained L-type calcium currents in dissociated deep dorsal horn neurons of the rat: characteristics and modulation. Neuroscience 102: 461-472, 2001.

Yang K, Wang D, and Li Y. Distribution and depression of the GABAb receptor in the spinal dorsal horn of adult rat. Brain Research Bulletin 55: 479-485, 2001.

Chapter 7: DISCUSSION

GENERAL IONIC MECHANISMS UNDERLYING SPASTICITY

The present results from the sacrocaudal spinal cord studied *in vitro*, together with the associated recording from awake sacral spinal rats, lead to the following interpretation of what causes spasticity syndrome after spinal cord injury. Immediately after injury, motoneurons receive unusually long polysynaptic EPSPs (200 - 500 ms) in response to low or high threshold afferent stimulation, especially cutaneous stimulation, consistent with the acute loss of descending brainstem innervation of the dorsal horn (Bennett et al. 2004; Bennett et al. 2001b; Li et al. 2004a). These EPSPs do not cause reflexes immediately after injury, because of the profound loss of motoneuron excitability that occurs with acute injury (Bennett et al. 2001a; Bennett et al. 2001b; Li et al. 2004a), primarily due to loss of intrinsic persistent inward current (PIC) that normally amplify and prolong synaptic inputs by many fold (Lee and Heckman 1999; Li and Bennett 2003). This loss of motoneuron excitability is likely the main reason for spinal shock that occurs in the first days after injury, considering that the excitatory synaptic inputs to motoneurons (EPSPs) are enhanced, rather than reduced, in this acute phase of injury. After about a month the motoneurons recover their excitability, and the same low threshold polysynaptic inputs (EPSPs) to the motoneurons are profoundly amplified and prolonged by PICs that regeneratively activate, cause plateau potentials and ultimately produce many seconds long discharges (Bennett et al. 2001a; Bennett et al. 2001b; Li and Bennett 2003; Li et al. 2004a). Thus, normally innocuous stimulation, such as gently rubbing the skin, evokes these polysynaptic EPSPs, which in turn trigger PICs and plateaus that ultimately cause many seconds long reflex responses and whole limb

spasms. Even passive movement of the limb would trigger such low-threshold long-lasting reflexes, and thus trigger spontaneous spasms. Finally, movements caused by the long-lasting reflexes reactivate low threshold afferents and trigger further polysynaptic EPSPs, which likely get larger with repetition due to the windup of the polysynaptic reflexes. This should ultimately lead to low frequency clonus, with a period of oscillation longer than the 200 ms EPSP duration (< 5 Hz clonus). These results from the sacral spinal rat model thus explain many of the characteristic features of the spinal spasticity syndrome, including spasms, clonus, hyperreflexia and hypersensitivity to normally innocuous stimulation (Kuhn and Macht 1948). Similar cellular mechanisms likely underlie spasticity in humans after spinal cord injury (Gorassini et al. 1999; Gorassini et al. 2003).

FUTURE RESEARCH DIRECTIONS

Mechanisms of the recovery of motoneuron PICs

It is still a mystery how motoneurons regain their ability to activate PICs after chronic spinal cord injury. However, as mentioned in the Introduction, some 5-HT does persist in the spinal cord below a chronic transection (Newton and Hamill 1988; Shapiro 1997), and the very small number of interneurons containing monoamines in the cord could increase with chronic injury (Cassam et al. 1997). Thus, one possibility for the redevelopment of PICs in chronic injury is markedly enhanced sensitivity of PICs to these residual monoamines.

Our study (Li and Bennett 2003) has indicated that two currents contribute to the recovery of the PIC: L-type Ca current (Ca PIC; likely due to CaV 1.3 channels) and persistent Na current (Na PIC; channel type unknown, but possibly NaV 1.1 or 1.6) (Goldin 2001). Other currents may yet be shown to play a role. Both Ca PIC and Na PIC currents are under the control of G protein coupled pathways activated by receptors for 5-HT and NE (Alaburda et al. 2002; Cantrell and Catterall 2001). The regulation of the PIC is thus a complex system, and the recovery of the PIC in chronic injury and its supersensitivity to monoamines could be due to changes in 3 different components: 1) the 5-HT or NE receptors, 2) the G protein coupled pathway or 3) the Ca or Na channels that generate the PIC. Monoaminergic receptors do transiently increase in number caudal to a spinal transection, but then return to baseline levels within two months (Giroux et al. 1999). Supersensitivity to monoamines may occur via changes in binding to

monoaminergic receptors or, perhaps more likely, alterations in the G protein pathways. In addition, because the PIC is largely generated within dendritic regions, its amplitude is strongly dependent on the location and density of the dendritic Ca and Na channels. Changes in Ca and Na channels could also be very important in the post-injury recovery of the PIC.

Pharmacological control of spasticity

Spasticity in spinal cord injury is such a severe problem for quality of life that most patients require constant antispastic medication. Blocking the PICs by motoneuron hyperpolarization or administration of L-type calcium channel/persistent sodium channel blockers to the *in vitro* preparation eliminates the long-lasting reflexes that contribute to spasticity (Li et al. 2004a), indicating that the PICs play a fundamental role in spasticity production in chronic injury. Thus, agents that control the PICs are prime targets for developing new strategies to control spasticity. The standard treatment of spinal spasms in human patients is the $GABA_B$ agonist baclofen. Our *in vitro* work shows that baclofen's main action is to produce powerful presynaptic inhibition of reflex pathways at low nanomolar doses. It can also suppress the PICs in normal motoneurons, but only at very high doses (micromolar) that cannot be obtained clinically; furthermore, even high doses of baclofen failed to inhibit the PICs after chronic injury (Li et al. 2004b). Our proposed studies consider the possibility that subtype specific antagonists for monoamine receptors can control PICs in motoneurons independently from actions on spasm-inducing afferent inputs, providing much more selective and effective control of spasms than is possible with a general suppressant like baclofen.

REFERENCES

Alaburda A, Perrier JF, and Hounsgaard J. Mechanisms causing plateau potentials in spinal motoneurones. In: *Adv Exp Med Biol*, 2002, p. 219-226.

Bennett D, Sanelli L, and Cooke C. Long-lasting polysynaptic reflexes that produce spasms after sacral spinal cord injury in rats. *J Neurophysiology* accepted, 2004.

Bennett DJ, Li Y, Harvey PJ, and Gorassini M. Evidence for plateau potentials in tail motoneurons of awake chronic spinal rats with spasticity. *J Neurophysiol* 86: 1972-1982, 2001a.

Bennett DJ, Li Y, and Siu M. Plateau potentials in sacrocaudal motoneurons of chronic spinal rats, recorded in vitro. *J Neurophysiol* 86: 1955-1971, 2001b.

Cantrell AR and Catterall WA. Neuromodulation of Na+ channels: an unexpected form of cellular plasticity. In: *Nat Rev Neurosci*, 2001, p. 397-407.

Cassam AK, Llewellyn-Smith IJ, and Weaver LC. Catecholamine enzymes and neuropeptides are expressed in fibres and somata in the intermediate gray matter in chronic spinal rats. In: *Neuroscience*, 1997, p. 829-841.

Giroux N, Rossignol S, and Reader TA. Autoradiographic study of alpha1- and alpha2-noradrenergic and serotonin1A receptors in the spinal cord of normal and chronically transected cats. In: *J Comp Neurol*, 1999, p. 402-414.

Goldin AL. Resurgence of sodium channel research. In: *Annu Rev Physiol*, 2001, p. 871-894.

Gorassini M, Bennett D, and Yang JF. Excitability of motor units in persons with spasticity from spinal cord injury. *Soc Neurosci Abstr 25:120*, 1999.

Gorassini MA, Knash M, Harvey PJ, Bennett DJ, and Yang JF. Role of motoneuron plateau potentials in the generation of involuntary muscle activity after spinal cord injury. *Brain*: submitted, 2003.

Kuhn RA and Macht MB. Some manifestations of reflex activity in spinal man with particular reference to the occurrence of extensor spasm. *Bull Johns Hopkins Hosp* 84: 43-75, 1948.

Lee RH and Heckman CJ. Enhancement of bistability in spinal motoneurons in vivo by the noradrenergic alpha1 agonist methoxamine. *J Neurophysiol* 81: 2164-2174, 1999.

Li Y and Bennett DJ. Persistent sodium and calcium currents cause plateau potentials in motoneurons of chronic spinal rats. *J Neurophysiol* 90: 857-869, 2003.

Li Y, Gorassini MA, and Bennett DJ. Role of persistent sodium and calcium currents in motoneuron firing and spasticity in chronic spinal rats. *J Neurophysiology* 91: 767-783, 2004a.

Li Y, Li X, Harvey PJ, and Bennett DJ. Effect of baclofen on spinal reflexes and persistent inward currents in motoneurons of acute and chronic spinal rats. *J Neurophysiology* (submitted), 2004b.

Newton BW and Hamill RW. The morphology and distribution of rat serotoninergic intraspinal neurons: an immunohistochemical study. In: *Brain Res Bull*, 1988, p. 349-360.

Shapiro S. Neurotransmission by neurons that use serotonin, noradrenaline, glutamate, glycine, and gamma-aminobutyric acid in the normal and injured spinal cord. In: *Neurosurgery*, 1997, p. 168-176; discussion 177.